

# **Problems in Laser Physics**



**G. Cerullo, S. Longhi,  
M. Nisoli, S. Stagira,  
and O. Svelto**



Cover photograph: "Homage to Arnolfo di Cambio": Drawing with a green beam of a copper-vapor laser from *Torre di Arnolfo*, *Palazzo Vecchio* (*Palazzo della Signoria*) to Brunelleschi Dome in Florence; realization of the laser EL.EN. S.p.A. Detail: exhibition of Dani Karavan, June 1999 (Firenze: *Palazzo Vecchio & Piazza della Signoria* – Prato: *Museo Pecci*—Fattoria Celle—Pistoia: *Piazza del Duomo*).



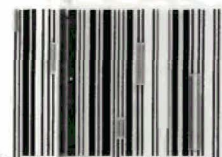
**KLUWER ACADEMIC /  
PLENUM PUBLISHERS**

233 Spring Street, New York, New York 100131578

PRINTED IN U.S.A.

ISBN 0-306-46649-X

90000



9 780306 466496

# **PROBLEMS IN LASER PHYSICS**

**G. Cerullo, S. Longhi, M. Nisoli,  
S. Stagira, and O. Svelto**

*Politecnico di Milano  
Milano, Italy*

**KLUWER ACADEMIC/PLENUM PUBLISHERS**  
**New York, Boston, Dordrecht, London, Moscow**

Library of Congress Cataloging in Publication Data

---

Problems in laser physics/G. Cerullo ... [et al.]

p. cm.

Includes bibliographical references and index.

ISBN 0-306-46649-X

1. Lasers—Problems, exercises, etc. I. Cerullo, G.

QC688 .P77 2001

621.36'6—dc21

2001041357

---

ISBN 0-306-46649-X

© 2001 Kluwer Academic/Plenum Publishers, New York  
233 Spring Street, New York, New York 10013

<http://www.wkap.nl/>

10 9 8 7 6 5 4 3 2 1

A C.I.P. record for this book is available from the Library  
of Congress

All rights reserved

No part of this book may be reproduced, stored in a  
retrieval system, or transmitted in any form or by any  
means, electronic, mechanical, photocopying,  
microfilming, recording, or otherwise, without written  
permission from the Publisher

Printed in the United States of America

# Preface

There is hardly any book that aims at solving problems typically encountered in the laser field, and this book intends to fill the void. Following some initial exercises related to general aspects in laser physics (Chapt. 1), the subsequent problems are organized along the following topics: (i) Interaction of radiation with matter either made of atoms or ions, weakly interacting with surrounding species, or made of more complicated elements such as molecules or semiconductors (Chapters 2 and 3). (ii) Wave propagation in optical media and optical resonators (Chapters 4 and 5). (iii) Optical and electrical pumping processes and systems (Chapter 6). (iv) Continuous wave and transient laser behaviors (Chapters 7 and 8). (v) Solid-state, dye, semiconductor, gas and X-ray lasers (Chapters 9 and 10). (vi) Properties of the output beam and beam transformation by amplification, frequency conversion and pulse compression or expansion (Chapters 11 and 12).

Problems are proposed here and solved following the contents of Orazio Svelto's *Principles of Lasers* (fourth edition; Plenum Press, New York, 1998). Whenever needed, equations and figures of the book mentioned above are currently used with an appropriate reference [e.g., Eq. (1.1.1) of the book is referred to as Eq. (1.1.1) of PL]. One can observe, however, that the types of problems proposed and discussed are of general validity and many of these problems have actually been suggested by our own long-time experience in performing theoretical and experimental researches in the field. Some of these problems are also directly related to real-world lasers (i.e., lasers, laser components and laser systems commonly found in research laboratories or commercially available). Therefore, the reader should be able to solve most of these problems even if his knowledge in laser physics has been acquired through studying other textbooks.

In each chapter, problems are first proposed all together and then solved at the end. This should encourage the reader to solve the problem by himself without immediately looking at the solution. Three **kinds** of problems are considered with attention being paid to a good balance between them:

1. Problems where one just needs to insert appropriate numbers into some important equation already provided in the previously mentioned book (applicative problems): they should help students to become more acquainted with important equations in laser physics and with the typical values of the corresponding parameters that are involved.
2. Problems where students are asked to prove some relevant equation left unproven

in the textbook (*demonstrative problems*): their purpose is to test the maturity acquired by demonstrating some, generally simple, passages.

3. Problems where students are asked to develop topics which go beyond those covered in the above book as well as in many other textbooks in the field (*evolutional problems*): their purpose is to increase the depth of knowledge in the laser field. Whenever appropriate, some hints for the solutions are also added, particularly for some more advanced demonstrative or evolutional **problems**. However, when the level of difficulty is deemed to be particularly high, a warning in the form "level of difficulty higher than average" is added at the end of the corresponding problem. This should help the reader, on the one hand, know when to apply himself harder and, on the other hand, not to get discouraged at a possible failure. Reading the solution should allow students to considerably enrich their basic knowledge in the field.

Lastly, care has been taken not to have the solution of one problem be dependent on the solution of a preceding problem in the chapter. This should allow more freedom for tackling problems not necessarily in sequential order.

Given the number of problems proposed and their wide variety, it is believed that a proficient student, upon solving these problems, should become more than well prepared to begin a research activity in laser physics and engineering as well as in the general field of photonics.

Giulio Cerullo  
Stefano Longhi  
Mauro Nisoli  
Salvatore Stagira  
Orazio Svelto

Milan, February 2001

# Contents

	<b>P</b>	<b>A</b>
<b>1. Introductory Concepts .....</b>	<b>1</b>	
<b>1.1. Spectrum of laser emission .....</b>	<b>1</b>	<b>5</b>
<b>1.2. Spectrum of visible light .....</b>	<b>1</b>	<b>5</b>
<b>1.3. Energy of a photon .....</b>	<b>1</b>	<b>5</b>
<b>1.4. Thermal energy .....</b>	<b>1</b>	<b>6</b>
<b>1.5. Population under thermal equilibrium of two levels .....</b>	<b>2</b>	<b>6</b>
<b>1.6. Small-signal gain of a ruby laser amplifier .....</b>	<b>2</b>	<b>7</b>
<b>1.7. Threshold inversion of a laser cavity .....</b>	<b>2</b>	<b>7</b>
<b>1.8. Temporal evolution of the population densities in a three-level system .....</b>	<b>2</b>	<b>8</b>
<b>1.9. Brightness of a diffraction limited beam .....</b>	<b>3</b>	<b>10</b>
<b>1.10. Comparison between the brightness of a lamp and that of an argon laser .....</b>	<b>3</b>	<b>11</b>
<b>1.11. Intensity on the retina of the sun light and of a He-Ne laser beam .....</b>	<b>3</b>	<b>11</b>
<b>1.12. Power spectrum of a wave-train of finite duration .....</b>	<b>4</b>	<b>12</b>
<b>1.13. Coherence time and coherence length of filtered light .....</b>	<b>4</b>	<b>13</b>
<b>1.14. Radiation pressure of a laser beam .....</b>	<b>4</b>	<b>14</b>
<b>1.15. Radiation pressure .....</b>	<b>4</b>	<b>14</b>
<b>2. Interaction of Radiation with Atoms and Ions .....</b>	<b>17</b>	
<b>2.1. Intensity and energy density of a plane em wave .....</b>	<b>17</b>	<b>23</b>
<b>2.2. Photon flux of a plane monochromatic wave .....</b>	<b>17</b>	<b>24</b>
<b>2.3. Number of modes of a blackbody cavity .....</b>	<b>17</b>	<b>24</b>
<b>2.4. Wien's law .....</b>	<b>17</b>	<b>26</b>

	<b>P</b>	<b>A</b>
2.5. Blackbody cavity filled with a dispersive medium .....	18	27
2.6. Power irradiated by a blackbody emitter .....	18	28
2.7. Average mode energy .....	18	29
2.8. Spontaneous and stimulated emission rates .....	18	30
2.9. Natural broadening .....	18	30
2.10. Doppler broadening .....	19	33
2.11. Temperature of a blackbody with the same energy density of a He-Ne laser .....	19	33
2.12. Spontaneous lifetime and cross section .....	19	34
2.13. Radiative lifetime and quantum yield of the ruby laser transition .....	19	35
2.14. Radiative lifetime of the strongest transition of the Nd:YAG laser .....	20	35
2.15. Transient response of a two-level system to an applied signal .....	20	36
2.16. Gain saturation intensity .....	20	39
2.17. Population inversion of a homogeneously broadened laser transition .....	21	41
2.18. Strongly coupled levels .....	21	42
2.19. Amplification of a monochromatic em wave .....	21	43
2.20. Amplified Spontaneous Emission in a Nd:YAG rod .....	22	44
2.21. Saturated absorption coefficient .....	22	45
2.22. Peak absorption coefficient and linewidth .....	22	45
 <b>3. Energy Levels. Radiative. and Nonradiative Transitions in Molecules and Semiconductors .....</b>	 <b>47</b>	
3.1. Vibrational frequency of a diatomic molecule .....	47	53
3.2. Calculation of the elastic constant of a molecule.....	47	54
3.3. From the potential energy to the vibrational frequency.....	47	54
3.4. The Morse potential energy .....	47	55
3.5. Calculation of the <b>Franck-Condon</b> factor .....	48	56
3.6. Rotational constant of a diatomic molecule .....	48	57
3.7. Far-infrared absorption spectrum of an HCl molecule .....	49	58
3.8. The most heavily populated rotational level .....	49	59
3.9. The emission lines of a CO <sub>2</sub> molecule .....	49	60
3.10. The law of mass action.....	49	60
3.11. Energies of the quasi-Fermi levels.....	50	62
3.12. The quasi-Fermi levels in GaAs .....	50	63
3.13. Derivation of the Bernard-Duraffourg condition .....	50	63
3.14. Laser levels in a semiconductor .....	50	64

	P	A
3.15. Frequency dependence of the gain of an inverted semiconductor.....	50	65
3.16. Gain calculation in a GaAs amplifier .....	51	67
3.17. Differential gain of a GaAs amplifier .....	51	68
3.18. Thickness of a quantum well: an order of magnitude estimate.....	51	69
3.19. An ideal quantum well.....	51	70
3.20. Energies of the quasi-Fermi levels in a semiconductor quantum well .....	52	71
3.21. Calculation of the gain bandwidth in a GaAs quantum well	52	73
 <b>4. Ray and Wave Propagation through Optical Media.....</b>	<b>75</b>	
4.1. ABCD matrix of a spherical dielectric interface .....	75	81
4.2. ABCD matrix of a thin lens .....	75	83
4.3. ABCD matrix of a piece of glass.....	75	83
4.4. Reflection at a plane interface .....	75	84
4.5. An high reflectivity dielectric mirror .....	76	86
4.6. A Fabry-Perot interferometer.....	76	87
4.7. A scanning Fabry-Perot interferometer .....	76	88
4.8. An imaging optical system .....	76	88
4.9. The ABCD law for gaussian beams .....	77	89
4.10. A collimating lens .....	77	92
4.11. A simple optical processing system .....	77	93
4.12. A laser driller .....	78	94
4.13. An earth to moon laser rangefinder .....	78	95
4.14. An He-Ne laser .....	78	95
4.15. An Argon laser.....	78	96
4.16. Gaussian beam propagation through an optical system.....	79	97
4.17. Power conservation for a gaussian beam .....	79	99
4.18. A "soft" or gaussian aperture .....	79	100
4.19. A waist imaging system.....	79	101
4.20. Gaussian beam transformation by a lens.....	79	102
4.21. Focusing a gaussian beam inside a piece of glass .....	80	103
 <b>5. Passive Optical Resonators .....</b>	<b>105</b>	
5.1. Stability of a resonator with concave mirrors .....	105	112
5.2. A concave-convex resonator .....	105	113
5.3. A simple two-mirror resonator.....	105	113

## CONTENTS

	P	A
5.4. Number of longitudinal modes in a resonator .....	105	113
5.5. Resonators for an Argon laser .....	106	114
5.6. A resonator for a CO <sub>2</sub> laser .....	106	115
5.7. A near-planar resonator .....	106	116
5.8. Single-mode selection in a He-Ne laser .....	106	117
5.9. Spot sizes on the mirrors of a stable resonator .....	107	117
5.10. A <b>plano-concave</b> resonator .....	107	118
5.11. A near-concentric resonator .....	107	120
5.12. The unlucky graduate student .....	107	121
5.13. Resonator with an intracavity lens .....	108	122
5.14. Resonator for a cw-pumped Nd:YAG laser .....	108	124
5.15. Resonator for a <b>Ti:sapphire</b> laser .....	108	124
5.16. Location of the beam waist in a stable resonator .....	109	127
5.17. Properties of a symmetric confocal resonator .....	109	128
5.18. Asymmetric confocal resonators.....	109	129
5.19. A confocal unstable resonator.....	110	130
5.20. Unstable resonator with gaussian minors: properties of the output beam .....	110	131
5.21. Designing a gaussian mirror for an unstable resonator .....	110	132
5.22. Unstable resonator with a supergaussian mirror .....	110	133
 <b>6. Pumping Processes .....</b>	 135	
6.1. Critical pump rate in a lamp-pumped Nd:YLF laser.....	135	141
6.2. Pump rate expression for longitudinal pumping .....	135	142
6.3. Laser spot size in a longitudinally pumped Ti:Al <sub>2</sub> O <sub>3</sub> laser under optimum pumping conditions.....	135	143
6.4. Optical pumping of a Ti:Al <sub>2</sub> O <sub>3</sub> laser: a design problem.....	136	143
6.5. Doping in a solid-state laser medium.....	136	144
6.6. A transversely pumped high-power Nd:YAG laser.....	136	145
6.7. Longitudinal vs. transverse pumping in Nd:YAG laser.....	136	145
6.8. Threshold power in a double-end pumped Nd:YVO <sub>4</sub> laser...	137	146
6.9. Threshold power in a quasi-three level laser: the Yb:YAG case.....	137	146
6.10. Threshold pump power of a Nd:glass fiber laser.....	137	147
6.11. Pump absorption in a Nd:glass fiber laser.....	138	147
6.12. Maximum output intensity in a Nd:glass amplifier.....	138	149
6.13. Electron temperature in a <b>Boltzmann</b> distribution.....	138	149
6.14. How to reduce the size of a He-Ne laser tube?.....	138	150
6.15. Thermal and drift velocities of electrons in a He-Ne laser...	139	150
6.16. A He-Ne laser: pump rate vs. pump current.....	139	151

	P	A
6.17. Scaling laws and performances in longitudinally pumped gas lasers.....	139	152
6.18. Pump rate vs. pumping current in Ar <sup>+</sup> lasers.....	139	152
6.19. Ar <sup>+</sup> lasers: pump efficiency vs. pump power .....	140	153
<b>7. Continuous Wave Laser Behavior .....</b>	<b>155</b>	
7.1. Calculation of logarithmic loss.....	155	163
7.2. Calculation of cavity photon lifetime.....	155	163
7.3. Four-level laser with finite lifetime of the lower laser level..	155	164
7.4. Rate equations analysis of a three-level laser.....	156	165
7.5. Threshold condition in a ruby laser.....	156	167
7.6. Thermal lensing in a microchip Nd:YAG laser.....	156	167
7.7. Transverse efficiency in an end-pumped four-level laser ....	157	168
7.8. Threshold and slope-efficiency calculations in a longitudinally-pumped Nd:YAG laser .....	157	169
7.9. Estimate of internal laser losses. ....	157	171
7.10. Calculation of optimum output coupling.....	158	171
7.11. Longitudinal efficiency in a standing-wave laser.....	158	172
7.12. Dispersion relation for a Lorentzian line.....	158	175
7.13. Frequency pulling in a homogeneously-broadened laser.....	159	178
7.14. Calculation of frequency pulling in a He-Xe laser.....	159	180
7.15. Quantum limit to the laser linewidth.....	159	180
7.16. Tuning of a Ti:sapphire laser by a birefringent filter.....	159	182
7.17. Transverse mode selection.....	160	183
7.18. Single longitudinal mode oscillation in an inhomogeneous broadened laser.....	160	184
7.19. Suppression of spatial hole burning by the twisted-mode technique.....	160	184
7.20. Single-longitudinal mode selection by an intracavity etalon.....	161	185
<b>8. Transient Laser Behavior .....</b>	<b>187</b>	
8.1. Relaxation oscillations in a Nd:YAG laser.....	187	193
8.2. Noise spectrum of the output power for a four-level laser...	187	193
8.3. Fast Q-switching in a Nd:YLF laser.....	187	195
8.4. Calculation of the pulse energy and pulse duration in a repetitively Q-switched Nd:YAG laser.....	188	196
8.5. Quarter-wave voltage in a Q-switch Pockels cell.....	188	197
8.6. Active Q-switching in a three-level laser.....	188	198
8.7. Calculation of the beam deflection angle by an acousto-optic modulator.....	189	200

## CONTENTS

	P	A
8.8. Mode-locking of sidebands modes with random amplitudes.....	189	201
8.9. Chirped Gaussian pulses with quadratic phase locking relations.....	189	202
8.10. On the periodicity of mode-locked signals.....	189	203
8.11. Phase locking condition for second-harmonic mode-locking.....	190	204
8.12. Pulsewidth calculation in an actively mode-locked Nd:YAG laser.....	190	205
8.13. Gaussian pulse analysis of frequency mode locking .....	190	206
8.14. Mode-locking in a He-Ne laser .....	190	208
8.15. Harmonic mode-locking of a laser in a linear cavity.....	191	209
8.16. Calculation of pulse energy and peak power in a passively mode-locked Nd:YAG laser.....	191	210
8.17. Pulse duration in an idealized Kerr lens mode-locked Ti:Sapphire laser.....	191	210
8.18. Pulse duration in a soliton-type Ti:sapphire mode-locked laser.....	192	212
8.19. Pulse broadening in a quartz plate.....	192	212
8.20. Self-imaging of a mode-locked pulse train.....	192	213
 <b>9. Solid-State, Dye, and Semiconductor Lasers .....</b>	 215	
9.1. Slope efficiency in a Ti:Al <sub>2</sub> O <sub>3</sub> laser.....	215	221
9.2. Output power from a Nd:YAG laser.....	215	221
9.3. A Nd:YVO <sub>4</sub> laser in the fog.....	215	222
9.4. A green solid-state laser.....	216	222
9.5. Yb:YAG laser vs. Nd:YAG laser.....	216	224
9.6. Anisotropy in a Cr:LiSAF laser rod.....	217	225
9.7. Threshold pump power in longitudinal pumping: ground and excited states contribution.....	217	227
9.8. Threshold pump power in a dye laser: triplet-triplet contribution.....	218	228
9.9. Slope efficiency in a dye laser.....	218	230
9.10. A laser cascade.....	218	232
9.11. Longitudinal modes in a semiconductor laser.....	218	232
9.12. Beam astigmatism in a semiconductor laser.....	219	233
9.13. Current threshold in a GaAs/AlGaAs laser.....	219	234
9.14. Slope efficiency in a GaAs/AlGaAs laser.....	219	235
9.15. Distributed feedback in a semiconductor laser.....	220	236
9.16. Current threshold in a quantum-well laser.....	220	237
9.17. Carrier density in a VCSEL at threshold.....	220	237

	P	A
<b>10. Gas, Chemical, Free-Electron, and X-Ray Lasers .....</b>	<b>239</b>	
10.1. Low-density laser emitting in the infrared.....	239	243
10.2. Low-density laser emitting in the UV - soft X region.....	239	243
10.3. High-power lasers for material processing.....	239	244
10.4. Internal structure of He-Ne lasers.....	239	244
10.5. Maximum output power in He-Ne lasers.....	240	245
10.6. Internal structure of high-power Ar <sup>+</sup> lasers.....	240	246
10.7. Output vs. <b>pump</b> power in Ar <sup>+</sup> lasers.....	240	246
10.8. Current density in a low power CO <sub>2</sub> laser.....	240	247
10.9. Voltage drop in a low power CO <sub>2</sub> laser tube.....	240	248
10.10. Rotational transitions in a CO <sub>2</sub> laser.....	241	248
10.11. Mode locking of a CO <sub>2</sub> laser.....	241	249
10.12. ASE threshold for a N <sub>2</sub> laser.....	241	250
10.13. Pump power in a KrF excimer laser at threshold.....	242	251
10.14. Cold reaction in a HF chemical laser.....	242	252
10.15. Transition linewidths in the soft-X-ray spectral region.....	242	252
10.16. A free-electron laser operating in the soft-X-ray region.....	242	253
<b>11. Properties of Laser Beams .....</b>	<b>255</b>	
11.1. Complex degree of coherence for a quasi monochromatic wave .....	255	261
11.2. Measurement of the spatial coherence by a Young interferometer .....	255	262
11.3. Destroy of spatial coherence by rotation of a ground glass..	255	262
11.4. Comparison of temporal coherence between a thermal source and a laser.....	256	263
11.5. Temporal coherence of white light.....	256	264
11.6. Relation between first-order degree of temporal coherence and <b>fringe</b> visibility in a Michelson interferometer.....	256	264
11.7. Degree of temporal coherence for a low-pressure discharge lamp .....	256	266
11.8. Temporal coherence of a gas laser oscillating on N axial modes .....	257	268
11.9. An interference experiment with partially coherent light....	257	269
11.10. Spatial coherence of the light from the sun.....	257	269
11.11. An astronomic calculation based on spatial coherence of stellar <b>radiation</b> .....	258	270
11.12. Beam divergence of a partially-coherent laser beam.....	258	270
11.13. Focusing of a perfectly-coherent spatial beam.....	258	271
11.14. <b>M</b> <sup>2</sup> factor of a Nd:YAG laser .....	258	272

	P	A
11.15. Brightness of a high-power CO <sub>2</sub> laser .....	259	272
11.16. Grain size of the speckle pattern as observed on a screen....	259	273
11.17. Grain size of the speckle pattern as seen by a human observer.....	259	274
11.18. Correlation function and power spectrum of a single-longitudinal mode laser.....	259	274
<b>12. Laser Beam Transformation: Propagation. Amplification. Frequency Conversion. Pulse Compression. and Pulse Expansion</b>	<b>277</b>	
12.1. Propagation of a multimode beam .....	277	285
12.2. Amplification of long pulses by a Nd:YAG amplifier .....	277	286
12.3. Amplification of short pulses by a Nd:YAG amplifier .....	277	286
12.4. Extraction efficiency of a two-pass amplifier .....	278	287
12.5. Saturation fluence in a quasi-three-level amplifier .....	278	289
12.6. Maximum output fluence from an amplifier with losses .....	278	290
12.7. Theoretical limit to the maximum intensity of an amplifier .	279	291
12.8. Index of refraction of an extraordinary wave in a uniaxial crystal .....	279	292
12.9. Double refraction in a uniaxial crystal .....	279	293
12.10. Second harmonic conversion of a Ti:sapphire laser in a BBO crystal .....	279	294
12.11. Second harmonic conversion efficiency in a KDP crystal ...	280	296
12.12. Second harmonic generation with a Gaussian beam .....	280	297
12.13. Frequency doubling of a Gaussian beam in a KDP crystal ..	281	298
12.14. Effective nonlinear coefficient of a KDP crystal .....	281	299
12.15. Threshold pump intensity of an optical parametric oscillator .....	282	301
12.16. Collinear parametric generation in a BBO crystal .....	282	301
12.17. Noncollinear parametric generation in a BBO crystal .....	282	302
12.18. Nonlinear index $n_2$ of sapphire .....	283	305
12.19. Pulse spectral broadening due to self-phase modulation in a Kerr medium .....	283	305
12.20. Spectral broadening of a 20-fs pulse in a hollow fiber filled with argon .....	283	306
12.21. Group delay dispersion of a medium .....	284	307
12.22. Dispersion-induced broadening of a 10-fs pulse in a fused silica plate .....	284	308

# **PROBLEMS IN LASER PHYSICS**

# CHAPTER 1

## Introductory Concepts

### PROBLEMS

#### 1.1P Spectrum of laser emission.

The part of the ~~ern~~ **spectrum** of interest in ~~the~~ laser field starts from the **submillimeter** wave region and decreases in wavelength to the x-ray region. This covers the following regions in succession: far infrared, near infrared, visible, UV, vacuum ultraviolet (WV), soft x-ray, x-ray: From standard textbooks find the wavelength intervals of ~~these~~ regions.

#### 1.2P Spectrum of visible light.

From standard textbooks find the **wavelength** intervals **corresponding to the** different colors of the visible **spectrum**, and calculate the corresponding frequency intervals.

#### 1.3P Energy of a photon.

Calculate the frequency in hertz and **wavenumbers** ( $\text{cm}^{-1}$ ) and ~~the~~ energy in electronvolts of a photon of wavelength  $\lambda=1 \mu\text{m}$  in **vacuum**.

#### 1.4P Thermal energy.

Calculate the **wavenumbers** corresponding to an energy spacing of  $kT$ , where  $k$  is the **Boltzmann** constant and  $T$  is ~~the~~ absolute temperature. Assume  $T=300 \text{ K}$ .

### **1.5P Population under thermal equilibrium of two levels.**

Determine the ratio between the thermal equilibrium population of two levels separated by the energy difference  $\Delta E$  equal to: (a)  $10^{-4}$  eV, which is a value equivalent to the spacing of rotational levels for many molecules; (b)  $5 \times 10^{-2}$  eV, which corresponds to molecular vibrational levels; (c) 3 eV, which is of the order of magnitude of electronic excitation of atoms and molecules. Assume that the two levels have the same degeneracy and that the temperature is 100 K, 300 K (room temperature) and 1000 K.

### **1.6P Small-signal gain of a ruby laser amplifier.**

The small-signal gain of a ruby laser amplifier using a **15-cm-long** rod is 12. Neglecting gain saturation, calculate **the** small-signal gain of a **20-cm-long** rod with the same population inversion.

### **1.7P Threshold inversion of a laser cavity.**

**A** laser cavity consists of two mirrors with reflectivity  $R_1 = 1$  and  $R_2 = 0.5$ , while the internal loss per pass is  $L_i = 1\%$ . Calculate **the** total logarithmic losses per pass. If **the** length of the active material is  $l = 7.5$  cm and **the** transition cross section is  $\sigma = 2.8 \times 10^{-19}$  cm<sup>2</sup>, calculate the threshold inversion.

### **1.8P Temporal evolution of the population densities in a three-level system.**

**Consider** the energy level scheme shown in Fig. 1.1. Atoms are raised from level 0 to level 2 at a **pump rate**  $R_p$ . The lifetime of levels 1 and 2 are  $\tau_1$  and  $\tau_2$  respectively. Assuming that **the** ground state 0 is not depleted to **any significant extent** and neglecting stimulated **emission**: (i) write **the** rate equations for the population densities,  $N_1$  and  $N_2$ , of level 1 and 2 respectively; (ii) calculate  $N_1$  and  $N_2$  as a function of time; (iii) plot the population densities in **the** following two cases: (a)  $\tau_1 = 2 \mu\text{s}$ ,  $\tau_2 = 1 \mu\text{s}$ ; (b)  $\tau_1 = 1 \mu\text{s}$ ,  $\tau_2 = 2 \mu\text{s}$ . **Assume** that levels 1 and 2 **have the same degeneracy**.

[Hint: **the** differential equation for **the** population of level 1 i.e.  $(dN_1/dt) + (N_1/\tau_1) = f(t)$ , can be solved multiplying both sides by the factor  $\exp(t/\tau_1)$ . In this way

the left-hand side of the preceding differential equation becomes a perfect differential]

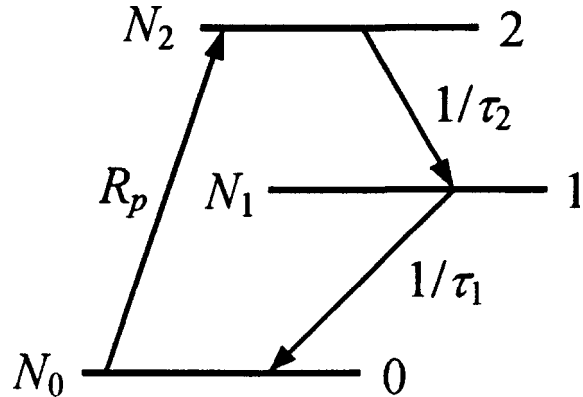


Fig. 1.1 Energy level scheme of the three-level system described in 1.8P

### 1.9P Brightness of a diffraction limited beam.

Show that the brightness of a diffraction-limited beam is given by  $B = (2/\beta\pi\lambda)^2 P$ , where:  $P$  is the power;  $\lambda$  is the wavelength;  $\beta$  is a numerical coefficient, of the order of unity, characterizing a diffraction-limited beam, whose value depends on the shape of the amplitude distribution of the beam.

### 1.10P Comparison between the brightness of a lamp and that of an argon laser.

The brightness of probably the brightest lamp so far available (PEK Labs type 107/109™, excited by 100 W of electrical power) is about 95 W/cm<sup>2</sup> sr in its most intense green line ( $\lambda = 546$  nm). Compare this brightness with that of a 1-W argon laser ( $\lambda = 514.5$  nm), which can be assumed to be diffraction limited.

### 1.11P Intensity on the retina of the sun light and of a He-Ne laser beam.

At the surface of the earth the intensity of the sun is approximately 1 kW m<sup>-2</sup>. Calculate the intensity at the retina that results when looking directly at the sun. Assume that: (i) the pupil of a bright-adapted eye is 2 mm in diameter; (ii) the

focal length of the eye is 22.5 mm; (iii) the Sun **subtends** an angle of **0.5°**. Compare this intensity with that resulting when looking into a **1-mW** He-Ne laser ( $\lambda=632.8$  nm) with a 2-mm diameter [the diameter of the beam in the focus of a lens of focal length  $f$  can be calculated as  $D_f = 4f\lambda / (\pi D_0)$ , where  $D_0$  is the beam diameter on the lens and  $\lambda$  is the laser wavelength].

### **1.12P Power spectrum of a wave-train of finite duration.**

Calculate the power spectrum of a single wave-train,  $f(t)$ , of finite duration  $\tau_0$  [ $f(t) = \exp(i 2\pi\nu_0 t)$  for  $-\tau_0/2 < t < \tau_0/2$ ,  $f(t)=0$  otherwise] and show that the full width at half maximum (FWHM) of the power spectrum is given by  $\Delta\nu = 1/\tau_0$ .

### **1.13P Coherence time and coherence length of filtered light.**

An interference filter with a pass band of 10 nm centered at 500 nm is used to obtain approximately **monochromatic** light from a white source. Calculate the coherence time of the filtered light and its coherence length.

[Hint: the coherence length,  $l_c$ , is defined as  $l_c = c \tau_0$ , where  $\tau_0$  is the coherence time]

### **1.14P Radiation pressure of a laser beam.**

A 10-W laser beam is **focused** to a spot of 1-mm diameter on a perfectly absorbent target. Calculate the radiation pressure on the target using the following relationship between pressure,  $p$ , and intensity,  $I$ :  $p = I/c$ .

### **1.15P Radiation pressure.**

Since the **momentum** of a photon of frequency  $\nu$  is given by  $q = \hbar k$ , where  $k = 2\pi\nu/c$ , show that the pressure exerted by a light beam of intensity  $I$  impinging normally on a perfectly absorbing surface is  $Ilc$ .

## 1. INTRODUCTORY CONCEPTS

## ANSWERS

### 1.1A Spectrum of laser emission.

The electromagnetic spectrum of interest in the laser field covers the following regions:

- |       |                    |   |
|-------|--------------------|---|
| i.    | far infrared       | $1 \text{ mm} > \lambda > 30 \mu\text{m}$   |
| ii.   | medium infrared    | $30 \mu\text{m} > \lambda > 3 \mu\text{m}$  |
| iii.  | near infrared      | $3 \mu\text{m} > \lambda > 780 \text{ nm}$  |
| iv.   | visible            | $780 \text{ nm} > \lambda > 380 \text{ nm}$ |
| v.    | ultraviolet        | $380 \text{ nm} > \lambda > 180 \text{ nm}$ |
| vi.   | vacuum ultraviolet | $180 \text{ nm} > \lambda > 40 \text{ nm}$  |
| vii.  | soft x-ray         | $40 \text{ nm} > \lambda > 1 \text{ nm}$    |
| viii. | x-ray              | $1 \text{ nm} > \lambda > 10 \text{ pm}$    |

### 1.2A Spectrum of visible light.

Since in vacuum  $\lambda\nu=c$ , where: A is the wavelength; v is the frequency; c is the velocity of light in **vacuum**, the frequency is obtained as  $\nu=c/\lambda$ .

The different colors of the visible **spectrum** correspond to the following wavelength and frequency intervals:

- |      |        |   |   |
|------|--------|---|---|
| i.   | red    | $780 \text{ nm} > \lambda > 620 \text{ nm}$ | $3.83 \times 10^{14} \text{ Hz} < \nu < 4.85 \times 10^{14} \text{ Hz}$ |
| ii.  | orange | $620 \text{ nm} > \lambda > 580 \text{ nm}$ | $4.85 \times 10^{14} \text{ Hz} < \nu < 5.15 \times 10^{14} \text{ Hz}$ |
| iii. | yellow | $580 \text{ nm} > \lambda > 560 \text{ nm}$ | $5.15 \times 10^{14} \text{ Hz} < \nu < 5.35 \times 10^{14} \text{ Hz}$ |
| iv.  | green  | $560 \text{ nm} > \lambda > 490 \text{ nm}$ | $5.35 \times 10^{14} \text{ Hz} < \nu < 6.1 \times 10^{14} \text{ Hz}$  |
| v.   | blue   | $490 \text{ nm} > \lambda > 460 \text{ nm}$ | $6.1 \times 10^{14} \text{ Hz} < \nu < 6.5 \times 10^{14} \text{ Hz}$   |
| vi.  | violet | $460 \text{ nm} > \lambda > 380 \text{ nm}$ | $6.5 \times 10^{14} \text{ Hz} < \nu < 7.9 \times 10^{14} \text{ Hz}$   |

### 1.3A Energy of a photon.

Since in vacuum  $\lambda\nu=c$  we obtain:

$$\nu = c/\lambda \approx 3 \times 10^{14} \text{ Hz} \quad (1)$$

## ANSWERS

The photon energy is given by:

$$E = h\nu = 1.99 \times 10^{-19} \text{ J} \quad (2)$$

Since  $1 \text{ eV} = 1.6 \times 10^{-19} \text{ J}$  we obtain:  $E = 1.24 \text{ eV}$ , which is the same as the kinetic energy of an electron that has been accelerated by a potential difference of 1.24 V. The reciprocal wavelength,  $\tilde{\nu} = \nu/c$ , is often used as a unit of frequency and it is expressed in  $\text{cm}^{-1}$ , also called wavenumbers:  $\tilde{\nu} = \nu/c = 10^4 \text{ cm}^{-1}$ .

Notes:

- (i) The conversion formula between energy in eV and wavelength measured in  $\mu\text{m}$  is simply:  $E(\text{eV}) \geq 1.24/\lambda (\mu\text{m})$
- (ii) The relationship between wavenumbers and energy is  $\tilde{\nu} = \nu/c = E/(hc)$ ;
- (iii)  $1 \text{ cm}^{-1}$  corresponds to  $1.24 \times 10^4 \text{ eV}$ ;  
 $1 \text{ eV}$  corresponds to  $8065.5 \text{ cm}^{-1}$

### 1.4A Thermal energy.

The thermal energy at  $T = 300 \text{ K}$  is given by:

$$kT = 4.14 \times 10^{-21} \text{ J} \quad (1)$$

As noted in 1.3A the relationship between wavenumbers and energy is  $\tilde{\nu} = \nu/c = E/(hc)$ ; one therefore obtains:

$$\tilde{\nu} = \frac{E}{hc} = \frac{kT}{hc} = 208.5 \text{ cm}^{-1} \quad (2)$$

### 1.5A Population under thermal equilibrium of two levels.

The ratio between the thermal equilibrium population of two levels separated by the energy difference  $\Delta E = E_2 - E_1$  ( $\Delta E > 0$ ) is given by Eq. (1.2.2) of PL:

$$\frac{N_2}{N_1} = \frac{g_2}{g_1} \exp\left(-\frac{\Delta E}{kT}\right) \quad (1)$$

where:  $N_1$  and  $N_2$  are the population densities of level 1 and 2, respectively;  $g_1$  and  $g_2$  are the degeneracies of the two levels. Using Eq. (1) and assuming that

the two levels have the same degeneracy ( $g_1 = g_2$ ) we obtain the following results:

$\Delta E$ (eV)	$T = 100$ K	$T = 300$ K	$T = 1000$ K
$10^{-4}$	0.9885	0.9962	0.9988
$5 \times 10^{-2}$	$3 \times 10^{-3}$	$1.45 \times 10^{-1}$	$5.6 \times 10^{-1}$
3	$5 \times 10^{-164}$	$8 \times 10^{-49}$	$8 \times 10^{-16}$

Note:

We have obtained that, for  $\Delta E = 10^{-4}$  eV, the two levels are almost equally populated at all temperatures considered. At  $\Delta E = 5 \times 10^{-2}$  eV, the population of the upper level is already significant at room temperature, so that some molecules are in an excited vibrational state at room temperature. In the case of  $\Delta E = 3$  eV, the population of the upper level is completely negligible. Therefore, at room temperature, most atoms and molecules are in their ground electronic state.

### 1.6A Small-signal gain of a ruby laser amplifier.

The small-signal gain of an active material of length  $l$  is given by:

$$G = \exp\{\sigma[N_2 - (g_2 N_1 / g_1)]/l\} \quad (1)$$

where:  $\sigma$  is the stimulated emission cross section;  $N_1$  and  $N_2$  are the population densities of the lower and upper laser level, respectively, and  $g_1$  and  $g_2$  are the corresponding degeneracies. Since using a 15-cm-long ruby rod the small-signal gain is  $G=12$ , from Eq. (1) one obtains:

$$\sigma[N_2 - (g_2 N_1 / g_1)] = \log G/l = 0.166 \text{ cm}^{-1} \quad (2)$$

Therefore, the small-signal gain of a 20-cm-long rod is:

$$G = \exp(0.166 \cdot 20) = 27.5 \quad (3)$$

### 1.7A Threshold inversion of a laser cavity.

The total logarithmic loss per pass is given by Eq. (1.2.6) of PL:

## ANSWERS

$$\gamma = \gamma_1 + \frac{\gamma_1 + \gamma_2}{2} \quad (1)$$

where  $\gamma_1$ ,  $\gamma_2$  and  $\gamma_i$  are defined by Eqs. (1.2.4) of PL:

$$\gamma_1 = -\ln R_1 = 0 \quad (2a)$$

$$\gamma_2 = -\ln R_2 = 0.693 \quad (2b)$$

$$\gamma_i = -\ln(1 - L_i) = 0.01 \quad (2c)$$

Therefore, one obtains:  $y = 0.357$ . The threshold inversion is given by Eq. (1.2.5) of PL:

$$N_c = \gamma / (\sigma l) = 1.7 \times 10^{17} \text{ cm}^{-3} \quad (3)$$

### 1.8A Temporal evolution of the population densities in a three-level system.

Referring to Fig. 1.1, the rate equations of level 1 and 2 can be written as:

$$\frac{dN_1}{dt} = \frac{N_2}{\tau_2} - \frac{N_1}{\tau_1} \quad (1a)$$

$$\frac{dN_2}{dt} = R_p - \frac{N_2}{\tau_2} \quad (1b)$$

Equation (1b) can be readily solved using the initial condition:  $N_2 = 0$  at  $t = 0$ :

$$N_2(t) = R_p \tau_2 [1 - \exp(-t/\tau_2)] \quad (2)$$

Equation (1a) can obviously be written as:

$$\frac{dN_1}{dt} + \frac{N_1}{\tau_1} = \frac{N_2}{\tau_2} \quad (3)$$

To solve this equation we multiply both sides by the factor  $\exp(t/\tau_1)$ . In this way the left-hand side of Eq. (3) becomes a perfect differential:

$$\frac{d}{dt}[N_1(t)\exp(t/\tau_1)] = \frac{N_2(t)}{\tau_2}\exp(t/\tau_1) \quad (4)$$

Using the initial condition:  $N_1 = 0$  at  $t = 0$ , from Eq. (4) we obtain:

$$N_1(t) = \frac{\exp(-t/\tau_1)}{\tau_2} \int_0^t N_2(t') \exp(-t'/\tau_1) dt' \quad (5)$$

Using the expression for  $N_2(t)$  given by Eq. (2) it is possible to calculate the integral in Eq. (5) as:

$$N_1(t) = R_p \tau_1 \left[ 1 + \frac{\tau_1}{\tau_2 - \tau_1} \exp\left(-\frac{t}{\tau_1}\right) - \frac{\tau_2}{\tau_2 - \tau_1} \exp\left(-\frac{t}{\tau_2}\right) \right] \quad (6)$$

As  $t \rightarrow \infty$ , a steady-state is reached with  $N_1(\infty) = R_p \tau_1$  and  $N_2(\infty) = R_p \tau_2$ . These steady-state populations of levels 1 and 2 could be readily obtained directly from Eqs. (1) by equating to zero the two time derivatives.

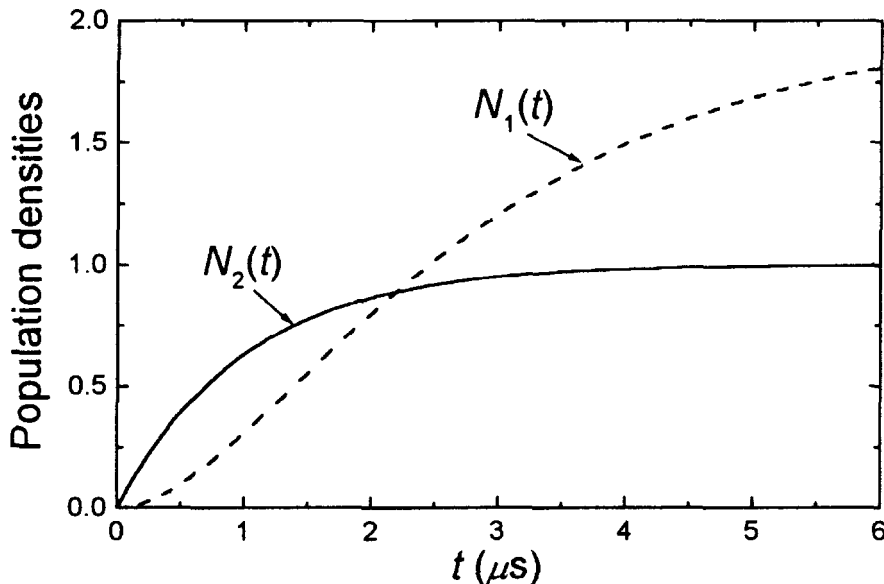


Fig. 1.2 Population densities  $N_1(t)$  and  $N_2(t)$  assuming  $\tau_1 = 2 \mu s$  and  $\tau_2 = 1 \mu s$

The variations with time of the population densities  $N_1(t)$  and  $N_2(t)$  assuming  $\tau_1 = 2 \mu s$  and  $\tau_2 = 1 \mu s$  are shown in Fig. 1.2. In this situation gain ( $N_2 - N_1 > 0$ ) is possible only for the short initial time interval of the order of  $\tau_2$ . Therefore, if such a system is used for a laser, the excitation must be in the form of a fast rising pulse.

The population densities assuming  $\tau_1 = 1 \mu s$  and  $\tau_2 = 2 \mu s$  are shown in Fig. 1.3.

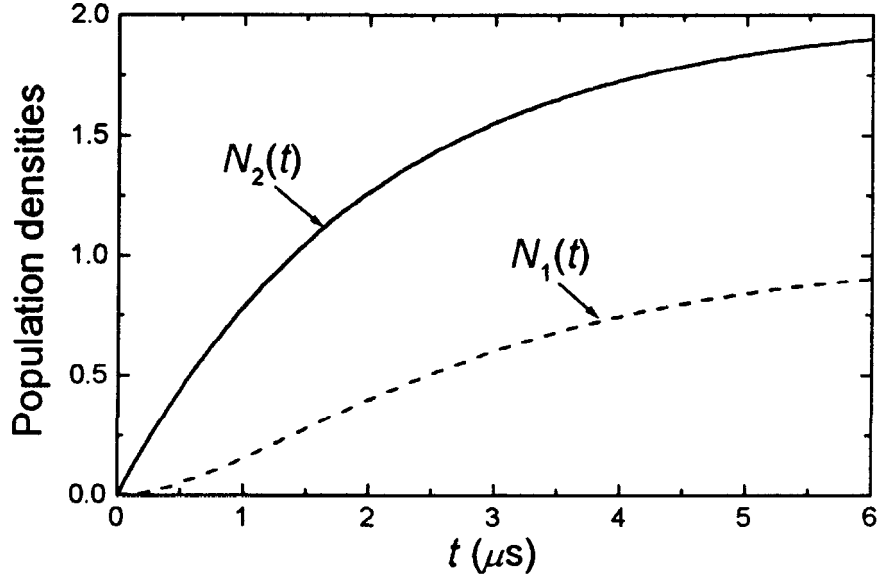


Fig. 1.3 Population densities assuming  $\tau_1 = 1 \mu\text{s}$  and  $\tau_2 = 2 \mu\text{s}$

### 1.9A Brightness of a diffraction limited beam.

The brightness of a given source of **em** waves is defined as the power emitted per unit surface area per unit solid angle. If  $dS$  is the elemental surface area of the source, the power  $dP$  emitted by  $dS$  into the solid angle  $d\Omega$  around a direction making the angle  $\theta$  with respect to the normal to the surface, can be written as [see Eq. (1.4.3) of **PL**]:

$$dP = B \cos \theta dS d\Omega \quad (1)$$

Let us consider a diffraction-limited laser beam of power  $P$ , with a circular cross section of diameter  $D$  and with a divergence  $\theta_d$ . Using Eq. (1) we obtain:

$$P = S \int_0^{\theta_d} B \cos \theta (2\pi \sin \theta) d\theta = \pi B S \int_0^{\theta_d} \sin 2\theta d\theta = \frac{1}{2} \pi B S (1 - \cos 2\theta_d) \quad (2)$$

where the beam cross section  $S$  is given by  $S = \pi D^2/4$ . Since  $\theta_d$  is very small we can use the following approximation:

$$\cos(2\theta_d) \approx 1 - (2\theta_d)^2/2 \quad (3)$$

Using this approximation in Eq. (2) one obtains  $P = \pi B S \theta_d^2$  and therefore:

$$B = \frac{P}{\pi S \theta_d^2} = \left( \frac{2}{\pi D \theta_d} \right)^2 P \quad (4)$$

Using Eq. (1.4.1) of PL, which gives the divergence of a diffraction limited beam as  $\theta_d = \beta \lambda / D$ , we get:

$$B = \left( \frac{2}{\beta \pi \lambda} \right)^2 P \quad (5)$$

### 1.10A Comparison between the brightness of a lamp and that of an argon laser.

Using Eq. (1.4.5) of PL and assuming  $\beta = 1$  we obtain:

$$B = \left( \frac{2}{\beta \pi \lambda} \right)^2 P = 1.53 \times 10^8 \text{ W cm}^{-2} \text{ sr}^{-1}$$

Therefore, the brightness of a 1-W argon laser turns out to be  $\sim 1.6 \times 10^6$  times larger than that of the brightest lamp so far available.

### 1.11A Intensity on the retina of the sun light and of a He-Ne laser beam.

The pupil area of bright-adapted eye is  $A = \pi D^2 / 4 = 3.14 \text{ mm}^2$ . The sun power passing through the pupil is therefore,  $P = 3.14 \text{ mW}$ . Assuming that the focal length of the eye is  $f_E = 22.5 \text{ mm}$  and that the total angle subtended by the Sun is  $\theta_S = 0.5^\circ$ , the image of the Sun on the retina has a diameter  $D_S$ , which can be calculated as follows:

$$D_S = 2 f_E \tan(\theta_S / 2) = 0.2 \text{ mm} \quad (1)$$

Therefore the intensity at the retina resulting when looking directly at the sun is given by:

$$I_S = \frac{4 P}{\pi D_S^2} = 10^5 \text{ W m}^{-2} \quad (2)$$

In the case of a 1-mW He-Ne laser beam ( $\lambda = 632.8 \text{ nm}$ ), the diameter of the spot onto the retina can be calculated as follows:

$$D_L = \frac{4 f_E \lambda}{\pi D_0} = 9 \mu\text{m} \quad (3)$$

This results in an intensity at the retina given by:

$$I_L = \frac{4 P_L}{\pi D_L^2} = 1.6 \times 10^7 \text{ W m}^{-2} \quad (4)$$

that is 160 times the intensity resulting when looking directly at the sun. Therefore extreme caution must be used in working with any type of laser.

### 1.12A Power spectrum of a wave-train of finite duration.

The Fourier transform of the function  $f(t)$  is given by:

$$\begin{aligned} g(\nu) &= \int_{-\infty}^{+\infty} f(t) \exp(-i 2 \pi \nu t) dt = \int_{-\tau_0/2}^{\tau_0/2} \exp[-i 2 \pi (\nu - \nu_0) t] dt = \\ &= \frac{\sin[\pi(\nu - \nu_0)\tau_0]}{\pi(\nu - \nu_0)} \end{aligned} \quad (1)$$

The power **spectrum**  $G(\nu) = |g(\nu)|^2$  is given by:

$$G(\nu) = \frac{\sin^2[\pi(\nu - \nu_0)\tau_0]}{n^2(\nu - \nu_0)^2} \quad (2)$$

Figure 1.4 shows the calculated power spectrum. We see that the spectral distribution is maximum at  $\nu = \nu_0$ , where  $G(\nu_0) = \tau_0^2$ , and drops to zero for  $\nu = \nu_0 \pm 1/\tau_0$ . One therefore sees that as  $\tau_0$  increases the peak value of the power spectrum becomes larger and its width narrower. As clearly shown in Fig. 1.4 most of the spectrum is contained in the frequency region between the first two minima on either side of the central maximum at  $\nu = \nu_0$ . Since the width  $\Delta\nu_0$  (FWHM) of  $G(\nu)$  is approximately equal to the frequency separation between the first minimum and the central maximum we have:  $\Delta\nu_0 = 1/\tau_0$ .

Note:

In the case of a sinusoidal electric field undergoing phase jumps at time intervals equal to  $\tau_0$ , the power spectrum is the same as that of the wave train given above. In this case the wave is said to have partial temporal coherence,

with a coherence time equal to  $\tau_0$ . Moreover, it is possible to demonstrate that any stationary em wave with coherence time  $\tau_0$  has a bandwidth  $\Delta\nu_0 \cong 1/\tau_0$ .

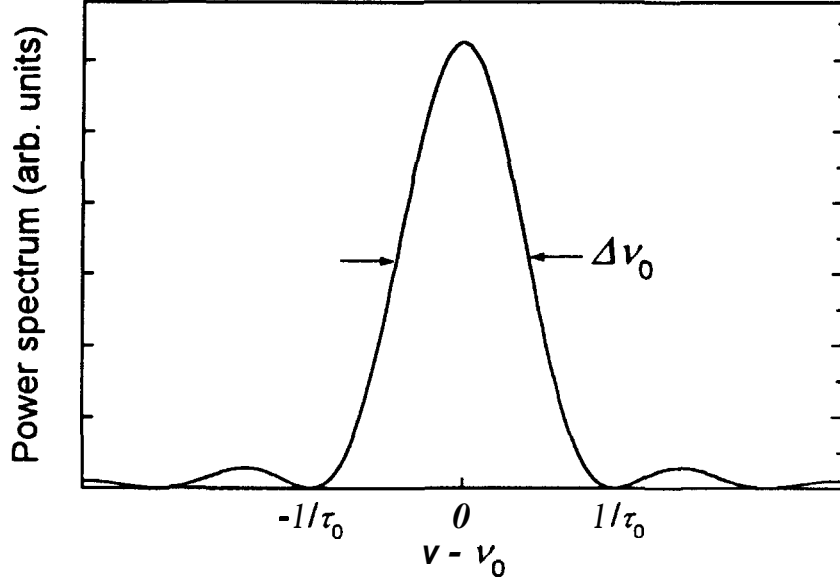


Fig. 1.4 Power spectrum of a single wave train of finite duration  $\tau_0$ .

### 1.13A Coherence time and coherence length of filtered light.

Any stationary em wave with coherence time  $\tau_0$  has a bandwidth  $\Delta\nu_0 \cong 1/\tau_0$ . We now take the reverse argument, namely, if a stationary em wave has a bandwidth  $\Delta\nu_0$  the corresponding coherence time is given by  $\tau_0 \cong 1/\Delta\nu_0$ . Using the relationship,  $\lambda\nu = c$ , between the wavelength of an em wave and its frequency, we obtain:

$$|\Delta\nu| = \frac{c}{\lambda^2} |\Delta\lambda| \quad (1)$$

Then the coherence time of the filtered light is obtained as:

$$\tau_0 \cong \frac{1}{\Delta\nu} = \frac{\lambda^2}{c \Delta\lambda} = 83 \text{ fs} \quad (2)$$

while the coherence length is:

$$l_c = c \tau_0 = \frac{\lambda^2}{\Delta\lambda} = 2.5 \times 10^{-5} \text{ m} \quad (3)$$

### 1.14A Radiation pressure of a laser beam.

The beam intensity is given by  $I = P/\pi w^2$ , where  $P$  is the power and  $w$  is the beam spot size. We thus get:

$$I = \frac{P}{\pi w^2} = 1.27 \times 10^{13} \text{ W m}^{-2} \quad (1)$$

The radiation pressure is then given by:

$$p = \frac{I}{c} = 4.2 \times 10^4 \text{ Pa} = 0.42 \text{ bar} \quad (2)$$

Note that **the radiation** pressure is comparable, in **this** case, to atmospheric pressure.

### 1.15A Radiation pressure.

Assuming that total **momentum** is conserved, a photon **must** transfer its **momentum** to the perfectly absorbing surface. If  $F$  is **the** photon flux (number of photons per unit area per unit time), the total **momentum** transferred to **the** surface  $\Delta S$  in the **time** interval  $\Delta t$  is given by:

$$Q = F q \Delta S \Delta t \quad (1)$$

The force,  $F$ , exerted on  $\Delta S$  by **the** incident photons can be calculated, using the impulse theorem, as  $F \Delta t = Q$ . Therefore the radiation pressure is obtained as:

$$p = \frac{F}{\Delta S} = \frac{Q}{\Delta S \Delta t} = F q = F \frac{h \nu}{c} \quad (2)$$

The intensity,  $I$ , is given by:  $I = F h \nu$ , consequently:  $p = I/c$ .

*Note:*

If the surface is perfectly reflecting, then **the** pressure is twice **the** above value, i.e.,  $p = 2 I/c$ . This is because the **change** of **photon** momentum upon reflection is now  $Aq = q - (-q) = 2q$ . Therefore **each** photon transfers twice as much **momentum** to the surface compared to the case of absorption.

In **the** case the light **beam** is incident on the absorbing surface at angle  $\theta$  the total **momentum transferred** to **the** surface  $\Delta S$  in the **time** interval  $\Delta t$  in **the** direction orthogonal to the surface is:

$$Q = F q (\Delta S \cos \theta) \Delta t \quad (3)$$

Since the pressure is the magnitude of the normal component of the force per unit area we obtain:

$$p = \frac{F \cos \theta}{A S} = F q \cos^2 \theta = \frac{I}{c} \cos^2 \theta \quad (4)$$



## CHAPTER 2

### Interaction of Radiation with Atoms and Ions

### PROBLEMS

#### 2.1P Intensity and energy density of a plane em wave.

Calculate the electric field amplitude and the energy density of a plane wave of intensity  $I=100 \text{ W m}^{-2}$ .

#### 2.2P Photon flux of a plane monochromatic wave.

Calculate the photon flux (photons  $\text{m}^{-2} \text{ s}^{-1}$ ) of a plane monochromatic wave of intensity  $I=200 \text{ W m}^{-2}$  and with a wavelength of either 500 nm or 100  $\mu\text{m}$ .

#### 2.3P Number of modes of a blackbody cavity.

For a cavity volume  $V=1 \text{ cm}^3$  calculate the number of modes that fall within a bandwidth  $\Delta\lambda=10 \text{ nm}$  centred at  $\lambda=600 \text{ nm}$ .

#### 2.4P Wien's law.

Prove Wien's law for blackbody radiation, namely  $\lambda_m T = 2898 \mu\text{m K}$ , where  $\lambda_m$  is the wavelength corresponding to the maximum of the energy density  $\rho_\lambda$  of the blackbody at absolute temperature  $T$ .  $\rho_\lambda$  is such that  $\rho_\lambda d\lambda$  gives the energy density for em waves of wavelengths between  $\lambda$  and  $\lambda+d\lambda$ .

### 2.5P Blackbody cavity filled with a dispersive medium.

Prove that if a black-body cavity is filled with a dispersive medium the radiation mode density,  $p_\nu$ , is given by:  $p_\nu = 8\pi\nu^2 n^2 n_g / c^3$ , where  $n_g$  is the group index given by  $n_g = n + v dn/dv$ . Prove that  $n$ , can also be expressed as  $n_g = n - \lambda dn/d\lambda$ .

### 2.6P Power irradiated by a blackbody emitter.

Calculate the power irradiated from a  $1\text{-mm}^2$  surface of a blackbody emitter at temperature  $T=300$  K (room temperature) over a wavelength interval of  $0.1\text{ }\mu\text{m}$  around the wavelength of  $1\text{ }\mu\text{m}$ .

[Hint: The relationship between the energy density in a blackbody cavity,  $\rho_\nu$ , and the intensity per unit frequency emitted by its walls,  $I_B(\nu)$ , is:  $I_B(\nu) = c \rho_\nu / 4$ ]

### 2.7P Average mode energy.

Prove that the average energy,  $\langle E \rangle$ , contained in each mode of a cavity is given by the relation (2.2.21) of PL:  $\langle E \rangle = h\nu [\exp(h\nu/kT) - 1]$ .

[Hint:  $\sum_{n=0}^{\infty} nh\nu \exp(-\frac{nh\nu}{kT}) = -\frac{d}{d(1/kT)} \sum_{n=0}^{\infty} \exp(-\frac{nh\nu}{kT})$ ]

### 2.8P Spontaneous and stimulated emission rates.

For a system in thermal equilibrium calculate the temperature at which the spontaneous and stimulated emission rates are equal for a wavelength of 500 nm, and the wavelength at which these rates are equal at a temperature of 4000 K.

### 2.9P Natural broadening.

Calculate the lineshape function for natural broadening assuming that the electric field of a decaying atom is  $E(t) = E_0 \exp(-t/2\tau_{sp}) \cos(\omega_0 t)$ .

**2.10P Doppler broadening.**

Calculate the Doppler broadened line width for the **488-nm** transition of an argon ion laser, given that the temperature of the discharge is **6000 K** and the atomic mass of argon is **39.95**. Repeat the previous calculation for the **632.8-nm** line of a He-Ne laser, where the temperature of the discharge is about **400 K**. The atomic mass of neon is **20.18**.

**2.11P Temperature of a blackbody with the same energy density of a He-Ne laser.**

The **linewidth** of a He-Ne laser ( $\lambda=632.8 \text{ nm}$ ) is one fifth of the Doppler linewidth. The temperature of the discharge is about **400 K**. **Assume** that the power inside the cavity is **200 mW** and that the cavity mode has a constant diameter of 1 mm, and a uniform intensity. Calculate the temperature of a blackbody, whose energy density at **632.8 nm** is equal to the energy density of the em wave inside **the** laser cavity. **The** atomic mass of neon is **20.18**.

**2.12P Spontaneous lifetime and cross section.**

Find the relation between spontaneous emission lifetime and cross section for a simple atomic transition.

**2.13P Radiative lifetime and quantum yield of the ruby laser transition.**

The  $R_1$  laser transition of ruby has to a good approximation a **Lorentzian** shape of width (**FWHM**) **330 GHz** at room temperature. **The** measured peak transition cross section is  $\sigma=2.5\times10^{-20} \text{ cm}^2$ . Calculate the radiative lifetime (the refractive index is **n=1.76**). Since the observed room temperature lifetime is 3 ms, what is the fluorescence quantum yield ?

**2.14P Radiative lifetime of the strongest transition of the Nd:YAG laser.**

In a Nd:YAG laser the  $^4F_{3/2} \rightarrow ^4I_{11/2}$  transition is the strongest one. The  $1.064\text{-}\mu\text{m}$  transition occurs between the sublevel  $m=2$  of the  $^4F_{3/2}$  level to sublevel  $l=3$  of the  $^4I_{11/2}$  level ( $R_2 \rightarrow Y_3$  transition). The two sublevels are each doubly degenerate. The energy separation between the two sub-levels of the upper state is  $\Delta E = 84 \text{ cm}^{-1}$ ; the fluorescent lifetime of the upper level is  $\tau_2 = 230 \text{ }\mu\text{s}$ ; the fluorescence quantum yield is  $\phi = 0.56$ ; the ratio between the amount of spontaneous radiation on the actual  $1.064\text{-}\mu\text{m}$  laser transition and the total radiative emission from both  $^4F_{3/2}$  sub-levels is 0.135. Calculate the radiative lifetime of the  $R_2 \rightarrow Y_3$  transition.

**2.15P Transient response of a two-level system to an applied signal.**

Suppose that a two-level system has an initial population difference  $\Delta N(0)$  at time  $t=0$ , different from the thermal equilibrium value  $\Delta N^e$ . Assume that a monochromatic em wave of constant intensity,  $I$ , and frequency  $\nu = (E_2 - E_1)/h$  (where  $E_1$  and  $E_2$  are the energy of the lower and upper states respectively) is then turned on at  $t=0$ . Calculate the evolution of the population difference  $\Delta N(t)$ .

**2.16P Gain saturation intensity.**

Prove that the gain saturation intensity in a homogeneous broadened transition is given by:

$$I_s = \frac{h\nu}{\sigma\tau_2} \left[ 1 + \frac{\tau_1}{\tau_2} \left( 1 - \frac{\tau_2}{\tau_{21}} \right) \frac{g_2}{g_1} \right]^{-1}$$

where:  $\tau_1$  and  $\tau_2$  are the lifetimes of the lower and upper states, respectively;  $1/\tau_{21}$  is the decay rate from the upper to the lower state;  $g_1$  and  $g_2$  are the degeneracies of the lower and upper states, respectively.

## 2.17P Population inversion of a homogeneously broadened laser transition

The rate of spontaneous emission,  $A_{21}$ , of a homogeneously broadened laser transition at  $\lambda=10.6 \mu\text{m}$  is  $A_{21}=0.34 \text{ s}^{-1}$ , while its linewidth  $\Delta\nu_0$  is  $\Delta\nu_0=1\text{GHz}$ . The degeneracies of lower and upper level are  $g_1=41$  and  $g_2=43$ , respectively. Calculate the stimulated emission cross section at line center. Calculate the population inversion to obtain a gain coefficient of  $5 \text{ m}^{-1}$ . Also calculate the gain saturation intensity assuming that the lifetime of the upper state is  $10 \mu\text{s}$  and that of the lower state  $0.1 \mu\text{s}$ .

## 2.18P Strongly coupled levels.

Prove relations (2.7.16a-b) of PL:

$$f_{2j} = \frac{N_{2j}}{N_2} = \frac{g_{2j} \exp(-E_{2j}/kT)}{\sum_{m=1}^{g_2} g_{2m} \exp(-E_{2m}/kT)}$$

$$f_{1i} = \frac{N_{1i}}{N_1} = \frac{g_{1i} \exp(-E_{1i}/kT)}{\sum_{m=1}^{g_1} g_{1m} \exp(-E_{1m}/kT)}$$

where:  $f_{2j}(f_{1i})$  is the fraction of total population of level 2 (level 1) that is found in sublevel  $j(i)$  at thermal equilibrium;  $E_{2m}$  and  $E_{1i}$  are sublevel energies in the upper and lower level, respectively, and  $g_{2m}$  and  $g_{1i}$  are their corresponding degeneracies. The upper level, 2, and lower level, 1, consist of  $g_2$  and  $g_1$  sublevels, respectively.

## 2.19P Amplification of a monochromatic em wave.

The homogeneously broadened transition of a 5-cm-long gain medium has an unsaturated gain coefficient at line center of  $g_0=5 \text{ m}^{-1}$  and a saturation intensity of  $5 \text{ W m}^{-2}$ . A monochromatic em wave, resonant with the gain transition, with an intensity of  $10 \text{ W m}^{-2}$  enters the gain medium. Calculate the output intensity.

## 2.20P Amplified Spontaneous Emission in a Nd:YAG rod

A cylindrical rod of Nd:YAG with diameter of 6.3 mm and length of 7.5 cm is pumped very hard by a suitable flashlamp. The peak cross section for the 1.064- $\mu\text{m}$  laser transition is  $\sigma = 2.8 \times 10^{-19} \text{ cm}^2$ , and the refractive index of YAG is  $n=1.82$ . Calculate the critical inversion for the onset of the ASE process (the two rod end faces are assumed to be perfectly antireflection-coated, i.e., nonreflecting). Also calculate the maximum energy that can be stored in the rod if the ASE process is to be avoided.

## 2.21P Saturated absorption coefficient

Instead of observing saturation as in Fig. 2.19 of PL, we can use just the beam  $I(\nu)$  and measure the absorption coefficient for this beam at sufficiently high values of intensity  $I(\nu)$ . For a homogeneous line, show that the absorption coefficient is in this case:

$$\alpha(\nu - \nu_0) = \frac{\alpha_0(0)}{1 + [2(\nu - \nu_0) / \Delta\nu_0]^2 + (I / I_{s0})}$$

where  $\alpha_0(0)$  is the unsaturated ( $I \ll I_{s0}$ ) absorption coefficient at  $\nu = \nu_0$  and  $I_{s0}$  is the saturation intensity, as defined by Eq. (2.8.11) of PL at  $\nu = \nu_0$ :  $I_{s0} = h\nu_0 / 2\sigma\tau$ .

## 2.22P Peak absorption coefficient and linewidth.

From the expression derived in Problem 2.21, find the behavior of the peak absorption coefficient and the linewidth versus  $I$ . How would you measure the saturation intensity  $I_{s0}$ ?

## ANSWERS

### 2.1A Intensity and energy density of a plane em wave.

The intensity of an em wave is the time **average** of the amount of energy that flows per unit time **through** a unit area **perpendicular** to the energy flow. The intensity is thus related to the time average of the Poynting vector,  $S=(E \times B)/\mu$ , where  $E$  and  $B$  are the electric and magnetic fields of the em wave, respectively, and  $\mu$  is the medium permeability. For a plane em wave  $E$  and  $B$  are **perpendicular** to each other and  $B=E/c_n$ , where  $c_n=(\epsilon\mu)^{-1/2}$  is the velocity of light in the medium. We **thus** obtain:

$$I = \langle |S| \rangle = \frac{\langle E^2 \rangle}{c_n \mu} = \epsilon c_n \langle E^2 \rangle = \epsilon_0 c n \langle E^2 \rangle \quad (1)$$

where  $c$  is the velocity of light in vacuum,  $n$  is the refractive index of the medium and  $\epsilon_0$  is the vacuum **permittivity**. Eq.(1) can be rewritten as follows:

$$I = \frac{\langle E^2 \rangle}{Z} = \frac{n}{Z_0} \langle E^2 \rangle \quad (2)$$

where  $Z$  is the medium impedance,  $Z=(\mu/\epsilon)^{1/2}$ , and  $Z_0$  is the vacuum **impedance**:  $Z_0=(\mu_0/\epsilon_0)^{1/2}=377 \Omega$ . In the case of a plane monochromatic em wave we obtain:

$$I = \frac{n E_0^2}{Z_0} \langle \cos^2(\omega t - \mathbf{k} \cdot \mathbf{r}) \rangle = \frac{n E_0^2}{2Z_0} \quad (3)$$

If  $I=100 \text{ W/m}^2$ , from (3) we obtain ( $n=1$ ):

$$E_0 = \sqrt{2 Z_0 I} = 274.6 \text{ V/m} \quad (4)$$

The time average energy density  $\langle \rho \rangle$  of the em wave is:

$$\langle \rho \rangle = \frac{1}{2} \epsilon \langle E^2 \rangle + \frac{1}{2} \mu \langle H^2 \rangle \quad (5)$$

For a plane em wave Eq.(5) becomes:

$$\langle \rho \rangle = \epsilon \langle E^2 \rangle \quad (6)$$

The substitution of (6) into (1), gives:

## ANSWERS

$$\langle \rho \rangle = \frac{nI}{c} \quad (7)$$

For  $I=100 \text{ W/m}^2$  from (7) we obtain:

$$\langle \rho \rangle = 3.3 \times 10^{-7} \text{ J/m}^3 \quad (8)$$

*Note:*

Consider a surface  $S$  perpendicular to the direction of propagation of an em plane wave (see Fig. 2.1). The energy,  $E$ , flowing through  $S$  in the time interval  $\Delta t$  is equal to the energy contained in a cylinder with base  $S$  and height  $l=c\Delta t/n$ . Since  $E=IS\Delta t$ , the energy density is given by:  $\rho=E/(Sl)=nI/c$ , as obtained above.

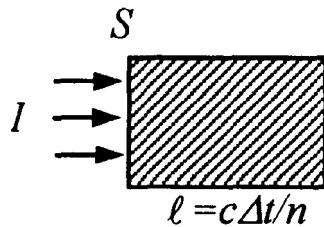


Fig. 2.1 Energy density of an em wave

### 2.2A Photon flux of a plane monochromatic wave.

The photon flux of a plane **monochromatic** wave of intensity  $I$  is given by:

$$F = \frac{I}{h\nu} = \frac{I\lambda}{hc}$$

If  $\lambda=500 \text{ nm}$ , we get:  $F=5\times 10^{20} \text{ ph m}^{-2} \text{ s}^{-1}$

If  $\lambda=100 \mu\text{m}$ , then:  $F=1\times 10^{23} \text{ ph m}^{-2} \text{ s}^{-1}$ .

### 2.3A Number of modes of a blackbody cavity.

The number of modes per unit volume and per unit frequency range is given by (2.2.16) of PL:

$$p_\nu = \frac{1}{V} \frac{dN}{d\nu} = \frac{8\pi\nu^2}{c^3} \quad (1)$$

where we have considered an empty cavity ( $n=1$ ). The number of modes for a cavity volume  $V$  that fall within a frequency bandwidth  $\Delta\nu$  is given by:

$$N \approx p_\nu V |\Delta\nu| \quad (2)$$

where we assume  $p_\nu$  constant over  $\Delta\nu$ . To solve the problem we have to find **the** relationship between  $A_\nu$  and  $\Delta\lambda$ . Since  $\lambda\nu=c$ , we have:

$$\Delta\nu \approx -\frac{c}{\lambda^2} \Delta\lambda \quad (3)$$

Using (1) and (3) in Eq.(2) we finally obtain:

$$N \approx \frac{8\pi}{\lambda^4} V \Delta\lambda = 1.9 \times 10^{12} \quad (4)$$

**Notes:**

(i) Another way to solve **the** problem is to calculate the number of modes per unit volume and per unit wavelength range,  $p_\lambda$ , which is related to  $p_\nu$  by the following relation:

$$p_\lambda d\lambda = -p_\nu d\nu \quad (5)$$

where we use the minus sign because  $d\lambda$  and  $d\nu$  have opposite signs, while  $p_\lambda$  and  $p_\nu$  are both positive. From (5) we get:

$$p_\lambda = -p_\nu \frac{d\nu}{d\lambda} = p_\nu \frac{c}{\lambda^2} \quad (6)$$

Replacing  $p_\nu$  in (6) by the expression given in (1), we obtain:

$$p_\lambda = \frac{8\pi}{\lambda^4} \quad (7)$$

The number of modes falling within the bandwidth  $\Delta\lambda$  for a cavity volume  $V$  is therefore given by:

$$N \approx p_\lambda V \Delta\lambda = \frac{8\pi}{\lambda^4} V \Delta\lambda \quad (8)$$

(ii) Expression (3) can be rewritten in the following compact and **useful** way:

$$\frac{\Delta\nu}{\nu} = -\frac{\Delta\lambda}{\lambda} \quad (9)$$

## ANSWERS

### 2.4A Wien's law.

We define  $\rho_\lambda$  according to the relationship :

$$\rho_\lambda d\lambda = -\rho_\nu d\nu \quad (1)$$

where we use the minus sign because  $d\lambda$  and  $d\nu$  have opposite signs, while  $\rho_\lambda$  and  $\rho_\nu$  are both positive. Since  $\nu=c/\lambda$ , we have:

$$\frac{d\nu}{d\lambda} = -\frac{c}{\lambda^2} \quad (2)$$

from (1) and (2) we get:

$$\rho_\lambda = -\rho_\nu \frac{d\nu}{d\lambda} = \frac{c}{\lambda^2} \rho_\nu \quad (3)$$

Using the expression (2.2.22) of PL for  $\rho_\nu$ , we obtain:

$$\rho_\lambda = \frac{8\pi hc}{\lambda^5} \frac{1}{\exp\left(\frac{hc}{\lambda kT}\right) - 1} \quad (4)$$

To find the maximum of  $\rho_\lambda$ , we first calculate  $d\rho_\lambda/d\lambda$  and equate it to zero. We get:

$$5 \left[ \exp\left(\frac{hc}{\lambda kT}\right) - 1 \right] = \frac{hc}{\lambda kT} \text{ ex~[\%]} \quad (5)$$

Taking  $y = (hc/\lambda kT)$ , Eq.(5) can be rewritten as:

$$5[1 - \exp(-y)] = y \quad (6)$$

This is a transcendental equation, which can be solved by successive approximations. Since we expect that  $(hc/\lambda kT) = h\nu/kT \gg 1$ , we also expect that  $\exp(-y) \ll 1$ . As a first guess we can then assume  $y=5$ . Substituting this value in the left hand side of Eq.(6) we obtain  $y=4.966$ . Proceeding in the same way we rapidly obtain the solution of Eq.(6):  $y=4.9651$ . We thus obtain:

$$\frac{hc}{kT\lambda_m} = 4.9651 \quad (7)$$

which can be written in the following form:

$$\lambda_m T = 2898 \mu\text{m K} \quad (8)$$

which is the Wien's law.

Note:

The iterative procedure to find the point of intersection between two functions, converges if we start with the function with the smaller slope near the point of intersection. Consider, for example, two functions  $f(x)$  and  $g(x)$  (see Fig.(2.2)).  $g(x)$  has the smaller slope near the intersection point. First we calculate  $g(x_0)$ , where  $x_0$  is the guessed solution. Then we solve the equation  $f(x) = g(x_0)$  and we find the next order solution  $x=x_1$ . Then we calculate  $g(x_1)$  and we proceed as before. In this way we generally have a fast convergence of the solution.

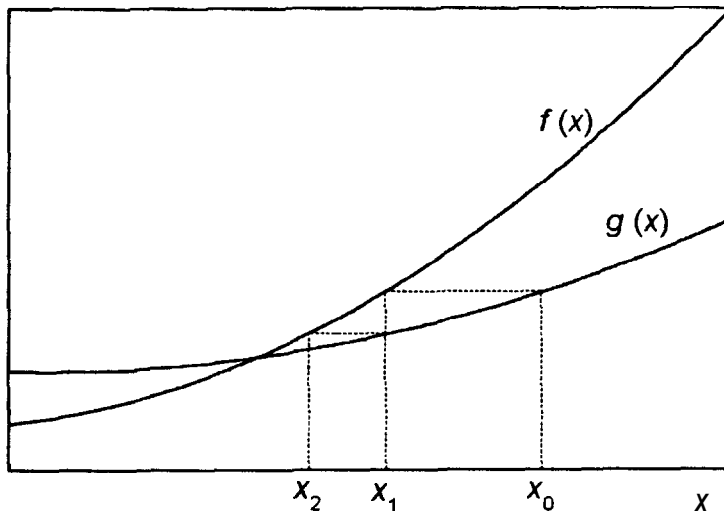


Fig. 22 Iterative procedure to find the intersection between two functions.

### 2.5A Blackbody cavity filled with a dispersive medium.

The number of modes per unit volume and per unit frequency range (radiation mode density) is given by (2.2.16) of PL:

$$p_\nu = \frac{1}{V} \frac{dN(\nu)}{d\nu} \quad (1)$$

where  $N(\nu)$  is the number of resonant modes with frequency between 0 and  $\nu$ . According to (2.2.15) of PL it is given by:

$$N(\nu) = \frac{8\pi\nu^3}{3c_n^3}V = \frac{8\pi\nu^3n^3}{3c^3}V \quad (2)$$

where  $c$  is the velocity of light in vacuum and  $n = n(\nu)$  is the refractive **index** of the dispersive **medium** filling **the** blackbody cavity. Using Eq.(2) in (1), we obtain:

$$p_\nu = \frac{8\pi}{3c^3} \frac{d}{d\nu} [\nu^3 n^3(\nu)] = \frac{8\pi}{c^3} \nu^2 n^2 \left( n + \nu \frac{dn}{d\nu} \right) = \frac{8\pi\nu^2 n^2 n_g}{c^3} \quad (3)$$

Since

$$\frac{dn}{d\nu} = \frac{d\lambda}{d\nu} \frac{dn}{d\lambda} = -\frac{c}{\nu^2} \frac{dn}{d\lambda} = -\frac{\lambda^2}{c} \frac{dn}{d\lambda} \quad (4)$$

the group **index**  $n_g$  can also be expressed as follows:

$$n_g = n + \nu \frac{dn}{d\nu} = n + \frac{c}{\lambda} \left( -\frac{\lambda^2}{c} \frac{dn}{d\lambda} \right) = n - \lambda \frac{dn}{d\lambda} \quad (5)$$

#### *Notes:*

- i) If **the** refractive **index** does not significantly vary **with** wavelength in a given spectral region, we can assume  $n_g \approx n$ .
- ii) Material dispersion is due to **the** wavelength dependence of the refractive index of **the** material. Given a homogeneous medium, such as a piece of glass or an optical fiber, characterized by a dispersion relation  $\beta = \beta(\omega)$ , the group velocity is given by  $v_g = d\omega/d\beta = (d\beta/d\omega)^{-1}$ . where  $\omega = 2\pi\nu$  and  $\beta = \nu n/c$ . Thus we have:

$$\frac{d\beta}{d\omega} = \frac{1}{c} \left[ n + \omega \frac{dn}{d\omega} \right] = \frac{1}{c} \left[ n + \nu \frac{dn}{d\nu} \right] = \frac{n_g}{c} \quad (6)$$

Therefore we obtain  $v_g = c/n_g$ .

## 2.6A Power irradiated by a blackbody emitter.

The relationship **between** the energy density in a blackbody cavity,  $\rho_\nu$ , and the intensity per unit frequency **emitted** by its walls,  $I_B(\nu)$ , is:

$$I_B(\nu) = \frac{c}{4} \rho_\nu \quad (1)$$

Assuming  $\rho_\nu$  constant over the frequency interval  $A\nu$  around the frequency  $\nu_0$  the power irradiated from a surface  $S$  of the blackbody emitter over  $A\nu$  is given by:

$$P = \frac{c}{4} \rho_{\nu_0} |\Delta\nu| S \quad (2)$$

Since  $|\Delta\nu| = \frac{c}{\lambda_0^2} |\Delta\lambda|$ , from Eq.(2) we obtain:

$$P = 5.3 \times 10^{-20} \text{ W}$$

## 2.7A Average mode energy.

The average energy of a mode is given by (2.2.21) of PL:

$$\langle E \rangle = \frac{\sum_{n=0}^{\infty} n h \nu \exp(-n h \nu / kT)}{\sum_{n=0}^{\infty} \exp(-n h \nu / kT)} \quad (1)$$

The denominator of Eq.(1) is a geometric series whose sum is:

$$\sum_{n=0}^{\infty} \exp(-n h \nu / kT) = \frac{1}{1 - \exp(-h \nu / kT)} \quad (2)$$

Taking the derivative of both sides of Eq.(2) with respect to  $(1/kT)$  we obtain:

$$\sum_{n=0}^{\infty} n h \nu \exp(-n h \nu / kT) = \frac{h \nu \exp(-h \nu / kT)}{[1 - \exp(-h \nu / kT)]^2} \quad (3)$$

The substitution of Eqs.(3) and (2) in the right-hand side of Eq.(1) leads to:

$$\langle E \rangle = \frac{h \nu}{\exp(h \nu / kT) - 1} \quad (4)$$

## 2.8A Spontaneous and stimulated emission rates.

The ratio of the rate of spontaneous emission, A, to the rate of stimulated emission, W, is given by:

$$R = \frac{A}{W} = \frac{A}{B\rho_{\nu_0}} \quad (1)$$

Where A and B are the Einstein coefficients, whose ratio is given by (2.4.42) of PL:

$$\frac{A}{B} = \frac{8\pi h\nu_0^3 n^3}{c^3} \quad (2)$$

Using the **Planck** formula (2.2.22) of PL for the energy density,  $\rho_{\nu_0}$ , in (1), we obtain:

$$R = \exp\left(\frac{h\nu}{kT}\right) - 1 = \exp\left(\frac{hc}{kT\lambda}\right) - 1 \quad (3)$$

The temperature at which R = 1 is thus given by:

$$T = \frac{hc}{k\lambda \ln 2} \quad (4)$$

Assuming  $\lambda = 500$  nm we obtain T = 41562 K.

Assuming T = 4000 K the wavelength at which R = 1 is given by:

$$\lambda = \frac{hc}{kT \ln 2} = 5.2 \text{ } \mu\text{m} \quad (5)$$

## 2.9A Natural broadening.

The natural or intrinsic broadening originates from spontaneous emission. Using quantum electrodynamics theory of spontaneous emission it is possible to show that the corresponding spectrum  $g(\nu - \nu_0)$  is described by a **Lorentzian** line characterized by a width (FWHM) given by:

$$\Delta\nu_0 = \frac{1}{2\pi\tau_{sp}} \quad (1)$$

To justify this result we can note that, since the power emitted by the atom decays as  $\exp(-t/\tau_{sp})$ , the corresponding electric field can be thought as decaying according to the relationship:

$$E(t) = E_0 \exp\left(-\frac{t}{2\tau_{sp}}\right) \cos(\omega_0 t) \quad (2)$$

valid for  $t \geq 0$  (for  $t < 0$   $E(t) = 0$ ).

To calculate the frequency distribution of this signal we take its Fourier transform:

$$E(\omega) = \frac{1}{2\pi} \int_{-\infty}^{+\infty} E(t) \exp(-i\omega t) dt \quad (3)$$

Using (2) in (3), we obtain:

$$\begin{aligned} E(\omega) &= \frac{E_0}{4\pi} \int_0^{+\infty} [e^{\left[i(\omega_0 - \omega) - \frac{1}{2\tau_{sp}}\right]t} + e^{-\left[i(\omega_0 + \omega) + \frac{1}{2\tau_{sp}}\right]t}] dt = \\ &= \frac{E_0}{4\pi} \left[ \frac{1}{i(\omega_0 + \omega) + \frac{1}{2\tau_{sp}}} - \frac{1}{i(\omega_0 - \omega) - \frac{1}{2\tau_{sp}}} \right] = \\ &= \frac{E_0}{2\pi} \frac{\frac{1}{2\tau_{sp}} + i\omega}{\omega_0^2 - \omega^2 + \left(\frac{1}{2\tau_{sp}}\right)^2 + i\frac{\omega}{\tau_{sp}}} \end{aligned} \quad (4)$$

The power spectrum is  $S(\omega) = |E(\omega)|^2 = E(\omega) \cdot E^*(\omega)$ :

$$S(\omega) = \frac{E_0^2}{4\pi^2} \frac{\omega^2 + \left(\frac{1}{2\tau_{sp}}\right)^2}{\left[\omega_0^2 - \omega^2 + \left(\frac{1}{2\tau_{sp}}\right)^2\right]^2 + \left(\frac{\omega}{\tau_{sp}}\right)^2} \quad (5)$$

Eq. (5) can be simplified making a few approximations. We can expect that  $S(\omega)$  is strongly peaked around  $\omega = \omega_0$  so that we can write  $\omega + \omega_0 \approx 2\omega_0$ . Furthermore we neglect  $(1/2\tau_{sp})^2$  with respect to  $\omega^2$  and  $\omega_0^2$ . We thus obtain:

$$\frac{4\pi^2}{E_0^2} S(\omega) = \frac{\omega_0^2}{(\omega_0 - \omega)^2 (\omega_0 + \omega)^2 + \left(\frac{\omega}{\tau_{sp}}\right)^2} = \frac{1}{4} \frac{1}{(\omega_0 - \omega)^2 + \left(\frac{1}{2\tau_{sp}}\right)^2} \quad (6)$$

Equation (6) is usually expressed in terms of frequency as:

$$S(\nu) = \frac{A}{(\nu - \nu_0)^2 + \left(\frac{1}{4\pi\tau_{sp}}\right)^2} \quad (7)$$

where A is a constant. The full width half maximum (FWHM),  $\Delta\nu_0$ , of this function can be found from Eq.(7) as:

$$\Delta\nu_0 = \frac{1}{2\pi\tau_{sp}} \quad (8)$$

Eq.(7) can then be written as follows:

$$S(\nu) = \frac{A}{(\nu - \nu_0)^2 + (\Delta\nu_0/2)^2} \quad (9)$$

The line shape function  $g(\nu)$  can be taken proportional to  $S(\nu)$  and hence be written as:

$$g(\nu) = \frac{B}{(\nu - \nu_0)^2 + (\Delta\nu_0/2)^2} \quad (10)$$

where the constant B is obtained from the normalization condition:

$$\int_{-\infty}^{+\infty} g(\nu) d\nu = 1 \quad (11)$$

Using Eq.(10) in Eq.(11) we get:

$$\begin{aligned} \int_{-\infty}^{+\infty} \frac{B}{(\nu - \nu_0)^2 + (\Delta\nu_0/2)^2} d\nu &= B \left( \frac{2}{\Delta\nu_0} \right)^2 \int_{-\infty}^{+\infty} \frac{1}{1 + \left[ \frac{2(\nu - \nu_0)}{\Delta\nu_0} \right]^2} d\nu = \\ &= B \frac{2}{\Delta\nu_0} \int_{-\infty}^{+\infty} \frac{1}{1 + x^2} dx = \frac{2B}{\Delta\nu_0} \tan^{-1} x \Big|_{-\infty}^{+\infty} = \frac{2B\pi}{\Delta\nu_0} = 1 \end{aligned}$$

## 2. INTERACTION OF RADIATION...

Thus we obtain  $B = \Delta\nu_0/2\pi$  and from Eq.(10):

$$g(\nu) = \frac{\Delta\nu_0}{2\pi[(\nu - \nu_0)^2 + (\Delta\nu_0/2)^2]} = \frac{(2/\pi\Delta\nu_0)}{1 + [2(\nu - \nu_0)/\Delta\nu_0]^2} \quad (12)$$

Which is a **Lorentzian** function. Since natural broadening is the same for each emitting atom it is a homogenous **broadening** mechanism.

Note:

The uncertainty in the energy **can** be obtained **from** (8) as:  $\Delta E = h \Delta\nu_0 = h/(2\pi\tau_{sp})$ , so that we have  $\Delta E \tau_{sp} = \hbar$ , in agreement with the Heisenberg principle.

### 2.10A Doppler broadening.

The Doppler linewidth is given by (2.5.18)of PL:

$$\Delta\nu_0^* = 2\nu_0 \left( \frac{2kT \ln 2}{Mc^2} \right)^{1/2} \quad (1)$$

The argon atom mass is :  $M = 39.95 \text{ amu}$ , where  $1 \text{ amu} = 1.66 \times 10^{-27} \text{ kg}$  is the atomic mass unit. Since  $\nu_0 = c/\lambda_0$ , where  $\lambda_0 = 488 \text{ nm}$ , and  $T = 6000 \text{ K}$ , from Eq.(1) we obtain:

$$\Delta\nu_0^* = 5.39 \text{ GHz}$$

In the case of the He-Ne laser we have:  $M_{He} = 20.18 \text{ amu}$ ,  $\lambda_0 = 632.8 \text{ nm}$ ,  $T = 400 \text{ K}$ , so that the Doppler linewidth is:

$$\Delta\nu_0^* = 1.5 \text{ GHz}$$

### 2.11A Temperature of a blackbody with the same energy density of a He-Ne laser.

Using the result of the previous problem, we have that the Doppler linewidth of the He-Ne laser is  $\Delta\nu_0^* = 1.5 \text{ GHz}$ . The laser linewidth is thus:

$$\Delta\nu_L = \Delta\nu_0^*/5 = 0.3 \text{ GHz} \quad (1)$$

The energy density,  $\rho$ , inside **the** laser cavity is given by:

$$\rho = 2I/c \quad (2)$$

where  $\mathbf{I}$  is the em wave intensity. The factor 2 appearing in Eq.(2) is due to the fact that a standing em wave is present in the laser cavity. From Eq.(2) we get:

$$\rho = \frac{2P}{\pi r^2 c} = 1.7 \times 10^{-3} \text{ J/m}^3 \quad (3)$$

where  $P$  is the power inside the laser cavity and  $r$  the mode radius. In Eq.(3) we have assumed that the laser beam is uniform over the beam cross section.

The energy density per unit frequency,  $\rho_\nu$ , is given by:

$$\rho_\nu = \frac{\rho}{\Delta\nu_L} \quad (4)$$

The temperature of a blackbody with the same energy density  $\rho_\nu$ , can be obtained from Eq.(2.2.22) of PL

$$T = \frac{h\nu}{k \ln\left(\frac{8\pi h\nu^3}{\rho_\nu c^3} + 1\right)} = 1.97 \times 10^6 \text{ K} \quad (5)$$

## 2.12A Spontaneous lifetime and cross section.

According to (2.4.29) of PL, the transition cross section  $\sigma$  is given by:

$$\sigma = \frac{2\pi^2}{3n\epsilon_0 ch} |\mu|^2 \nu_0 g_t (\nu - \nu_0) \quad (1)$$

The lifetime for spontaneous emission is given by Eq. (2.3.15) of PL:

$$\tau_{sp} = \frac{3h\epsilon_0 c^3}{16\pi^2 \nu_0^3 n |\mu|^2} \quad (2)$$

From (1) and (2) it is possible to obtain a simple relation between  $\sigma$  and  $\tau_{sp}$ , independent of the dipole moment  $\mu$ :

$$\sigma(\nu) = \frac{\lambda_0^2}{8\pi n^2} \frac{g_t(\nu - \nu_0)}{\tau_{sp}} \quad (3)$$

where  $\lambda_0 = c/\nu_0$  is the wavelength (in vacuum) of an e.m. wave whose frequency corresponds to the center of the line.

Equation (3) can be used either to obtain the value of  $a$ , when  $\tau_{sp}$  is known, or the value of  $\tau_{sp}$  when  $a$  is known. If  $\sigma(v)$  is known, to calculate  $\tau_{sp}$  from (3) we multiply both sides by  $d\nu$  and integrate. Since  $\int g_t(v - \nu_0) d\nu = 1$ , we get:

$$\tau_{sp} = \frac{\lambda_0^2}{8\pi n^2} \frac{1}{\int \sigma(\nu) d\nu} \quad (4)$$

### 2.13A Radiative lifetime and quantum yield of the ruby laser transition.

From Eq.(3) in Problem 2.12 we have:

$$\tau_{sp} = \frac{\lambda_0^2}{8\pi n^2} \frac{g_t(\nu - \nu_0)}{\sigma} \quad (1)$$

For a **Lorentzian** lineshape at  $\nu = \nu_0$  we have  $g(0) = (2/\pi A\nu_0)$ . For  $\lambda_0 = 694$  nm, we obtain from Eq.(1) the spontaneous emission lifetime (i.e., the radiative lifetime)

$$\tau_{sp} = \frac{\lambda_0^2}{8\pi n^2} \frac{2}{\pi \Delta\nu_0 \sigma} = 4.78 \text{ ms} \quad (2)$$

According to (2.6.22) of PL, the fluorescence quantum yield  $\phi$  is given by:

$$\phi = \frac{\tau}{\tau_{sp}} = 0.625 \quad (3)$$

### 2.14A Radiative lifetime of the Nd:YAG laser transition.

The number of **atoms** decaying **radiatively** per unit volume and unit time on the actual laser transition is given by:

$$r_{22} = \frac{N_{22}}{\tau_{r,22}} \quad (1)$$

Where  $N_{22}$  is the population of the sublevel **m=2** of the upper laser state, and  $\tau_{r,22}$  is the radiative lifetime of the  $R_2 \rightarrow Y_3$  transition. The total number of atoms decaying radiatively from the two sublevels of the upper state per unit volume and unit time is:

$$r_2 = \frac{N_2}{\tau_{r,2}} \quad (2)$$

where:  $N_2$  and  $\tau_{r,2}$  are the total population and the effective radiative lifetime of the upper level, respectively. Since the ratio between (1) and (2) is equal to 0.135,  $\tau_{r,22}$  is given by:

$$\tau_{r,22} = \frac{N_{22}}{N_2} \frac{\tau_{r,2}}{0.135} = f_{22} \frac{\tau_{r,2}}{0.135} \quad (3)$$

where  $f_{22}$  represents the fraction of the total population found in the sublevel  $m=2$ . Since the two sublevels are each doubly degenerate, then, according to Eq. (2.7.3) of PL, one has:

$$N_{22} = N_{21} \exp\left(-\frac{\Delta E}{kT}\right) \quad (4)$$

where  $\Delta E$  is the energy separation between the two sublevels.  
We then obtain:

$$f_{22} = \frac{N_{22}}{N_{21} + N_{22}} = \frac{1}{1 + \exp\left(-\frac{\Delta E}{kT}\right)} \quad (5)$$

For  $\Delta E = 84 \text{ cm}^{-1}$  and  $kT = 208 \text{ cm}^{-1}$  ( $T = 300 \text{ K}$ ), we obtain  $f_{22} = 0.4$ . The radiative lifetime  $\tau_{r,2}$  is given by:

$$\tau_{r,2} = \frac{\tau_2}{\phi} = \frac{230}{0.56} \mu\text{s} = 410.7 \mu\text{s} \quad (6)$$

where  $\phi$  is the quantum yield. Substituting the calculated values of  $f_{22}$  and  $\tau_{r,2}$  in Eq.(3) we finally obtain:

$$\tau_{r,22} = 1.2 \text{ ms}$$

## 2.15A Transient response of a two-level system to an applied signal.

We consider a two level system, and we assume that the two levels have the same degeneracy ( $g_1=g_2$ ). We suppose that at time  $t=0$  the population difference  $\Delta N(0)=N_1(0)-N_2(0)$  is different from the thermal equilibrium value,  $\Delta N^e=N_1^e-N_2^e$ . A monochromatic em wave with constant intensity  $I$  is then

turned on at  $t=0$ . The rate of change of the upper state population  $N_2$  due to the combined effects of absorption, stimulated emission and spontaneous decay (radiative and **nonradiative**) can be written as:

$$\frac{dN_2}{dt} = W(N_1 - N_2) - \frac{N_2 - N_2^e}{\tau} \quad (1)$$

where  $W=\sigma I/hv$ . The term describing the spontaneous decay takes explicitly into account that, without any applied external signal (**i.e.**, for  $I=0$ ), the population density  $N_2$  relaxes toward the thermal equilibrium value  $N_2^e$ .

We then indicate by  $N_t$  the total population density and by  $\Delta N$  the population difference:

$$N_t = N_1 + N_2 \quad (2)$$

$$\Delta N = N_1 - N_2 \quad (3)$$

Using (2) and (3) in (1) we get:

$$\frac{d\Delta N}{dt} = -2W\Delta N - \frac{\Delta N - (N_t - 2N_2^e)}{\tau} \quad (4)$$

Since **Eqs.(2)** and (3) are valid also at thermal equilibrium, we obtain:

$$\Delta N^e = N_1^e - N_2^e = N_t - 2N_2^e \quad (5)$$

From (4) and (5) we obtain the final form of the rate equation for the population difference  $\Delta N$ :

$$\frac{d\Delta N}{dt} = -2W\Delta N - \frac{\Delta N - \Delta N^e}{\tau} \quad (6)$$

which can be easily solved, by variable separation, with the initial condition:  $\Delta N = \Delta N(0)$  at  $t=0$ . We obtain:

$$\Delta N(t) = \frac{\Delta N^e}{1+2W\tau} + \left[ \Delta N(0) - \frac{\Delta N^e}{1+2W\tau} \right] \exp\left(-\frac{1+2W\tau}{\tau}t\right) \quad (7)$$

**From (7)** we see that, with no applied signal (**i.e.**, when  $I=0$ , and hence  $W=0$ ), the population difference  $\Delta N(t)$  relaxes from the initial value  $\Delta N(0)$  toward the thermal **equilibrium** value  $\Delta N^e$  with the exponential time constant  $\tau$ . In the presence of an em wave of constant intensity  $I$ , the population difference  $\Delta N(t)$  is driven toward a steady-state value  $\Delta N_\infty$  given by:

## ANSWERS

$$\Delta N_{\infty} = \frac{\Delta N^e}{1+2W\tau} = \frac{\Delta N^e}{1+\frac{2\sigma\tau}{h\nu}I} = \frac{\Delta N^e}{1+\frac{I}{I_s}} \quad (8)$$

where  $I_s = (h\nu/2\sigma\tau)$  is the saturation intensity. The time constant,  $\tau'$ , by which this equilibrium is reached is seen from Eq.(7) to be given by:

$$\tau' = \frac{\tau}{1+I/I_s} \quad (9)$$

and it decreases upon increasing  $I$ .

Note that, from Eq.(8), it is apparent that  $\Delta N_{\infty} < \Delta N^e$ . Using (8) and (9), Eq.(7) can be rewritten in the following more compact form:

$$\Delta N(t) = \Delta N_{\infty} + [\Delta N(0) - \Delta N_{\infty}] \exp\left(-\frac{t}{\tau'}\right) \quad (10)$$

Figure 2.3 shows the temporal behavior of  $\Delta N(t)$  for different values of the normalized intensity,  $I/I_s$ .

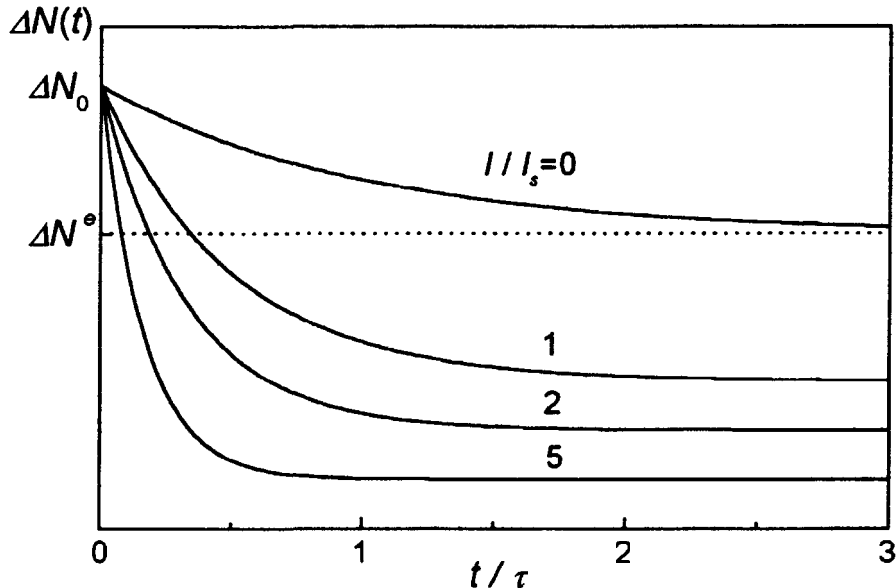


Fig. 2.3 Temporal evolution of the population difference  $\Delta N(t)$  for different values of the normalized intensity  $I/I_s$ .

## 2, INTERACTION OF RADIATION..

### 2.16A Gain saturation intensity.

We consider the case where the transition  $2 \rightarrow 1$  exhibits net gain. We assume that the medium behaves as a four-level system (see Fig.2.4), and the inversion between levels 2 and 1 is produced by some suitable pumping process.

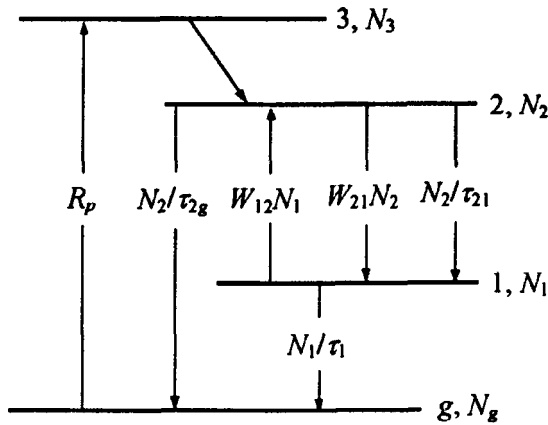


Fig. 24 Energy levels and transitions involved in gain saturation of a four-level laser.

We further assume that transition  $3 \rightarrow 2$  is so rapid that we can set  $N_3 \approx 0$ . We denote by  $1/\tau_{21}$  and  $1/\tau_{2g}$  the decay rates (radiative and nonradiative) of the transitions  $2 \rightarrow 1$  and  $2 \rightarrow g$ , respectively, where  $g$  denotes the ground state. The total decay rate of level 2 is thus given by:

$$\frac{1}{\tau_2} = \frac{1}{\tau_{21}} + \frac{1}{\tau_{2g}} \quad (1)$$

With these assumptions, we can write the following rate equations for the populations of levels 1 and 2:

$$\begin{aligned} \frac{dN_2}{dt} &= R_p - \frac{N_2}{\tau_2} - W_{21}N_2 + W_{12}N_1 \\ \frac{dN_1}{dt} &= \frac{N_2}{\tau_{21}} - \frac{N_1}{\tau_1} + W_{21}N_2 - W_{12}N_1 \end{aligned} \quad (2)$$

where  $R_p$  is the pumping rate. In Eq.(2) we have [Eq.(1.1.8) of PL]:

$$W_{12} = \frac{g_2}{g_1} W_{21} \quad (3)$$

where:  $g_1$  and  $g_2$  are the degeneracies of the levels 1 and 2, respectively.  
Eqs.(2) can thus be written as follows:

$$\begin{aligned}\frac{dN_2}{dt} &= R_p - \frac{N_2}{\tau_2} - W_{21} \left( N_2 - \frac{g_2}{g_1} N_1 \right) \\ \frac{dN_1}{dt} &= \frac{N_2}{\tau_{21}} - \frac{N_1}{\tau_1} + W_{21} \left( N_2 - \frac{g_2}{g_1} N_1 \right)\end{aligned}\quad (4)$$

In the steady state (i.e., for  $dN_1/dt=dN_2/dt=0$ ) Eqs.(4) reduce to a simple system:

$$\begin{aligned}\left( \frac{1}{\tau_2} + W_{21} \right) N_2 - W_{21} \frac{g_2}{g_1} N_1 &= R_p \\ \left( \frac{1}{\tau_{21}} + W_{21} \right) N_2 - \left( W_{21} \frac{g_2}{g_1} + \frac{1}{\tau_1} \right) N_1 &= 0\end{aligned}\quad (5)$$

Using Cramer's rule to solve this system we get:

$$\begin{aligned}N_2 &= -\frac{R_p}{\Delta} \left( \frac{g_2}{g_1} W_{21} + \frac{1}{\tau_1} \right) \\ N_1 &= -\frac{R_p}{\Delta} \left( \frac{1}{\tau_{21}} + W_{21} \right)\end{aligned}\quad (6)$$

where A is the determinant of the ~~matrix~~ of coefficients of the system (5):

$$\Delta = \frac{1}{\tau_1} - \frac{1}{\tau_2} + \frac{1}{\tau_2} \frac{g_2}{g_1} - \frac{1}{\tau_{21}} \frac{g_2}{g_1} W_{21} \quad (7)$$

From (6) the population inversion can be written as follows:

$$N_2 - \frac{g_2}{g_1} N_1 = \frac{R_p \tau_2 \left( 1 - \frac{g_2}{g_1} \frac{\tau_1}{\tau_{21}} \right)}{1 + \left( \tau_1 \frac{g_2}{g_1} + \tau_2 - \frac{\tau_1 \tau_2}{\tau_{21}} \frac{g_2}{g_1} \right) W_{21}} \quad (8)$$

Since  $W_{21}=\sigma_{21} F = \sigma_{21} I/h\nu$ , Eq.(8) can be rewritten as follows:

$$N_2 - \frac{g_2}{g_1} N_1 = \frac{\Delta N_0}{1 + \frac{I}{\sigma}} \quad (9)$$

where  $A N_0 \equiv \left( N_2 - \frac{g_2}{g_1} N_1 \right)_0 = R_p \tau_2 \left( 1 - \frac{g_2}{g_1} \frac{\tau_1}{\tau_{21}} \right)$  is the population inversion in the absence of the saturating beam (i.e., for  $I=0$ ) and:

$$I_s = \frac{h\nu}{\sigma\tau_2} \frac{1}{1 + \frac{\tau_1}{\tau_2} \frac{g_2}{g_1} \left( 1 - \frac{\tau_2}{\tau_{21}} \right)} \quad (10)$$

is the gain saturation intensity [in (10)  $\sigma=\sigma_{21}$ ]. From (10) it is apparent that if  $\tau_1 \ll \tau_2$ , or  $\tau_2 \approx \tau_{21}$ , or  $g_2 \ll g_1$  or any combination of the previous conditions, then the saturation intensity can be approximated as follows:

$$I_s \approx \frac{h\nu}{\sigma\tau_2} \quad (11)$$

## 2.17A Population inversion of a homogeneously broadened laser transition

As shown in Problem 2.12, the stimulated emission cross section  $\sigma(\nu)$  is given by:

$$\sigma(\nu) = \frac{\lambda_0^2}{8\pi n^2} \frac{g_t(\nu - \nu_0)}{\tau_{sp}} = A_{21} \frac{\lambda_0^2}{8\pi n^2} g_t(\Delta\nu) \quad (1)$$

The cross section at line center is thus given by:

$$\sigma(0) = A_{21} \frac{\lambda_0^2}{8\pi n^2} g_t(0) \quad (2)$$

For a **Lorentzian** lineshape (homogeneous broadening) at  $\Delta\nu=0$  we have [see (2.4.9b) of PL]:

$$g_t(0) = g(0) = \frac{2}{\pi \Delta\nu_0} \quad (3)$$

Assuming  $n=1$  we get:

$$\sigma(0) = A_{21} \frac{\lambda_0^2}{8\pi} \frac{2}{\pi \Delta\nu_0} = 9.68 \times 10^{-22} \text{ m}^2 \quad (4)$$

The gain coefficient at line center is given by (2.7.14) of PL:

$$g = \sigma \left( N_2 - N_1 \frac{g_2}{g_1} \right) = 5 \text{ m}^{-1} \quad (5)$$

The population inversion is thus given by:

$$N_2 - N_1 \frac{g_2}{g_1} = \frac{g}{\sigma} = 5.16 \times 10^{21} \text{ m}^{-3} \quad (6)$$

The gain saturation intensity is given by (11) in Problem 2.16. Since  $\tau_2 \gg \tau_1$  and  $g_1 \approx g_2$  we can use Eq.(12) of Problem 2.16:

$$I_s \approx \frac{\hbar\nu}{\sigma\tau_2} = \frac{\hbar c}{\sigma(0)\lambda\tau_2} = 1.9 \text{ MW/m}^2 \quad (7)$$

## 2.18A Strongly coupled levels.

To prove Eq.(2.7.16a) of PL we assume that the upper level, 2, consists of  $g_2$  sublevels with different energies but with very rapid relaxation **among** them. Each sublevel,  $2j$  ( $j=1, 2, \dots, g_2$ ), may also consist of many degenerate levels,  $2jk$  ( $k=1, 2, \dots, g_{2j}$ , where  $g_{2j}$  is the degeneracy of sublevel  $2j$ ). Due to the rapid relaxation, **Boltzmann** statistics can be taken to hold for the population of each individual level. We can then write:

$$N_{2jk} = N_{21i} \exp\left(-\frac{E_{2j} - E_{21}}{kT}\right) \quad (1)$$

where  $N_{2jk}$  is the population of the **degenerate** level  $k$  of the sublevel  $2j$ . Since the degenerate levels of a single sublevel are also in thermal equilibrium, their population must be all equal, thus:

$$N_{2jk} = \frac{N_{2j}}{g_{2j}} \quad (2a)$$

where  $N_{2j}$  is the population of the sublevel  $2j$ . Similarly, for the first sublevel, 21, we have:

$$N_{21i} = \frac{N_{21}}{g_{21}} \quad (2b)$$

From (2) and (1) we then obtain:

$$N_{2j} = N_{21} \frac{g_{2j}}{g_{21}} \exp\left(-\frac{E_{2j} - E_{21}}{kT}\right) \quad (3)$$

The total population,  $N_2$ , of the upper level is thus given by:

$$N_2 = \sum_{m=1}^{g_2} N_{2m} = \frac{N_{21}}{g_{21}} \exp\left(\frac{E_{21}}{kT}\right) \sum_{m=1}^{g_2} g_{2m} \exp\left(-\frac{E_{2m}}{kT}\right) \quad (4)$$

From (3) and (4) the fraction of total population of level 2 that is found in sublevel  $j$  at thermal equilibrium is thus given by:

$$f_{2j} = \frac{N_{2j}}{N_2} = \frac{g_{2j} \exp(-E_{2j}/kT)}{\sum_{m=1}^{g_2} g_{2m} \exp(-E_{2m}/kT)} \quad (5)$$

The proof of Eq.(2.7.16b) of PL follows a similar argument

## 2.19A Amplification of a monochromatic em wave.

The increase of the photon flux  $F$  for a propagation  $dz$  in the gain medium is given by  $dF = gFdz$ . Since  $F=I/h\nu$ , the corresponding intensity increase,  $dl$ , is:

$$dl = g I dz \quad (1)$$

where  $g$  is the gain coefficient given by (2.8.25) of PL:

$$g = \frac{g_0}{1 + I/I_s} \quad (2)$$

Using (2) in Eq.(1) we obtain:

$$\left( \frac{1}{I} + \frac{1}{I_s} \right) dl = g_0 dz \quad (3)$$

The solution of this equation, with the initial condition  $I=I_0$  for  $z=0$ , is:

$$I = I_0 \exp\left(g_0 l - \frac{I - I_0}{I_s}\right) \quad (4)$$

where  $I$  is the length of the gain medium. Eq.(4) must be solved iteratively. If saturation were negligible the output intensity would be:

$$I = I_0 \exp(g_0 l) = 12.84 \text{ W m}^{-2} \quad (5)$$

Therefore we expect that the solution of **Eq.(4)** is contained in the interval:  $I_0 < I < I_0 \exp(g_o l)$ . Taking into account the note of Problem 2.4, since the function at the left hand side of **Eq.(4)** has the smaller slope around the solution, we take the first-order solution  $I=I_1$  (where  $10 \text{ W m}^{-2} < I_1 < 12.84 \text{ W m}^{-2}$ ) on the left hand side of **Eq.(4)**. We then solve the equation:

$$I_0 \exp\left(g_o l - \frac{I - I_0}{I_s}\right) = I_1 \quad (6)$$

from which we get the solution to second order:

$$I_2 = I_0 - I_s \left( \ln \frac{I_1}{I_0} - g_o l \right) \quad (7)$$

and so on. This iterative procedure then rapidly converges to the value:

$$I = 10.84 \text{ W} \quad (8)$$

## 2.20A Amplified Spontaneous Emission in a Nd:YAG rod.

The single-pass gain for the onset of ASE for a Lorentzian line is given by (2.9.4a) of PL:

$$G = \frac{4\pi^{3/2}}{\phi \Omega} (\ln G)^{1/2} \quad (1)$$

where the emission solid angle  $\Omega$  is given by (2.9.1) of PL:

$$\Omega = \frac{\pi D^2}{4l^2} = 5.5 \times 10^{-3} \text{ sr} \quad (2)$$

Assuming a fluorescence quantum yield  $\phi=1$ , from **Eq.(1)**, using a fast iterative procedure, we obtain:  $G=1.24 \times 10^4$ . Since  $G=\exp[\sigma N_{th} l]$ , where  $N_{th}$  is the threshold inversion for ASE, we get:

$$N_{th} = \frac{\ln G}{\sigma l} = 4.49 \times 10^{18} \text{ cm}^{-3} \quad (3)$$

The **maximum** energy,  $E_m$ , that can be stored in the rod, if the ASE process is to be avoided, is then:

$$E_m = N_{th} \frac{\pi D^2 l}{4} h\nu = 1.96 \text{ J} \quad (4)$$

## 2. INTERACTION OF RADIATION...

### 2.21A Saturated absorption coefficient.

The absorption coefficient,  $\alpha$ , of a homogeneous line is given by (2.8.12) of PL:

$$\alpha(\nu - \nu_0) = \frac{\alpha_0}{1 + I/I_s} \quad (1)$$

where  $\alpha_0$  is the unsaturated absorption coefficient, given by (2.8.13) of PL:

$$\alpha_0 = \frac{2\pi^2}{3n\epsilon_0 ch} |\mu|^2 \nu g(\nu - \nu_0) \Delta N^e = \alpha_0(0) \frac{g(\nu - \nu_0)}{g(0)} \quad (2)$$

In Eq.(2)  $\Delta N^e$  is the population difference,  $N_1 - N_2$ , in the absence of the saturating beam ( $I=0$ ), and thus corresponds to the thermal equilibrium value. Moreover,  $\alpha_0(0)$  is the unsaturated absorption coefficient at  $\nu = \nu_0$ :

$$\alpha_0(0) = \frac{2\pi^2}{3n\epsilon_0 ch} |\mu|^2 \nu_0 g(0) \Delta N^e = \sigma(0) \Delta N^e \quad (3)$$

where  $\sigma(0)$  is the cross section at  $\nu = \nu_0$ .

The saturation intensity,  $I_s$ , is given by (2.8.11) of PL:

$$I_s = \frac{h\nu}{2\sigma\tau} = \frac{h\nu}{2\sigma(0)\tau} \frac{g(0)}{g(\nu - \nu_0)} = I_{s0} \frac{g(0)}{g(\nu - \nu_0)} \quad (4)$$

where  $I_{s0} = h\nu/(2\sigma(0)\tau)$  is the saturation intensity at  $\nu = \nu_0$ . Using (2) and (4) in (1) we obtain:

$$\alpha(\nu - \nu_0) = \frac{\alpha_0(0)}{\frac{g(0)}{g(\nu - \nu_0)} + \frac{I}{I_{s0}}} = \frac{\alpha_0(0)}{1 + \left[ \frac{2(\nu - \nu_0)}{\Delta\nu_0} \right]^2 + \frac{I}{I_{s0}}} \quad (5)$$

### 2.22A Peak absorption coefficient and linewidth.

The peak absorption coefficient is given by Eq.(5) in Problem 2.21 evaluated at  $\nu = \nu_0$ :

$$\alpha(0) = \frac{\alpha_0(0)}{1 + I/I_{s0}} \quad (1)$$

In order to calculate the **linewidth**, we first evaluate the frequency  $\nu'$  corresponding to an absorption coefficient  $\alpha(\nu'-\nu_0)=\alpha(0)/2$ :

$$\frac{\alpha_0(0)}{1 + [2(\nu' - \nu_0) / \Delta\nu_0]^2 + I / I_{s0}} = \frac{\alpha_0(0)}{2(1 + I / I_{s0})} \quad (2)$$

From (2) we obtain:

$$|\nu' - \nu_0| = \frac{\Delta\nu_0}{2} \sqrt{1 + I / I_{s0}} \quad (3)$$

The linewidth is thus given by:

$$\Delta\nu_s = \Delta\nu_0 \sqrt{1 + I / I_{s0}} \quad (4)$$

Therefore, when the intensity  $I$  increases, **the** absorption line still retains its **Lorentzian** shape; its linewidth, however, increases by a factor  $F = \sqrt{1 + I / I_{s0}}$ , while its peak value decreases by  $F^2$ .

It is possible to measure the saturation intensity  $I_{s0}$  by using either Eq.(1) or Eq.(4). In a measurement of the peak absorption coefficient, one first measures the absorption coefficient at low intensity (i.e., at  $I << I_{s0}$ ). In this way one obtains  $\alpha_0(0)$ . Then the absorption coefficient is measured at high intensity,  $I$ , in order to cause saturation. In **this** case one obtains  $\alpha(0)$ . From (1) one then obtains:

$$I_{s0} = \frac{\alpha(0)}{\alpha_0(0) - \alpha(0)} I \quad (5)$$

## CHAPTER 3

# Energy levels, Radiative, and Nonradiative Transitions in Molecules and Semiconductors

## PROBLEMS

### 3.1P Vibrational frequency of a diatomic molecule.

Show that the vibrational frequency of a diatomic molecule consisting of two atoms of masses  $M_1$  and  $M_2$  is  $\nu = (1/2\pi)(k_0/M_r)^{1/2}$ , where  $k_0$  is the constant of the elastic restoring force and  $M_r$  is the so-called reduced mass, such that  $1/M_r = 1/M_1 + 1/M_2$ .

### 3.2P Calculation of the elastic constant of a molecule.

The observed vibrational frequency of iodine ( $I_2$ ) molecule is  $\tilde{\nu} = 213 \text{ cm}^{-1}$ . Knowing the mass of each iodine atom ( $M = 21.08 \cdot 10^{-26} \text{ kg}$ ), calculate the elastic constant of the molecule.

[Hint: use the result of the previous problem]

### 3.3P From the potential energy to the vibrational frequency.

Assume that the electronic energy of a **homonuclear** diatomic molecule is known, either analytically or numerically, as a **function** of the **internuclear distance  $R$** :  $U = U(R)$ . Use **this** expression to calculate the vibrational frequency of the molecule.

### 3.4P The Morse potential energy.

A frequently used empirical expression for the electronic energy curve of diatomic molecules is the so-called Morse potential, given by:

$$U(R) = D_e \{1 - \exp[-\beta(R - R_0)]\}^2$$

Using this expression, find the dissociation energy and calculate the vibrational frequency of a symmetric molecule made of two atoms of mass  $M$ .

### 3.5P Calculation of the Franck-Condon factor.

Consider a vibronic transition and suppose that the energy curves of ground and excited states have the same curvature (corresponding to the same force constant  $k_0$ ) and minima corresponding to two different internuclear separations  $R_{0g}$  and  $R_{0e}$ . Calculate the **Franck-Condon** factor for the transition from the first vibrational level ( $\nu'' = 0$ ) of the ground state to the first vibrational level ( $\nu' = 0$ ) of the excited state.

[Hints: recall that the wavefunction of the lowest energy level of an harmonic oscillator can be written as:

$$\psi_0 = \left( \frac{1}{\alpha \pi^{1/2}} \right)^{1/2} \exp\left(-\frac{y^2}{2}\right)$$

where  $y = R/\alpha$ , the quantity  $\alpha$  being given by  $\alpha = \hbar^{1/2}/(mk)^{1/4}$ , where  $m$  is the oscillator mass and  $k$  is the constant of the elastic restoring force. Use in

addition the following mathematical result:  $\int_{-\infty}^{+\infty} \exp(-x^2) dx = \pi^{1/2}$

*(Level of difficulty higher than average)*

### 3.6P Rotational constant of a diatomic molecule.

Consider the rigid rotation of a diatomic molecule, made of two atoms with masses  $M_1$  and  $M_2$  at an internuclear distance  $R_0$ .

- (a) calculate **the** moment of inertia  $I$  about an axis passing through the center of mass and perpendicular to the internuclear axis;
- (b) recalling the quantization rule of angular momentum,  $L^2 = \hbar^2 J(J+1)$ , with  $J$  positive integer, express the rotational constant  $B$  of the molecule.

### 3.7P Far-infrared absorption spectrum of an HCl molecule.

Measurements of the far-infrared absorption bands of the HCl molecule allow direct access to the pure rotational transitions. Some of the obtained results are as follows:

$\Delta E = 83.32 \text{ cm}^{-1}$  for the  $J = 3 \rightarrow J = 4$  transition;

$\Delta E = 104.13 \text{ cm}^{-1}$  for the  $J = 4 \rightarrow J = 5$  transition;

$\Delta E = 124.73 \text{ cm}^{-1}$  for the  $J = 5 \rightarrow J = 6$  transition.

- Verify the consistency of the measurements and obtain the rotational constant B for the HCl molecule;
- calculate the internuclear distance of the molecule (mass of the hydrogen atom  $m_H = 1 \text{ m}_u$ , mass of the chlorine atom  $m_{Cl} = 35.5 \text{ m}_u$ , where  $m_u = 1.67 \times 10^{-27} \text{ kg}$ ).

### 3.8P The most heavily populated rotational level.

Derive Eq. (3.1.10) in PL giving the quantum number  $J$  of the most heavily populated rotational level of a given vibrational level. From this expression calculate the most heavily populated rotational level of the ICl molecule ( $B = 0.114 \text{ cm}^{-1}$ ) at room temperature.

### 3.9P The emission lines of a CO<sub>2</sub> molecule.

The wavelength of the light emitted from the (001)  $\rightarrow$  (100)  $P(12)$  vibrational-rotational transition in a CO<sub>2</sub> molecule is  $\lambda = 10.5135 \text{ pm}$ , while the wavelength emitted from the (001)  $\rightarrow$  (100)  $P(38)$  transition is  $\lambda = 10.742 \text{ pm}$ .

- calculate the rotational constant B of the CO<sub>2</sub> molecule;
- calculate the energy difference between the (001) and the (100) levels.

### 3.10P The law of mass action.

Consider a semiconductor in thermal equilibrium, with its Fermi level within the **bandgap** but away from its edges by an energy of at least several times  $kT$ . Prove that the product of electron and hole concentrations is constant, independent of the position of the Fermi level (i.e. of the doping level).

[Hint: use the mathematical result:  $\int_0^{\infty} \exp(-x)x^{1/2} dx = \pi^{1/2}/2$ ]

## PROBLEMS

### 3.11P Energies of the quasi-Fermi levels.

Under the **limit** condition  $T = 0$  K, calculate the energies of the **quasi-Fermi** levels in a semiconductor, as a function of the electron and hole densities,  $N_e$  and  $N_h$ .

### 3.12P The quasi-Fermi levels in GaAs.

Using the results of the previous problem, calculate the **quasi-Fermi** levels for GaAs at  $T = 0$  K and for an injected carrier density  $N_e = N_h = 2 \times 10^{18} \text{ cm}^{-3}$  (effective masses in **GaAs** are  $m_e = 0.067 m_0$ ,  $m_h = 0.46 m_0$ ). Evaluate the validity of this approximation for the temperature  $T = 300$  K and compare it to the exact results.

[Hint: use Fig. 3.15(a) in PL for an exact calculation of the **quasi-Fermi** levels].

### 3.13P Derivation of the Bernard-Duraffourg condition.

Prove the **Bernard-Duraffourg** condition for net gain in a bulk semiconductor:  
 $E'_2 - E'_1 < E'_{Fc} - E'_{Fv}$ .

### 3.14P Laser levels in a semiconductor.

Derive an expression of the upper and lower levels in a laser transition in a semiconductor at frequency  $\nu_0$  such that  $h\nu_0 > E_g$ . Use the results to calculate the upper and lower levels in **GaAs** for a transition at 1.45 eV [effective masses in GaAs are  $m_e = 0.067 m_0$ ,  $m_h = 0.46 m_0$ , while **bandgap** energy is  $E_g = 1.424$  eV].

### 3.15P Frequency dependence of the gain of an inverted semiconductor.

Consider an inverted bulk semiconductor.

- Give the analytical expression of the gain as a function of photon energy at  $T=0$  K and find the energy for which the gain is the highest;
- explain qualitatively how these results are expected to be modified at room temperature.

### **3.16P Gain and gain bandwidth calculation in a GaAs amplifier.**

Consider a bulk GaAs semiconductor at room temperature and assume the following expression for the absorption coefficient:

$$\alpha_0(v) = 19760 (hv - E_g)^{1/2}, \text{ where } \alpha_0 \text{ is expressed in cm}^{-1} \text{ and the photon energy } hv \text{ in eV.}$$

Calculate the gain coefficient at a photon energy exceeding the **bandgap** by **10 meV** and for a carrier injection  $N = 2 \times 10^{18} \text{ cm}^{-3}$  (**hint:** use Fig. 3.15(b) in PL to determine the energies of the quasi-Fermi levels). Calculate also the gain bandwidth. Compare the results **with those that** would have been obtained had the semiconductor been cooled to a **temperature** approaching **0 K**.

### **3.17P Differential gain of a GaAs amplifier.**

For a **carrier** injection of  $N = 2 \times 10^{18} \text{ cm}^{-3}$  and a photon energy exceeding the **bandgap** by **10 meV**, the gain **coefficient** of GaAs can be calculated to be  $g = 217 \text{ cm}^{-1}$ . Assuming a transparency density of  $N_{tr} = 1.2 \times 10^{18} \text{ cm}^{-3}$ , calculate **the** differential gain.

### **3.18P Thickness of a quantum well: an order of magnitude estimate.**

Consider a layer of GaAs of **thickness** L sandwiched between two AlGaAs barriers at room temperature ( $T = 300 \text{ K}$ ). Estimate the layer thickness for which quantum confinement effects start to play a role for electrons in the conduction band (effective mass for electrons in the conduction band in GaAs is  $m_c = 0.067 m_0$ ).

[Hint: calculate the De Broglie wavelength for **thermalized** electrons]

### **3.19P An ideal quantum well.**

Consider a particle of **mass** m in a one-dimensional potential well of **thickness** L, with infinite potential barriers at **the** boundaries. Using basic quantum mechanics calculate **the** discrete energy levels inside the well.

**3.20P Energies of the quasi-Fermi levels in a semiconductor quantum well.**

Consider a semiconductor quantum well under non-equilibrium conditions with an injected **carrier** density  $N_e = N_h = N$ . Show in detail how to calculate the energies of the quasi-Fermi levels in the conduction and valence bands, respectively.

*(Level of difficulty higher than average)*

**3.21P Calculation of the gain bandwidth in a GaAs quantum well.**

For a **10-nm** GaAs quantum well at room temperature ( $T = 300$  K) calculate (using Fig. 3.26 in PL) the overall bandwidth of **the** gain curve for an injected carrier density of  $N = 2 \times 10^{18} \text{ cm}^{-3}$ .

## ANSWERS

### 3.1A Vibrational frequency of a diatomic molecule.

Let us consider the two atoms as two masses bound by a spring of elastic constant  $k_0$ . Projecting the equations of motion on an  $x$  axis, we get

$$M_1 \frac{d^2 x_1}{dt^2} = k_0(x_2 - x_1) \quad (1a)$$

$$M_2 \frac{d^2 x_2}{dt^2} = -k_0(x_2 - x_1) \quad (1b)$$

Upon dividing Eqs. (1a) and (1b) by  $M_1$  and  $M_2$ , respectively, and then subtracting the resulting two equations, we get

$$\frac{d^2}{dt^2}(x_2 - x_1) = -k_0 \left( \frac{1}{M_1} + \frac{1}{M_2} \right) (x_2 - x_1) \quad (2)$$

Making the substitution  $y = x_2 - x_1$  and defining the reduced mass  $M_r$  as

$$\frac{1}{M_r} = \frac{1}{M_1} + \frac{1}{M_2} \quad (3)$$

we get the equation

$$\frac{d^2 y}{dt^2} + \frac{k_0}{M_r} y = 0 \quad (4)$$

This is the equation of a **harmonic** oscillator of mass  $M_r$  and elastic constant  $k_0$ . Its vibrational frequency is then given by

$$\nu = \frac{1}{2\pi} \sqrt{\frac{k_0}{M_r}} \quad (5)$$

For the particular case of a homonuclear diatomic molecule ( $M_1 = M_2 = M$ ) the vibrational frequency becomes

$$\nu = \frac{1}{2\pi} \sqrt{\frac{2k_0}{M}} \quad (6)$$

## ANSWERS

### **3.2A Calculation of the elastic constant of a molecule.**

Let us first express the vibrational frequency in Hz. Recalling that

$$\tilde{\nu} = \nu/c = 1/\lambda \quad (1)$$

we obtain

$$\nu = c\tilde{\nu} = 213\text{cm}^{-1} \cdot 3 \times 10^{10} \text{cm/s} = 6.4 \times 10^{12} \text{Hz} \quad (2)$$

Using Eq. (6) of the previous problem, which applies for a homonuclear diatomic molecule, we obtain the elastic constant of the molecule

$$k_0 = 4\pi^2\nu^2 \frac{M}{2} = 170 \frac{\text{N}}{\text{m}} \quad (3)$$

### **3.3A From the potential energy to the vibrational frequency.**

Let  $R_0$  be the equilibrium internuclear distance of the molecule, corresponding to a minimum of the electronic energy. From a second order Taylor expansion of the energy around  $R_0$ , we get

$$U(R) = U(R_0) + \left(\frac{dU}{dR}\right)_{R_0} (R - R_0) + \frac{1}{2} \left(\frac{d^2U}{dR^2}\right)_{R_0} (R - R_0)^2 + \dots \quad (1)$$

If  $R_0$  is a minimum position for the energy, we have  $(dU/dR)_{R_0} = 0$ , so from Eq. (1) we get

$$U(R) = U(R_0) + \frac{1}{2} \left(\frac{d^2U}{dR^2}\right)_{R_0} (R - R_0)^2 \quad (2)$$

Since this expression also gives the potential energy of the oscillator, the restoring force can be calculated as

$$F = -\frac{dU}{dR} = -\left(\frac{d^2U}{dR^2}\right)_{R_0} (R - R_0) \quad (3)$$

and is elastic, i.e. proportional to displacement, with a constant  $k_0 = (d^2U/dR^2)_{R_0}$ . Therefore the vibrational frequency of the molecule is:

$$\nu = \frac{1}{2\pi} \sqrt{\frac{2k_0}{M}} = \frac{1}{2\pi} \sqrt{\frac{2 \left( \frac{d^2 U}{dR^2} \right)_{R_0}}{M}} \quad (4)$$

and can thus be directly calculated from the electronic energy function, known from experiments or from *ab initio* calculations.

*Note:*

Any potential energy function, in the neighbourhood of the *stable* equilibrium position, can be approximated by a parabola: this explains the **importance** of the harmonic oscillator in **physics**.

### 3.4A The Morse potential energy.

It is a simple matter to show that  $R_0$  is a minimum position for the Morse potential energy and that the corresponding energy value is  $U(R_0) = 0$ . For large values of the internuclear distance, the Morse potential tends to its asymptotic value  $U(\infty) = D_e$ ; therefore the dissociation energy, i.e. the energy that must be delivered to the **molecule** to bring its nuclei far apart, is simply given by

$$U(\infty) - U(R_0) = D_e \quad (1)$$

To calculate the vibrational frequency, we can perform a Taylor expansion of the Morse function around  $R_0$ , as in the previous problem; more simply, we can expand the exponential function to the first order around  $R_0$ , getting

$$\exp[-\beta(R - R_0)] \approx 1 - \beta(R - R_0) \quad (2)$$

We can thus express the Morse potential around the equilibrium position as

$$U(R) \approx D_e \beta^2 (R - R_0)^2 = \frac{1}{2} k_0 (R - R_0)^2 \quad (3)$$

with  $k_0 = 2D_e \beta^2$ . The expression of the vibrational frequency for the molecule then follows from Eq. (6) of **problem 3.1**:

$$\nu = \frac{1}{2\pi} \sqrt{\frac{2k_0}{M}} = \frac{1}{2\pi} \sqrt{\frac{4D_e \beta^2}{M}} \quad (4)$$

## ANSWERS

### 3.5A Calculation of the Franck-Condon factor.

Assuming potential energies for ground and excited state with **the** same curvature, we can write the wavefunctions of the lowest vibrational levels in ground and excited states as

$$\psi_{0g} = \left( \frac{1}{\alpha \pi^{1/2}} \right)^{1/2} \exp\left(-\frac{y^2}{2}\right) \quad (1a)$$

$$\psi_{0e} = \left( \frac{1}{\alpha \pi^{1/2}} \right)^{1/2} \exp\left(-\frac{y'^2}{2}\right) \quad (1b)$$

with  $\alpha^2 = \hbar/(mk)^{1/2}$ ,  $y = (R - R_{0g})/\alpha$ ,  $y' = (R - R_{0e})/\alpha$ ,  $R_{0g}$  and  $R_{0e}$  being the equilibrium internuclear separations in the ground and excited state, respectively. It is for us more convenient to write  $y' = y - A$ , with  $A = (R_{0e} - R_{0g})/\alpha$ . To calculate the Franck-Condon factor, we need to evaluate the overlap integral

$$S_{00} = \int_{-\infty}^{+\infty} \psi_{0g}(R) \psi_{0e}(R) dR = \frac{1}{\alpha \pi^{1/2}} \int_{-\infty}^{+\infty} \exp\left[-\frac{y^2}{2}\right] \exp\left[-\frac{(y-A)^2}{2}\right] \alpha dy \quad (2)$$

By some simple mathematical manipulations, this expression can be put in the form

$$S_{00} = \frac{1}{\pi^{1/2}} \exp\left[-\frac{\Delta^2}{4}\right] \int_{-\infty}^{+\infty} \exp\left[-\left(y - \frac{\Delta}{2}\right)^2/2\right] dy \quad (3)$$

By making the additional substitution  $\xi = y - \Delta/2$  and recalling the mathematical result given in the text of **the** problem, we obtain

$$S_{00} = \exp\left[-\frac{\Delta^2}{4}\right] = \exp\left[-\frac{(R_{0e} - R_{0g})^2}{4\alpha^2}\right] \quad (4)$$

The Franck-Condon factor for the given vibronic transition is **then** given by

$$\left| \int_{-\infty}^{+\infty} \psi_{0g}(R) \psi_{0e}(R) dR \right|^2 = S_{00}^2 = \exp\left[-\frac{(R_{0e} - R_{0g})^2}{2\alpha^2}\right] \quad (5)$$

Note that the **Franck-Condon** factor rapidly decreases for increasing **difference** in equilibrium internuclear distances between ground and excited state.

### 3.6A Rotational constant of a diatomic molecule.

Let us first calculate the position of the center of mass of the molecule. Assuming an  $x$  axis oriented along the direction joining the two nuclei and with the origin on the first atom, we get

$$x_{cm} = \frac{M_1 \cdot 0 + M_2 R_0}{M_1 + M_2} = \frac{M_2 R_0}{M_1 + M_2} \quad (1)$$

The moment of inertia about an axis passing through the center of mass and perpendicular to the internuclear axis is then given by

$$I = M_1 x_{cm}^2 + M_2 (R_0 - x_{cm})^2 \quad (2)$$

By inserting Eq. (1) into Eq. (2) and by some **simple** algebraic manipulations, we obtain the expression

$$I = \frac{M_1 M_2}{M_1 + M_2} R_0^2 = M_r R_0^2 \quad (3)$$

where  $M_r = M_1 M_2 / (M_1 + M_2)$  is the reduced mass of the molecule as previously defined in problem 3.1.

According to classical mechanics, the kinetic energy of a rigid body rotating around a given axis can be written as  $E_k = L^2 / 2I$ , where  $L$  is the angular momentum and  $I$  is the moment of inertia about that axis. According to quantum mechanics, the angular momentum is quantized, i.e. it can have only discrete values, given by the quantization rule  $L^2 = \hbar^2 J(J+1)$ , where  $J$  is a positive integer. By substituting into the preceding expression for kinetic energy, we obtain

$$E_k = \frac{\hbar^2 J(J+1)}{2I} = B J(J+1) \quad (4)$$

with the rotational constant  $B$  given by

$$B = \frac{\hbar^2}{2I} = \frac{\hbar^2}{2M_r R_0^2} \quad (5)$$

*Note:*

For spectroscopic purposes, it is often convenient to express the rotational constant in inverse wavenumbers

$$\tilde{B} = \frac{B}{hc} = \frac{\hbar}{4\pi c \mu R_0^2} \quad (6)$$

### 3.7A Far-infrared absorption spectrum of an HCl molecule.

Let us first calculate the energy spacing between two consecutive rotational levels of rotational quantum numbers  $J-1$  and  $J$ :

$$\Delta E = E(J) - E(J-1) = B J(J+1) - B(J-1)J = 2BJ \quad (1)$$

We thus see that the energy difference between two consecutive rotational levels is not constant, but increases linearly with increasing quantum number  $J$ . This property proves to be consistent with the measured far infrared absorption spectra of the HCl molecule. We can in fact extract nearly the same rotational constant from the different transitions, namely

$$J = 3 \rightarrow J = 4 \quad \tilde{B} = \Delta E/8 = 10.41 \text{ cm}^{-1}$$

$$J = 4 \rightarrow J = 5 \quad \tilde{B} = \Delta E/10 = 10.4 \text{ cm}^{-1}$$

$$J = 5 \rightarrow J = 6 \quad \tilde{B} = \Delta E/12 = 10.39 \text{ cm}^{-1}$$

We can thus assume for the rotational constant of the molecule the value  $\tilde{B} = 10.4 \text{ cm}^{-1}$ . To determine the interatomic equilibrium distance starting from the rotational constant, let us first calculate the reduced mass of the molecule:

$$M_r = \frac{m_H m_{Cl}}{m_H + m_{Cl}} = 1.624 \times 10^{-27} \text{ kg} \quad (2)$$

The equilibrium interatomic distance can then be obtained from Eq. (6) of the previous problem as

$$R_0 = \sqrt{\frac{\hbar}{4\pi c M_r \tilde{B}}} = 0.128 \text{ nm} \quad (3)$$

*Note:*

The experimental data show a slight decrease of  $\tilde{B}$  for higher energy levels; this can be understood in terms of centrifugal effects. For the higher energy levels,

as the molecule is spinning more rapidly, the interatomic bond is elongated slightly, causing **an** increase of the moment of inertia and a corresponding decrease of  $\tilde{B}$ .

### 3.8A The most heavily populated rotational level.

It was shown in problem 3.6 that, in quantum mechanics, the angular momentum of a rotator is quantized according to the relationship:

$$L^2 = \hbar^2 J(J+1) \quad (1)$$

where  $J$  is an integer. Consequently, also its energy is quantized:

$$E = BJ(J+1) \quad (2)$$

However, also the direction of angular momentum is quantized; its projection on **an** arbitrary axis  $z$  can in fact assume the  $2J+1$  different values

$$L_z = m\hbar \quad m = 0, \pm 1, \dots, \pm J \quad (3)$$

Therefore a rotational level of quantum number  $J$  is **(2J+1)-fold** degenerate. The probability of occupation of a given rotational level can **then** be written as

$$p(J) = C(2J+1)\exp[-BJ(J+1)/kT] \quad (4)$$

where  $C$  is a suitable normalization constant. To calculate the most heavily populated level, we equal to zero the derivative of  $p$  with respect to  $J$ :

$$\frac{dp}{dJ} = C \exp[-BJ(J+1)/kT] \left\{ 2 - (2J+1)^2 B/kT \right\} = 0 \quad (5)$$

This equation holds for a rotational quantum number

$$J_{max} = \left( \frac{kT}{2B} \right)^{1/2} - \frac{1}{2} \quad (6)$$

It is easy to verify that this corresponds to a maximum for the level occupation probability.

Taking the ICl molecule ( $B = 0.114 \text{ cm}^{-1}$ ) and recalling that at **room** temperature ( $T = 300 \text{ K}$ )  $kT = 209 \text{ cm}^{-1}$ , we obtain  $J_{max} = 29.8$ . This means that the level with rotational quantum number  $J = 30$  is **the** most heavily populated for a ICl molecule at room temperature.

## ANSWERS

### 3.9A The emission lines of a CO<sub>2</sub> molecule.

In rotational-vibrational transitions for most diatomic and **triatomic** molecules (and in particular for CO<sub>2</sub>), selection rules require that the rotational quantum number is changed by one unit:

$$\Delta J = J'' - J' = \pm 1 \quad (1)$$

where  $J''$  and  $J'$  are the rotational **numbers** for the lower and upper vibrational states respectively. For the so called 'P – branch transitions we have  $\Delta J = +1$ , i.e. the rotational number of the lower vibrational state is higher,  $J'' = J' + 1$ ; this is referred to as the  $P(J'')$  transition. If we let  $\hbar\nu_0$  be the energy difference between the two vibrational levels, the energy of the  $P(J'')$  transition can be easily calculated as

$$E(J'') = \hbar\nu_0 + BJ'(J'+1) - BJ''(J''+1) = \hbar\nu_0 - 2BJ'' \quad (2)$$

In particular, taking the energy difference between two P-branch transitions with rotational numbers  $J''_1$  and  $J''_2$ , we get

$$E(J''_1) - E(J''_2) = 2B(J''_2 - J''_1) \quad (3)$$

Eq. (3) can be used to calculate the rotational constant of the molecule. For our problem, let us first express the energies of the two transitions in  $\text{cm}^{-1}$  [we recall that  $E(\text{cm}^{-1}) = 1/\lambda(\text{cm})$ ]. We obtain  $E(12) = 951.16 \text{ cm}^{-1}$ ,  $E(38) = 930.92 \text{ cm}^{-1}$ . With the help of Eq. (3), we obtain  $B = 0.389 \text{ cm}^{-1}$ .

The energy difference  $\hbar\nu_0$  between the two vibrational levels can then be obtained from Eq. (2):

$$\hbar\nu_0 = E(J'') + 2BJ'' \quad (4)$$

Using the previously obtained value of  $B$ , one easily calculates  $\hbar\nu_0 = 960.5 \text{ cm}^{-1}$ .

### 3.10A The law of mass action.

Let us write the expression of the electron density in the conduction band at thermal equilibrium, using the system of coordinates of Fig. 3.9a in PL (i.e. measuring energy in the conduction band **from the bottom** of the band upwards):

$$N_e = \int_0^{\infty} \rho_c(E_c) f_c(E_c) dE_c \quad (1)$$

with the density of states given by

$$\rho_c(E_c) = \frac{1}{2\pi^2} \left( \frac{2m_c}{\hbar^2} \right)^{3/2} E_c^{1/2} \quad (2)$$

and the level occupation probability given by the Fermi-Dirac distribution:

$$f_c(E_c) = \frac{1}{1 + \exp[(E_c - E_F)/kT]} \quad (3)$$

In our frame of reference one has  $E_F < 0$ , since the Fermi level is lying in the **bandgap**; if we additionally assume  $E_F \gg kT$ , we see that for any value of  $E_c$  the exponential function in the denominator will be much larger than 1. Therefore we can write:

$$f_c(E_c) \approx \exp[-(E_c - E_F)/kT] \quad (4)$$

which corresponds to using a **Boltzmann** approximation for the tail of the Fermi-Dirac distribution. By inserting (2) and (4) into (1), we get:

$$N_e \approx \frac{(2m_c)^{3/2}}{2\pi^2 \hbar^3} \exp(E_F/kT) \int_0^\infty E_c^{1/2} \exp(-E_c/kT) dE_c \quad (5)$$

By making the change of variables  $x = E_c/kT$  and recalling the mathematical result given in the text of the problem, we can easily obtain:

$$N_e \approx 2 \left( \frac{2\pi m_c k T}{\hbar^2} \right)^{3/2} \exp(E_F/kT) \quad (6)$$

Upon interchanging the index  $c$  with  $v$ , the same calculations can be repeated to obtain the hole density in the valence band. The only difference is that, in the coordinate system used in Fig. 3.9a for the valence band, the energy of the Fermi level is given by  $-E_g - E_F$ . Therefore one obtains the hole density as

$$N_h \approx 2 \left( \frac{2\pi m_v k T}{\hbar^2} \right)^{3/2} \exp[-(E_F + E_g)/kT] \quad (7)$$

The product of electron and hole concentrations is then given by:

$$N_e N_h \approx 4 \left( \frac{2\pi k T}{\hbar^2} \right)^3 (m_c m_v)^{3/2} \exp(-E_g/kT) \quad (8)$$

This product is independent of the position of the Fermi level within the **bandgap**, i.e. of the doping level of the semiconductor, and it applies as long as

the system is at thermal equilibrium. This important result of semiconductor physics is referred to as the "law of mass action".

### 3.11A Energies of the quasi-Fermi levels.

Let us calculate the electron density in the conduction band:

$$N_e = \int_0^{\infty} \rho_c(E_c) f_c(E_c) dE_c \quad (1)$$

with the density of states given by

$$\rho_c(E_c) = \frac{1}{2\pi^2} \left( \frac{2m_c}{\hbar^2} \right)^{3/2} E_c^{1/2} \quad (2)$$

For the ideal case of a semiconductor at  $T = 0$  K, the **Fermi-Dirac** distribution function simplifies and becomes

$$\begin{aligned} f_c(E_c) &= 1 & E_c < E_{Fc} \\ f_c(E_c) &= 0 & E_c > E_{Fc} \end{aligned} \quad (3)$$

Therefore expression (1) simplifies to

$$N_e = \int_0^{E_F} \frac{(2m_c)^{3/2}}{2\pi^2 \hbar^3} E_c^{1/2} dE_c = \frac{(2m_c)^{3/2}}{3\pi^2 \hbar^3} E_F^{3/2} \quad (4)$$

The energy of the quasi-Fermi level, with respect to the conduction band edge, is then readily obtained from (4) as:

$$E_{Fc} = (3\pi^2)^{2/3} \frac{\hbar^2}{2m_c} N_e^{2/3} \quad (5)$$

Upon interchanging the indexes  $c$  with  $v$  and  $e$  with  $h$ , an analogous expression can be obtained for the energy of the **quasi-Fermi** level in the valence band, calculated with respect to the valence band edge:

$$E_{Fv} = (3\pi^2)^{2/3} \frac{\hbar^2}{2m_v} N_h^{2/3} \quad (6)$$

Eqs. (5) and (6) show that, by increasing the injection density, the **quasi-Fermi** level move deeper in to the conduction and valence bands. They are rigorously

valid only at  $T = 0 \text{ K}$ , however they hold approximate validity at low temperatures or high injection levels, when  $E_{Fc,\nu} \gg kT$  and the Fermi-Dirac distribution can be approximated reasonably well by a step function.

### 3.12A The quasi-Fermi levels in GaAs.

The energy of the **quasi-Fermi** level in the conduction band can be calculated from the expression derived in the previous problem upon inserting the values of the constants relevant to our case:

$$E_{Fc} = \left(3\pi^2\right)^{2/3} \frac{\hbar^2}{2m_c} N_e^{2/3} = 86.4 \text{ meV} \quad (1)$$

The quasi-Fermi energy in **the** valence band can then be calculated as:

$$E_{Fv} = \frac{m_c}{m_v} E_{Fc} = 12.58 \text{ meV} \quad (2)$$

To evaluate whether **the** low-temperature approximation still holds at room temperature, we need to compare the above energies with  $kT$  ( $\approx 26 \text{ meV}$  at  $T = 300 \text{ K}$ ). Since  $E_{Fc} \gg kT$ , i.e. the **quasi-Fermi** level lies well within **the** conduction band, we expect the low-temperature approximation to hold reasonably well at room temperature; on the **other** hand, since  $E_{Fv} < kT$ , the valence band approximation is expected to be inaccurate in this case.

In fact, from an inspection of Fig. 3.15(b), **which** plots **the** results of exact calculations at room temperature, we see **that**, at an injected carrier density of  $2 \times 10^{18} \text{ cm}^{-3}$ , one has  $E_{Fc} = 3.2 kT \approx 83.2 \text{ meV}$ , while  $E_{Fv} = -kT \approx -26 \text{ meV}$ . This confirms the validity of the low-temperature approximation for the conduction band but not for the valence band.

### 3.13A Derivation of the Bernard-Duraffourg condition.

To have net gain in a semiconductor at a given frequency  $\nu_0 = (E_2' - E_1')/\hbar$ , the number of transitions available for stimulated emission must exceed the number of those available for absorption.

According to Eq. (3.2.31) in PL, the number of transitions available for stimulated emission is given by,

$$dN_{se} = dN f_c(E_2') [1 - f_\nu(E_1')] \quad (1)$$

where  $dN$  is the overall number of transitions between frequencies  $\nu_0$  and  $\nu_0 + d\nu_0$ ,  $f_c(E_2')$  is the probability that the upper level is **full** and **1-f<sub>v</sub>(E<sub>1</sub>)** is the probability that the lower level is empty.

The number of transitions available for absorption is, according to Eq. 3.2.30 in PL

$$dN_a = dN f_v(E_1') [1 - f_c(E_2')] \quad (2)$$

where, in this case,  $f_v(E_1')$  is the probability that the lower level is full and **1-f<sub>c</sub>(E<sub>2</sub>)** is the probability that the upper level is empty.

Their net difference is easily calculated as

$$dN_{se} - dN_a = dN [f_c(E_2') - f_v(E_1')] \quad (3)$$

Having net gain therefore requires that:

$$f_c(E_2') > f_v(E_1') \quad (4)$$

or, using Eqs. (3.2.11) in PL:

$$\frac{1}{1 + \exp[(E_2' - E_{Fc}')/kT]} > \frac{1}{1 + \exp[(E_1' - E_{Fv}')/kT]} \quad (5)$$

which becomes

$$E_1' - E_{Fv}' > E_2' - E_{Fc}' \quad (6)$$

or, equivalently

$$E_2' - E_1' < E_{Fc}' - E_{Fv}' \quad (7)$$

which is the sought condition.

### 3.14A Laser levels in a semiconductor.

Within the parabolic band approximation, the energies of electrons and holes in the conduction and valence bands are given by

$$E_2 = \frac{\hbar^2 k_c^2}{2m_c} \quad (1a)$$

$$E_1 = \frac{\hbar^2 k_v^2}{2m_v} \quad (1b)$$

We recall once again that the energy of the conduction band is measured from the bottom of the band upwards, while the energy of the valence band is measured **from** the top of the band downward.

Since the wave vector of a photon is negligible with respect to that of electron and holes, selection rules require that optical transition occur vertically in the E vs. k diagram, **i.e.** that the wave vector is conserved:

$$k_c = k' = k \quad (2)$$

The energy of the optical transition can thus be written as

$$\hbar\nu_0 = E_g + E_1 + E_2 = E_g + \frac{\hbar^2 k^2}{2} \left( \frac{1}{m_c} + \frac{1}{m_v} \right) = E_g + \frac{\hbar^2 k^2}{2m_r} \quad (3)$$

where  $m_r$  is the so-called reduced mass of the semiconductor, given by

$$\frac{1}{m_r} = \frac{1}{m_c} + \frac{1}{m_v} \quad (4)$$

From Eq. (3) the k value corresponding to a given transition energy  $\hbar\nu_0$  is readily calculated. Upon substituting the resulting expression into Eqs. (1), we obtain, in the usual frames of reference, the energies of the upper and lower laser levels

$$E_2 = (\hbar\nu_0 - E_g) \frac{m_r}{m_c} \quad (5a)$$

$$E_1 = (\hbar\nu_0 - E_g) \frac{m_r}{m_v} \quad (5b)$$

To apply these results to the case of GaAs, we first note that the reduced mass is given by:

$$m_r = \frac{m_v m_c}{m_v + m_c} = 0.0585 \text{ } m_0 \quad (6)$$

For  $E_g = 1.424 \text{ eV}$  and  $\hbar\nu_0 = 1.45 \text{ eV}$ , we then obtain:  $E_2 = 22.3 \text{ meV}$ ,  $E_1 = 3.3 \text{ meV}$ .

### 3.15A Frequency dependence of the gain in an inverted semiconductor.

According to Eq. (3.2.37) in PL, the gain coefficient of an inverted semiconductor is given by

$$g(\nu) = \alpha_0(\nu) [f_c(E'_2) - f_v(E'_1)] \quad (1)$$

with

$$\alpha_0(\nu) = \frac{\pi^3 \nu}{n \epsilon_0 c h^3} \frac{\mu^2}{3} (2m_r)^{3/2} (h\nu - E_g)^{1/2} \quad (2)$$

$$f_c(E'_2) = \frac{1}{1 + \exp[(E'_2 - E'_{Fc})/kT]} \quad (3)$$

$$f_v(E'_1) = \frac{1}{1 + \exp[(E'_1 - E'_{Fv})/kT]} \quad (4)$$

At T=0 K the **Fermi** distribution functions simplify considerably to become

$$f_c(E'_2) = \begin{cases} 1 & E'_2 < E'_{Fc} \\ 0 & E'_2 > E'_{Fc} \end{cases} \quad (5)$$

$$f_v(E'_1) = \begin{cases} 1 & E'_1 < E'_{Fv} \\ 0 & E'_1 > E'_{Fv} \end{cases} \quad (6)$$

We then get

$$f_c(E'_2) - f_v(E'_1) = \begin{cases} 1 & E'_2 - E'_1 < E'_{Fc} - E'_{Fv} \\ -1 & E'_2 - E'_1 > E'_{Fc} - E'_{Fv} \end{cases} \quad (7)$$

The gain coefficient can then be written as

$$g(\nu) = \begin{cases} \alpha_0(\nu) & \frac{E_g}{h} < \nu < \frac{E_{Fc} - E_{Fv}}{h} \\ -\alpha_0(\nu) & \nu > \frac{E_{Fc} - E_{Fv}}{h} \end{cases} \quad (8)$$

The maximum value of gain is achieved at  $\nu = \nu_{\max} = (E_{Fc} - E_{Fv})/h$ . For  $\nu > \nu_{\max}$  the gain changes abruptly sign and becomes absorption.

In the case of a room temperature semiconductor, the **Fermi** distribution function shows a smoother transition from 1 to 0 and also the abrupt frequency jump in the gain function disappears.

### 3.16A Gain calculation in a GaAs amplifier.

Let us first calculate the values of the energy for the two levels involved in laser action for a transition energy exceeding the **bandgap** by 10 meV. According to the results of problem 3.14, the energy of the upper level in the conduction band is

$$E_2 = (\hbar\nu - E_g) \frac{m_r}{m_c} = 10 \text{ meV} \frac{0.059 m_0}{0.067 m_0} = 8.8 \text{ meV} \quad (1)$$

while that of the lower level in the valence band is

$$E_1 = (\hbar\nu - E_g) \frac{m_r}{m_v} = 10 \text{ meV} \frac{0.059 m_0}{0.46 m_0} = 1.2 \text{ meV} \quad (2)$$

The optical gain of the **semiconductor** is then given by

$$g(\nu) = \alpha_0(\nu) [f_c(E_2) - f_v(E_1)] \quad (3)$$

where the absorption coefficient is

$$\alpha_0(\nu) = 19760 (\hbar\nu - E_g)^{1/2} = 1976 \text{ cm}^{-1} \quad (4)$$

To compute the **Fermi** occupation factors, the energies of the **quasi-Fermi** levels in the valence and conduction bands need to be known. From Fig. 3.15(b) in PL we obtain, for a carrier injection  $N = 2 \times 10^{18} \text{ cm}^{-3}$ :

$$E_{Fc} = 3 kT = 78 \text{ meV} \quad E_{Fv} = -1.5 kT = -39 \text{ meV} \quad (5)$$

The **Fermi** occupation factors can then be obtained as

$$f_c(E_2) = \frac{1}{1 + \exp[(E_2 - E_{Fc})/kT]} = 0.934 \quad (6)$$

$$f_v(E_1) = \frac{1}{1 + \exp[(E_{Fv} - E_1)/kT]} = 0.824 \quad (7)$$

Inserting the above values in Eq. (3), we obtain the gain coefficient as  $g = 217 \text{ cm}^{\prime\prime}$ .

If we consider the semiconductor at 0 K, the energies of the **quasi-Fermi** levels at a carrier injection density  $N = 2 \times 10^{18} \text{ cm}^{\prime\prime}$  can be calculated using the results of problem 3.11:

$$E_{Fc} = \frac{\hbar^2}{2m_c} [3\pi^2 N]^{2/3} = 86.4 \text{ meV} \quad (8)$$

$$E_{Fv} = \frac{m_c}{m_v} E_{Fc} = 12.58 \text{ meV} \quad (9)$$

Note that the energy of the **quasi-Fermi** level of the conduction band, which was lying well within the band already at room temperature, did not change much going to 0 K, while the **quasi-Fermi** energy of the conduction band experienced a large change. Recalling the **Fermi** occupation factors at T = 0 K, which were given in the previous problem, we obtain:

$$f_c(E_2) = 1 \quad f_v(E_1) = 0 \quad (10)$$

and therefore the gain coefficient becomes

$$g = \alpha_0 = 1976 \text{ cm}^{-1} \quad (11)$$

Therefore, going to low temperatures, the gain of the semiconductor increases significantly.

The gain bandwidth can be obtained from (3.2.39) of PL. Upon switching from the primed to the **unprimed** coordinate system, we write according to (3.2.3)

$$E_{Fc}' = E_{Fc} + E_g \quad E_{Fv}' = -E_{Fv} \quad (12)$$

so that, from (3.2.39) of PL, we get

$$E_g < h\nu < E_g + E_{Fc} + E_{Fv} \quad (13)$$

The gain bandwidth is then given by  $\Delta E = E_{Fc} + E_{Fv}$  and hence equal to  $\Delta E = 39 \text{ meV}$  at room temperature and  $\Delta E \approx 99 \text{ meV}$  at 0 K. Therefore, going to low temperatures, the gain bandwidth also increases significantly.

Note:

In terms of frequency units one has  $A\nu = \Delta E/h$  and one gets  $A\nu = 9.4 \text{ THz}$  and  $A\nu = 24 \text{ THz}$  for the two cases, respectively. This value is comparable to that of tunable solid-state lasers and much greater than that of e.g. Nd:YAG or Nd:glass (see Table 2.2 in PL).

### 3.17A Differential gain of a GaAs amplifier.

For typical gain coefficients of interest in **semiconductor** lasers, the gain vs. injection density relationship can be approximated as linear, i.e. can be written as

$$g = \sigma(N - N_r) \quad (1)$$

from which we can calculate the differential **gain** as

$$\sigma = \frac{g}{N - N_r} = \frac{217 \text{ cm}^{-1}}{0.8 \times 10^{18} \text{ cm}^{-3}} = 2.7 \times 10^{-16} \text{ cm}^2 \quad (2)$$

Note:

This value can be compared to the typical gain cross sections of **atomic** and molecular media. For example, in  $\text{Nd}^{3+}$  in different hosts,  $a$  ranges from  $10^{-19}$  to  $10^{-18} \text{ cm}^2$ , being therefore 2 to 3 orders of magnitude lower; such values are typical of solid state lasers exploiting forbidden transitions. On the other hand, for dye lasers exploiting allowed transitions, typical values of  $a$  are in the range  $1-4 \times 10^{-16} \text{ cm}^2$ , i.e. of the same order of magnitude as in semiconductors. Note however that the **comparison** is not fully legitimate, since the concept of cross section is not appropriate for a delocalized wavefunction, such as that of an electron in a semiconductor.

### 3.18A Thickness of a quantum well: an order of magnitude estimate.

Within the parabolic band approximation, electrons at the bottom of the conduction band can be considered as free particles with an effective mass  $m_c$ . According to statistical mechanics, their average thermal kinetic energy is:

$$\frac{1}{2}m_c v_{th}^2 = \frac{3}{2}kT \quad (1)$$

which gives:

$$v_{th} = \sqrt{\frac{3kT}{m_c}} \quad (2)$$

The De Broglie wavelength associated to the electron is given by

$$\lambda_c = \frac{h}{p_c} = \frac{h}{mv_{th}} = \frac{h}{\sqrt{3kTm_c}} \quad (3)$$

For the case of electron in **GaAs** at  $T = 300 \text{ K}$  we get

$$\lambda_c = \frac{6.626 \times 10^{-34} \text{ Js}}{\sqrt{3 \times 1.38 \times 10^{-23} \text{ J/K} \times 300 \text{ K} \times 0.067 \times 9.1 \times 10^{-31} \text{ kg}}} = 24 \text{ nm} \quad (4)$$

The De Broglie wavelength provides us with the order of magnitude estimate of the well thickness needed for sizable quantum confinement effects: if  $L \gg \lambda_c$ , no **significant** confinement will occur, while for  $L \ll \lambda_c$  the confinement will be relevant. This result shows us that quantum confined semiconductor structures require control of the layer thickness with nm precision; this is nowadays possible using sophisticated techniques such as molecular **beam epitaxy** or **metallo-organic** chemical vapor deposition.

### 3.19A An ideal quantum well.

Let us consider a **particle** of mass  $m$  inside the well. Its **eigenstates** are given by the solutions of the time-independent **Schrödinger** equation:

$$H\psi = E\psi \quad (1)$$

where  $H = -\left(\frac{\hbar^2}{2m}\nabla^2 + V\right)$  is the **hamiltonian** operator,  $V$  is **the** potential energy and  $E$  is the energy eigenvalue. If we set to zero the potential energy inside the well, we get the simple equation

$$-\frac{\hbar^2}{2m} \frac{d^2\psi}{dx^2} = E\psi \quad (2)$$

which can be cast in the form

$$\frac{d^2\psi}{dx^2} + k^2\psi = 0 \quad (3)$$

with  $k = \sqrt{2mE/\hbar^2}$ . This is the well known classical equation of a harmonic oscillator, which has the solutions:

$$\psi(x) = A \sin(kx) + B \cos(kx) \quad (4)$$

Being the well of infinite depth, the wavefunction cannot penetrate its borders, i.e.  $\psi(x) = 0$  for all  $x$  values outside the well. For the continuity of the wavefunction, we get the following boundary conditions for the wavefunction:

$$\psi(0) = 0 \quad (5a)$$

$$\psi(L) = 0 \quad (5b)$$

From the first condition we get  $B = 0$ ; the second gives us  $\sin(kL) = 0$ , which is **verified** when

$$k_n = \frac{n\pi}{L} \quad (6)$$

where  $n$  is an integer. We therefore get for the energy the discrete values

$$E_n = \frac{\hbar^2 n^2 \pi^2}{2mL^2} \quad (7)$$

### 3.20A Energies of the quasi-Fermi levels in a semiconductor quantum well.

Let us start by calculating the electron density in **the** conduction band. As in a bulk semiconductor, it can be obtained by integrating over the entire band the product of the density of states **times** the occupation probability:

$$N_e = \int_0^\infty \rho_c(E_c) f_c(E_c) dE_c \quad (1)$$

The **Fermi** distribution function is, as usual, given by

$$f_c(E_c) = \frac{1}{1 + \exp[(E_c - E_{Fc})/kT]} \quad (2)$$

while the density of states in the conduction band of a quantum well can **be** written as

$$\rho_c(E_c) = \sum_i \frac{m_c}{\pi\hbar^2 L_z} H(E - E_{ic}) \quad (3)$$

In Eq. (3)  $L_z$  is the well thickness,  $H$  is **the** Heaviside (step) function

$$H(E - E_{ic}) = \begin{cases} 0 & E < E_{ic} \\ 1 & E > E_{ic} \end{cases} \quad (4)$$

and  $E_{ic}$  are the energies of the discrete states in the conduction band of the quantum well. By plugging Eqs. (2) and (3) into Eq. (1), we get the expression:

$$N_e = \sum_i \frac{m_c}{\pi \hbar^2 L_z} \int_{E_k}^{\infty} \frac{1}{1 + \exp[(E_c - E_{Fc})/kT]} dE_c \quad (5)$$

To evaluate this expression we need to calculate the integral

$$I = \int_{E_k}^{\infty} \frac{1}{1 + \exp[(E_c - E_{Fc})/kT]} dE_c \quad (6)$$

which can also be rewritten as

$$I = \int_{E_k}^{\infty} \frac{\exp[-(E_c - E_{Fc})/kT]}{1 + \exp[-(E_c - E_{Fc})/kT]} dE_c \quad (7)$$

By making the substitution  $y = \exp[-(E_c - E_{Fc})/kT]$ , we obtain

$$I = kT \int_0^{\exp[-(E_k - E_{Fc})/kT]} \frac{dy}{1 + y} = kT \ln\{1 + \exp[(E_{Fc} - E_{ic})/kT]\} \quad (8)$$

By substituting Eq. (8) into (5), we obtain:

$$N_e = \frac{m_c kT}{\pi \hbar^2 L_z} \sum_i \ln\{1 + \exp[(E_{Fc} - E_{ic})/kT]\} \quad (9)$$

In Eq. (9) the sum is extended over all **subbands** and we assume that the effective mass of the electrons does not vary in the different subbands. By interchanging the subscript *c* with *v* we get, analogously, the hole density in the valence band

$$N_h = \frac{m_v kT}{\pi \hbar^2 L_z} \sum_i \log\{1 + \exp[(E_{Fv} - E_{iv})/kT]\} \quad (10)$$

Equations (9) and (10) can be used to obtain two plots of  $N_e$  vs.  $E_{Fc}$  and  $N_h$  vs.  $E_{Fv}$ , respectively. From these two plots, the values of  $E_{Fc}$  and  $E_{Fv}$ , for a given value of the carrier injection  $N = N_e = N_h$ , can then be obtained.

### 3.21A Calculation of the gain bandwidth in a GaAs quantum well.

The condition for net gain in a semiconductor quantum well can be written as [see (3.3.26) in PL]

$$E_g + E_{1c} + E_{1v} < \hbar\nu < E_{Fc}' - E_{Fv}' \quad (1)$$

Upon switching from the primed to the unprimed coordinate system we write according to (3.2.3) of PL

$$E_{Fc}' = E_{Fc} + E_g \quad E_{Fv}' = -E_{Fv} \quad (2)$$

so that relationship (1) becomes

$$E_g + E_{1c} + E_{1v} < \hbar\nu < E_g + E_{Fc} + E_{Fv} \quad (3)$$

The gain bandwidth of the quantum well amplifier is then given by

$$\Delta E = E_{Fc} + E_{Fv} - E_{1c} - E_{1v} \quad (4)$$

From Fig. 3.26 in PL we extract, for an injection density  $N = 2 \times 10^{18} \text{ cm}^{-3}$ , the following values for the differences between the quasi-Fermi energies and the energies of the  $n = 1$  subband:

$$E_{Fc} - E_{1c} = 2.8 \text{ } kT = 70 \text{ meV} \quad (5a)$$

$$E_{Fv} - E_{1v} = -kT = -25 \text{ meV} \quad (5b)$$

By inserting Eqs. (5) into (4), we finally get the gain bandwidth of the quantum-well amplifier

$$\Delta E = 45 \text{ meV} \quad (6)$$

The corresponding value in frequency units is then given by  $\Delta\nu = \Delta E/\hbar = 11 \text{ THz}$ .

Note:

This value is comparable to that of tunable solid-state lasers and much larger than that of e.g. Nd:YAG or Nd:glass [see Table 2.2 in PL].



## CHAPTER 4

# Ray and Wave Propagation through optical media

## PROBLEMS

### 4.1P ABCD matrix of a spherical dielectric interface.

Calculate the ABCD matrix for a ray entering a spherical dielectric interface from a medium of refractive index  $n_1$  to a medium of refractive index  $n_2$ , with radius of curvature  $R$  (assume  $R > 0$  if the center is to the left of the surface).

### 4.2P ABCD matrix of a thin lens.

Use the results of the previous exercise to calculate the ABCD matrix of a thin spherical lens, made up of two closely spaced dielectric interfaces, of radii  $R_1$  and  $R_2$ , enclosing a material of refractive index  $n_2$ . The lens is immersed in a medium of refractive index  $n_1$ .

### 4.3P ABCD matrix of a piece of glass.

Calculate the ABCD matrix for a piece of glass of length  $L$  and refractive index  $n$ .

### 4.4P Reflection at a plane interface.

A plane electromagnetic wave is incident at the plane interface between two media of refractive indices  $n_1$  and  $n_2$ , with direction orthogonal to the interfaces. Derive the expressions for the electric field reflectivity and transmission and demonstrate that the sum of intensity reflectivity and intensity transmission is 1.

## PROBLEMS

### 4.5P An high reflectivity dielectric mirror.

Consider an highly reflective dielectric mirror made by alternating  $\lambda/4$  layers of high and low refractive index materials, with the sequence starting and ending with an high-index material.  $\text{TiO}_2$  ( $n_H = 2.28$  at  $1.064 \mu\text{m}$ ) and  $\text{SiO}_2$  ( $n_L = 1.45$  at  $1.064 \mu\text{m}$ ) are used as high- and low-index materials respectively, while the substrate is made of BK7 glass ( $n_S = 1.54$  at  $1.064 \mu\text{m}$ ). Design the mirror (layer thickness and number of layers) so that it has a power reflectivity  $R > 99\%$  at the Nd:YAG wavelength  $\lambda_0 = 1.064 \mu\text{m}$ .

### 4.6P A Fabry-Perot interferometer.

A Fabry-Perot interferometer consisting of two identical mirrors, air-spaced by a distance  $L$ , is illuminated by a monochromatic em wave of tunable frequency. From a measurement of the transmitted intensity versus the frequency of the input wave we find that the free spectral range of the interferometer is  $3 \times 10^9 \text{ Hz}$  and its resolution is 30 MHz. Calculate the spacing  $L$  of the interferometer, its finesse, and the mirror reflectivity.

### 4.7P A scanning Fabry-Perot interferometer.

A Nd:YAG laser is oscillating at the wavelength of  $1.064 \mu\text{m}$  on 100 longitudinal modes spaced by 100 MHz; design a scanning Fabry-Perot interferometer made of two air-spaced mirrors that is able to resolve all these modes. In addition, specify the piezoelectric transducer sweep corresponding to one free spectral range of the interferometer.

### 4.8P An imaging optical system.

Prove that an optical system described by an ABCD matrix with  $B = 0$  images the input plane onto the output plane, and that  $A$  gives the magnification. Verify this on a single thin lens, imaging at a distance  $d_i$  an object placed at a distance  $d_0$  from the lens.

[Hint: according to geometrical optics,  $1/d_0 + 1/d_i = 1/f$ ]

### 4.9P The ABCD law for gaussian beams.

Demonstrate the *ABCD* law for a gaussian beams, stating that a gaussian beam of complex parameter  $q_1$ :

$$u(x_1, y_1, z_1) = \exp\left\{-jk \frac{x_1^2 + y_1^2}{2q_1}\right\}$$

is transformed into the following gaussian beam:

$$u(x, y, z) = \frac{1}{A + B/q_1} \exp\left\{-jk \frac{x^2 + y^2}{2q}\right\}$$

where  $q$  is related to  $q_1$  by the law:

$$q = \frac{Aq_1 + B}{Cq_1 + D} .$$

*(Zavel & difficulty higher than average)*

### 4.10P A collimating lens.

A positive lens of focal length  $f$  is placed at a distance  $d$  from the waist of a gaussian beam of waist spot size  $w_0$ . Derive an expression of the focal length  $f$  (in terms of  $w_0$  and  $d$ ) required so that the beam leaving the lens has a plane wavefront. In addition, find the distance from the waist for which the shortest focal length lens is required to collimate the beam.

### 4.11P A simple optical processing system.

Consider the propagation of an optical beam with field amplitude  $u_1(x_1, y_1, z_1)$  through an optical system made up of a free space propagation of length  $f$ , a lens of focal length  $f$ , and a subsequent free space propagation of length  $f$ . Calculate the field amplitude at the output plane of the system. Discuss a possible application of this optical system.

*(Level & diflculty higher than average).*

## PROBLEMS

### 4.12P A laser driller.

For a material processing application, a  $\text{TEM}_{00}$  beam at  $\lambda = 532 \text{ nm}$  from a frequency doubled **Nd:YAG** laser is focused using a lens with focal length  $f = 50 \text{ mm}$  and numerical aperture  $\text{NA} = 0.3$ . To avoid excessive diffraction effects at the lens edge due to **truncation** of the gaussian field by the lens, one usually chooses the lens diameter according to the criterion  $D \geq 2.25 w_1$ . Assuming that the equality holds in the previous expression and that the waist of the incident beam is located at the lens, i.e.  $w_1 = w_0$ , find the spot size in the focus.

### 4.13P An earth to moon laser rangefinder.

Suppose that a  $\text{TEM}_{00}$  gaussian beam from a ruby laser ( $\lambda = 694.3 \text{ nm}$ ) is transmitted through a **1-m** diameter diffraction-limited telescope to illuminate a spot on **the** surface of the moon. Assuming an earth-to-moon distance of  $z \cong 348,000 \text{ km}$  and using the relation  $D = 2.25 w_0$  between the telescope objective diameter and the beam spot size (see previous problem), calculate the beam spot size on the moon. (Distortion effects from the atmosphere can be important, but they are neglected here).

### 4.14P An He-Ne laser.

A given He-Ne laser oscillating in a pure gaussian  $\text{TEM}_{00}$  mode at  $\lambda = 632.8 \text{ nm}$  with an output power of  $P = 5 \text{ mW}$  is advertised as having a far-field divergence-angle of **1 mrad**. Calculate spot size, peak intensity, and peak electric field at **the** waist position.

### 4.15P An Argon laser.

A gaussian  $\text{TEM}_{00}$  beam from an Argon laser at  $\lambda = 514.5 \text{ nm}$  with an output power of **1 W** is sent to a target at a distance  $L = 500 \text{ m}$ . Assuming that the beam is initially at its waist, find the spot size that guarantees the highest peak intensity on the target and calculate this intensity.

**4.16P Gaussian beam propagation through an optical system.**

Given a gaussian beam of spot size  $w_1$  and radius of curvature  $R_1$  propagating through an optical system described by a *real*  $ABCD$  matrix, calculate the beam spot size  $w$  at the output plane of the system.

*(Level of difficulty higher than average)*

**4.17P Power conservation for a gaussian beam.**

Show that, when a gaussian beam is propagated through an optical system described by an  $ABCD$  matrix with *real* elements, its power is conserved.

*(Level of difficulty higher than average)*

**4.18P A "soft" or gaussian aperture.**

Calculate the  $ABCD$  matrix for a "soft" or gaussian aperture, with the following field amplitude transmission:

$$t(x, y) = \exp\left[-\frac{x^2 + y^2}{w_a^2}\right]$$

where  $w_a$  is a constant.

**4.19P A waist imaging system.**

Find the conditions under which an optical system, described by an  $ABCD$  matrix, transforms a gaussian beam with waist  $w_{01}$  on the input plane of the system into a beam with waist  $w_{02}$  on the output plane.

**4.20P Gaussian beam transformation by a lens.**

Use the results of the previous problem to discuss the **transformation**, using a lens of focal length  $f$ , of a gaussian beam with spot size at the beam waist  $w_{01}$  and a waist-lens distance  $d_1 > f$ .

**4.21P Focusing a gaussian beam inside a piece of glass.**

Consider a **gaussian** beam with spot size  $w_{01}$  and plane wavefront entering a lens of focal length  $f$  (assume  $z_{R1} \gg f$ ). A long block of glass with **refractive** index  $n$  is placed at a distance  $L < f$  from the lens. Find the position of the beam waist inside the glass.

## ANSWERS

**4.1A ABCD matrix of a spherical dielectric interface.**

Let us consider for simplicity a convex interface ( $R < 0$ ) and an incident ray forming an angle  $\theta_i$  with the normal (see Fig. 4.1); the angle  $\theta_t$  formed by the transmitted ray is obtained from Snell's law:

$$n_1 \sin \theta_i = n_2 \sin \theta_t \quad (1)$$

Assuming small angular displacements, one can use the **paraxial approximation** ( $\sin \theta \approx \theta$ ); Snell's law then becomes:

$$n_1 \theta_i = n_2 \theta_t \quad (2)$$

Let us now consider the triangle ABC in Fig. 4.1; using the well known property that an external angle in a triangle is equal to the sum of the two non adjacent internal angles, we get:

$$\theta_i = \theta_t + \alpha \quad (3)$$

In the same way, considering the triangle BCD, we obtain:

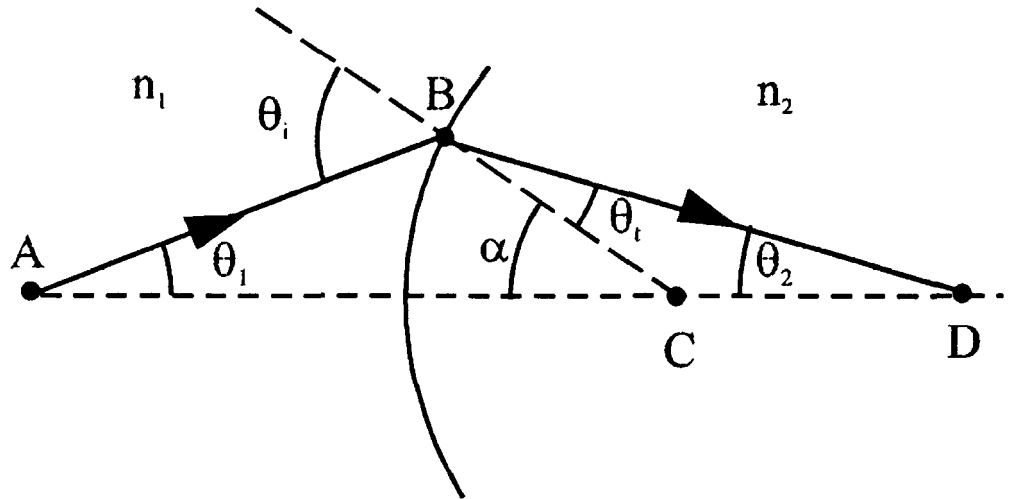


Fig. 4.1: incident and transmitted rays at a spherical dielectric interface.

$$\alpha = \theta_t + \theta_i \quad (4)$$

From Eqs. (2), (3) and (4) one can **eliminate**  $\theta_i$  and  $\theta_t$  to obtain:

$$n_1 \theta_1 + n_2 \theta_2 = (n_2 - n_1) \alpha \quad (5)$$

From Fig. 4.1 and again using the paraxial approximation, we have  $a \approx \tan a = r_1/|R| = -r_1/R$ . The angles  $\theta_1$  and  $\theta_2$  correspond, on the other hand, to the slopes of the rays in the two media. According to the sign convention usually adopted an angle is positive if the vector must be rotated clockwise to make it coincide with the positive direction of the  $z$  axis. We thus obtain:  $r_1' = \theta_1, r_2' = \theta_2$ . The substitution of these relationships into Eq. (5) gives:

$$n_1 r_1' - n_2 r_2' = -(n_2 - n_1) \frac{r_1}{R} \quad (6)$$

We can therefore write:

$$r_2 = r_1 \quad (7a)$$

$$r_2' = \frac{n_2 - n_1}{n_2 R} r_1 + \frac{n_1}{n_2} r_1' \quad (7b)$$

Recalling the relationships that connect displacements and slopes of the optical rays on the input and output planes of the system:

$$r_2 = A r_1 + B r_1' \quad (8a)$$

$$r_2' = C r_1 + D r_1' \quad (8b)$$

we obtain:  $A = 1, B = 0, C = (n_2 - n_1)/R, D = n_2/n_1$ . The  **$ABCD$**  matrix of the interface is therefore:

$$\begin{vmatrix} A & B \\ C & D \end{vmatrix} = \begin{vmatrix} 1 & 0 \\ \frac{n_2 - n_1}{n_2 R} & \frac{n_1}{n_2} \end{vmatrix} \quad (9)$$

For the particular case of plane interface ( $R = \infty$ ) the **matrix** simplifies to:

$$\begin{vmatrix} A & B \\ C & D \end{vmatrix} = \begin{vmatrix} 1 & 0 \\ 0 & \frac{n_1}{n_2} \end{vmatrix} \quad (10)$$

Note that the determinant of the matrix is  $AD - BC = n_1/n_2$ , i.e. the ratio of the refractive indexes in the entrance and exit planes of the system. If  $n_1 = n_2$  we obtain  $AD - BC = 1$ .

### 4.2A ABCD matrix of a thin lens.

A thin lens can be thought of as the cascade of two spherical dielectric interfaces, of the kind discussed in the previous exercise. The overall ABCD matrix is thus the product of the two:

$$\begin{vmatrix} A & B \\ C & D \end{vmatrix} = \begin{vmatrix} 1 & 0 \\ \frac{n_2 - n_1}{n_2 R_2} & \frac{n_1}{n_2} \end{vmatrix} \begin{vmatrix} 1 & 0 \\ \frac{n_1 - n_2}{n_1 R_1} & \frac{n_2}{n_1} \end{vmatrix} = \begin{vmatrix} 1 & 0 \\ \frac{n_1 - n_2}{n_1 R_1} + \frac{n_2 - n_1}{n_1 R_2} & 1 \end{vmatrix} \quad (1)$$

Since a lens of focal length  $f$  is characterized by the ABCD matrix:

$$\begin{vmatrix} A & B \\ C & D \end{vmatrix} = \begin{vmatrix} 1 & 0 \\ -\frac{1}{f} & 1 \end{vmatrix} \quad (2)$$

the comparison of Eqs. (1) and (2) gives the following expression for  $f$ :

$$\frac{1}{f} = \frac{n_2 - n_1}{n_1} \left( \frac{1}{R_2} - \frac{1}{R_1} \right) \quad (3)$$

*Notes:*

- i) as usual, the order in which the matrices appear in the product is the opposite of the order in which the corresponding optical elements are traversed by the light ray;
- ii) for the second interface, the refractive indexes of inner and outer medium are interchanged.
- iii) For a biconcave lens one has  $R_1 < 0$  and  $R_2 > 0$  and Eq. (3) gives

$$\frac{1}{f} = \frac{n_2 - n_1}{n_1} \left( \frac{1}{R_2} + \frac{1}{|R_1|} \right) \quad (4)$$

### 4.3A ABCD matrix of a piece of glass.

This optical system can be thought of as the cascade of a **vacuum/glass** interface, a propagation in glass, and a **glass/vacuum** interface. The corresponding matrix is:

$$\begin{vmatrix} A & B \\ C & D \end{vmatrix} = \begin{vmatrix} 1 & 0 \\ 0 & n \end{vmatrix} \begin{vmatrix} 1 & L \\ 0 & 1 \end{vmatrix} \begin{vmatrix} 1 & 0 \\ 0 & \frac{1}{n} \end{vmatrix} = \begin{vmatrix} 1 & 0 \\ 0 & n \end{vmatrix} \begin{vmatrix} 1 & \frac{L}{n} \\ 0 & \frac{1}{n} \end{vmatrix} = \begin{vmatrix} 1 & \frac{L}{n} \\ 0 & \frac{1}{n} \end{vmatrix} \quad (1)$$

This is equivalent to the ABCD matrix for a free space propagation of length  $L/n$ .

Note:

From the point of view of the angular propagation of a light beam, a piece of optical material of length  $L$  and refractive index  $n$  is equivalent to a shorter length,  $L/n$ , of vacuum propagation. On the other hand, considering the temporal propagation of a light pulse, the same piece of optical material is equivalent to a longer length,  $nL$ , of propagation in vacuum, since the speed of light is reduced in the material.

#### 4.4A Reflection at a plane interface.

To calculate the reflected and transmitted electric fields, we start from the boundary conditions at the interface between two media, which state that the tangential components of the electric field  $E$  and the magnetic field  $H$  are conserved. In medium 1 the e.m. wave is made by the superposition of the incident and reflected waves, while in medium 2 it is given by the transmitted wave. The incident, transmitted and reflected waves are shown in Fig. 2: note that the vectors are drawn in such way that  $E$ ,  $H$  and the wave-vector  $k$  always form a right-handed tern.

Conservation of the tangential component yields the equations:

$$E_i + E_r = E_t \quad (1)$$

$$H_i - H_r = H_t \quad (2)$$

We recall now that, for a plane e.m. wave, one has  $H = E/(\mu v) = nE/(\mu c_0)$ , where  $\mu$  is the permeability of the material and  $c$  is the light velocity, and considering that, for all media of interest in optics, one has  $\mu \approx \mu_0$ , where  $\mu_0$  is the permeability of vacuum and eq. (2) becomes:

$$n_1 (E_i - E_r) = n_2 E_t \quad (3)$$

By combining Eqs. (1) and (3), it is straightforward to derive the field reflection coefficient:

$$r = \frac{E_r}{E_i} = \frac{n_1 - n_2}{n_1 + n_2} \quad (4)$$

and the field transmission coefficient:

$$t = \frac{E_t}{E_i} = \frac{2n_1}{n_1 + n_2} \quad (5)$$

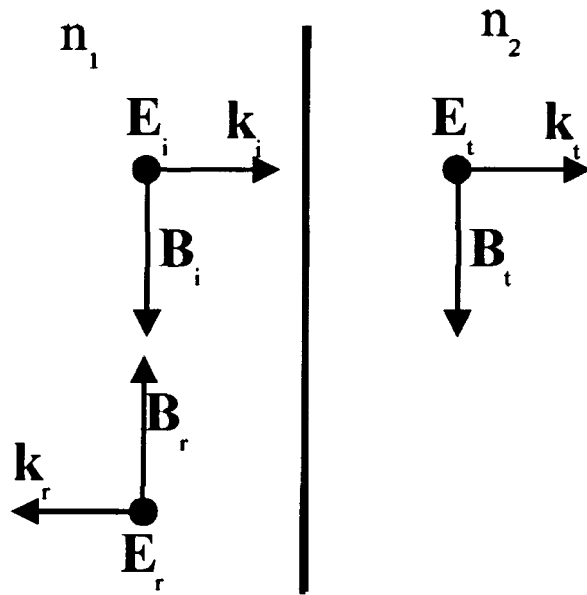


**Fig. 4.2:** incident, transmitted and reflected e.m. waves at the interface between two dielectric media.

To derive the intensity reflection and transmission coefficients, we recall that:

$$I = \frac{1}{2} \frac{c}{n} \varepsilon |E|^2 = \frac{1}{2} c \varepsilon_0 n |E|^2 \quad (6)$$

where  $\varepsilon = n^2 \varepsilon_0$  and  $\varepsilon_0$  is the vacuum permittivity. We then obtain:

$$R = \frac{I_r}{I_i} = \left| \frac{E_r}{E_i} \right|^2 = |r|^2 = \left( \frac{n_1 - n_2}{n_1 + n_2} \right)^2 \quad (7)$$

$$T = \frac{I_t}{I_i} = \frac{n_2}{n_1} \left| \frac{E_t}{E_i} \right|^2 = \frac{n_2}{n_1} |t|^2 = \frac{4n_1 n_2}{(n_1 + n_2)^2} \quad (8)$$

It is now easy to show that:

$$R + T = \frac{(n_1 - n_2)^2 + 4n_1 n_2}{(n_1 + n_2)^2} = 1 \quad (9)$$

*Notes:*

- i) Relationship (9) is required by the conservation of energy. It is however not true that  $|r|^2 + |t|^2 = 1$ .
- ii) Considering a typical air/glass interface ( $n_1 = 1, n_2 = 1.5$ ) we get:  $R = 0.04$ , which means that 4% of the power is lost on reflection. If many interfaces are present or if they are located inside a laser cavity, these so-called "Fresnel losses" may impede laser action. This problem can be solved by the use of suitable antireflection coatings.

#### 4.5A An high reflectivity dielectric mirror.

Let us first specify the layer thickness. To obtain a high reflectivity coating, both the high and the low reflectivity layer must have optical thickness of  $\lambda_0/4$ . In this case we have:

$$l_H = \frac{\lambda_0}{4n_H} = 116.6 \text{ nm} \quad l_L = \frac{\lambda_0}{4n_L} = 183.4 \text{ nm} \quad (1)$$

To calculate the number of layers required to reach the specified reflectivity, we recall that the expression for the power reflectivity of a multilayer stack made up of an odd number of layers is given by (see Eq. (4.4.1) in PL):

$$R = \left( \frac{n_H^{J+1} - n_L^{J-1} n_S}{n_H^{J+1} + n_L^{J-1} n_S} \right)^2 \quad (2)$$

where  $J$  is the number of layers (we note that, to have  $J$  given by an odd number, the stack should start and end with an high reflectivity layer). With some simple manipulations, this expression can be rewritten as:

$$\left( \frac{n_H}{n_L} \right)^J = \left( \frac{1 - \sqrt{R}}{1 + \sqrt{R}} \right) \frac{n_S}{n_L n_H} \quad (3)$$

which gives:

$$J = \frac{\log \left[ \left( \frac{1+\sqrt{R}}{1-\sqrt{R}} \right) \frac{n_S}{n_L n_H} \right]}{\log \left( \frac{n_H}{n_L} \right)} \quad (4)$$

Substituting the numerical values into this expression, we get  $J = 11.5$ . Therefore the **minimum** number of layers which gives the specified reflectivity is  $J = 13$ ; in this **case** we get from Eq.(2):  $R = 99.48\%$

#### 4.6A A Fabry-Perot interferometer.

For a Fabry-Perot interferometer made of air-spaced mirrors, the free spectral range is:  $\Delta\nu_{FSR} = c/(2L)$ . The mirror spacing in our case is then given by:

$$L = \frac{c}{2\Delta\nu_{FSR}} = \frac{3 \times 10^{11} \text{ mm s}^{-1}}{2 \times 3 \times 10^9 \text{ s}^{-1}} = 50 \text{ mm} \quad (1)$$

The finesse of the interferometer, i.e. the ratio of free spectral range to width of the transmission peak, is:

$$F = \frac{\Delta\nu_{FSR}}{\Delta\nu_C} = \frac{3 \times 10^9 \text{ Hz}}{30 \times 10^6 \text{ Hz}} = 100 \quad (2)$$

The finesse is a function of the mirror reflectivity; in the case of equal mirrors we have (see Eq. (4.5.14a) in PL):

$$F = \frac{\pi\sqrt{R}}{1-R} \quad (3)$$

which gives the equation:

$$R^2 - \left[ 2 + \left( \frac{\pi}{F} \right)^2 \right] R + 1 = 0 \quad (4)$$

the solution of which is:  $R = 0.968$ .

*Note:*

Eq.(4) can be written in the form:

$$R^2 - 2(1+\alpha^2)R + 1 = 0 \quad (5)$$

## ANSWERS

where  $a = \pi/\sqrt{2}F$ . Assuming  $\alpha \ll 1$ , we get:

$$R = 1 + \alpha^2 - \sqrt{(1 + \alpha^2)^2 - 1} \approx 1 - \sqrt{2}\alpha = 1 - \frac{\pi}{F} \quad (6)$$

and obtain for the finesse the following simple expression, valid for large values of  $F$ :

$$F = \frac{\pi}{1-R} = \frac{\pi}{T} \quad (7)$$

### 4.7A A scanning Fabry-Perot interferometer.

Given **100** oscillating longitudinal modes spaced by **100** MHz, the laser linewidth is **10 GHz**. To avoid frequency ambiguity, therefore we must set the free spectral range  $\Delta\nu_{FSR} > 10$  GHz. Leaving a safety margin, we can choose:  $\Delta\nu_{FSR} = 15$  GHz. This corresponds to a mirror distance:

$$L = \frac{c}{2\Delta\nu_{FSR}} = \frac{3 \times 10^{11} \text{ mm s}^{-1}}{2 \times 15 \times 10^9 \text{ s}^{-1}} = 10 \text{ mm}$$

The resolving power of the interferometer is given by  $A\nu_M = A\nu_{FSR}/F$ , where  $F$  is the finesse of the **instrument**. To observe the single longitudinal modes, we need to have  $\Delta\nu_M < 100$  MHz; again leaving **some** margin, we can choose  $\Delta\nu_M = 75$  MHz, which corresponds to a finesse  $F = 200$ . Assuming to use two mirrors with the same reflectivity and using the result of the previous problem, we obtain the required mirror reflectivity:  $R = 1 - \pi/F = 0.984$ . Finally, to get the excursion of the piezotransducer we recall that, to cover a free spectral range of the interferometer, the mirror **distance** should be varied by half a wavelength, i.e.  $\Delta L_{FSR} = \lambda/2 = 0.532$  nm.

### 4.8A An imaging optical system.

The matrix formulation of geometrical optics relates the position  $r_1$  and the slope  $r'_1$  of a ray of light at the input plane of an optical system to the corresponding position and slope at the output plane, according to:

$$\begin{aligned} r_2 &= Ar_1 + Br'_1 \\ r'_2 &= Cr_1 + Dr'_1 \end{aligned} \quad (1)$$

#### 4. RAY AND WAVE PROPAGATION.

If  $B = 0$ , we get:

$$r_2 = Ar_1 \quad (2)$$

This condition means that all the rays emerging from a point source in the input plane of the system located at a distance  $r_1$  from the axis, regardless of their slopes  $r'_1$ , will converge to a point in the output plane at a distance  $Ar_1$  from the axis: the system thus images the input plane onto the output plane with **magnification**  $A$ .

We can **verify** this condition considering **an** optical system made of a propagation  $d_o$ , a thin lens of focal length  $f$  and a propagation  $d_i$ . The corresponding ABCD matrix is:

$$\begin{aligned} \begin{vmatrix} A & B \\ C & D \end{vmatrix} &= \begin{vmatrix} 1 & d_i \\ 0 & 1 \end{vmatrix} \begin{vmatrix} 1 & 0 \\ -\frac{1}{f} & 1 \end{vmatrix} \begin{vmatrix} 1 & d_o \\ 0 & 1 \end{vmatrix} = \\ \begin{vmatrix} 1 - \frac{d_i}{f} & d_i \\ -\frac{1}{f} & 1 \end{vmatrix} \begin{vmatrix} 1 & d_o \\ 0 & 1 \end{vmatrix} &= \begin{vmatrix} 1 - \frac{d_i}{f} & d_0 + d_i - \frac{d_o d_i}{f} \\ -\frac{1}{f} & 1 - \frac{d_o}{f} \end{vmatrix} \end{aligned} \quad (3)$$

If the imaging condition of geometrical optics is satisfied ( $1/d_o + 1/d_i = 1/f$ ), it is easy to verify that  $B = 0$  and  $A = d_i/d_o = M$ , i.e. the magnification predicted by geometrical optics.

#### 4.9A The ABCD law for gaussian beams.

According to the extension of the Huygens principle to a general optical system, the field  $u(x, y, z)$  at the output plane of a general **paraxial** optical system is given by (see Eq. (4.6.9) in PL):

$$\begin{aligned} u(x, y, z) &= \frac{j}{B\lambda} \iint_S u(x_1, y_1, z_1) \\ &\exp \left\{ -jk \left[ \frac{A(x_1^2 + y_1^2) + D(x^2 + y^2) - 2x_1 x - 2y_1 y}{2B} \right] \right\} dx_1 dy_1 \end{aligned} \quad (1)$$

Let us assume that at the input plane of the system we have a lowest order gaussian beam. In this case the field distribution, apart from a (possibly complex) multiplying constant, can be written as:

$$u_1(x_1, y_1, z_1) = \exp\left\{-jk[(x_1^2 + y_1^2)/2q_1]\right\} \quad (2)$$

By substituting (2) into (1), it is easy to see that the double integral can be separated into the product of two simple integrals:

$$u(x, y, z) = I_1(x, z)I_2(y, z) \quad (3)$$

where:

$$I_1(x, z) = \sqrt{\frac{j}{B\lambda}} \int_{-\infty}^{+\infty} \exp\left[-j\frac{kx_1^2}{2q_1}\right] \exp\left[-j\frac{k}{2B}(Ax_1^2 + Dx^2 - 2xx_1)\right] dx_1 \quad (4)$$

and  $I_2(y, z)$  can be obtained from  $I_1(x, z)$  by interchanging  $x$  with  $y$  and  $x_1$  with  $y_1$ .  $I_1(x, z)$  can be rewritten in the following way:

$$I_1(x, z) = \sqrt{\frac{j}{B\lambda}} \exp\left[-j\frac{kDx^2}{2B}\right] \int_{-\infty}^{+\infty} \exp\left\{-j\frac{k}{2B}\left[\left(A + \frac{B}{q_1}\right)x_1^2 - 2xx_1\right]\right\} dx_1 \quad (I)$$

We now have to evaluate an integral of the kind:

$$\int_{-\infty}^{+\infty} \exp(-ax_1^2 - 2bx_1) dx_1 \quad (6)$$

where  $a$  and  $b$  are complex constants:

$$a = \frac{jk}{2B} \left( A + \frac{B}{q_1} \right) b = \frac{jkx}{2B} \quad (7)$$

The integral can be easily calculated with the following change of variables:

$$\xi = \sqrt{a}x_1 + \frac{b}{\sqrt{a}} \quad (8)$$

We then get:

$$\int_{-\infty}^{+\infty} \exp(-ax_1^2 - 2bx_1) dx_1 = \frac{\exp\left(\frac{b^2}{a}\right)}{\sqrt{a}} \int_{-\infty}^{+\infty} \exp(-\xi^2) d\xi = \sqrt{\frac{\pi}{a}} \exp\left(\frac{b^2}{a}\right) \quad (9)$$

Using this result, after some easy manipulations we can write  $I_1(x, z)$  as:

$$I_1(x, z) = \frac{1}{\sqrt{A + \frac{B}{q_1}}} \exp\left(-j \frac{kDx^2}{2B}\right) \exp\left(j \frac{kx^2}{2B} \frac{1}{A + \frac{B}{q_1}}\right) = \\ \frac{1}{\sqrt{A + \frac{B}{q_1}}} \exp\left[-j \frac{kx^2}{2B} \left(D - \frac{q_1}{Aq_1 + B}\right)\right] \quad (10)$$

Remembering that  $AD - BC = 1$ , the expression in brackets can be rearranged as:

$$D - \frac{q_1}{Aq_1 + B} = \frac{(AD - 1)q_1 + BD}{Aq_1 + B} = B \frac{Cq_1 + D}{Aq_1 + B} \quad (11)$$

Using this result, we can simplify  $I_1(x, z)$  to:

$$I_1(x, z) = \frac{1}{\sqrt{A + \frac{B}{q_1}}} \exp\left(-j \frac{kx^2}{2q}\right) \quad (12)$$

where:

$$q = \frac{Aq_1 + B}{Cq_1 + D} \quad (13)$$

We can derive an analogous expression for  $I_2(y, z)$  and thus obtain:

$$u(x, y, z) = I_1(x, z)I_2(y, z) = \frac{1}{\sqrt{A + \frac{B}{q_1}}} \exp\left[-\frac{jk}{2q} (x^2 + y^2)\right] \quad (14)$$

This is the sought result, showing that an optical system described by an ***ABCD*** ~~matrix~~ transforms a gaussian beam into another gaussian beam, with a complex parameter given by the so-called "***ABCD*** law".

This result is very important because it considerably simplifies the task of propagating a gaussian beam through an optical system. Instead of having to calculate a two-dimensional integral, in fact, we just need to compute algebraically the new  $q$  parameter of the beam.

## ANSWERS

### 4.10A A collimating lens.

The lens changes the complex **parameter**  $q$  of the gaussian beam according to the ABCD law:

$$\frac{1}{q_2} = \frac{C + \frac{D}{q_1}}{A + \frac{B}{q_1}} = \frac{1}{q_1} - \frac{1}{f} \quad (1)$$

Recalling that  $1/q = 1/R - j\lambda/(πw^2)$ , we see that the lens only changes the radius of curvature of the gaussian beam:

$$\frac{1}{R_2} = \frac{1}{R_1} - \frac{1}{f} \quad (2)$$

Therefore, to obtain a collimated beam after **the** lens ( $R_2 = \infty$ ) we need to choose the focal length equal to the radius of curvature of the impinging **beam**:

$$f = R_1 \quad (3)$$

The radius of curvature of the **beam** incident on **the** lens is in **turn** given by:

$$R_1 = d \left[ 1 + \left( \frac{z_R}{d} \right)^2 \right] \quad (4)$$

where, as usual,  $z_R = \pi w_0^2 / \lambda$ . Depending on the distance from **the** waist, therefore, a different focal **length** will be required in order to collimate the beam. Note that for  $d \gg z_R$  we get  $R_1 \approx d$  and the gaussian beam becomes a spherical wave originating from **the** waist, while for  $d \ll z_R$  we have  $R_1 \gg d$ , i.e. the gaussian beam behaves like a plane wave. The minimum focal length is needed at the distance **from the** waist for which the radius of curvature is minimum:

$$\frac{\partial R_1}{\partial d} = 1 - \frac{z_R^2}{d^2} = 0 \quad (5)$$

This occurs for  $d = z_R$ ; in **that** case we have  $R_1 = 2 z_R$ .

Note that it is a general property of gaussian **beams** that **the** minimum radius of curvature is reached at a **distance** from the waist equal to the Rayleigh range (see Fig. 4.16(b) in PL).

### 4.11A A simple optical processing system.

The  $ABCD$  matrix of this optical system can be calculated as:

$$\begin{vmatrix} A & B \\ C & D \end{vmatrix} = \begin{vmatrix} 1 & f \\ 0 & 1 \end{vmatrix} \begin{vmatrix} 1 & 0 \\ -\frac{1}{f} & 1 \end{vmatrix} \begin{vmatrix} 1 & f \\ 0 & 1 \end{vmatrix} = \begin{vmatrix} 1 & f \\ 0 & 1 \end{vmatrix} \begin{vmatrix} 1 & f \\ -\frac{1}{f} & 0 \end{vmatrix} = \begin{vmatrix} 0 & f \\ -\frac{1}{f} & 0 \end{vmatrix} \quad (1)$$

This matrix has the peculiarity of having both  $A = 0$  and  $D = 0$ . This simplifies considerably the **Kirchhoff-Fresnel** integral, which becomes:

$$u(x, y, z) = \frac{j}{B\lambda} \int_{-\infty}^{+\infty} \int_{-\infty}^{+\infty} u_1(x_1, y_1, z_1) \exp\left[j \frac{2\pi}{\lambda f} (xx_1 + yy_1)\right] dx_1 dy_1 \quad (2)$$

Recalling the definition of the two-dimensional Fourier transform of a function:

$$U(\xi, \eta) = \int_{-\infty}^{+\infty} \int_{-\infty}^{+\infty} u_1(x_1, y_1) \exp[j 2\pi (\xi x_1 + \eta y_1)] dx_1 dy_1 \quad (3)$$

the field of the output plane can be written as

$$u(x, y, z) = \frac{j}{B\lambda} U\left(\frac{x}{\lambda f}, \frac{y}{\lambda f}\right) \quad (4)$$

The physical interpretation of this very important result is straightforward: the field in the input plane of the optical system can be thought of as a superposition of plane waves, with different wave-vector (the so-called "angular spectrum" of the field): an ideal thin lens focuses each wave into a point in the focal plane. There is thus a one-to-one correspondence between plane waves and points in the focal plane, which can be expressed by a Fourier **transform**.

Note that, if the distance of the input plane of the system from the lens is  $d \neq f$ , then the  $ABCD$  matrix becomes:

$$\begin{vmatrix} A & B \\ C & D \end{vmatrix} = \begin{vmatrix} 1 & f \\ 0 & 1 \end{vmatrix} \begin{vmatrix} 1 & 0 \\ -\frac{1}{f} & 1 \end{vmatrix} \begin{vmatrix} 1 & d \\ 0 & 1 \end{vmatrix} = \begin{vmatrix} 0 & f \\ -\frac{1}{f} & 1 - \frac{d}{f} \end{vmatrix} \quad (5)$$

In this case one only has  $A = 0$ . The field in the output plane is then:

## ANSWERS

$$\begin{aligned}
 u(x, y, z) = & \frac{j}{B\lambda} \int_{-\infty}^{+\infty} \int_{-\infty}^{+\infty} u_1(x_1, y_1, z_1) \exp \left[ -\frac{j\pi}{\lambda f} \left( 1 - \frac{d}{f} \right) (x^2 + y^2) \right] \\
 & \times \exp \left[ j \frac{2\pi}{\lambda f} (x_1 x + y_1 y) \right] dx_1 dy_1 = \\
 & \frac{j}{B\lambda} \exp \left[ -\frac{j\pi}{\lambda f} \left( 1 - \frac{d}{f} \right) (x^2 + y^2) \right] U \left( \frac{x}{\lambda f}, \frac{y}{\lambda f} \right)
 \end{aligned} \tag{6}$$

We see that the output field is again given by the Fourier transform of the input field, but this time multiplied by a phase factor.

### 4.12A A laser driller.

The numerical aperture of a lens is defined as  $NA = \sin\theta$ , where  $\theta = \tan^{-1}(D/f)$ . In our case we get:

$$\theta = \sin^{-1}(0.3) = 17.5^\circ, \quad D = f \tan(\theta) = 15.7 \text{ mm} \tag{1}$$

The spot size that fully exploits the lens aperture is therefore

$$w_{01} = \frac{D}{2.25} \approx 7 \text{ mm} \tag{2}$$

In this case the Rayleigh range of the beam is:

$$z_{R1} = \frac{\pi w_{01}^2}{\lambda} = \frac{\pi \times 49 \text{ mm}^2}{0.532 \times 10^{-3} \text{ mm}} = 289 \text{ m} \tag{3}$$

Since  $z_{R1} \gg f$ , we can use for the spot size in the focus the simplified expression:

$$w_f = \frac{\lambda f}{\pi w_{01}} = \frac{0.532 \times 10^{-3} \text{ mm} \times 50 \text{ mm}}{\pi \times 7 \text{ mm}} = 1.2 \mu\text{m} \tag{4}$$

#### *Notes:*

- i) The spot size is of the same order of magnitude as the wavelength; in fact a diffraction limited optical beam can at best be focused to a dimension of the order of its wavelength. In order to get the tightest focusing, therefore, wavelengths as short as possible should be used;

- ii) Contrary perhaps to intuition, the spot size in the focal plane of the lens is smaller for increasing spot size on the lens; therefore, to get tight focusing we should fill the whole aperture of the lens with the laser **beam**;
- iii) For small  $\theta$ , we can make the approximation  $\theta \approx \tan\theta \approx \sin\theta$  and we get:  $NA \approx D/f$ , so that  $w_f \propto \lambda/NA$ . Therefore the tightest focusing can be achieved using a lens with large numerical aperture;
- iv) The previous calculations are valid under the assumption that the lens does not introduce any aberrations, i.e. for so-called “**diffraction-limited**” optics. It is often impossible to obtain diffraction limited focusing with **large** numerical aperture using a simple thin lens: in this case lens combinations, such as doublets and triplets, **that** compensate for the aberrations, must be used.

#### 4.13A An earth to moon laser rangefinder.

In order to minimize the beam divergence, we should choose the **maximum** spot size at the beam waist, i.e. the one that completely fills the telescope objective. In this case we obtain:  $w_0 = 012.25 = 0.444$  m. Assuming **that** the beam has a waist at the telescope objective, the spot size at a distance  $z$  is given by:

$$w(z) = w_0 \sqrt{1 + \left(\frac{z}{z_R}\right)^2} \quad (1)$$

where, as usual,  $z_R = \pi w_0^2 / \lambda$ . In our case:

$$z_R = \frac{\pi \times (0.444)^2 \text{ m}^2}{0.694 \times 10^{-6} \text{ m}} = 892 \text{ km} . \quad (2)$$

On the surface of the moon, since  $z \gg z_R$ , the previous expression simplifies to:

$$w(z) = w_0 \frac{z}{z_R} = \frac{\lambda z}{\pi w_0} = \frac{0.694 \times 10^{-6} \text{ m} \times 384 \times 10^6 \text{ m}}{\pi \times 0.444 \text{ m}} = 191 \text{ m} \quad (3)$$

#### 4.14A An He-Ne laser.

If we let  $w_0$  be the waist of the **gaussian** beam, we get:

$$w(z) = w_0 \sqrt{1 + \left(\frac{z}{z_R}\right)^2} \quad (1)$$

with the Rayleigh range given by  $z_R = \pi w_0^2 / \lambda$ . The far-field condition is reached when  $z \gg z_R$ ; in this case we have:

$$w(z) \approx w_0 \frac{z}{z_R} = \frac{\lambda z}{\pi w_0} = \theta_d z \quad (2)$$

The beam divergence is therefore:  $\theta_d = \lambda / (\pi w_0)$ . Knowing the divergence, we can thus calculate the waist spot size:

$$w_0 = \frac{\lambda}{\pi \theta_d} = \frac{0.632 \times 10^{-3} \text{ mm}}{\pi \times 10^{-3} \text{ rad}} \approx 0.2 \text{ mm} \quad (3)$$

Recalling that the power of the gaussian beam is related to its peak intensity  $I_0$  by:  $P = (\pi w_0^2 / 2) I_0$ , we obtain:

$$I_0 = \frac{2P}{\pi w_0^2} = \frac{2 \times 5 \times 10^{-3} \text{ W}}{\pi \times (0.2)^2 \text{ mm}^2} = 79.5 \frac{\text{mW}}{\text{mm}^2} \quad (4)$$

For a monochromatic e.m. wave, the relationship between intensity and peak electric field  $E_0$  is  $I_0 = \epsilon_0 c E_0^2 / 2 = E_0^2 / (2Z_0)$ , where  $Z_0 = \sqrt{\mu_0 / \epsilon_0} = 377 \Omega$  is the vacuum impedance. The **peak** electric field in the wait plane is therefore:

$$E_0 = \sqrt{2I_0 Z_0} = \sqrt{2 \times 79.5 \frac{\text{mW}}{\text{cm}^2} \times 377 \Omega} \approx 77 \frac{\text{V}}{\text{cm}} \quad (5)$$

#### 4.15A An Argon laser.

According to the law for gaussian beam propagation in free space, the spot size at a distance  $L$  from the beam waist is:

$$w(L) = w_0 \sqrt{1 + \left(\frac{L}{z_R}\right)^2} \quad (1)$$

where  $z_R = \pi w_0^2 / \lambda$  is the Rayleigh distance. By taking the square of this expression, we obtain:

$$w^2(L, w_0) = w_0^2 + \frac{L^2 \lambda^2}{\pi^2 w_0^2} \quad (2)$$

We thus see that the square of the spot size is the sum of two contributions: one that grows with growing initial spot size  $w_0$  (since, as it is obvious, the spot size will be greater than the value at the waist) and one that grows for decreasing spot sizes (since diffraction effects become more important for smaller waists); there must therefore be an optimum waist spot size, that guarantees the highest intensity on the target. This can be formally calculated by taking the derivative of (2) with respect to  $w_0$ :

$$2w \frac{\partial w}{\partial w_0} = 2w_0 - 2 \frac{L^2 \lambda^2}{\pi^2 w_0^3} = 0 \quad (3)$$

This equation allows to calculate the waist spot size for the highest intensity on the target:

$$w_0 = \sqrt{\frac{L\lambda}{\pi}} \quad (4)$$

Under those conditions, the spot size in the target plane can be easily calculated to be:

$$w(L) = \sqrt{2} w_0 = \sqrt{\frac{2 \times 5 \times 10^5 \text{ mm} \times 0.514 \times 10^{-3} \text{ mm}}{\pi}} = 12.8 \text{ mm} \quad (5)$$

and the peak intensity of the beam on the screen is:

$$I_0 = \frac{2P}{\pi w_0^2} = \frac{2 \times 1 \text{ W}}{\pi \times 1.28^2 \text{ cm}^2} = 0.5 \frac{\text{W}}{\text{cm}^2} \quad (6)$$

Note that the previous condition corresponds to:  $L = \pi w_0^2 / \lambda = z_R$ , i.e. we must choose the beam waist so that the Rayleigh range of the beam matches the distance from the screen.

#### 4.16A Gaussian beam propagation through an optical system.

The complex parameter  $q_1$  of the gaussian beam entering the system is given by:

$$\frac{1}{q_1} = \frac{1}{R_1} - j \frac{\lambda}{\pi w_1^2} \quad (1)$$

The complex parameter at the output plane can be calculated using the **ABCD** law:

$$\frac{1}{q} = \frac{C + \frac{D}{q_1}}{A + \frac{B}{q_1}} = \frac{C + \frac{D}{R_1} - j \frac{\lambda D}{\pi w_1^2}}{A + \frac{B}{R_1} - j \frac{\lambda B}{\pi w_1^2}} = \frac{\left( C + \frac{D}{R_1} - j \frac{\lambda D}{\pi w_1^2} \right) \left( A + \frac{B}{R_1} + j \frac{\lambda B}{\pi w_1^2} \right)}{\left( A + \frac{B}{R_1} \right)^2 + \left( \frac{\lambda B}{\pi w_1^2} \right)^2} \quad (2)$$

The spot size  $w$  at the output plane of the system is related to the imaginary part of  $1/q$ :

$$\text{Imag}\left(\frac{1}{q}\right) = -\frac{\lambda}{\pi w^2} = -\frac{\frac{\lambda}{\pi w_1^2} \left( AD + \frac{BD}{R_1} - BC - \frac{BD}{R_1} \right)}{\left( A + \frac{B}{R_1} \right)^2 + \left( \frac{\lambda B}{\pi w_1^2} \right)^2} \quad (3)$$

After straightforward manipulations and remembering the property **AD - BC = 1**, this expression can be rewritten as:

$$w^2 = w_1^2 \left[ \left( A + \frac{B}{R_1} \right)^2 + \left( \frac{\lambda B}{\pi w_1^2} \right)^2 \right] \quad (4)$$

which is the sought result.

*Notes:*

- i) The derived expression can be verified for the simple case of an imaging system ( $B = 0$ , see problem 4.4); in this case we get  $w_2 = A w_1$ , i.e. the input spot size is, as expected, magnified by a factor **A**.
- ii) Eq. (4) can be rewritten in a more useful form by noting that:

$$\left| A + \frac{B}{q_1} \right|^2 = \left( A + \frac{B}{R_1} \right)^2 + \left( \frac{B\lambda}{\pi w_1^2} \right)^2 \quad (5)$$

We then obtain the result

$$w^2 = w_1^2 \left| A + \frac{B}{q_1} \right|^2 \quad (6)$$

a useful expression which will be employed in the following problem.

#### 4. RAY AND WAVE PROPAGATION...

##### 4.17A Power conservation for a gaussian beam.

The electric field of the gaussian beam on the input plane of the system **can** be written as:

$$u_1(x_1, y_1) = U_0 \exp\left[-\frac{jk}{2q_1}(x_1^2 + y_1^2)\right] = \\ U_0 \exp\left[-\frac{jk}{2R_1}(x_1^2 + y_1^2)\right] \exp\left[-\frac{x_1^2 + y_1^2}{w_1^2}\right] \quad (1)$$

while its intensity is:

$$I_1(x_1, y_1) = \frac{1}{2} c \epsilon |u_1(x_1, y_1)|^2 = \frac{1}{2} c \epsilon U_0^2 \exp\left[-2 \frac{x_1^2 + y_1^2}{w_1^2}\right] \quad (2)$$

The power of the beam can be calculated as:

$$P_1 = \int_{-\infty}^{+\infty} \int_{-\infty}^{+\infty} I_1(x_1, y_1) dx_1 dy_1 = \frac{1}{2} c \epsilon U_0^2 \int_{-\infty}^{+\infty} \int_{-\infty}^{+\infty} \exp\left[-2 \frac{x_1^2 + y_1^2}{w_1^2}\right] dx_1 dy_1 \quad (3)$$

The double **integral** over the entire  $x_1$ - $y_1$  plane **can** be calculated more easily in polar coordinates. We then get :

$$x_1^2 + y_1^2 = r^2 \quad dx_1 dy_1 = 2\pi r dr \quad (4)$$

$$P_1 = \frac{1}{2} c \epsilon U_0^2 \int_0^{\infty} \exp\left[-2 \frac{r^2}{w_1^2}\right] 2\pi r dr \quad (5)$$

By making the additional change of variables:  $\rho = 2r^2/w_1^2$  we obtain:

$$P_1 = \frac{1}{2} c \epsilon U_0^2 \frac{w_1^2}{2} \int_0^{\infty} \exp(-\rho) d\rho = \frac{1}{4} c \epsilon U_0^2 w_1^2 \quad (6)$$

This is a useful expression connecting the power of a gaussian beam of spot size  $w_1$  to its **peak** electric field  $U_0$ . At the output plane of the optical system we have a gaussian beam with complex parameter  $q$  given by the ABCD law and amplitude:

$$U = \frac{U_0}{A + \frac{B}{q_1}} \quad (7)$$

By repeating the previous calculation, the beam power on the output plane is given by:

$$P = \frac{1}{4} c \epsilon U^2 \pi w^2 = \frac{1}{4} c \epsilon U_0^2 \pi w_1^2 \left( \frac{w}{w_1} \right)^2 \frac{1}{\left| A + \frac{B}{q_1} \right|^2} \quad (8)$$

Recalling the relationship, derived in the previous exercise,

$$\left( \frac{w}{w_1} \right)^2 = \left| A + \frac{B}{q_1} \right|^2 \quad (9)$$

we obtain  $P = P_0$ , i.e. the power of the gaussian beam is conserved.

*Note:*

The previous derivation is valid under the hypotheses that:

- i) the ABCD matrix of the system has real elements;
- ii) there are no limiting apertures in the optical system, so that the integral of the gaussian beam intensity can be calculated from  $-\infty$  to  $+\infty$ .

In these cases the power of the beam is conserved; if the ABCD matrix has complex elements, in general the power of the beam is not conserved. We will see an example of this in the following exercise.

#### 4.18A A "soft" or gaussian aperture.

If a gaussian beam of complex parameter  $q_1$  is impinging on the aperture, the electric field beyond the aperture is simply given by:

$$\begin{aligned} u(x, y) &= \exp \left[ -j \cdot 2 \frac{k}{q_1} (x^2 + y^2) \right] t(x, y) = \exp \left[ -j \cdot 2 \frac{k}{2q_1} (x^2 + y^2) \right] \\ &\exp \left[ -\frac{x^2 + y^2}{w_1^2} \right] = \exp \left[ -j \cdot 2 \frac{k}{2q_1} (x^2 + y^2) \right] \end{aligned} \quad (1)$$

where:

$$\frac{1}{4} = \frac{1}{4l} - \frac{j\lambda}{\pi w_a^2} \quad (2)$$

This expression can be rewritten in the form:

$$q = \frac{q_1}{1 - \frac{j\lambda q_1}{\pi w_a^2}} \quad (3)$$

Recalling the ABCD law for a gaussian beam transformation, it is easy to see that the aperture can be described by an ***ABCD*** matrix with the following parameters:

$$A = 1 \quad B = 0 \quad C = -\frac{j\lambda}{\pi w_a^2} \quad D = 1 \quad (4)$$

The soft aperture is thus described by an ***ABCD*** matrix with complex elements.

*Notes:*

- i) The “soft” aperture has an ***ABCD*** matrix equivalent to that of a thin lens, but with an imaginary focal length.
- ii) Gaussian apertures are encountered in laser physics and engineering: they can be used to simulate the effect of a “hard aperture or to model the radial gain profile in a longitudinally pumped system;
- iii) Apertures with a gaussian transmittance profile can also be obtained using special mirrors with radially variable reflectivity profile; these mirrors are specially used in connection with unstable resonators (see problems **5.20-5.22** in this book);
- iv) Now we can understand why, in an ***ABCD*** matrix with complex elements, power is not conserved: the gaussian aperture in fact, having a transmittance less than unity, causes some losses to the beam.

#### 4.19A A waist imaging system.

Since the beam has a waist on the input plane of the system, its complex parameter can be written as  $q_1 = j z_{R1}$ , with  $z_{R1} = \pi w_{01}^2 / \lambda$ . On the output plane of the system, the beam is transformed according to the ***ABCD*** law, so:

$$q_2 = \frac{Aq_1 + B}{Cq_1 + D} = \frac{jAz_{R1} + B}{jCz_{R1} + D} = \frac{BD + ACz_{R1}^2 + jz_{R1}}{C^2 z_{R1}^2 + D^2} \quad (1)$$

If the output plane of the system has to be a waist, we require that  $q_2 = j z_{R2}$ , which means:

$$\operatorname{Re}[q_2] = 0 \quad \text{or} \quad BD + AC z_{R1}^2 = 0 \quad (2)$$

which is the sought condition. In that case it is straightforward to derive the spot size on the output plane:

$$w_{02} = \frac{w_{01}}{\sqrt{\left(\frac{\pi C w_{01}^2}{\lambda}\right)^2 + D^2}} \quad (3)$$

#### 4.20A Gaussian beam transformation by a lens.

Let us call  $d_2$  the distance of the transformed beam waist from the lens. The *ABCD matrix* for the system is:

$$\begin{vmatrix} A & B \\ C & D \end{vmatrix} = \begin{vmatrix} 1 & d_2 \\ 0 & 1 \end{vmatrix} \begin{vmatrix} 1 & 0 \\ -\frac{1}{f} & 1 \end{vmatrix} \begin{vmatrix} 1 & d_1 \\ 0 & 1 \end{vmatrix} = \begin{vmatrix} 1 - \frac{d_2}{f} & d_1 + d_2 - \frac{d_1 d_2}{f} \\ -\frac{1}{f} & 1 - \frac{d_1}{f} \end{vmatrix} \quad (1)$$

In the previous problem we derived the condition in order to have a beam waist on the output plane:

$$AC z_{R1}^2 + BD = 0 \quad (2)$$

which, in our case, becomes:

$$\left(d_1 + d_2 - \frac{d_1 d_2}{f}\right) \left(1 - \frac{d_1}{f}\right) - \frac{z_{R1}^2}{f} \left(1 - \frac{d_2}{f}\right) = 0 \quad (3)$$

This equation allows to calculate the distance  $d_2$  of the new waist from the lens:

$$d_2 = f + \frac{f^2(d_1 - f)}{z_{R1}^2 + (d_1 - f)^2} \quad (4)$$

The spot size of this new beam waist is (using again the results of the previous problem):

$$w_{02} = \frac{w_{01}}{\sqrt{C^2 z_{R1}^2 + D^2}} = \frac{w_{01}}{\sqrt{\left(\frac{z_{R1}}{f}\right)^2 + \left(1 - \frac{d_1}{f}\right)^2}} \quad (5)$$

*Notes:*

- i) the position of the waist created by the lens depends on the initial spot size  $w_{01}$ , so the imaging condition for the waists of gaussian beams is different from that of geometrical optics;
- ii) if  $z_{R1} \gg d_1 - f$ , we get:

$$d_2 \approx f + \frac{f^2}{d_1 - f} - \frac{d_1 f}{d_1 - f} \quad (6)$$

and we recover the usual imaging condition of geometrical optics:

$$\frac{1}{d_1} + \frac{1}{d_2} = \frac{1}{f} \quad (7)$$

In that case the spot size becomes:

$$w_{02} = \frac{w_{01}}{\left|1 - \frac{d_1}{f}\right|} = \frac{d_2}{d_1} w_{01} \quad (8)$$

i.e. we get the magnification  $d_2/d_1$  predicted by geometrical optics. Under those conditions, in fact, the gaussian beam essentially behaves like a spherical wave.

- iii) If the beam waist is in the front focal plane of the lens,  $d_1 = f$ , we get

$$d_2 = f \quad (9)$$

i.e. the new waist is in the back focal plane of the lens. This result is in stark contrast with the predictions of geometrical optics, yielding  $d_2 = \infty$ .

#### 4.21A Focusing a gaussian beam inside a piece of glass.

Let us call  $x$  the distance of the waist of the gaussian beam from the input face of the material. In this case, the ABCD matrix of the propagation from the lens to the waist is:

$$\begin{vmatrix} A & B \\ C & D \end{vmatrix} = \begin{vmatrix} 1 & x \\ 0 & 1 \end{vmatrix} \begin{vmatrix} 1 & 0 \\ 0 & \frac{1}{n} \end{vmatrix} \begin{vmatrix} 1 & L \\ 0 & 1 \end{vmatrix} \begin{vmatrix} 1 & 0 \\ -\frac{1}{f} & 1 \end{vmatrix} = \begin{vmatrix} 1 & \frac{x}{n} \\ 0 & \frac{1}{n} \end{vmatrix} \begin{vmatrix} 1 - \frac{L}{f} & L \\ -\frac{1}{f} & 1 \end{vmatrix} =$$

$$\begin{vmatrix} 1 - \frac{L}{f} - \frac{x}{nf} & L + \frac{x}{n} \\ -\frac{1}{nf} & \frac{1}{n} \end{vmatrix} \quad (1)$$

Recalling the result, derived in problem 4.19, for the transformation of a waist into another waist:

$$BD + ACz_{R1}^2 = 0 \quad (2)$$

we get in our case:

$$\frac{L}{n} + \frac{x}{n^2} - \frac{z_{R1}^2}{nf} \left( 1 - \frac{L}{f} - \frac{x}{nf} \right) = 0 \quad (3)$$

With some easy manipulations and using the hypothesis  $z_{R1} \gg f$  we obtain:

$$x = n(f - L) \quad (4)$$

which reduces to  $x = f - L$  for  $n = 1$ . Thus, as expected, the focus is shifted to the right with respect to the vacuum case.

# CHAPTER 5

## Passive Optical Resonators

### PROBLEMS

#### 5.1P Stability of a resonator with concave mirrors.

Consider a resonator made of two concave mirrors ( $R_1 > 0, R_2 > 0$ ) spaced by a distance  $L$ . Find the values of  $L$  for which the resonator is stable.

What would be the stability range for a resonator made of two convex mirrors?

#### 5.2P A concave-convex resonator.

Consider a resonator made of a convex mirror (radius  $R_1 < 0$ ) and a concave mirror (radius  $R_2 > 0$ ) at a distance  $L$ . Find the values of  $L$  for which the resonator is stable (consider both the cases  $|R_1| > R_2$  and  $|R_1| < R_2$ ).

#### 5.3P A simple two-mirror resonator.

A two-mirror resonator is formed by a convex mirror of radius  $R_1 = -1$  m and a concave mirror of radius  $R_2 = 1.5$  m. What is the maximum possible mirror separation if this is to remain a stable resonator?

#### 5.4P Number of longitudinal modes in a resonator.

Consider the active medium Nd:YAG (refractive index  $n = 1.82$ , linewidth  $\Delta\nu = 120$  GHz).

- Consider first a resonator with length  $L = 50$  cm, employing a rod of length  $l = 10$  cm. Find the number of longitudinal modes falling within the FWHM gain linewidth;
- Consider then a resonator made upon coating the end mirrors directly onto the active material surfaces (microchip laser). What is the maximum thickness  $l$  that allows oscillation of only one longitudinal mode?

## PROBLEMS

### **5.5P Resonators for an Argon laser.**

Consider a resonator consisting of two concave spherical mirrors both with radius of curvature  $4\text{ m}$  and spaced by a distance of  $1\text{ m}$ .

- (a) Calculate the spot size of the  $\text{TEM}_{\infty}$  mode at the resonator center and on the mirrors when laser oscillation **occurs** at the  $\text{Ar}^+$  laser wavelength  $\lambda_{\text{Ar}} = 0.514\text{ }\mu\text{m}$ .
- (b) Calculate the spot sizes on the mirrors if mirror  $M_1$  is replaced by a plane mirror.

### **5.6P A resonator for a $\text{CO}_2$ laser.**

Repeat the calculations of point (a) in problem 5.5 if **the** resonator is **employed** for the  $\text{CO}_2$  laser wavelength  $\lambda_{\text{CO}_2} = 10.6\text{ }\mu\text{m}$ .

### **5.7P A near-planar resonator.**

Consider a symmetric near-planar resonator, made of two mirrors of radii  $R_1 = R_2 = R$ , separated by a distance  $L$ , with  $L \ll R$ .

- (a) Obtain an approximate expression for the spot sizes at the beam waist and on the end mirrors.
- (b) Calculate the spot sizes for a resonator oscillating at  $\lambda = 514\text{ nm}$  (**an** argon laser wavelength) with  $L = 1\text{ m}$  and  $R = 8\text{ m}$ .
- (c) Compare the results to those obtained by a confocal resonator of the same length.

### **5.8P Single-mode selection in a He-Ne laser.**

Consider a He-Ne laser, oscillating at the wavelength  $\lambda = 0.633\text{ }\mu\text{m}$  and using a symmetric confocal resonator with mirror radius  $R = 0.5\text{ m}$ . Assume that the **aperturing** effect produced by the bore of the capillary containing the He-Ne gas mixture can be simulated by a diaphragm of radius  $a$  in front of the spherical mirrors. If the power gain per pass of the He-Ne laser is  $2 \times 10^{-2}$ , calculate the diaphragm radius needed to suppress the  $\text{TEM}_{01}$  mode

**5.9P Spot sizes on the mirrors of a stable resonator.**

For a generic stable resonator:

- (a) express the spot sizes on the end mirrors as a functions of the single-pass propagation **matrix** elements  $A_1$ ,  $B_1$ ,  $C_1$  and  $D_1$ ;
- (b) show that the resonator is at a stability limit when either  $A_1$ ,  $B_1$ ,  $C_1$  or  $D_1$  are zero;
- (c) evaluate the spot sizes on the end mirrors **corresponding** to these four stability limits.

**5.10P A plano-concave resonator.**

Consider a plano-concave resonator where the radius of the concave mirror is  $R$  and the resonator distance is  $L$ . Calculate the  $\text{TEM}_{00}$  mode spot sizes at the two end mirrors.

**5.11P A near-concentric resonator.**

Consider a near-concentric resonator made of two concave mirrors of radius  $R$  spaced by the distance  $L = 2R - \Delta L$ . Give an approximate expression of the spot sizes at the beam waist and on the mirrors as a function of  $L$  and  $\Delta L$ .

**5.12P The unlucky graduate student.**

A graduate student is instructed by **his** advisor to align a laser with a confocal resonator using two mirrors of nominal radius of curvature  $R = 200$  mm. Unfortunately, due to manufacturing errors, the radii of curvature of the two mirrors are  $R_1 = R + \Delta R$ ,  $R_2 = R - \Delta R$ , with  $\Delta R = 3$  mm. After **spending** unsuccessfully long nights in the lab trying to achieve laser action at the nominally confocal distance  $L = 200$  mm, the student finds that the laser works if the two mirrors are moved either slightly closer or slightly farther **than** the confocal position. Explain this result and find the mirror spacing at **which** the laser starts working.

### 5.13P Resonator with an intracavity lens.

A resonator consists of two plane mirrors with a lens inserted between them. If the focal length of the lens is  $f$ , and  $L_1$ ,  $L_2$  are the distances of the mirrors from the lens, calculate the values of the focal length  $f$  for which the cavity is stable. (*Level of difficulty higher than average*)

### 5.14P Resonator for a cw-pumped Nd:YAG laser.

In high power cw-pumped Nd:YAG lasers with a cylindrical gain medium, due to pump-induced thermal effects, the rod can be simulated by a thin lens with **dioptric** power proportional to the **pump** power,  $1/f = k P_{\text{pump}}$ . Consider a simple resonator for such a laser, consisting of two plane mirrors at distances  $L_1 = 0.5$  m,  $L_2 = 1$  m from the rod. Assuming  $k = 0.5 \text{ m}^{-1} \text{ kW}^{-1}$  and using the results of the previous problem, calculate the pump power stability range for this resonator.

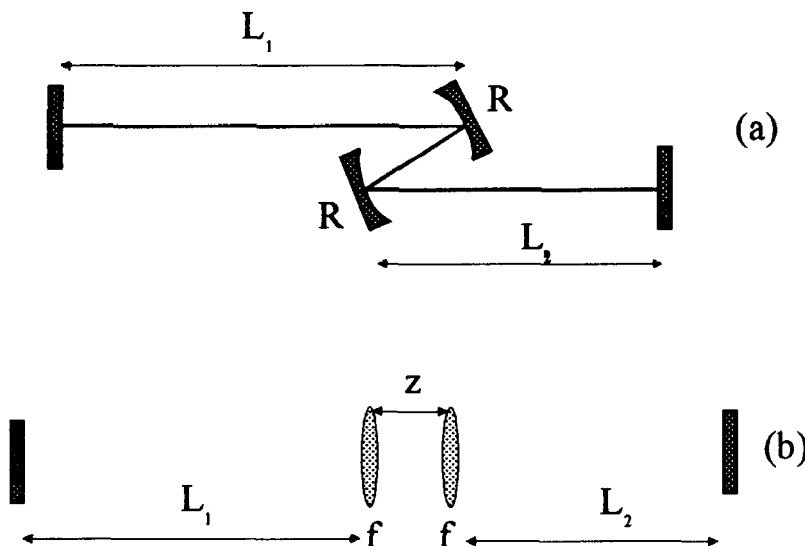


Fig. 5.1: Schematic of a resonator used for a **Ti:sapphire** laser (a) and equivalent representation (b).

### 5.15P Resonator for a Ti:sapphire laser.

Typical cw-pumped Ti:sapphire lasers employ a four-mirror resonator of the type shown in Fig. 5.1(a), with two plane end mirrors and two curved folding

mirrors. The **Ti:sapphire** medium consists of a platelet inserted, at Brewster angle, between the two folding mirrors. Neglecting the astigmatism produced by the two folding mirrors and by the platelet, the resonator can be represented as in Fig. 5.1(b), with two **intracavity** lenses of focal length  $f$  separated by a distance  $z$ . Assume the following parameters, typical of a Kerr lens mode-locked **Ti:sapphire** laser:  $L_1 = 500 \text{ mm}$ ,  $L_2 = 1000 \text{ mm}$ ,  $f = 50 \text{ mm}$ . Find the values of the folding mirrors distance  $z$  for which the resonator is stable, knowing that the stability condition, in terms of the  $(A_1, B_1, C_1, D_1)$  one-way matrix elements, can be written as  $0 < A_1 D_1 < 1$ .

*(Level of difficulty higher than average)*

### 5.16P Location of the beam waist in a stable resonator.

Consider a stable resonator consisting of two mirrors, of radii  $R_1$  and  $R_2$ , separated by a distance  $L$ . Find the location of the beam waist of the fundamental mode of the resonator.

[Hint: recalling that the end mirrors are **equiphase** surfaces for the resonator mode, try to match a **gaussian** mode to the end mirrors]

*(Level of difficulty higher than average)*

### 5.17P Properties of a symmetric confocal resonator.

Consider a symmetric confocal resonator, made of two mirrors of radius  $R$  separated by a distance  $L = R$ .

- (a) Prove that any symmetric field distribution on one mirror will be reproduced after one roundtrip.
- (b) Prove that the field distributions on the two end mirrors are related to each other by a Fourier transform.

[Hint: write the field distribution on one mirror as:

$$u_1(x_1, y_1) = A_1(x_1, y_1) \exp[jk(x_1^2 + y_1^2)/2R]$$

*(Level of difficulty higher than average)*

### 5.18P Asymmetric confocal resonators.

Show that all confocal resonators can be represented, in the  $g_1$ - $g_2$  plane, by an hyperbola having asymptotes  $g_1 = 1/2$  and  $g_2 = 1/2$ . Show then that all asymmetric confocal resonators are unstable.

## PROBLEMS

### **5.19P A confocal unstable resonator.**

Consider an unstable resonator for a **CO<sub>2</sub>** laser ( $\lambda = 10.6 \mu\text{m}$ ) consisting of two mirrors, of radii  $R_1 = 4 \text{ m}$  and  $R_2 = -2 \text{ m}$ .

- (a) find the mirror separation L so that the resonator is confocal;
- (b) calculate the resonator **magnification**;
- (c) calculate the mirror sizes so that the resonator is **single-ended** and the equivalent Fresnel number is  $N_{eq} = 0.5$ ;
- (d) **calculate** the output coupling losses using the geometrical optics and the diffractive optics approaches.

### **5.20P Unstable resonator with gaussian mirrors: properties of the output beam.**

Consider an unstable resonator with magnification M, employing an output coupling mirror with gaussian reflectivity profile  $R(r) = R_0 \exp(-2r^2/w_m^2)$ .

- (a) Prove that the output **beam** presents a dip in the center when  $R_0 > 1/M^2$ ;
- (b) prove that when  $R_0 M^2 = 1$  (the so-called maximally flat case) the output coupling losses for the resonator are given by  $\gamma = 1 - 1/M^4$ .

### **5.21P Designing a gaussian mirror for an unstable resonator.**

A diode-pumped **Nd:YAG** laser is equipped with an unstable resonator with gaussian output coupler. By operating **the** laser with a stable resonator, the optimum output coupling loss  $\gamma_{OPT} = 0.6$  is determined. The laser uses a rod with 3.2 mm radius placed as close as possible to the gaussian mirror. Using the results of the previous problem, design a gaussian mirror so that: (a) the laser is optimally coupled; (b) the output beam is maximally flat; (c) the mode efficiently fills the laser rod (assume a clipping of the mode by the beam aperture at an intensity that is 2% of the peak value).

### **5.22P Unstable resonator with a supergaussian mirror.**

Consider an unstable resonator consisting of a convex mirror (mirror 1) of radius  $R_1$  and a plane mirror (mirror 2) separated by a distance  $L = 50 \text{ cm}$ . Assume that the plane mirror has a super-Gaussian reflectivity profile with a super-Gaussian order  $n = 6$  and peak power-reflectivity  $R_0 = 0.5$ . Assume also that **the** active medium consists of a cylindrical rod (**e.g.** a **Nd:YAG** rod) with

radius  $a = 3.2$  mm placed just in front of mirror 2. To limit round-trip losses to an acceptable value, assume also a round-trip magnification  $M = 1.4$ . Calculate: (a) the spot size  $w$  of the field intensity  $I_{in}$  for a  $2 \times 10^{-2}$  intensity truncation by the active medium; (b) the corresponding mirror spot size  $w_m$ ; (c) the cavity round-trip losses; (d) the radius of curvature of the convex mirror.

## ANSWERS

### ANSWERS

#### **5.1A Stability of a resonator with concave mirrors.**

Let us assume  $R_1 < R_2$ . The stability condition for the resonator, according to Eq. 5.4.11 in PL, can be written as:

$$0 < g_1 g_2 < 1 \quad (1)$$

where  $g_1 = 1 - L/R_1$ ,  $g_2 = 1 - L/R_2$ . The stability condition is equivalent to the two inequalities

$$\left(1 - \frac{L}{R_1}\right) \left(1 - \frac{L}{R_2}\right) > 0 \quad (2a)$$

$$\left(1 - \frac{L}{R_1}\right) \left(1 - \frac{L}{R_2}\right) < 1 \quad (2b)$$

The first one can be rearranged as

$$\frac{L^2}{R_1 R_2} - L \left( \frac{1}{R_1} + \frac{1}{R_2} \right) + 1 > 0 \quad (3)$$

and is satisfied when  $L < R_1$  and  $L > R_2$ . Inequality (2b) can be rewritten as

$$\frac{L^2}{R_1 R_2} - L \left( \frac{1}{R_1} + \frac{1}{R_2} \right) < 0 \quad (4)$$

which is valid when  $L > 0$  and  $L < R_1 + R_2$ . Combining the results, we find for the resonator the following two stability regions:

$$0 < L < R_1 \quad R_2 < L < R_1 + R_2 \quad (5)$$

Note that the two stability regions have, in terms of the mirrors distance  $L$ , the same width  $\Delta L = \min(R_1, R_2)$ . If the resonator is symmetric, the two regions coalesce into one.

If both mirrors are convex ( $R_1 < 0$ ,  $R_2 < 0$ ), then both  $g_1$  and  $g_2$  are greater than 1, and  $g_1 g_2 > 1$ , so that the stability condition can never be satisfied.

### 5.2A A concave-convex resonator.

The stability condition for a simple two-mirror resonator results in the two inequalities:

$$g_1 g_2 > 0 \quad (1a)$$

$$g_1 g_2 < 1 \quad (1b)$$

where  $g_1 = 1 - L/R_1$ ,  $g_2 = 1 - L/R_2$ . In our case, since  $R_1 < 0$ , we have  $g_1 > 0$  for all values of L; therefore (1a) becomes  $g_2 > 0$  or equivalently  $L < R_2$ . The second condition is:

$$\left(1 - \frac{L}{R_1}\right) \left(1 - \frac{L}{R_2}\right) < 1 \quad (2)$$

which, after straightforward manipulations, becomes:

$$\frac{L}{R_1 R_2} < \frac{1}{R_1} + \frac{1}{R_2} \quad (3)$$

Multiplying both sides of (3) by  $R_1 R_2$  and recalling that, upon multiplication by a negative constant, the sign of an inequality is reversed, we obtain:

$$L > R_1 + R_2 \quad (4)$$

Note that, if  $|R_1| > R_2$ , (4) is always satisfied. In conclusion, the mirrors distance range for which the resonator remains stable is:

$$\begin{array}{lll} R_1 + R_2 < L < R_2 & \text{if} & |R_1| < R_2 \\ 0 < L < R_2 & \text{if} & |R_1| > R_2 \end{array}$$

### 5.3A A simple two-mirror resonator.

Using the analysis of the previous problem, since  $|R_1| < R_2$ , we find that the resonator remains stable when  $R_1 + R_2 < L < R_2$ , i.e. for  $L > 0.5$  m and  $L < 1.5$  m.

### 5.4A Number of longitudinal modes in a resonator.

The frequency spacing between longitudinal modes in the resonator is given by

$$\Delta\nu = \frac{c}{2L'} \quad (1)$$

## ANSWERS

where

$$L' = (L - l) + n l = L + (n - 1) l = 58.2 \text{ cm} \quad (2)$$

is the equivalent resonator length. We recall that, since the light speed in a material of refractive index  $n$  is  $c/n$ , the propagation in a material of length  $l$  is equivalent to a free space propagation over a length  $nl$ . From Eqs. (1) and (2) we obtain  $\Delta\nu = 258.6 \text{ MHz}$ . The number of longitudinal modes falling within the Nd:YAG gain linewidth is thus:

$$N = \frac{\Delta\nu_{\text{YAG}}}{\Delta\nu} \approx 464 \quad (3)$$

For the case of end mirrors directly coated onto the surfaces of the laser rod (microchip laser) the longitudinal mode separation is

$$\Delta\nu = \frac{c}{2nl} \quad (4)$$

In order to achieve single longitudinal mode operation, the mode spacing must be such that  $\Delta\nu \geq \Delta\nu_{\text{YAG}}/2$ ; this way, in fact, if one mode is tuned to coincide with the center of the gain curve, the two adjacent longitudinal modes are far away enough from the line center that, for a laser not too far above threshold, they cannot oscillate. It is then easy to obtain:

$$l \leq \frac{c}{n \Delta\nu_{\text{YAG}}} = 1.4 \text{ mm} \quad (5)$$

which is a thickness quite easy to manufacture. Single-longitudinal mode Nd:YAG laser based on the microchip concept are thus easily feasible. In fact they are commercially available.

### **5.5A A resonator for an Argon laser.**

Since the resonator is symmetric, the beam waist is located at the resonator center. The g parameters of this cavity are

$$g_1 = g_2 = g = 1 - \frac{L}{R} = 0.75 \quad (1)$$

One has therefore  $g_1 g_2 = 0.562$  and the cavity is stable. The spot size at the beam waist, according to Eq. (5.5.10b) of PL, is given by

$$w_0 = \left( \frac{L\lambda}{\pi} \right)^{1/2} \left[ \frac{1+g}{4(1-g)} \right]^{1/4} \quad (2)$$

Using the given parameters, it is easy to calculate  $w_0 = 0.465$  mm. The spot sizes on the end mirrors, according to Eq. (5.5.10a) in PL, are given by

$$w = \left( \frac{\lambda L}{\pi} \right)^{1/2} \left( \frac{1}{1-g^2} \right)^{1/4} \quad (3)$$

Inserting the given values, we obtain  $w = 0.497$  mm. We can thus see that the  $\text{TEM}_{\infty}$  mode spot size remains nearly constant along the resonator axis.

If mirror  $M_1$  becomes planar, the resonator is asymmetric. In this case  $g_1 = 1$ ,  $g_2 = 0.75$ , so that  $g_1 g_2 = 0.75$  and the resonator is again stable. The spot sizes on the mirrors can be calculated using Eqs. (5.5.8) from PL:

$$w_1 = \left( \frac{L\lambda}{\pi} \right)^{1/2} \left[ \frac{g_2}{g_1(1-g_1g_2)} \right]^{1/4} \quad (4)$$

$$w_2 = \left( \frac{L\lambda}{\pi} \right)^{1/2} \left[ \frac{g_1}{g_2(1-g_1g_2)} \right]^{1/4} \quad (5)$$

Inserting the relevant numerical values in Eqs. 4 and 5, we obtain  $w_1 = 0.532$  mm,  $w_2 = 0.614$  mm. The spot sizes are thus somewhat larger than those obtained with the previous symmetric cavity. Note that the beam waist occurs at the plane mirror location. Thus  $w_1$  is also the spot size at the beam waist  $w_0$ .

### 5.6A A resonator for a CO<sub>2</sub> laser.

The results obtained for the Argon laser wavelength in the previous problem can be easily scaled to the CO<sub>2</sub> case by observing that the spot size is proportional to the square root of wavelength. We can thus obtain:

$$w_{CO2} = \left( \frac{\lambda_{CO2}}{\lambda_{Ar}} \right)^{1/2} w_{Ar} = 2.25 \text{ mm} \quad (1)$$

$$w_{0CO2} = \left( \frac{\lambda_{CO2}}{\lambda_{Ar}} \right)^{1/2} w_{0Ar} = 2.11 \text{ mm} \quad (2)$$

Note that, for a similar resonator design, the  $\text{TEM}_{\infty}$  mode spot size is about a factor of four larger in the CO<sub>2</sub> laser. For both the Argon and the CO<sub>2</sub> lasers, the

**calculated** mode sizes fit quite well the bore radii of **typical** discharge tubes, so that efficient single transverse mode operation can be obtained quite easily.

### 5.7A A near-planar resonator.

Since the resonator is symmetric, the spot size at the **beam** waist is obtained from Eq. (5.5.10a) of PL:

$$w_0 = \left( \frac{L\lambda}{\pi} \right)^{1/2} \left[ \frac{1+g}{4(1-g)} \right]^{1/4} = \left( \frac{L\lambda}{\pi} \right)^{1/2} \left[ \frac{2 - \frac{L}{R}}{4 \frac{L}{R}} \right]^{1/4} \quad (1)$$

Since  $L \ll R$ , eq. (1) **can be approximated** to:

$$w_0 \approx \left( \frac{L\lambda}{\pi} \right)^{1/2} \left( \frac{R}{2L} \right)^{1/4} \quad (2)$$

The spot sizes at the end mirrors can be obtained from Eq. (5.5.10b) of PL:

$$w_1 = w_2 = \left( \frac{L\lambda}{\pi} \right)^{1/2} \left( \frac{1}{1-g^2} \right)^{1/4} \quad (3)$$

Recalling that  $L/R \ll 1$ , we obtain:

$$g^2 = \left( 1 - \frac{L}{R} \right)^2 = 1 + \left( \frac{L}{R} \right)^2 - 2 \frac{L}{R} \approx 1 - 2 \frac{L}{R} \quad (4)$$

Substituting Eq. (4) into Eq. (3), we obtain:

$$w_1 = w_2 \approx \left( \frac{L\lambda}{\pi} \right)^{1/2} \left( \frac{R}{2L} \right)^{1/4} \quad (5)$$

In the near-planar resonator approximation, therefore, the spot sizes at the beam waist and on the mirror surfaces are the same.

For the Argon laser resonator given in the problem, we obtain:

$$w_0 = w_1 = w_2 = \left( \frac{10^3 \text{ mm} \times 0.514 \times 10^{-3} \text{ mm}}{\pi} \right)^{1/2} (4)^{1/4} = 0.57 \text{ mm} \quad (6)$$

A confocal resonator of the same length as the near-planar one has mirror radii  $R_1 = R_2 = 1$  m; in this case  $g_1 = g_2 = 0$  and, again using Eqs. (5.5.10), we obtain:

$$w_0 = \left( \frac{L\lambda}{2\pi} \right)^{1/2} \approx 0.29 \text{ mm} \quad w = \left( \frac{L\lambda}{\pi} \right)^{1/2} \approx 0.4 \text{ mm} \quad (7)$$

We thus see that, compared to a confocal resonator, a near-planar one allows to obtain larger spot sizes, even if the increase is not **dramatic**.

### 5.8A Single mode selection in a He-Ne laser.

To fulfill the **confocality** condition, the resonator length must be  $L = R = 0.5$  m. Its  $g$  parameters are  $g_1 = g_2 = 0$ . In order to suppress the  $\text{TEM}_{01}$  mode, the mirror aperture must cause on this mode a loss per transit greater than 0.01. From Fig. 5.13b of PL, we see that 1% losses for the  $\text{TEM}_{01}$  mode are obtained for a Fresnel number  $N = a^2/L\lambda \cong 1$ . From this expression one readily gets the value for the bore radius as:

$$a = (NL\lambda)^{1/2} \cong 0.562 \text{ mm} \quad (1)$$

Note that, for the quoted value of the Fresnel number, the losses of the  $\text{TEM}_{\infty}$  mode (see Fig. 5.13a in PL) are much lower, less than 0.1%.

### 5.9A Spot sizes on the mirrors of a stable resonator.

Let us consider a generic resonator made of two plane mirrors containing an optical system with single pass propagation matrix  $A_1, B_1, C_1, D_1$ ; the scheme of such a resonator is shown in Fig. 5.8d of PL. The  $q$  parameters on the end mirrors can be easily obtained [see Eqs. (5.5.6) in PL]:

$$q_1 = j \sqrt{-\frac{B_1 D_1}{A_1 C_1}} \quad q_2 = j \sqrt{\frac{A_1 B_1}{C_1 D_1}} \quad (1)$$

The  $q$  parameter is related to the radius of curvature  $R$  and spot size  $w$  of the modes by the:

$$\frac{1}{q} = \frac{1}{R} - \frac{j\lambda}{\pi w^2} \quad (2)$$

Since the end mirrors are **equiphasic** surfaces for the resonator, the phase fronts on these mirrors are flat, i.e.  $R_1 = R_2 = \infty$ , and Eq. (2) becomes:

$$q = j \frac{\pi w^2}{\lambda} \quad (3)$$

By combining (1) and (3), we can obtain the spot sizes on the end mirrors as a function of the single-pass **matrix** elements:

$$w_1 = \left( \frac{\lambda}{\pi} \right)^{1/2} \left( -\frac{B_1 D_1}{A_1 C_1} \right)^{1/4} \quad w_2 = \left( \frac{\lambda}{\pi} \right)^{1/2} \left( -\frac{A_1 B_1}{C_1 D_1} \right)^{1/4} \quad (4)$$

To obtain the stability limits, we recall that the stability condition, in terms of the single-pass **matrix** elements, becomes:

$$0 \leq A_1 D_1 \leq 1 \quad (5)$$

Eq. (5) shows that  $A_1 = 0$  and  $D_1 = 0$  correspond indeed to stability limits. The other limits are obtained when  $A_1 D_1 = 1$ . Recalling the property of any ABCD matrix of having unitary determinant ( $A_1 D_1 - B_1 C_1 = 1$ ), this second condition becomes  $B_1 C_1 = 0$ ; thus also  $B_1 = 0$  and  $C_1 = 0$  are stability limits.

Using Eqs. 4, we can now evaluate the mode spot sizes at the stability limits. We obtain:

$$A_1 \rightarrow 0 \quad w_1 \rightarrow \infty \quad w_2 \rightarrow 0 \quad (6a)$$

$$B_1 \rightarrow 0 \quad w_1 \rightarrow 0 \quad w_2 \rightarrow 0 \quad (6b)$$

$$C_1 \rightarrow 0 \quad w_1 \rightarrow \infty \quad w_2 \rightarrow \infty \quad (6c)$$

$$D_1 \rightarrow 0 \quad w_1 \rightarrow 0 \quad w_2 \rightarrow \infty \quad (6d)$$

Of course, at the stability limits the gaussian beam analysis is no more valid; nevertheless, Eqs. (6) are **useful** to predict the trend of the  $\text{TEM}_{\infty}$  mode size on the mirrors as the resonator approaches the stability limits.

## 5.10A A plano-concave resonator.

The g parameters of the plano-concave resonator are:

$$g_1 = 1 \quad g_2 = 1 - \frac{L}{R} \equiv g \quad (1)$$

For  $R>0$ ,  $g_2<1$ , so  $g_1 g_2 < 1$  for any value of  $L$ ; the resonator becomes unstable when  $g_2<0$ , i.e. when  $L>R$ . To calculate the mode spot sizes on the mirrors, let us first write the single pass propagation matrix:

$$\begin{vmatrix} A_1 & B_1 \\ C_1 & D_1 \end{vmatrix} = \begin{vmatrix} 1 & 0 \\ -\frac{1}{R} & 1 \end{vmatrix} \begin{vmatrix} 1 & L \\ 0 & 1 \end{vmatrix} = \begin{vmatrix} 1 & L \\ -\frac{1}{R} & 1 - \frac{L}{R} \end{vmatrix} \quad (2)$$

Using the results of the previous problem, we can easily calculate the spot sizes on the end mirrors:

$$w_1 = \left(\frac{\lambda}{\pi}\right)^{1/2} \left(-\frac{B_1 D_1}{A_1 C_1}\right)^{1/4} = \left(\frac{\lambda}{\pi}\right)^{1/2} [L(R-L)]^{1/4} \quad (3)$$

$$w_2 = \left(\frac{\lambda}{\pi}\right)^{1/2} \left(-\frac{A_1 B_1}{C_1 D_1}\right)^{1/4} = \left(\frac{\lambda}{\pi}\right)^{1/2} R \left(\frac{L}{R-L}\right)^{1/4} \quad (4)$$

Note that, as the resonator approaches the stability limit ( $L \rightarrow R$ ,  $D_1 \rightarrow 0$ ), the spot size tends to vanish on mirror  $M_1$  and to diverge on mirror  $M_2$ , in agreement with the analysis of the previous problem.

Note:

In the following we outline an alternative procedure for solving the problem. The beam waist occurs at the plane mirror and if we let  $w_0$  be the spot size at this waist we can write [see Eq. (4.7.17b) of PL]

$$R(z) = z \left[ 1 + \left( \frac{z_R}{z} \right)^2 \right] \quad (5)$$

where  $R$  is the radius of curvature of the equiphase surface at the distance  $z$  from the waist and  $z_R = \pi w_0^2 / \lambda$  is the Rayleigh distance. At the position of the concave mirror the equiphase surface must coincide with the mirror surface,  $R$ . We thus have  $R(L) = R$  and from Eq. (5) we get

$$z_R = L \left[ \left( \frac{R}{L} \right) - 1 \right]^{1/2} \quad (6)$$

The spot size at the beam waist, i.e. at the plane mirror, can then be obtained as

$$w_0 = w_1 = \left(\frac{\lambda L}{\pi}\right)^{1/2} \left[ \frac{R}{L} - 1 \right]^{1/4} \quad (7)$$

The spot size at the concave mirror,  $w_2$ , is then obtained from the relation [see (4.7.17a) of PL]

$$w(z) = w_0 \left[ 1 + \left( \frac{z}{z_R} \right)^2 \right]^{1/2} \quad (8)$$

Upon setting  $w(z) = w_2$  and  $z = L$ , with the help of Eq. (7) we readily get

$$w_2 = \left( \frac{\lambda}{\pi} \right)^{1/2} R \left( \frac{L}{R - L} \right)^{1/4} \quad (9)$$

### 5.11A A near-concentric resonator.

As stated in the text, in a near-concentric resonator the mirrors distance fulfills the condition:

$$L = 2R - \Delta L \quad (1)$$

with  $\Delta L \ll L$ . The cavity g-parameters can thus be written as

$$g_1 = g_2 = g = 1 - \frac{L}{R} = 1 - 2 + \frac{2\Delta L}{L + \Delta L} \approx -1 + \frac{2\Delta L}{L} \quad (2)$$

Note that, for  $\Delta L = 0$ , one has  $g_1 g_2 = 1$ , i.e. the resonator is at a stability limit (concentric cavity). With the help of Eq. (5.5.10b) of PL, the spot size at the beam waist can be calculated as

$$\begin{aligned} w_0 &= \left( \frac{L\lambda}{\pi} \right)^{1/2} \left[ \frac{1+g}{4(1-g)} \right]^{1/4} \approx \\ &\left( \frac{L\lambda}{\pi} \right)^{1/2} \left[ \frac{1-1+2\Delta L/L}{4(1+1-2\Delta L/L)} \right]^{1/4} \approx \left( \frac{L\lambda}{\pi} \right)^{1/2} \left[ \frac{\Delta L}{4L} \right]^{1/4} \end{aligned} \quad (3)$$

The spot sizes at the mirrors can be calculated using Eq. (5.5.10a) of PL as:

$$\begin{aligned}
 w_1 = w_2 &= \left( \frac{L\lambda}{\pi} \right)^{1/2} \left[ \frac{1}{1-g^2} \right]^{1/4} = \\
 &\left( \frac{L\lambda}{\pi} \right)^{1/2} \left[ \frac{1}{1 - 1 - 4(\Delta L/L)^2 + 4\Delta L/L} \right]^{1/4} \cong \left( \frac{L\lambda}{\pi} \right)^{1/2} \left[ \frac{L}{4\Delta L} \right]^{1/4}
 \end{aligned} \tag{4}$$

Note:

From Eqs. (3) and (4) it can easily be seen that, as  $\Delta L \rightarrow 0$ , i.e. as the resonator approaches the concentric condition, the spot size at the beam waist vanishes, while that on the mirrors becomes progressively larger. Upon approaching the stability limit, the resonator mode thus tends to a spherical wave originating at the resonator center.

### 5.12A The unlucky graduate student.

When the student places the two mirrors in the nominally confocal position, at a distance  $L = R = 200$  mm, the stability parameters of the cavity are:

$$g_1 = 1 - \frac{R}{R + \Delta R} > 0 \quad g_2 = 1 - \frac{R}{R - \Delta R} < 0 \tag{1}$$

One therefore has  $g_1 g_2 < 0$  and the cavity is unstable. To move the cavity into a stable configuration, one must have  $g_1 g_2 > 0$ , i.e.:

$$\left( 1 - \frac{L}{R + \Delta R} \right) \left( 1 - \frac{L}{R - \Delta R} \right) > 0 \tag{2}$$

which can be cast into the form:

$$L^2 - 2RL + (R + \Delta R)(R - \Delta R) > 0 \tag{3}$$

It is easy to show that inequality (3) is satisfied for  $L > R + AR$  and  $L < R - AR$ . Therefore the student has to move the mirrors by  $AR = 3$  mm either closer or farther than the confocal position to bring the resonator into the stable region and thus achieve laser action.

### 5.13A Resonator with an intracavity lens.

We recall that the stability condition for a resonator can be written as:

$$-1 < \frac{A + D}{2} < 1 \quad (1)$$

where  $A$  and  $D$  are the **roundtrip matrix** elements. For a general resonator with plane minors, this expression turns out to be simpler in terms of the elements of the one-way propagation **matrix**. One has in fact [see Fig. 5.8 of PL]:

$$A = D = 2A_1D_1 - 1 \quad (2)$$

and the inequality (1) becomes

$$0 < A_1D_1 < 1 \quad (3)$$

The one-way matrix for the resonator of the problem can be simply calculated as:

$$\begin{vmatrix} A_1 & B_1 \\ C_1 & D_1 \end{vmatrix} = \begin{vmatrix} 1 & L_2 \\ 0 & 1 \end{vmatrix} \begin{vmatrix} \frac{1}{f} & 0 \\ -\frac{1}{f} & 1 \end{vmatrix} \begin{vmatrix} 1 & L_1 \\ 0 & 1 \end{vmatrix} = \begin{vmatrix} 1 - \frac{L_2}{f} & L_1 + L_2 - \frac{L_1 L_2}{f} \\ -\frac{1}{f} & 1 - \frac{L_1}{f} \end{vmatrix} \quad (4)$$

The stability condition (3) then becomes simply

$$0 < \left(1 - \frac{L_2}{f}\right) \left(1 - \frac{L_1}{f}\right) < 1 \quad (5)$$

which corresponds to the two inequalities

$$L_1 L_2 \left(\frac{1}{f}\right)^2 - (L_1 + L_2) \left(\frac{1}{f}\right) + 1 > 0 \quad (6a)$$

$$L_1 L_2 \left(\frac{1}{f}\right)^2 - (L_1 + L_2) \left(\frac{1}{f}\right) < 0 \quad (6b)$$

Let us now assume that  $L_2 > L_1$ . In this case, it can easily be shown that (6a) is valid when

$$\frac{1}{f} < \frac{1}{L_1} \quad \frac{1}{f} > \frac{1}{L_2} \quad (7a)$$

while (6b) is satisfied when

$$\frac{1}{f} > 0 \quad \frac{1}{f} < \frac{1}{L_1} + \frac{1}{L_2} \quad (7b)$$

Both inequalities are verified when

$$0 < \frac{1}{f} < \frac{1}{L_2} \quad \frac{1}{L_1} < \frac{1}{f} < \frac{1}{L_1} + \frac{1}{L_2} \quad (8)$$

We see therefore, that, as the focal length of the intracavity lens is varied, the resonator crosses two stability regions. These regions have the same width in terms of the lens dioptric power  $1/f$ :

$$\Delta\left(\frac{1}{f}\right) = \frac{1}{L_2} \quad (9)$$

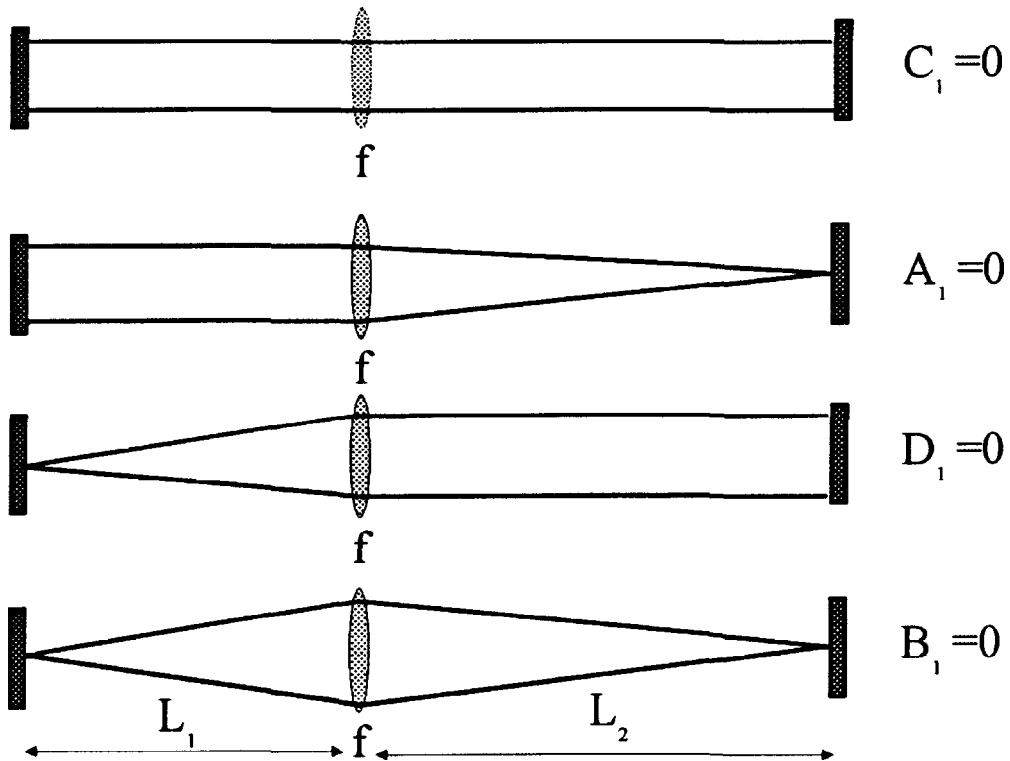


Fig. 5.2 Geometrical optics predictions for the cavity modes for the resonator of problem 5.13 at the stability limits.

Note:

It is interesting to consider the geometrical optics prediction for the resonator modes corresponding to the stability limits, shown in Fig. 5.2. When  $1/f = 0$  ( $C_1 = 0$ ) the lens has **infinite** focal length, i.e. there is no lens inside the resonator. In this case we have a plane-parallel resonator and the mode is a **plane** wave. When  $1/f = 1/L_2$  ( $A_1 = 0$ ) we have, according to the results of problem 5.9,  $w_1 \rightarrow \infty$  and  $w_2 \rightarrow 0$ . In this **case** the mode can be **pictured**, by **geometrical** optics, as a plane wave on mirror  $M_1$  which is focused by the lens on mirror  $M_2$ . When  $1/f = 1/L_1$  ( $D_1 = 0$ ) we have  $w_1 \rightarrow 0$  and  $w_2 \rightarrow \infty$ . In this **case** the mode can be pictured as a spherical wave originating on mirror  $M_1$  which is collimated by the lens and transformed into a plane wave on mirror  $M_2$ . Finally, when  $1/f = 1/L_1 + 1/L_2$  ( $B_1 = 0$ ) we have  $w_1 \rightarrow 0$  and  $w_2 \rightarrow 0$ . In this case the lens images a spherical wave originating on mirror  $M_1$  onto mirror  $M_2$ . Although a gaussian beam analysis loses validity at the stability limits, these considerations can help predicting the mode size behavior on the mirrors as the stability limit is approached (for example, focusing on one end mirror can result in catastrophic damage or can be used to enhance some intensity-dependent nonlinear optical process taking place close to the mirror).

### 5.14A Resonator for a cw-pumped Nd:YAG laser.

Let us first calculate the values of the **dioptric** power for the **intracavity** lens corresponding to the stability limits. Using the results of the previous problem, we obtain:

$$\frac{1}{f_a} = 0 \text{ m}^{-1} \quad \frac{1}{f_b} = \frac{1}{L_2} = 1 \text{ m}^{-1} \quad \frac{1}{f_c} = \frac{1}{L_1} = 2 \text{ m}^{-1} \quad \frac{1}{f_d} = \frac{1}{L_1} + \frac{1}{L_2} = 3 \text{ m}^{-1} \quad (1)$$

Given the linear relationship between thermal lens dioptric power and pump power, we can easily calculate the pump power stability limits:

$$P_a = 0 \text{ kW} \quad P_b = 2 \text{ kW} \quad P_c = 4 \text{ kW} \quad P_d = 6 \text{ kW} \quad (2)$$

### 5.15A Resonator for a Ti:sapphire laser.

Let us calculate the single-pass propagation matrix for the resonator of Fig. 5.1b:

$$\begin{vmatrix} A_1 & B_1 \\ C_1 & D_1 \end{vmatrix} = \begin{vmatrix} 1 & L_2 \\ 0 & 1 \end{vmatrix} \begin{vmatrix} 1 & 0 \\ -\frac{1}{f} & 1 \end{vmatrix} \begin{vmatrix} 1 & z \\ 0 & 1 \end{vmatrix} \begin{vmatrix} 1 & 0 \\ -\frac{1}{f} & 1 \end{vmatrix} \begin{vmatrix} 1 & L_1 \\ 0 & 1 \end{vmatrix} \quad (1)$$

After some lengthy but **straightforward** calculations, this **matrix** can be expressed as:

$$\begin{vmatrix} A_1 & B_1 \\ C_1 & D_1 \end{vmatrix} = \begin{vmatrix} \left(1 - \frac{L_2}{f}\right)\left(1 - \frac{z}{f}\right) - \frac{L_2}{f} & L_1 \left[ \left(1 - \frac{L_2}{f}\right)\left(1 - \frac{z}{f}\right) - \frac{L_2}{f} \right] + L_2 + z \left(1 - \frac{L_2}{f}\right) \\ -\frac{1}{f} - \frac{1}{f} \left(1 - \frac{z}{f}\right) & -\frac{L_1}{f} - \frac{L_1}{f} \left(1 - \frac{z}{f}\right) + 1 - \frac{z}{f} \end{vmatrix} \quad (2)$$

Eq. (2) shows that, as expected, the single-pass matrix elements are functions of the distance  $z$ . From the stability condition  $0 < A_1 D_1 < 1$ , since  $A_1 D_1 - B_1 C_1 = 1$ , one readily obtains that the condition  $A_1 D_1 < 1$  is equivalent to the condition  $B_1 C_1 < 0$ . The stability condition can thus equivalently be written as

$$A_1 D_1 > 0 \quad (3a)$$

$$B_1 C_1 < 0 \quad (3b)$$

The stability of the cavity is thus closely related to the sign of the one-way matrix elements. Let us assume  $L_1, L_2 > f$  (which is true for any realistic Ti:sapphire resonator) and let us also take  $L_1 < L_2$ . The conditions under which the matrix elements are positive can be easily calculated from Eq. (2) as:

$$A_1 > 0 \quad z < z_A = f + \frac{f L_2}{L_2 - f} \quad (4)$$

$$B_1 > 0 \quad z > z_B = \frac{L_1 f}{L_1 - f} + \frac{L_2 f}{L_2 - f} \quad (5)$$

$$C_1 > 0 \quad z > z_C = 2f \quad (6)$$

$$D_1 > 0 \quad z < z_D = f + \frac{L_1 f}{L_1 - f} \quad (7)$$

It is easy to show that  $z_C < z_A < z_D < z_B$ . The stability condition given by Eq. (3a) is satisfied when  $z < z_A$  and  $z > z_D$ , while the stability condition expressed by Eq. (3b) holds for  $z > z_C$  and  $z < z_B$ ; combining the two inequalities, we obtain the following stability ranges for the distance  $z$  between the two folding mirrors:

$$z_C < z < z_A \quad z_D < z < z_B \quad (8)$$

We thus obtain two stability ranges for this distance  $z$ , both of which have the same width:

$$\Delta z = \frac{f^2}{L_2 - f} \quad (9)$$

For the numerical values given in the problem, we find the following stability ranges:

$$100 \text{ mm} < z < 102.63 \text{ mm} \quad 105.55 \text{ mm} < z < 108.18 \text{ mm} \quad (10)$$

The width of each stability region is just  $\Delta z = 2.63 \text{ mm}$ , and thus careful measurement of the folding mirrors distance is required to achieve laser action.

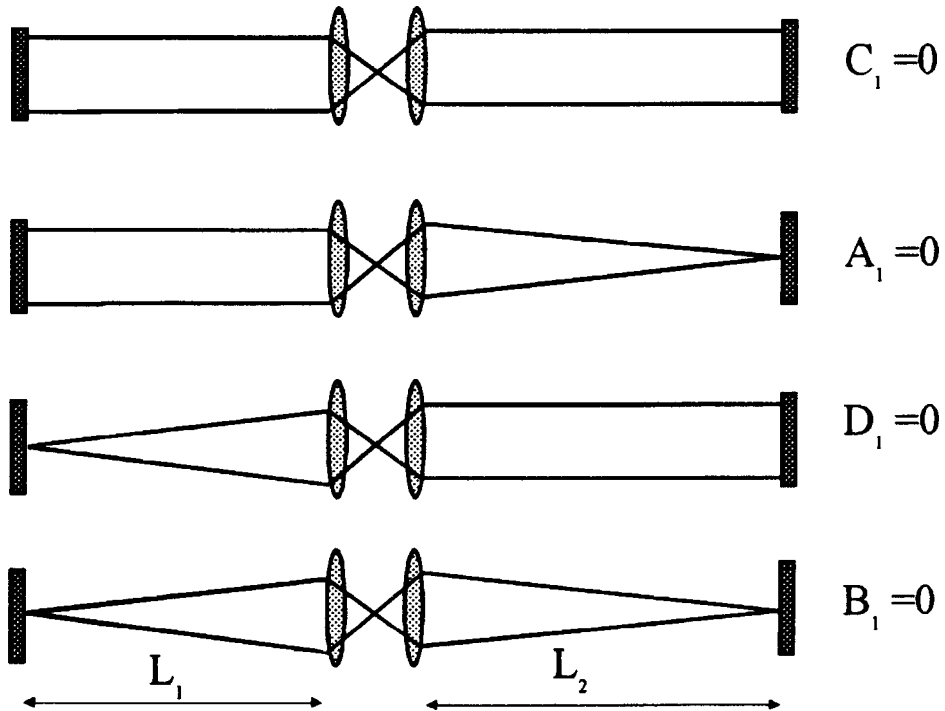


Fig. 5.3 Geometrical optics predictions for the cavity modes for the resonator of problem 5.15 at the stability limits.

Note:

Also in this case some useful physical insight can be obtained by considering the geometrical optics description of the modes at the stability limits: this is illustrated in Fig. 5.3 (the derivation of the modes is left to the reader). It can be seen that, for example, in the second stability region the mode remains focused on  $M_1$ , while its size on  $M_2$  decreases gradually.

### 5.16A Location of the beam waist in a stable resonator.

To solve this problem, let  $z = 0$  correspond to the location of the beam waist and let us assume  $z > 0$  going from the left to the right. The radius of curvature of the gaussian beam is given by the well-known expression:

$$R(z) = z + \frac{z_R^2}{z} \quad (1)$$

where  $z_R = \pi w_0^2 / \lambda$  is the Rayleigh range. Let  $z_1$  and  $z_2$  be the distances of the mirrors from the beam waist, respectively (if both mirrors are concave, the waist occurs between the two mirrors and one has  $z_1 < 0$  and  $z_2 > 0$ ). The mirrors distance  $L$  can then be expressed as:

$$L = z_2 - z_1 \quad (2)$$

We now have to impose the condition that the mirrors are **equiphasic** surfaces for the mode, i.e. the mirror radii match the radii of curvature of the Gaussian beam. We can then write the simple equations:

$$-R_1 = z_1 + \frac{z_R^2}{z_1} \quad (3)$$

$$R_2 = z_2 + \frac{z_R^2}{z_2} \quad (4)$$

Note the minus sign on the left-hand side of Eq. (3), due to the fact that the radius of a gaussian beam is assumed negative to the left of the beam waist, while the radius of curvature of mirror  $M_1$  is assumed positive if it is concave. (1), (3) and (4) are a set of three equations in the unknowns  $z_1$ ,  $z_2$  and  $z_R$ : solving them will yield the distances of the beam waist from the end mirrors as well as the its spot size. By expressing the mirror radii as a function of the cavity  $g$  parameters ( $g_i = 1 - L/R_i$ ), Eqs. (3) and (4) can be recast into the form:

$$-\frac{Lz_1}{1-g_1} = z_1^2 + z_R^2 \quad (5)$$

$$\frac{Lz_2}{1-g_2} = z_2^2 + z_R^2 \quad (6)$$

**Subtracting** (5) from (6) and exploiting (2), we obtain the equation:

$$(z_1 + L)^2 - z_1^2 = \frac{(z_1 + L)L}{1-g_2} + \frac{Lz_1}{1-g_1} \quad (7)$$

It is now a matter of simple algebra to solve Eq. (7) and obtain:

$$z_1 = -\frac{Lg_2(1-g_1)}{g_1+g_2-2g_1g_2} \quad (8)$$

From Eq. (2) we then obtain:

$$z_2 = z_1 + L = \frac{Lg_1(1-g_2)}{g_1+g_2-2g_1g_2} \quad (9)$$

Eqs. (8) and (9) are the solutions to our problem. The results can be usefully checked by considering the limiting cases of resonators with one plane mirror. If  $R_1 = \infty$ , then  $g_1 = 1$  and Eqs. (8)-(9) give, as expected,  $z_1 = 0$  and  $z_2 = L$  (similarly, for  $R_2 = \infty$ , we get  $g_2 = 1$ ,  $z_2 = 0$  and  $z_1 = -L$ ).

Finally, by inserting for example Eq. (9) into Eq. (6) we get, after some simple algebra:

$$z_R^2 = \frac{L^2 g_1 g_2 (1-g_1 g_2)}{(g_1+g_2-2g_1g_2)^2} \quad (10)$$

The spot size at the beam waist is then obtained as:

$$w_0 = \left( \frac{L\lambda}{\pi} \right)^{1/2} \left[ \frac{g_1 g_2 (1-g_1 g_2)}{(g_1+g_2-2g_1g_2)^2} \right]^{1/4} \quad (11)$$

which is the same result obtained in PL (Eq. 5.5.9) using a different procedure.

### 5.17A Properties of a symmetric confocal resonator.

Let us consider a stable confocal resonator, with mirror radii  $R_1 = R_2 = R$  and mirrors distance  $L = R$ . The first point of the problem can be easily proven by considering the resonator roundtrip matrix, starting from mirror  $M_1$ :

$$\begin{aligned} \begin{vmatrix} A & B \\ C & D \end{vmatrix} &= \begin{vmatrix} 1 & 0 \\ -\frac{2}{R} & 1 \end{vmatrix} \begin{vmatrix} 1 & R \\ 0 & 1 \end{vmatrix} \begin{vmatrix} 1 & 0 \\ -\frac{2}{R} & 1 \end{vmatrix} \begin{vmatrix} 1 & R \\ 0 & 1 \end{vmatrix} = \\ &= \begin{vmatrix} 1 & R \\ -\frac{2}{R} & -1 \end{vmatrix} \begin{vmatrix} 1 & R \\ -\frac{2}{R} & -1 \end{vmatrix} = \begin{vmatrix} -1 & 0 \\ 0 & -1 \end{vmatrix} \end{aligned} \quad (1)$$

We thus see that, apart from a change of sign, the roundtrip matrix is the **unitary** matrix, i.e. the **matrix** corresponding to a plane mirror. Thus any field distribution on one **mirror** will be reproduced **after** one **roundtrip**.

To prove the second point, let us consider a generic self-consistent field distribution on mirror  $M_1$ . Since the mirror surface is an **equiphase** surface, this distribution can be written as:

$$u_1(x_1, y_1) = A(x_1, y_1) \exp\left[-\frac{jk(x_1^2 + y_1^2)}{2(-R)}\right] = A(x_1, y_1) \exp\left[\frac{jk(x_1^2 + y_1^2)}{2R}\right] \quad (2)$$

In Eq. (2),  $A(x_1, y_1)$  is a real function and we adopt the usual sign convention for **the** radius of curvature. The field distribution on **mirror**  $M_2$  can be simply obtained by applying the Huygens-Fresnel integral to a **propagation** over a distance  $R$ :

$$u_2(x_2, y_2) = \frac{j}{\lambda R} \int_{-\infty}^{+\infty} \int_{-\infty}^{+\infty} u_1(x_1, y_1) \exp\left\{-jk\left[\frac{x_1^2 + y_1^2 + x_2^2 + y_2^2 - 2x_1x_2 - 2y_1y_2}{2R}\right]\right\} dx_1 dy_1 \quad (3)$$

Inserting Eq. (2) into Eq. (3), we obtain:

$$u_2(x_2, y_2) = \frac{j}{\lambda R} \exp\left[-\frac{jk(x_2^2 + y_2^2)}{2R}\right] \int_{-\infty}^{+\infty} \int_{-\infty}^{+\infty} u_1(x_1, y_1) \exp\left[\frac{jk}{2R}(2x_1x_2 + 2y_1y_2)\right] dx_1 dy_1 \quad (4)$$

which, apart from a phase factor, represents the two-dimensional Fourier transform of **the** field distribution on mirror  $M_1$ .

### 5.18A Asymmetric confocal resonators.

A resonator is confocal if the mirrors distance  $L$  equals the sum of their focal lengths:

$$L = f_1 + f_2 \quad (1)$$

where  $f_1 = R_1/2$  and  $f_2 = R_2/2$ . Equation (1) can be rewritten in the form:

$$1 - \frac{R_1}{L} + 1 - \frac{R_2}{L} = 0 \quad (2)$$

or, recalling the definitions of  $g_1$  and  $g_2$ ,

$$1 - \frac{1}{1-g_1} + 1 - \frac{1}{1-g_2} = 0 \quad (3)$$

With some easy manipulations, Eq. (3) can be cast into the form

$$2g_1g_2 - g_1 - g_2 = 0 \quad (4)$$

which can alternatively be written as

$$(2g_1 - 1)(2g_2 - 1) = 1 \quad (5)$$

Eq. (5) represents an hyperbola having asymptotes  $g_1 = \frac{1}{2}$ ,  $g_2 = \frac{1}{2}$ . The curve lies outside the stability region of the resonator except for the two points  $g_1 = g_2 = 1$  (plane-parallel resonator) and  $g_1 = g_2 = 0$  (symmetric confocal resonator) which are at the boundaries of the stability region. Thus all asymmetric confocal resonators are unstable

### 5.19A A confocal unstable resonator.

The mirrors separation required to have a confocal resonator is:

$$L = (R_1 + R_2)/2 = 1 \text{ m} \quad (1)$$

The self-consistent mode in this case can be described as a spherical wave originating at the common focus, which is collimated by mirror  $M_1$  and turned again into a spherical wave by mirror  $M_2$  (see Fig. 5.18 of PL). In this case the **roundtrip magnification** is simply given by:

$$M = \frac{|R_1|}{|R_2|} = 2 \quad (2)$$

If the resonator is single ended, the equivalent Fresnel number is given by:

$$N_{eq} = \frac{(M-1)a_2^2}{2L\lambda} \quad (3)$$

To achieve  $N_{eq} = 0.5$  from Eq. (3) we calculate the mirror radius as  $a_2 = 3.26$  mm. To insure single-ended operation, the radius  $a_1$  of mirror  $M_1$  must fulfill the condition  $a_1 > Ma_2 = 6.52$  mm.

The coupling losses can first be calculated from geometrical optics as

$$\gamma_G = 1 - \frac{1}{M^2} \quad (4)$$

In our **case**, we obtain  $\gamma_G = 0.75$ . The value for the coupling losses, according to **diffractive** optics, *can* then be obtained from Fig. 5.22 of PL for a **magnification**  $M = 2$  and an equivalent **Fresnel** number  $N_{eq} = 0.5$ . We get  $\gamma_D = 0.4$ . Note that **diffractive** optics yields **significantly** lower values for the output coupling losses. Physically, this result is due to the fact that radial intensity distribution of the mode, instead of being flat as predicted by geometrical optics, has a bell shape **peaking** on the axis.

### 5.20A Unstable resonator with gaussian mirrors: properties of the output beam.

The radial intensity distribution of the beam incident on the gaussian mirror can be written as:

$$I_{in}(r) = I_0 \exp(-2r^2/w_i^2) \quad (1)$$

where:  $w_i^2 = w_m^2(M^2 - 1)$ . The intensity distribution of the transmitted beam is:

$$I_t(r) = I_{in}(r) [1 - R(r)] = I_0 \exp(-2r^2/w_i^2) [1 - R_0 \exp(-2r^2/w_m^2)] \quad (2)$$

Eq. (2) can be rewritten as:

$$I_t(r) = I_0 [\exp(-2r^2/w_i^2) - R_0 \exp(-2M^2 r^2/w_i^2)] \quad (3)$$

This distribution presents a dip for  $r = 0$  when it has a **maximum** for  $r > 0$ ; this occurs at the radial position for which  $dr/dl = 0$ , i.e.:

$$I_0 \left[ -\frac{4r^2}{w_i^2} \exp(-2r^2/w_i^2) + R_0 \frac{4rM^2}{w_i^2} \exp(-2r^2M^2/w_i^2) \right] = 0 \quad (4)$$

Eq. (4) has the solution, which can be easily verified to correspond to a maximum:

$$r_{max} = \left[ \frac{w_i^2}{M^2 - 1} \log(R_0 M^2) \right]^{1/2} \quad (5)$$

In order for  $r_{max}$  to be a real positive number,  $\log(R_0 M^2) > 0$  is required, i.e.

$$R_0 > \frac{1}{M^2} \quad (6)$$

The situation in which the dip just begins to appear (the so-called maximally flat condition) is achieved when  $R_0 M^2 = 1$ . Let us calculate, under this condition, the average mirror reflectivity:

$$\bar{R} = \frac{P_{ref}}{P_{in}} \quad (7)$$

where  $P_{ref}$  and  $P_{in}$  are reflected and incident powers, respectively. These can be easily calculated as:

$$P_{in} = \int_0^\infty I_0 \exp\left(-2r^2/w_i^2\right) 2\pi r dr = \frac{\pi w_i^2}{2} I_0 \quad (8)$$

$$\begin{aligned} P_{ref} &= \int_0^\infty I_0 R_0 \exp\left[-2r^2\left(\frac{1}{w_i^2} + \frac{1}{w_m^2}\right)\right] 2\pi r dr = \\ &\int_0^\infty I_0 R_0 \exp\left(-2\frac{r^2 M^2}{w_i^2}\right) 2\pi r dr = \frac{\pi w_i^2}{2} \frac{R_0}{M^2} I_0 \end{aligned} \quad (9)$$

By taking the ratio of (9) and (8), we obtain the radially averaged reflectivity as:  $\bar{R} = R_0/M^2$ . For the case of a maximally flat profile ( $R_0 = 1/M^2$ ) we obtain  $\bar{R} = 1/M^4$  and the output coupling losses are  $\gamma = 1 - 1/M^4$ .

### 5.21A Designing a gaussian mirror for an unstable resonator.

For a maximally flat output beam, the output coupling losses are given by (see previous problem):

$$\gamma = 1 - \frac{1}{M^4} \quad (1)$$

In our case, for  $\gamma = 0.6$ , the resonator magnification is obtained from Eq. (1) as  $M = 1.257$ . The peak reflectivity of the gaussian mirror that satisfies the maximally flat condition is:

$$R_0 = \frac{1}{M^2} = 0.632 \quad (2)$$

We now need to design the spot size of the mirror reflectivity profile,  $w_m$ . To this purpose, let us first calculate the desired mode size  $w_i$  incident on the

output coupler. To achieve 2% clipping of the mode intensity at the rod edge ( $r = a = 3.2$  mm) we need to impose:

$$I_0 \exp\left(-2\sigma^2/w_i^2\right) = 0.02I_0 \quad (3)$$

Solving Eq. (3) we obtain  $w_i = 2.29$  mm. Finally the mirror spot size is given by:

$$w_m = \frac{w_i}{\sqrt{M^2 - 1}} = 3 \text{ mm} \quad (4)$$

The mirror design is now complete; the final step in the resonator design will require selecting the appropriate mirror radii and their distance so as to achieve the required magnification.

### 5.22A Unstable resonator with supergaussian mirrors.

To answer question (a), we recall that the radial intensity profile of a supergaussian mode of order  $n$  is:

$$I(r) = I_0 \exp\left[-2\left(\frac{r}{w}\right)^n\right] \quad (1)$$

In our case, the required mode truncation by the active medium corresponds to:

$$I(a) = I_0 \times 2 \times 10^{-2} \quad (2)$$

or equivalently:

$$\exp\left[-2\left(\frac{a}{w}\right)^n\right] = 2 \times 10^{-2} \quad (3)$$

Solving Eq. (3), we obtain:  $w = 2.86$  mm. The mode spot size on the supergaussian mirror is related to the mirror spot size  $w_m$  and the roundtrip magnification by:

$$w = w_m (M^n - 1)^{1/n} \quad (4)$$

From Eq. (4) one gets  $w_m = 2.09$  mm. The cavity roundtrip losses  $\gamma$  depend only on the roundtrip magnification and the peak mirror reflectivity  $R_0$ :

## ANSWERS

$$\gamma = 1 - \frac{R_0}{M^2} \quad (5)$$

From Eq. (5) we obtain  $\gamma = 0.745$ .

In order to choose the radius  $R_1$  needed to obtain the assumed magnification, we need the relationship between magnification and the cavity g parameters. This is given by Eq. (5.6.4) of PL which, in our case ( $g_2 = 1$ ), becomes:

$$M = 2g_1 - 1 + 2g_1 \left(1 - \frac{1}{g_1}\right)^{1/2} \quad (6)$$

After some straightforward manipulations Eq. (6) can be solved for  $g_1$ , giving:

$$g_1 = \frac{(M+1)^2}{4M} = 1.0286 \quad (7)$$

The radius of curvature of mirror  $M_1$  is then given by:

$$R_1 = \frac{L}{1-g_1} = -17.5 \text{ m} \quad (8)$$

# CHAPTER 6

## Pumping Processes

### PROBLEMS

#### 6.1P Critical pump rate in a lamp-pumped Nd:YLF laser.

A Nd:YLF rod 5 mm in diameter, 6.5 cm long, with  $1.3 \times 10^{20}$  Nd atoms/cm<sup>3</sup> is cw-pumped by two lamps in a **close-coupled** configuration. Energy separation between upper laser level and ground level approximately corresponds to a wavelength of 940 nm. The electrical pump power spent by each lamp at **threshold**, when the rod is inserted in the laser cavity, is  $P_{\text{lamp}} = 1$  kW. Assuming that the rod is uniformly pumped with an overall pump efficiency  $\eta_p = 4\%$ , calculate the corresponding critical pump rate.

#### 6.2P Pump rate expression for longitudinal pumping.

Prove that, for longitudinal pumping, the pump rate is  $R_p(r,z) = a I_p(r,z)/h\nu_p$ , where  $I_p(r,z)$  is the pump intensity in the active medium and  $a$  is the absorption coefficient at the frequency  $\nu_p$  of the pump.

#### 6.3P Laser spot size in a longitudinally pumped Ti:Al<sub>2</sub>O<sub>3</sub> laser under optimum pumping conditions.

A Ti:Al<sub>2</sub>O<sub>3</sub> rod is inserted in a z-shaped folded linear cavity (see Fig. 6.11c of PL) and is longitudinally pumped, only from one side, by the focused beam of an Ar<sup>+</sup> laser at the pump wavelength  $\lambda_p = 514$  nm. Assume a round trip loss of the cavity  $\gamma_r = 6\%$ , an effective stimulated-emission cross section  $\sigma_e = 3 \times 10^{-19}$  cm<sup>2</sup>, a lifetime of the upper laser level  $\tau = 3 \mu\text{s}$  and a pump efficiency  $\eta_p = 30\%$ . Under optimum pumping conditions **calculate** the designed laser spot size  $w_0$  in the active rod, so that a threshold pump power  $P_{th} = 1$  W **is** achieved.

### **6.4P Optical pumping of a Ti:Al<sub>2</sub>O<sub>3</sub> laser: a design problem.**

With reference to the Ti:Al<sub>2</sub>O<sub>3</sub> laser configuration considered in the previous problem, assume that the spot size  $w_{pl}$  of the pump beam at the focusing lens is equal to 0.7 mm. Assume that the pump beam is focused in the active **medium** throughout one of the folding spherical mirror of the resonator (see Fig. 6.11c of PL). Also assume that this mirror consists of a **plane-concave** mirror with refractive index  $n = 1.5$  and radius of curvature of the concave surface  $R = 220$  mm. Calculate the focal length of the pump-focussing lens so that a pump spot size  $w_p = 27 \mu\text{m}$  is obtained in the active medium.

### **6.5P Doping in a solid-state laser medium.**

The density of a YAG (Y<sub>3</sub>Al<sub>5</sub>O<sub>12</sub>) crystal is 4.56 g cm<sup>-3</sup>. Calculate the density of Yb ions in the crystal when 6.5% of Yttrium ions are substituted by Ytterbium ions (6.5 atom.% Yb).

### **6.6P A transversely pumped high-power Nd:YAG laser.**

A Nd:YAG rod with a diameter of 4 mm, a length of 6.5 cm and 1 atom.% Nd doping is transversely pumped at 808 nm wavelength in the pump configuration of Fig. 6.15 of PL. Assume that 90% of the optical power emitted from the pumping fibers is uniformly absorbed in the rod and that the mode spot size is 0.7 **times** the rod radius (optimal spot). To obtain high power from the laser, an output mirror of 15% transmission is used. Including other internal losses, a loss per single pass of  $\gamma = 10\%$  is estimated. If the effective stimulated emission cross section is taken as  $\sigma_e = 2.8 \times 10^{-19} \text{ cm}^2$  and the upper laser level lifetime is  $\tau = 230 \mu\text{s}$ , calculate the optical power required **from** the fibers to reach laser threshold.

### **6.7P Longitudinal vs. transverse pumping in Nd:YAG laser.**

The Nd:YAG rod of problem 6.6 is longitudinally pumped in the **pump** configuration of Fig. 6.11a of PL. Assume that: (a) the single pass loss  $\gamma = 10\%$  and the mode spot size  $w_0 = 1.4$  mm to be the same as in the previous problem; (b) the transmission at pump wavelength of the HR mirror directly coated on the rod is 95%; (c) the absorption **coefficient** of the active medium at pump wavelength is  $a = 4 \text{ cm}^{-1}$ ; (d) optimum pumping conditions are realized.

**Calculate** the optical pump power required at threshold and compare this value with that obtained for problem 6.6.

### 6.8P Threshold power in a double-end pumped Nd:YVO<sub>4</sub> laser.

A Nd:YVO<sub>4</sub> laser is based on a z-shaped folded linear cavity as that shown in Fig. 6.11c of PL. The laser rod is longitudinally pumped, from both sides, by two laser diode bars coupled to the cavity by optical fiber bundles. The **diodes** emit at 800 nm with a radiative efficiency  $\eta_r = 50\%$ , each fiber bundle has a transfer **efficiency**  $\eta_t = 87\%$  and the absorption efficiency is  $\eta_a = 97\%$ . Determine the overall pump efficiency. Assuming a round trip loss  $\gamma_{rt} = 18\%$ , an upper laser level lifetime  $\tau = 98 \mu\text{s}$ , an effective stimulated emission cross section  $\sigma_e = 7.6 \times 10^{-19} \text{ cm}^2$  and a laser spot size of 500  $\mu\text{m}$  inside the Nd:YVO<sub>4</sub> rod, calculate the threshold electrical power required for each of the two diode bars under optimum **pump** conditions.

### 6.9P Threshold power in a quasi-three level laser: the Yb:YAG case.

An **Yb:YAG** laser platelet 1.5 mm long with  $8.9 \times 10^{20} \text{ Yb ions/cm}^3$  (6.5 atom% Yb) is longitudinally pumped in a laser configuration such as that in Fig. 6.11a of PL by the output of an InGaAs/GaAs QW array at a 940 nm wavelength. The beam of the array is suitably reshaped so as to produce an approximately round spot in the active medium with a spot size approximately matching the laser-mode spot size  $w_0 = 100 \mu\text{m}$ . The effective cross section for stimulated emission and absorption at the  $\lambda = 1.03 \mu\text{m}$  lasing wavelength, at room temperature, can be taken as  $\sigma_e = 1.9 \times 10^{-20} \text{ cm}^2$  and  $\sigma_a = 0.11 \times 10^{-20} \text{ cm}^2$ , while the effective upper state lifetime is  $\tau = 1.5 \text{ ms}$ . Transmission of the output coupling mirror is 3.5%, so that, including other internal losses, single-pass loss can be estimated as  $\gamma = 2\%$ . **Calculate** the threshold pump power under the stated conditions.

### 6.10P Threshold pump power of a Nd:glass fiber laser.

Consider a **Nd:glass** fiber laser with  $N_t = 6 \times 10^{17} \text{ Nd ions/cm}^3$  pumped at 800 nm and assume that the fiber core radius is 5  $\mu\text{m}$ . Assume a lifetime of the upper

laser level  $\tau = 300 \mu\text{s}$ , an effective stimulated emission cross section  $\sigma_e = 4 \times 10^{-20} \text{ cm}^2$ , an optical pump efficiency  $\eta_p = 38\%$  and a single pass loss  $\gamma = 3\%$ . Calculate the optical pump power at threshold.

### 6.11P Pump absorption in a Nd:glass fiber laser.

In the fiber laser of problem 6.10 the unsaturated absorption coefficient of the active medium at pump wavelength is  $\alpha_0 = 0.015 \text{ cm}^{-1}$ . Calculate the fiber length which is required to absorb 90% of the incident pump power when this power is equal to  $P_p = 200 \text{ mW}$ .

*(Level of difficulty higher than average)*

### 6.12P Maximum output intensity in a Nd:glass amplifier.

A single-pass CW laser amplifier consists of a 2 cm thick Nd:glass disk with  $3.2 \times 10^{20} \text{ Nd ions/cm}^3$ ; assume an effective stimulated-emission cross section  $\sigma_e = 4 \times 10^{-20} \text{ cm}^2$ , a lifetime of the upper laser level  $\tau = 300 \mu\text{s}$  and an overall scattering loss in the amplifier of  $\gamma = 3\%$ .

On account of the presence of this loss and for a given unsaturated **gain** coefficient  $g_0$ , show that there is a maximum intensity which can be obtained at the amplifier output. Using the numerical values indicated above, calculate the pump rate which is required to obtain a maximum output intensity of  $3 \times 10^5 \text{ W/cm}^2$ .

### 6.13P Electron temperature in a Boltzmann distribution.

Calculate the electron temperature for an electronic gas characterized by a **Maxwell-Boltzmann** energy distribution with an average kinetic energy of 10 eV.

### 6.14P How to reduce the size of a He-Ne laser tube?

A laser company produces a He-Ne laser consisting of a tube **5 mm** in diameter, **25 cm** long, containing **4 torr** of the gas mixture; the laser **tube** requires an operating voltage of **520 V**. The producer wants to reduce laser tube diameter to **3 mm** and its length to **15 cm**. Calculate the pressure and the operating voltage that are required in this laser.

### 6.15P Thermal and drift velocities of electrons in a He-Ne laser.

The He-Ne mixture used in the laser of problem 6.14 has a 6:1 ratio between He and Ne partial pressure, so elastic collisions of electron with He atoms can be considered as the dominant process. Assuming an elastic cross section  $\sigma_{el} = 5 \times 10^{-16} \text{ cm}^2$  for He, a gas temperature  $T = 400 \text{ K}$ , an average electron energy  $E_e = 10 \text{ eV}$ , a total pressure of the mixture of 4 torr, an operating voltage of 520 V and a tube length of 25 cm, calculate the thermal and drift velocities of the electrons in this laser.

### 6.16P A He-Ne laser: pump rate vs. pump current.

In the He-Ne laser considered in problem 6.14 one has  $(w) = 5 \times 10^{-11} \text{ cm}^3 \text{ s}^{-1}$ , where  $w$  is electron velocity and  $a$  is the electron impact cross section for He excitation. Assuming an unitary energy transfer efficiency between He and Ne atoms, taking a drift velocity  $v_d \approx 4.05 \times 10^6 \text{ cm/s}$  and a tube diameter of 5 mm and assuming a He atomic density  $N = 8.28 \times 10^{16} \text{ atoms/cm}^3$  in the gas mixture, calculate the pump rate corresponding to a 70 mA pumping current.

### 6.17P Scaling laws and performances in longitudinally pumped gas lasers.

A gas laser consist of a gas tube with diameter  $D$ , length  $l$ , containing a gas mixture at a pressure  $p$ . The laser has a pump power at threshold  $P_{th} = 1 \text{ W}$ , corresponding to an absorbed current  $I = 1 \text{ mA}$ . If the tube diameter were doubled, how much would be the absorbed current at threshold? (Assume that the pump efficiency  $\eta_p$  remains the same).

### 6.18P Pump rate vs. pumping current in $\text{Ar}^+$ lasers.

In  $\text{Ar}^+$  lasers the active species are Argon ions which are produced at the high current density of the discharge and which are then excited to the upper laser level by electronic impact. Which is in this case the functional relation between pump rate and current density?

**6.19P Ar<sup>+</sup> lasers: pump efficiency vs. pump power.**

An A . laser has a pump efficiency  $\eta_p = 8 \times 10^{-4}$  at 0.5 kW electrical pump power. Evaluate the pump efficiency at 9 kW pump power.

## ANSWERS

### 6.1A Critical pump rate in a lamp-pumped Nd:YLF laser.

The pump **efficiency**  $\eta_p$  of a given laser is defined as the ratio between the minimum pump power  $P_m$  required to produce a given pump **rate**  $R_p$  in the laser medium and the actual power  $P_p$  entering the pumping system:

$$\eta_p = \frac{P_m}{P_p} \quad (1)$$

We recall that the pump rate is the number of active species (atoms, molecules) excited in the unit volume and unit time inside the active medium by the pumping system. If  $R_p$  is not uniform in the laser medium, the average pump rate  $\bar{R}_p$  must be considered in defining pump **efficiency**.

In the lamp pumping configuration we can assume an uniform pump rate in the laser rod, so Eq. (1) can be directly used to derive  $R_p$ . Let  $d$  and  $l$  be respectively the diameter and the length of the Nd:YLF rod considered.

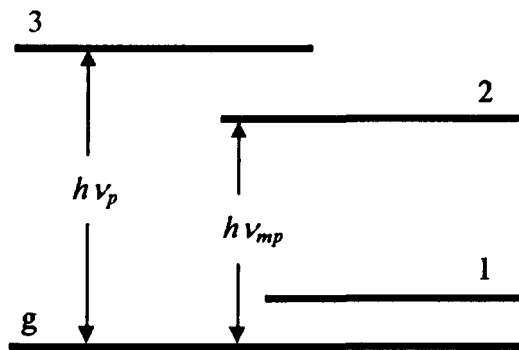


Fig. 6.1 Four level laser scheme.

The minimum pump power  $P_m$  required to produce a pump rate  $R_p$  is then given by:

$$P_m = R_p h\nu_{mp} \frac{\pi d^2 l}{4} \quad (2)$$

where  $h\nu_{mp}$  is the energy difference between upper laser level and ground level (see Fig. 6.1). Using eq. (1) in (2) we obtain:

$$R_p = \frac{4\eta_p P}{\pi h v_{mp} d^2 l} \quad (3)$$

For  $P = P_{th} = 2P_{lamp}$ , Eq. (3) gives the critical pump rate  $R_{cp}$  for the considered laser. Using the values reported in the problem, the critical pump rate turns out to be  $R_{cp} = 2.96 \times 10^{20} \text{ cm}^{-3} \text{ s}^{-1}$ .

### 6.2A Pump rate expression for longitudinal pumping.

Consider a rod-shaped active medium longitudinally-pumped by a laser beam and let  $z$  be the longitudinal coordinate along the rod axis, starting from the entrance face of the rod. Let  $r$  be the radial distance from the rod axis. Consider now an infinitesimal element  $dV$  of the active medium at the coordinate  $r_0, z_0$  with a thickness  $dz$  and surface area  $dS$  (Fig. 6.2).

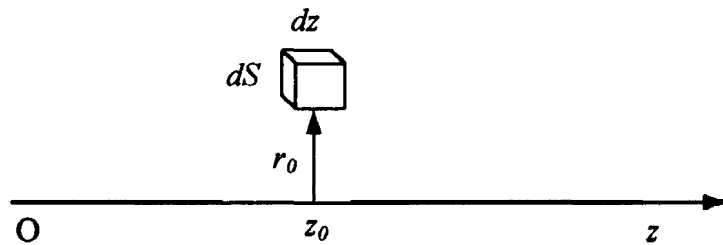


Fig. 6.2 Pump rate determination in longitudinal pumping

Let also  $I_p(r, z)$  describe the pump intensity distribution within the active medium and  $\alpha$  be the absorption coefficient of the medium at the pump frequency  $v_p$ . According to Eq. (2.4.17) and to Eq. (2.4.31-34) of PL, the elemental power  $dP$  absorbed within volume  $dV$  can be written as

$$\begin{aligned} dP &= [I_p(r_0, z_0) - I_p(r_0, z_0 + dz)] dS \\ &= -\left(\frac{dI_p}{dz}\right)_{z=z_0} dz dS = \\ &= \alpha I_p(r_0, z_0) dV \end{aligned} \quad (1)$$

By definition, we then have

$$dP = R_p h v_p dV \quad (2)$$

The comparison of (1) and (2) then shows that:

$$R_p(r_0, z_0) = \frac{\alpha I_p(r_0, z_0)}{h\nu_p} \quad (3)$$

Note that Eq. (3) also holds in the saturation regime; in this case the absorption coefficient  $\alpha = \alpha(I_p)$  is a function of the pump intensity, thus it depends on the position inside the active medium (see answer 6.11).

### 6.3A Laser spot size in a longitudinally pumped $\text{Ti:Al}_2\text{O}_3$ laser under optimum pumping conditions.

The threshold pump power  $P_{th}$  of a longitudinally pumped four-level laser can be written as [see Eq. (6.3.20) of PLJ]:

$$P_{th} = \left( \frac{\gamma}{\eta_p} \right) \left( \frac{h\nu_p}{\tau} \right) \left[ \frac{\pi(w_0^2 + w_p^2)}{2\sigma_e} \right] \quad (1)$$

where:  $\gamma$  is the single pass loss;  $\eta_p$  is the pump efficiency;  $\tau$  is the lifetime of the upper laser level;  $\nu_p$  is the pump frequency;  $\sigma_e$  is the **effective** stimulated emission cross section;  $w_p$  and  $w_0$  are the spot sizes of the pump and laser beams in the active medium, respectively. Optimum pumping conditions corresponds to a situation where  $w_p = w_0$ . Furthermore the single pass loss is given by  $\gamma \approx \gamma_n/2$ . Under these conditions, from Eq. (1) we get:

$$w_0 = w_p = \left[ \frac{2P_{th}\eta_p\tau\sigma_e}{\pi\gamma_n h\nu_p} \right]^{1/2} \quad (2)$$

Upon using the numerical values given in the problem, we obtain  $w_0 = w_p = 27 \mu\text{m}$ .

### 6.4A Optical pumping of a $\text{Ti:Al}_2\text{O}_3$ laser: a design problem.

The pumping **configuration** is indicated in Fig. 6.3, where, for simplicity, the end faces of the active medium are taken orthogonal to both pump and laser beams. Assume now that the wave front of the pump beam incident on the

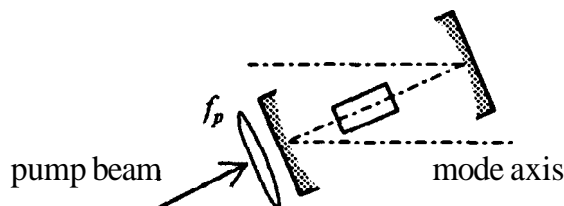


Fig. 63 Longitudinal pumping in a **z-shaped** folded linear cavity.

pumping lens is plane. Also assume that the pumping lens and the **folding** mirror are so close one another that their effect can be simulated by a single lens of an effective focal length  $f_e$  given by :

$$\frac{1}{f_e} = \frac{1}{f_p} + \frac{1}{f_m} \quad (1)$$

where  $f_m$  is the focal length of the folding mirror, acting on the pump beam as a defocusing lens. The pump spot size at the beam waist inside the active medium *can* then be approximately expressed [see Eq. (4.7.28) of PL] as

$$w_p \cong \frac{\lambda_p f_e}{\pi w_{pl}} \quad (2)$$

where  $\lambda_p$  is the pump wavelength. For  $\lambda_p = 514 \text{ nm}$ ,  $w_p = 27 \mu\text{m}$  and  $w_{pl} = 700 \mu\text{m}$ , we then obtain  $f_e = 11.5 \text{ cm}$ . On the other hand  $f_m$  is obtained by the lens-maker law:

$$\frac{1}{f_m} = (n - 1) \left[ \frac{1}{R_1} - \frac{1}{R_2} \right] \quad (3)$$

where  $R_1$  and  $R_2$  are the radii of curvature of the two surfaces of the mirror and  $n$  is the refractive index of the mirror medium. For  $n = 1.5$ ,  $R_1 = \infty$  and  $R_2 = 22 \text{ cm}$  we get from Eq. (3) that  $f_m = -44 \text{ cm}$ . From Eq. (1) the focal length of the pumping lens is then readily obtained as  $f_p = 9.15 \text{ cm}$ .

## 6.5A Doping in a solid-state laser medium.

From the element periodical table one gets the atomic weights of **yttrium**, aluminum and oxygen, as  $p_Y = 88.91$ ,  $p_{Al} = 26.98$  and  $p_O = 16$  respectively. Thus the weight of 1 mole of YAG ( $\text{Y}_3\text{Al}_5\text{O}_{12}$ ) is

$$W_{YAG} = 3 p_Y + 5 p_{Al} + 12 p_O = 593.63 \text{ g} \quad (1)$$

which corresponds to the Avogadro number  $n_A = 6.022 \times 10^{23}$  of  $\text{Y}_3\text{Al}_5\text{O}_{12}$  molecules and hence to a number of Y ions  $n_Y = 3 n_A = 18.066 \times 10^{23}$  ions. On the other hand  $W_{YAG} = 593.63 \text{ g}$  of YAG occupy a volume

$$V = W_{YAG}/\rho_{YAG} = 130.18 \text{ cm}^3 \quad (2)$$

where  $\rho_{YAG} = 4.56 \text{ g} \times \text{cm}^{-3}$  is the YAG density. The density of Y ions is then given by  $N_Y = n_Y/V = 1.388 \times 10^{22} \text{ ions/cm}^3$ . If 6.5% of Y ions are replaced by Yb ions, the density of the Yb ions is  $N_{Yb} = 6.5 \times 10^{-2} N_Y = 9.02 \times 10^{20} \text{ ions/cm}^3$ .

### 6.6A A transversely pumped high-power Nd:YAG laser.

The threshold pump power  $P_{th}$  of the Nd:YAG laser can be expressed as [see eq. (6.3.21) of PL]:

$$P_{th} = \left( \frac{\gamma}{\eta_p} \right) \left( \frac{h\nu_p}{\tau} \right) \left[ \frac{\pi a^2}{\sigma_e \{1 - \exp[-2a^2/w_0^2]\}} \right] \quad (1)$$

where:  $\gamma$  is the single pass loss;  $\eta_p$  is the pump efficiency;  $\tau$  is the upper laser level lifetime;  $\nu_p$  is the pump frequency;  $\sigma_e$  is the effective stimulated emission cross section;  $a$  and  $w_0$  are the rod radius and laser spot size in the active medium respectively. The optimum mode spot corresponds to  $w_{0,opt} = 0.7a$ .

In our case the pump power emitted by the fibers at threshold is required. Accordingly  $\eta_p$  is only equal to the absorption efficiency, i.e. one has  $\eta_p = 0.9$ . Using the other numerical values given in the problem, we then get from Eq. (1)  $P_{th} = 54.25$  W.

### 6.7A Longitudinal vs. transverse pumping in Nd:YAG laser.

The threshold pump power is given by Eq. (6.3.20) of PL as:

$$P_{th} = \left( \frac{\gamma}{\eta_p} \right) \left( \frac{h\nu_p}{\tau} \right) \left[ \frac{\pi(w_0^2 + w_p^2)}{2\sigma_e} \right] \quad (1)$$

In the present case, assuming a good antireflection coating of both faces of the pumping lens (V-coating,  $R < 0.2\%$ ), the pumping efficiency  $\eta_p$  can be taken as the product of the HR mirror transmission,  $T_p$ , times the absorption efficiency  $\eta_a = [1 - \exp(-\alpha l)]$ , where  $\alpha$  is the absorption coefficient at pump wavelength and  $l$  is the length of the active medium [see Eq. (6.3.11) of PL]. We then get  $\eta_p = \eta_a T_p \cong T_p = 0.95$ . Under optimum pumping condition one then has  $w_p = w_0$  in Eq. (1). With the given values of the parameters involved, one then gets from Eq. (1)  $P_{th} = 24.77$  W, i.e. roughly half the value obtained for problem 6.6.

### 6.8A Threshold power in a double-end pumped Nd:YVO<sub>4</sub> laser.

The threshold pump power for longitudinal pumping is given by:

$$P_{th} = \left( \frac{\gamma}{\eta_p} \right) \left( \frac{h\nu_p}{\tau} \right) \left[ \frac{\pi(w_0^2 + w_p^2)}{2\sigma_e} \right] \quad (1)$$

In our **case** we can take  $\gamma = \gamma_r/2 = 9\%$ ,  $\eta_p = \eta_r\eta_t\eta_a = 42\%$  and  $w_0 = w_p = 500 \mu\text{m}$ . Using the given data for  $\nu_p = \lambda/c$ ,  $\sigma_e$  and  $\tau$  we then get from Eq. (1)  $P_{th} = 5.6 \text{ W}$ . Thus the power required from each diode bar at threshold is  $P = P_{th}/2 = 2.8 \text{ W}$ . Note **that**, compared to the previous problem,  $P_{th}$  is now about 4 times smaller, the difference mostly arising from the difference in spot size for the two cases (note that the product  $\sigma\tau$  is about the same for Nd:YAG and Nd:YVO<sub>4</sub>).

### 6.9A Threshold power in a quasi-three level laser: the Yb:YAG case.

The threshold pump power  $P_{th}$  of the Yb:YAG laser can be expressed as [see Eq. (6.3.25) of PL]:

$$P_{th} = \left( \frac{\gamma + \sigma_a N_t l}{\eta_p} \right) \left( \frac{h\nu_p}{\tau} \right) \left[ \frac{\pi(w_0^2 + w_p^2)}{2(\sigma_e + \sigma_a)} \right] \quad (1)$$

where:  $\gamma$  is the single pass loss;  $\eta_p$  is the pump efficiency;  $\tau$  is the upper laser level lifetime;  $\nu_p$  is the **pump** frequency;  $\sigma_e$  and  $\sigma_a$  are the effective stimulated emission and absorption cross section at lasing wavelength;  $N_t$  is the total population;  $l$  is the active medium length;  $w_p$  and  $w_0$  are the **pump** and laser mode spots sizes in the active medium. We assume a unitary transmission, at the pump wavelength, of the pumping lens and of the HR mirror coated on one face of the platelet (see Fig. 6.11a of PL). The pump efficiency can then be taken equal to the absorption efficiency, i.e.  $\eta_p = \eta_a = [1 - \exp(-\alpha l)]$ ; from Table 6.2 of PL, the absorption coefficient at pump wavelength is seen to be equal to  $\alpha = 5 \text{ cm}^{-1}$ . We then get  $\eta_p = 0.53$ . From Eq. (1), using the numerical values given for all other parameters, we obtain  $P_{th} = 0.69 \text{ W}$ .

### 6.10A Threshold pump power of a Nd:glass fiber laser.

Equation (1) in answer 6.3, which holds for longitudinal pumping, can be used here and the pump and laser spot sizes can be approximately taken equal to the core radius of the fiber. Using the given numerical values of the parameters involved, we get  $P_{th} = 1.3 \text{ mW}$ . Note the very small value of this power, compared to what required in bulk Nd laser, as arising from the very small values of both  $w_0$  and  $w_p$ .

### 6.11A Pump absorption in a Nd:glass fiber laser.

Assuming a uniform intensity distribution of the pump power in the fiber, the pump intensity in the core is  $I_p = 4P_p / \pi d^2 = 254.6 \text{ kW/cm}^2$ , where  $d$  is the core diameter. At such high intensities of the pump, depletion of the **ground-state** population cannot be neglected. To calculate pump absorption for this case we assume a very fast relaxation both from the pump level to the upper laser level and from the lower laser level to the ground level (ideal 4-level laser). Population will then be available only in the ground level and in the upper laser level. We let  $N_2$  be the population of the latter level and  $N_t$  the total population. Under steady state we can write that the number of **Nd<sup>3+</sup>** ions raised, per unit time, to the upper laser level must equal the number of ions spontaneously decaying from this level. Thus:

$$R_p = \frac{N_2}{\tau} \quad (1)$$

where  $R_p$  is the pump rate and  $\tau$  is the upper laser level lifetime. According to Eq. (6.3.2) of PL, the pump rate can be expressed as:

$$R_p = \frac{\alpha I_p}{h\nu_p} \quad (2)$$

where  $\alpha$  is the absorption **coefficient** of the medium at the pump frequency  $\nu_p$  (see also answer 6.2). According to Eq. (2.4.32) of PL, the absorption coefficient  $\alpha$  in an ideal 4-level medium is:

$$\alpha = \sigma_p (N_t - N_2) \quad (3)$$

being  $\sigma_p$  the pump absorption cross-section. Substituting Eq.(2-3) in Eq. (1), we get:

$$N_2 = N_t \frac{(I_p/I_s)}{1+(I_p/I_s)} \quad (4)$$

where

$$I_s = h\nu_p/\sigma_p\tau \quad (5)$$

is the **pump** saturation intensity.

If we now let  $N_g$  be the ground state population, since  $N_g = N_t - N_2$ , we obtain from Eq. (4):

$$N_g = \frac{N_t}{1+(I_p/I_s)} \quad (6)$$

The decay of the pump intensity along the z-coordinate of the fiber can then be described by:

$$\frac{dI_p}{dz} = -\sigma_p N_g I_p = -\frac{\alpha_0 I_p}{1+(I_p/I_s)} \quad (7)$$

where  $\alpha_0 = \sigma_p N_t$ , is the unsaturated absorption coefficient at the pump wavelength. We can separate the variables in Eq. (7) to obtain:

$$\frac{1+(I_p/I_s)}{I_p} dl = -\alpha_0 dz \quad (8)$$

Upon integrating both sides of Eq. (8) over the length,  $l$ , of the fiber we get:

$$\ln \left[ \frac{I_p(0)}{I_p(l)} \right] + \frac{I_p(0) - I_p(l)}{I_s} = \alpha_0 l \quad (9)$$

where  $I_p(0)$  and  $I_p(l)$  are the pump intensities at the beginning and at the end of the fiber respectively.

With the values given in our problem, we have  $I_p(l) = 0.1 I_p(0)$  and  $I_s = 33.1 \text{ kW/cm}^2$ . From Eq. (9) we then get  $\alpha_0 l = 9.22$ , which gives  $l = 615 \text{ cm}$ . Note that for pump intensities much smaller than the saturation intensity, Eq (9) can be simplified to:

$$\ln \left[ \frac{I_p(0)}{I_p(l)} \right] = \alpha_0 l \quad (10)$$

and the length required to absorb 90% of the pump power would decrease to  $l' = 153 \text{ cm}$ .

### 6.12A Maximum output intensity in a Nd:glass amplifier.

The elemental change of intensity  $dI$ , when the beam to be amplified traverses the thickness  $dz$  in the amplifier, can be written as:

$$dI = (g - \alpha) I dz \quad (1)$$

where  $g$  is the saturated gain and  $\alpha$  accounts for scattering losses. The saturated gain can then be expressed as:

$$g = \frac{g_0}{1 + (I/I_s)} \quad (2)$$

where  $g_0$  is the unsaturated gain and  $I_s = h\nu/\sigma_e\tau$  is the saturation intensity.

The substitution of Eq. (2) into Eq. (1) then shows that the net gain  $g_n(I) = g - \alpha$  approaches zero when, at some point inside the amplifier, the intensity reaches the maximum value

$$I_m = I_s [(g_0/\alpha) - 1] \quad (3)$$

From this point on, the intensity does not increase any more and all the energy stored in the amplifier is actually lost as scattering.

To calculate the required pump rate  $R_p$  we first write:

$$R_p = N_{20}/\tau = g_0/\sigma_e\tau \quad (4)$$

where  $N_{20}$  is the population of the upper laser level in the absence of saturation ( $I = 0$ ). The substitution of  $g_0$ , from Eq. (4) into Eq. (3), then leads to the following expression for  $R_p$ :

$$R_p = \frac{\alpha}{\sigma_e\tau} \left( 1 + \frac{I_m}{I_s} \right) \quad (5)$$

Using some numerical values given in the problem, we get  $\alpha = -\ln(1-\gamma)/l \approx 0.015 \text{ cm}^{-1}$ , where  $l = 2 \text{ cm}$  is the amplifier thickness. Using the remaining numerical values given in the problem, we then obtain  $R_p = 2.55 \times 10^{22} \text{ ions/(s cm}^3)$ .

### 6.13A Electron temperature in a Boltzmann distribution.

For a Maxwell-Boltzmann distribution, the relation between average kinetic energy  $E = m v_{th}^2/2$  and electron temperature  $T_e$  is:

$$T_e = (2/3k) (m v_{th}^2/2) \quad (1)$$

where:  $k$  is the **Boltzmann** constant;  $m$  is the electron mass;  $v_{th}$  is its thermal velocity. From Eq. (1) one sees that  $kT_e$  is equal to (213) times the average **kinetic** energy, i.e.  $kT_e = 6.67 \text{ eV}$ . Using the known values of the electron charge and of **Boltzmann** constant (see Appendix I of PL) we then get  $T_e = 77295 \text{ K}$ .

### 6.14A How to reduce the size of a He-Ne laser tube?

To calculate the new diameter  $D$  and gas pressure  $p$ , we can use the scaling laws [see Eqs. (6.4.23a and b) of PL]:

$$pD = (pD)_{opt} \quad (1a)$$

$$\left(\frac{\mathcal{E}}{p}\right) = \left(\frac{\mathcal{E}}{p}\right)_{opt} \quad (1b)$$

where  $\mathcal{E}$  is the electric field of the discharge. From Eq. (1a) we get  $p = p_0 D_0 / D = 6.67 \text{ torr}$ , where:  $p_0$  and  $D_0$  are the pressure and the diameter of the old tube;  $p$  and  $D$  are the corresponding values for the new tube. Assuming now that the electric field  $\mathcal{E}$  is uniform along the laser tube, we can write

$$\mathcal{E} = V/l \quad (2)$$

where  $V$  is the applied voltage and  $l$  is the tube length. From Eqs. (1b) and (2) we then get  $V = V_0 p l / (p_0 l_0) = 520 \text{ V}$ , where:  $V_0$  and  $l_0$  are the voltage and the length of the old tube;  $V$  and  $l$  are the corresponding values for the new tube. Note that, since the product  $pl$  remains unchanged in our case, the required voltage also remains unchanged.

### 6.15A Thermal and drift velocities of electrons in a He-Ne laser.

The thermal velocity  $v_{th}$  is related to the average electron energy  $E$  by the equation:

$$v_{th} = (2E/m)^{1/2} \quad (1)$$

where  $m$  is the electronic mass. From Eq. (1) we get  $v_{th} = 1.87 \times 10^8 \text{ cm/s}$ . According to Eq. (6.4.13) of PL, the **drift** velocity  $v_d$  is given by:

$$v_d = \frac{e\mathcal{E}l}{m v_{th}} \quad (2)$$

where  $e$  is the electronic charge,  $\sigma$  the applied electric field and  $l$  the electronic mean **free** path. The latter quantity can be expressed as:

$$l = 1/(N\sigma_{el}) \quad (3)$$

where  $N$  is the He atomic density and  $\sigma_{el}$  is the cross-section for elastic collision of an electron with a He atom. From the equation of state of gases, the atomic density of He atoms  $N$  is given by:

$$N = pN_A/RT \quad (4)$$

where:  $N_A$  is the Avogadro's number;  $p$  is the partial He pressure;  $T$  is the gas temperature and  $R$  is the gas constant. The **partial** He pressure is **(6/7)** times the pressure of the total gas mixture. From Eq. (4) we then get  $N = 8.28 \times 10^{16}$  atoms/cm<sup>3</sup>. Substituting in Eq. (3), we obtain  $l = 0.024$  cm. Assuming now that the electric field  $\sigma$  is uniform along the laser tube, we can write:

$$\sigma = V/L \quad (5)$$

where  $V$  is the applied voltage and  $L$  is the tube length. From Eq. (5) and using data given in the problem, we obtain  $\sigma = 20.8$  V/cm. From Eq. (1-2) we finally get  $v_d = 4.7 \times 10^6$  cm/s.

### 6.16A A He-Ne laser: pump rate vs. pump current.

In He-Ne lasers the main pumping process occurs through excitation of He atoms in a metastable state by electron impact; Ne excitation is then achieved by resonant energy transfer. In steady state, neglecting **de-excitation** of He atoms by electron impact and wall collisions, the rate of He excitation must equal the rate of Ne excitation. This assumption is not completely realistic, but simplifies our calculation. From Eq. (6.4.24) of PL, the pumping rate is seen to be given by:

$$R_p = N \frac{J}{e} \left( \frac{\langle v\sigma \rangle}{v_d} \right) \quad (1)$$

where:  $N$  is the density of He atoms;  $v_d$  is the drift velocity;  $J$  is the current density;  $e$  is the electron charge. Using the values given in the problem we can calculate the pump rate which turns out to be  $R_p = 2.27 \times 10^{18}$  atoms/(cm<sup>3</sup> s).

### 6.17A Scaling laws and performances in longitudinally pumped gas lasers.

The operating voltage of the gas laser is readily obtained as  $V = P_{th}/i = 1000$  V. From the scaling laws of a **gas** laser discharge [see Eq. (6.4.23a-b) of PL], one sees that doubling the tube diameter requires a reduction of both pressure and electric field to half their original values. In particular, this correspond to a reduction of the operating voltage to half its **original** value, **i.e.** to 500 V. The new threshold pump power can be obtained from Eq. (6.4.26) of PL, **i.e.** from:

$$R_{pc} = \eta_p \frac{P_{th}}{Alh\nu_{mp}} \quad (1)$$

where:  $R_{cp}$  is the critical pump rate;  $A$  is the cross-sectional area of the tube;  $l$  is its length and  $h\nu_{mp}$  is the **minimum** pump energy. The critical pump rate can be obtained from Eq. (6.3.19) of PL as

$$R_{pc} = \frac{\gamma}{\sigma_e l \tau} \quad (2)$$

where  $\gamma$  is the single-pass loss,  $\sigma_e$  is the stimulated emission cross-section and  $\tau$  is the lifetime of the upper laser level. Since all parameters on the right hand side of Eq. (2) remain unchanged between the two cases,  $R_{cp}$  will also remain unchanged. Since, furthermore,  $\eta_p$  remains unchanged, we then obtain from Eq. (1) that  $P_{th}/A$  must remain unchanged. Accordingly, the threshold pump power must increase four times (**i.e.**  $P_{th} = 4$  W) and the required current by 8 times (**i.e.**  $I_{th} = 8$  mA).

### 6.18A Pump rate vs. pumping current in $\text{Ar}^+$ lasers.

According to Eq. (6.4.24) of PL, the pump rate  $R_p$  is given **by**:

$$R_p = N_t \frac{J}{e} \left( \frac{\langle v\sigma \rangle}{v_d} \right) \quad (1)$$

where:  $N_t$  is the density of the active species ( $\text{Ar}^+$  ions);  $J$  is the current density;  $e$  is the electron charge;  $v$  is the electron velocity;  $\sigma$  is the electron impact cross-section and  $v_d$  is the **drift** velocity. Assuming a **maxwellian** electron-energy distribution and also assuming that the electron temperature remains unchanged (**i.e.**  $T_e = T_{opt}$ ) upon changing the current density  $J$ , one can

readily see from Eq. (6.4.6) of PL that (*uo*) remains unchanged. For a given electron temperature, on the other hand, the thermal velocity [since  $(mv_h^2/2) = 2kT_e/3$ ] remains unchanged and so it does the drift velocity  $v_d$  [see Eq. (6.4.16) of PL]. It then follows from (1) that  $R_p \propto J N_t$ . On the other hand, Ar<sup>+</sup> ions are generated by electron impact with neutral atoms. Thus their density  $N_t$  can be taken to be proportional to  $\mathbf{J}$ . Thus the pump rate is seen to be proportional to  $\mathbf{J}^2$ . The same result is derived if we consider the pumping process as two consecutive steps, involving two electron collisions. The probability of this process is the square the probability of single collision. Assuming that the probability of electron collision with an atom is proportional to the current density  $\mathbf{J}$  in the gas discharge, it then follows that the probability of a pumping process is proportional to  $J^2$ .

### 6.19A Ar<sup>+</sup> lasers: pump efficiency vs. pump power.

According to Eq. (6.4.26) of PL, the pump rate  $R_p$  can be written as:

$$R_p = \eta_p \frac{P}{Alh\nu_{mp}} \quad (1)$$

where:  $\eta_p$  is the pump efficiency;  $P$  is the pump power;  $A$  the cross-sectional area of the laser tube;  $l$  is its length and  $h\nu_{mp}$  is the minimum pump energy. For given tube parameters,  $R_p$  is seen to be proportional to both  $P$  and  $\eta_p$ . On the other hand, it was shown in the previous problem that  $R_p \propto J^2$ , where  $J$  is the current density, while  $P$ , being the voltage constant for the gas discharge, is expected to be proportional to  $J$ . It then follows that  $\eta_p$  must increase linearly with  $J$ . For this reason, we get:  $\eta_p(9 \text{ kW}) = \eta_p(0.5 \text{ kW}) \times (9/0.5) = 1.44 \times 10^{-2}$ .



# CHAPTER 7

## Continuous Wave Laser Behavior

### PROBLEMS

#### 7.1P Calculation of logarithmic loss.

Calculate the logarithmic loss per-pass  $\gamma$  of a Fabry-Perot laser cavity, with negligible internal loss, made of two mirrors with transmission  $T_1=80\%$  and  $T_2=5\%$ .

#### 7.2P Calculation of cavity photon lifetime.

A Nd:YAG ring laser of geometrical length  $L=10$  cm is made of a  $l=1$  cm long active crystal with refractive index  $n=1.82$ , placed inside a three-mirror optical resonator with **mirror** reflectivities  $R_1=95\%$ ,  $R_2=100\%$  and  $R_3=98\%$  at the laser wavelength. Neglecting internal cavity losses and assuming an effective stimulated emission cross-section  $\sigma_e=2.8 \times 10^{-19}$  cm<sup>2</sup> at the center of the laser transition, calculate:

- (a) The cavity photon lifetime when no pumping is applied to the crystal.
- (b) The cavity photon lifetime when the laser is below threshold and the pumping rate is half of its threshold value.
- (c) The cavity photon lifetime when the pumping rate is approaching the threshold value.
- (d) The population inversion needed to reach laser threshold.

#### 7.3P Four-level laser with finite lifetime of the lower laser level.

Consider a four-level laser below threshold and assume that: (i) the **branching** ratio of the  $2 \rightarrow 1$  transition, compared to the overall spontaneous transition rate, is  $\beta=0.5$ ; (ii) the overall upper-state lifetime is purely **radiative** and its value is

equal to  $\tau_2=234\text{ }\mu\text{s}$ . (**Data** refer to the 1.064- $\mu\text{m}$  transition of Nd:YAG). Under these conditions, how short **must** the lifetime  $\tau_1$  of the lower laser level be to ensure that  $N_1/N_2<1\%$ ?

### 7.4P Rate equations analysis of a three-level laser.

In a three-level laser scheme the lower laser level is the ground state and pumping occurs through a pump band which populates, by fast relaxation, the upper laser level. Assuming a total population  $N_t$  of the active specie, an upper level lifetime  $\tau$ , a cavity photon lifetime  $\tau_c$  and a pumping rate  $W_p$ , write the space-independent rate equations for the three-level laser. Assuming a total logarithmic loss  $y$ , a stimulated emission cross-section  $\sigma_e$  of the laser transition, and a length  $l$  of the active medium, calculate the pump rate needed to reach threshold.

### 7.5P Threshold condition in a ruby laser.

Using the result of problem 7.4P, calculate the population inversion necessary to achieve laser oscillation in a ruby laser at the wavelength  $\lambda=694.3\text{ nm}$ . Assume a Fabry-Perot resonator with **mirror** reflectivities  $R_1=100\%$  and  $R_2=96\%$ , a scattering loss of 3% per round-trip pass, and a **6-cm** long ruby rod. Assume also equal values for absorption and stimulated emission peak cross sections  $\sigma_a=\sigma_e=2.7\times10^{-20}\text{ cm}^2$ .

### 7.6P Thermal lensing in a microchip Nd:YAG laser.

In a Nd:YAG microchip laser, made of a 1-mm thick crystal (refractive index  $n=1.82$ ) with plane-parallel faces end-pumped **by** a diode laser, the **pump**-induced thermal lens in the crystal is well approximated by a thin lens placed at the center of the cavity. The equivalent focal length of the thermal lens can be estimated from divergence measurements of the microchip laser beam. Assuming that the laser is operating in the fundamental TEM<sub>00</sub> mode and that the beam divergence is  $\theta=5\text{ mrad}$ , estimate the value of the thermal lens.

### 7.7P Transverse efficiency in an end-pumped four-level laser.

Let us consider a four-level laser longitudinally-pumped by a  $\text{TEM}_{00}$  circular pump beam of nearly constant spot size  $w_p$ . Assuming that the laser beam consists of a Gaussian  $\text{TEM}_{00}$  mode, of spot size at beam waist  $w_0$ , and neglecting mode diffraction inside the gain medium, derive an analytical expression for the transverse **efficiency** of the laser close to threshold.

[Hint: From the expression of the normalized input-output curve  $y=y(x)$ , given by Eq.(7.3.33) of PL, calculate the threshold expressions for  $x$  and  $(dy/dx)$ . Then use these results to calculate the transverse slope **efficiency**]

*(Level of difficulty higher than average)*

### 7.8P Threshold and slope efficiency calculations in a longitudinally-pumped Nd:YAG laser.

A Nd:YAG laser ( $\lambda=1.064 \mu\text{m}$ ) consists of a  $L=5 \text{ mm}$  long crystal, placed inside a plano-concave resonator, end-pumped by a GaAs diode laser ( $\lambda_p=800 \text{ nm}$ ). The plane minor is directly coated on the plane surface of the YAG crystal and has nominally 100% reflectivity at the laser wavelength. The output mirror has a radius of curvature  $R=10 \text{ cm}$  and a transmission  $T=6\%$  at laser wavelength. The geometrical length of the cavity is  $L=9 \text{ cm}$ , and the internal losses per transit are  $\gamma_i=0.03$ . Assuming an overall pump efficiency  $\eta_p \approx 60\%$  and a Gaussian pump distribution with spot size  $w_p$  equal to  $\approx 123 \mu\text{m}$  and nearly constant along the crystal, calculate the threshold pump power. Let then calculate the laser slope efficiency when the pump power exceeds by a factor of  $x=10$  the minimum laser threshold. Assume, for Nd:YAG, an effective stimulated cross-section  $\sigma_e=2.8 \times 10^{-19} \text{ cm}^2$ , an upper level lifetime of  $\tau=230 \mu\text{m}$  and a refractive index  $n=1.82$ .

### 7.9P Estimate of internal laser losses.

To estimate the internal losses in a high-power diode-pumped Nd:YLF laser, the threshold pump power  $P_{th}$  was measured using two different output couplers with reflectivities  $R_1=90\%$  and  $R_2=95\%$ . The other cavity mirror has nominally 100% reflectivity at the laser wavelength. Knowing that the measured threshold pump powers are  $P_{th1}=1 \text{ W}$  and  $P_{th2} = 600 \text{ mW}$ , provide an estimate of the internal losses.

### 7.10P Calculation of optimum output coupling.

Calculate the optimum transmission of the output mirror when the laser of Problem 7.9P is pumped by a diode input power  $P_p=5$  W. Neglect, for the sake of simplicity, the transverse **spatial** variations of the pump and laser fields and use the results of optimum output coupling of plane-wave theory.

### 7.11P Longitudinal efficiency in a standing-wave laser.

Consider two identical laser systems which differ each other only by the resonator geometry. The first laser uses a unidirectional ring cavity, whereas the second one consists of a standing-wave (Fabry-Perot) cavity with one output coupler. The output coupling losses for the two lasers are given by  $\gamma_2^{(1)}=0.05$  and  $\gamma_2^{(2)}=0.1$ , respectively. Internal losses per round-trip are the same for the two lasers and given by  $\gamma_i=0.1$ . Assuming that in both lasers pump and transverse efficiency are the same, how do you compare the slope efficiency of the two lasers when (i) they are operated close to threshold, and (ii) when they are operated ten times above threshold?

(The answer to this problem contains a detailed discussion about the longitudinal efficiency in a four-level laser)

### 7.12P Dispersion relation for a Lorentzian line.

The  $R_1$  line of ruby at  $\lambda_0=694.3$  nm is well approximated by a two-level homogeneously-broadened transition with a collision broadening at room temperature of  $\Delta\nu_0\approx330$  GHz (FWHM). The bulk refractive index of ruby, for an electric field polarized parallel to the **c-crystal** axis, is  $n_0=1.763$ . Calculate the refractive index of ruby, taking into account the dispersion introduced by the  $R_1$  line, (i) at the center of the absorption line ( $\nu=\nu_0$ ), and (ii) at a frequency **blue-shifted** from  $\nu_0$  by  $A\nu_0/2$ . Assume a  $Cr^{3+}$  concentration of  $N=1.58\times10^{19}$  ions/cm<sup>3</sup> and an absorption cross section  $\sigma_a=1.22\times10^{-20}$  cm<sup>2</sup> for the  $R_1$  transition

(The answer to this problem contains a detailed discussion about the relation between the absorption **coefficient** and the refractive index for a homogeneously-broadened two-level transition)

### 7.13P Frequency pulling in a homogeneously-broadened laser.

Derive Eq.(7.9.1) of PL describing frequency pulling for a **homogeneously-broadened** laser transition.

[Hint: calculate the resonance frequencies of the optical cavity taking into account the dispersive curve of the gain medium with a Lorentzian line; see Eq.(7.10.2) of PL and problem 7.12P. Let then compare these resonance frequencies with those of the empty cavity, and use the fact that, at steady-state laser operation, gain equals losses. Finally, express cavity losses as functions of the width of cavity mode resonance]

*(Level of difficulty higher than average)*

### 7.14P Calculation of frequency pulling in a He-Xe laser.

In a high-gain low-pressure He-Xe laser operating on the **3.51  $\mu\text{m}$  transition** of Xe, the laser transition is mainly Doppler broadened with a **FWHM** of  $\Delta\nu_0 \approx 200 \text{ MHz}$ . Assuming a **logarithmic** loss per pass  $\gamma=0.5$  and an optical cavity length  $L_e=0.1 \text{ m}$ , calculate the ratio  $\Delta\nu/\Delta\nu_c$  between the width of laser transition and cavity mode resonance. Then estimate the frequency pulling of laser emission when the cavity mode resonance  $\nu_c$  is **detuned** from the center of the **gainline**  $\nu_0$  by  $\nu_0-\nu_c=50 \text{ MHz}$ .

### 7.15P Quantum limit to the laser linewidth.

Consider a single-longitudinal-mode **Nd:YAG** laser in a ring cavity oscillating at  $\lambda_L=1064 \text{ nm}$  which emits an output power of  $P=100 \text{ mW}$ . Assuming an optical length of the cavity  $L_e=12 \text{ cm}$  and a logarithmic loss per pass  $\gamma=0.01$ , estimate the Schawlow-Townes limit to the laser linewidth due to spontaneous emission.

*(The answer to this problem contains an heuristic derivation of the Schawlow-Towens formula of the laser linewidth due to spontaneous emission)*

### 7.16P Tuning of a Ti:sapphire laser by a birefringent filter.

A birefringent filter for laser tuning, made of a quartz plate, is inserted, at Brewster angle, in a **Ti:sapphire** laser operating at  $\lambda=780 \text{ nm}$ . The plate is rotated in such a way that the ordinary and extraordinary refractive indices of ordinary and extraordinary beams are  $n_o=1.535$  and  $n_e=1.544$ , respectively.

Calculate the plate **thickness** L in such a way that the wavelength separation between two consecutive transmission maxima be  $\Delta\lambda_{fsr}=6$  nm.

### 7.17P Transverse mode selection.

An Ar-ion laser, oscillating on its green  **$\lambda=514.4\text{-nm}$**  transition, has a 10% unsaturated gain per pass. The resonator consists of two concave spherical mirrors both of **radius** of curvature  **$R=5$**  m and separated by  **$L=100$**  cm. The output mirror has a  **$T_2=5\%$**  transmission; the other mirror is nominally 100% reflecting. **Identical** apertures are inserted at both ends of the resonator to obtain  $\text{TEM}_{00}$  mode operation. Neglecting all other types of losses, calculate the required aperture diameter.

### 7.18P Single longitudinal mode oscillation in an inhomogeneously-broadened laser.

The **linewidth**  $\Delta\nu_0=50$  MHz of a low-pressure CO<sub>2</sub> laser is predominantly established by Doppler broadening. The laser is operating with a pump power twice the threshold value. Assuming that one mode coincides with the transition peak and equal losses for all modes, calculate the maximum mirror spacing that still allows single longitudinal mode operation.

### 7.19P Suppression of spatial hole burning by the twisted-mode technique.

A method to eliminate the standing-wave pattern in a Fabry-Perot laser cavity is the so-called twisted-mode technique, where control of the polarization state of counterpropagating waves is achieved in a such a way that the oppositely traveling beams in the active medium consist of two circularly polarized waves of the same sence (both right or both left) and amplitude  $E_0$ . Using a polar representation of the polarization state of circular waves and denoting by A the laser wavelength, show that:

- (i) the interference of the two circularly-polarized waves, at a reference transverse plane  **$z=0$** , produces a linearly-polarized wave of amplitude  **$2E_0$** .
- (ii) the interference of the two circularly-polarized waves, at a generic **transverse** plane  **$z$**  at a distance d from the reference plane  **$z=0$** , produces a linearly-polarized wave of amplitude  **$2E_0$**  and direction of vibration forming an

angle  $\Delta\phi=2\pi d/\lambda$  with respect to the polarization direction at the reference plane  $z=0$ .

### 7.20P Single-longitudinal mode selection by an intracavity etalon.

An Ar-ion laser oscillating on its green  $\lambda=514.5$  nm transition has a total loss per pass  $\gamma=4\%$ , an unsaturated **peak gain**  $G_p=\exp(\sigma_p Nl)=1.3$ , and a cavity length  $L=100$  cm. To select a single-longitudinal mode, a tilted and coated **quartz** ( $n_r=1.45$ ) **Fabry-Perot** etalon with a  $1=2$  cm thickness is used inside the resonator. Assuming for simplicity that one cavity mode is coincident with the peak of the transition (whose linewidth is  $\Delta\nu_0=3.5$  GHz), calculate the **etalon** finesse and the reflectivity of the two etalon faces to ensure single-mode operation.



## ANSWERS

### 7.1A Calculation of logarithmic loss.

The logarithmic loss per-pass  $\gamma$  of a **Fabry-Perot** cavity is defined by:

$$\gamma = \frac{\gamma_1 + \gamma_2}{2} \quad , \quad (1)$$

where:

$$\gamma_1 = -\ln(1-T_1) \quad (2)$$

$$\gamma_2 = -\ln(1-T_2) \quad (3)$$

and  $T_1, T_2$  are the power transmissions of the two mirrors. For  $T_1=80\%$  and  $T_2=5\%$ , from Eqs.(2) and (3) one obtains  $\gamma_1 \approx 1.61$ ,  $\gamma_2 \approx 0.05$ , and thus from Eq.(1)  $\gamma \approx 0.83$ .

### 7.2A Calculation of cavity photon lifetime.

In order to derive a general expression of the cavity photon lifetime when the laser is below threshold, let us recall that the field intensity  $I(t)$  at a reference plane inside the ring cavity at time  $t$  satisfies the delayed equation:

$$I(t+\Delta t) = \exp[g + \ln(R_1 R_2 R_3)] I(t) \quad (1)$$

where  $g$  is the single-pass gain experienced by the field intensity when passing through the **Nd:YAG** rod and  $\Delta t$  is the cavity photon **transit** time. Assuming that the field varies slowly on the cavity round-trip time and that the net gain per-pass is small, we may set in Eq.(1)  $I(t+\Delta t) \approx I(t) + (dI/dt)\Delta t$  and  $\exp[g + \ln(R_1 R_2 R_3)] \approx 1 + [g + \ln(R_1 R_2 R_3)]$ , so that Eq.(1) can be cast in the form:

$$\frac{dI}{dt} = \frac{-g + \ln(R_1 R_2 R_3)}{\Delta t} I \quad (2)$$

The solution to Eq.(2) is given by:

$$I(t) = I_0 \exp(-t/\tau_c) \quad (3)$$

where  $I_0$  is the initial field intensity at time  $t=0$  and:

$$\tau_c = -\frac{\Delta t}{g + \ln(R_1 R_2 R_3)} \quad (4)$$

represents the cavity photon lifetime. Taking into account that:

$$g = \sigma_e N l \quad (5)$$

$$\Delta t = \frac{L_e}{c} \quad (6)$$

where  $N=N_2-N_1 \approx N_2$  is the **population** inversion established by the pumping process,  $c$  is the velocity of light in vacuum, and  $L_e=(n-1)l+L$  is the optical length of the cavity, substitution of Eqs.(5) and (6) into Eq.(4) yields:

$$\tau_c = -\frac{(n-1)l + L}{c[\sigma_e N l + \ln(R_1 R_2 R_3)]} \quad (7)$$

Equation (7) allows one to answer questions (ad).

(a) When no pumping is applied to the crystal, i.e. for  $N=0$ , from Eq.(7) we obtain:

$$\tau_c = -\frac{(n-1)l + L}{c \ln(R_1 R_2 R_3)} = -\frac{0.82 \times 10^{-1} \text{ m} + 10^{-1} \text{ m}}{3 \times 10^8 \frac{\text{m}}{\text{s}} \ln(0.95 \times 1 \times 0.98)} \approx 5 \text{ ns} \quad (8)$$

(b) Since the gain at threshold is given by  $g_{th}=-\ln(R_1 R_2 R_3)$ , at a pumping rate half of its threshold value, one has  $g=g_{th}/2$ . From Eq.(7) it then follows:

$$\tau_c = -2 \frac{(n-1)l + L}{c \ln(R_1 R_2 R_3)} \approx 10 \text{ ns} \quad (9)$$

(c) When the pumping rate approaches the threshold value,  $g$  tends toward  $g_{th}$  and, from Eq.(7), it follows that  $\tau_c \rightarrow \infty$ . This means that any initial field perturbation is damped out on a time scale  $\tau_c$  which diverges as the threshold for oscillation is attained. This phenomenon, known as critical slowing-down, is a typical feature of any physical system exhibiting a phase transition.

(d) The population inversion at threshold,  $N_{th}$ , is obtained by equating gain to cavity loss. We then get

$$N_{th} = -\frac{\ln(R_1 R_2 R_3)}{\sigma_e l} = -\frac{\ln(0.95 \times 1 \times 0.98)}{2.8 \times 10^{-19} \text{ cm}^2 \times 1 \text{ cm}} \approx 2.55 \times 10^{21} \text{ cm}^{-3} \quad (10)$$

### 7.3A Four-level laser with finite lifetime of the lower laser level.

Let us consider a four-level laser and assume that: (i) the lifetime  $\tau_1$  of the lower laser level (level 1) is comparable with the lifetime  $\tau_2$  of the upper laser level

(level 2); (ii) the lifetime of level 2 is purely radiative with a branching ratio  $\beta$  for the transition **2→1**. Under these conditions, the following set of rate-equations for the populations  $N_1$  and  $N_2$  of levels 1 and 2 can be written:

$$\frac{dN_2}{dt} = -\frac{N_2}{\tau_2} + R_p - B\phi(N_2 - N_1) \quad (1)$$

$$\frac{dN_1}{dt} = -\frac{N_1}{\tau_1} + \beta \frac{N_2}{\tau_2} + B\phi(N_2 - N_1) \quad (2)$$

where  $R_p$  is the pump rate,  $\phi$  is the number of photons in the cavity mode and  $B$  is the stimulated transition per photon, per mode. Notice that in Eq.(2) the radiative and non-radiative decays of level 1 to lower atomic levels are accounted for by the term  $-N_1/\tau_1$ , whereas  $\beta N_2/\tau_2$  accounts for the rate of atomic decay, **from** level 2 to level 1, due to spontaneous emission. When the laser is operated below threshold and in steady-state, from Eq.(2) with  $\phi=0$  one obtains:

$$\frac{N_1}{N_2} = \beta \frac{\tau_1}{\tau_2} \quad (3)$$

In order to have  $N_1/N_2 < 1\%$ , from Eq.(3) it follows that  $\tau_1 < 0.01(\tau_2/\beta)$ . Assuming  $\tau_2=234 \mu s$  and  $\beta=0.51$ , we obtain:

$$\tau_1 < \frac{234 \mu s}{100 \times 0.51} \cong 4.59 \mu s \quad (4)$$

Note:

The condition given by Eq.(4) is well satisfied for a **Nd:YAG** laser medium, for which the decay time of the lower laser level is a few hundredths of picoseconds.

#### 7.4A Rate equations analysis of a three-level laser.

For a three-level laser, under the assumption of fast decay from the pump band manifolds to the upper laser level, we need to consider only the populations  $N_1$  of the lower laser level 1 (ground state) and  $N_2$  of the upper laser level 2 (excited state). At any time, these populations satisfy the condition of population conservation:

$$N_1 + N_2 = N_t \quad (1)$$

where  $N_t$  is the total population of the active specie. If incoherent pumping **from** the ground state to the upper laser level is provided at a rate  $W_p$ , we can write

the following set of space-independent rate-equations for the population  $N_2$  of upper laser level and for the number of photons  $\phi$  in the cavity mode:

$$\frac{dN_2}{dt} = W_p N_1 - \frac{N_2}{\tau} - B\phi(N_2 - N_1) \quad (2)$$

$$\frac{d\phi}{dt} = -\frac{\phi}{\tau_c} + B\phi V_a (N_2 - N_1) \quad (3)$$

where  $\tau$  is the lifetime of the upper laser level,  $B$  is the stimulated transition rate per-photon per-mode,  $\tau_c$  is the cavity photon lifetime, and  $V_a$  is the volume of the mode in the active medium. Notice that, as compared to a quasi-three level laser (see PL, sec. 7.2.2), the basic difference of a purely three-level laser scheme is that the effective pump rate  $R_p = W_p N_1$  depends on the population of the lower laser level, which can not of course be taken constant. To calculate the threshold pump rate  $W_{pc}$  and the populations  $N_{1c}$  and  $N_{2c}$  of the laser levels at threshold, let us first observe that, at threshold, the overall growth rate of cavity photons must vanish. From Eq.(3) we then obtain:

$$V_a B(N_{2c} - N_{1c}) = \frac{1}{\tau_c} \quad (4)$$

Using the expressions for  $B$  and  $\tau_c$  given by Eqs. (7.2.13) and (7.2.14) of PL, respectively, Eq.(4) can be cast in the form:

$$\sigma_e (N_{2c} - N_{1c}) l = \gamma \quad (5)$$

where  $\gamma = L_e c / \tau_c$  is the **total** logarithmic loss per-pass,  $L_e$  is the optical cavity length,  $a_e$  is the stimulated emission cross-section of the laser transition, and  $l$  is the length of the gain medium. The expressions of  $N_{1c}$ ,  $N_{2c}$  are obtained from Eqs.(1) and (5) as:

$$N_{1c} = \frac{N_t - \gamma/\sigma_e l}{2} \quad (6)$$

$$N_{2c} = \frac{N_t + \gamma/\sigma_e l}{2} \quad (7)$$

The expression of  $W_{pc}$  is then readily obtained from Eq.(2) upon setting  $\phi=0$  and  $dN_2/dt=0$ . This yields  $W_{pc} = N_{2c}/(N_{1c}\tau)$  and hence, using Eqs.(6) and (7),

$$W_{pc} = \frac{N_t + \gamma/\sigma_e l}{\tau(N_t - \gamma/\sigma_e l)} \quad (8)$$

### 7.5A Threshold condition in a ruby laser.

The population inversion at threshold is given by **Eq.(5)** of Problem 7.4. The total **logarithmic** loss  $\gamma$  is given by:

$$\gamma = \gamma_i + \frac{\gamma_1 + \gamma_2}{2} \quad (1)$$

where  $\gamma_i=0.03$  are the internal losses,  $\gamma_1=-\ln R_1=0$  and  $\gamma_2=-\ln R_2 \cong 0.04$  are the logarithmic losses due to mirror transmissions. From **Eq.(1)** one then obtains  $\gamma \cong 0.05$ . From **Eq.(5)** of Problem 7.4 it then follows:

$$N_{2c} - N_{1c} = \frac{\gamma}{\sigma_e l} = \frac{0.05}{2.7 \times 10^{-20} \text{ cm}^2 \times 6 \text{ cm}} \cong 3.08 \times 10^{17} \text{ cm}^{-3} \quad (2)$$

### 7.6A Thermal lensing in a microchip Nd:YAG laser.

In presence of the thermally-induced lens, the laser cavity can be schematized by a symmetric flat-flat resonator, of length  $l=1\text{mm}$ , with a thin lens of focal length  $f$  placed at the center of the crystal. Due to the symmetry of the resonator, the two beam waists of the  $\text{TEM}_{00}$  Gaussian laser mode of equal spot size  $w_0$ , must occur at the two flat mirrors. The beam waist  $w_0$  can be then calculated from the divergence  $\theta_d=0.005 \text{ rad}$  using **Eq.(4.7.19)** of PL, i.e.:

$$w_0 = \frac{\lambda}{\pi\theta_d} = \frac{1.064 \mu\text{m}}{\pi \times 5 \times 10^{-2} \text{ rad}} \cong 67.7 \mu\text{m} \quad (1)$$

To relate the spot size  $w_0$  to the focal **length**  $f$ , we first observe that the radius of curvature  $R$  of the Gaussian mode, before the thin lens, must be equal and opposite in sign to that after the lens. From **Eq.(4.2.20)** of PL one readily obtains  $R=2f$  (see also **Example 4.5** of PL). On the other hand, the radius of curvature of a Gaussian beam is related to the propagation distance from the beam waist by **Eq.(4.7.17b)** of PL, so that one has:

$$R = 2f = d \left[ 1 + \left( \frac{\pi w_0^2}{d\lambda} \right)^2 \right] \quad (2)$$

where  $d=l/2 \cong 274.7 \mu\text{m}$  is the diffractive distance between the thin lens and the flat mirrors, and  $\lambda=1.064 \mu\text{m}$  is the laser wavelength in vacuum. The substitution of **Eq.(1)** into **Eq.(2)** then yields  $f \cong 33.4 \text{ cm}$ .

### 7.7A Transverse efficiency in an end-pumped four-level laser.

For a four-level laser with a **weakly-diffracting** Gaussian transverse distribution of both pump beam and laser cavity mode inside the gain medium, the transverse slope **efficiency** is provided by Eq.(7.3.35) of PL, i.e.:

$$\eta_t = \frac{\pi w_0^2}{\pi w_p^2} \frac{dy}{dx} = \delta \frac{dy}{dx} \quad (1)$$

where:  $w_0$  and  $w_p$  are the spot sizes of TEM<sub>00</sub> pump and laser modes, respectively, inside the gain medium;  $\delta = (w_0/w_p)^2$ ;  $x$  and  $y$  are the normalized pump power and output laser power, respectively, as defined in Eqs.(7.3.25) and (7.3.27) of PL. The normalized input-output curve  $y=y(x)$  is implicitly defined by Eq.(7.3.33) of PL, i.e.:

$$\frac{1}{x} = \int_0^1 \frac{t^\delta dt}{1+yt} \quad (2)$$

In order to derive an analytical expression of the transverse **efficiency** close to threshold, we need to calculate the derivative  $dy/dx$  at  $x=x_{th}$ , where  $x_{th}$  is the threshold value of the normalized pump power, which is readily obtained from Eq.(2) by setting  $y=0$ , i.e.:

$$x_{th} = \frac{1}{\int_0^1 t^\delta dt} = 1 + \delta \quad (3)$$

Upon differentiating both sides of Eq.(2) with respect to the variables  $x$  and  $y$ , we obtain:

$$\frac{1}{x^2} = \frac{dy}{dx} \int_0^1 \frac{t^{\delta+1} dt}{(1+yt)^2} \quad (4)$$

The derivative  $dy/dx$  at  $x=x_{th}$  is then readily obtained from Eq.(4) upon setting  $x=x_{th}$  and  $y=0$ . We get:

$$\left( \frac{dy}{dx} \right)_{x_{th}} = \frac{1}{x_{th}^2} \frac{1}{\int_0^1 t^{\delta+1} dt} = \frac{\delta+2}{x_{th}^2} \quad (5)$$

From Eq.(1) with the help of Eqs.(5) and (3), the transverse **efficiency** close to threshold can be written in the final **simple** form:

$$\eta_t = \frac{\delta(\delta + 2)}{(1 + \delta)^2} \quad (6)$$

Note:

- (i) The threshold transverse efficiency vanishes when  $\delta \rightarrow 0$ , i.e. when the laser spot size is much smaller than the pump spot size.
- (ii) The threshold transverse efficiency reaches its maximum value  $\eta_t = 1$  when  $\delta \rightarrow \infty$ , i.e. when the laser spot size is much larger than the pump spot size.
- (iii) At mode matching, i.e. when  $w_0 = w_p$ , the threshold value of  $\eta_t$  already attains the relatively large value of  $\eta_t = 3/4$ . Upon increasing the pump power above threshold,  $\eta_t$  is expected to increase up to its maximum value  $\eta_t = 1$  (see Fig. 7.10 of PL). The relatively modest increase, with pump power, of  $\eta_t$  is understood when one notices that, in this case, the input-output curve,  $y = y(x)$ , weakly differs from a linear curve (see Fig. 7.9 of PL).

### 7.8A Threshold and slope-efficiency calculations in a longitudinally-pumped Nd:YAG laser,

The calculation of the pump power at threshold  $P_{th}$  and of the laser slope efficiency  $\eta$  for the longitudinally-pumped Nd:YAG laser can be readily done by application of the results of the space-dependent model for a four-level laser under the assumption of nondiffracting Gaussian distribution of both pump and laser modes inside the gain medium (see sec. 7.3.2 of PL). In this case the pump power threshold  $P_{th}$  and the slope efficiency  $\eta$  are given by:

$$P_{th} = (1 + \delta)P_{mth} \quad (1)$$

$$\eta = \eta_p \eta_c \eta_q \eta_t \quad (2)$$

where:  $\delta = (w_0/w_p)^2$ ,  $w_0$  and  $w_p$  being the spot sizes of laser and pump modes inside the gain medium, respectively;  $P_{mth}$  is the minimum threshold for a Gaussian beam pumping, given by Eq.(7.3.32) of PL;  $\eta_p$  is the pump efficiency;  $\eta_c = \gamma_2/2y$  is the output coupling efficiency;  $\eta_q = h\nu/h\nu_p$  is the quantum efficiency;  $\eta_t$  is the transverse efficiency given by Eq.(7.3.35) of PL. Since the logarithmic loss per-pass of the laser is given by  $\gamma = \gamma_i - (1/2)\ln(1-T) \approx 0.06$ , where  $\gamma_i = 0.03$  are the internal losses per-transit and  $T = 0.06$  is the transmission of the output coupler, assuming  $w_p = 123 \mu\text{m}$ ,  $\eta_p = 0.6$ ,  $\tau = 230 \mu\text{s}$ ,  $h\nu_p = 1.87 \times 10^{-19} \text{ J}$  and  $\sigma_e = 2.8 \times 10^{-19} \text{ cm}^2$ , from Eq.(7.3.32) of PL one obtains:

$$P_{\text{th}} = \frac{\gamma}{\eta_p} \frac{h\nu_p}{\tau} \frac{\pi w_p^2}{2\sigma_e} = \frac{0.06}{0.6} \frac{1.87 \times 10^{-19} \text{ J}}{230 \mu\text{s}} \frac{\pi \times 123^2 \mu\text{m}^2}{2 \times 2.8 \times 10^{-19} \text{ cm}^2} \cong 69 \text{ mW} \quad (3)$$

In order to evaluate the other quantities entering into Eqs.(1) and (2), we first need to calculate the spot size  $w_0$  of the laser mode inside the **gain** medium. To this aim, let us notice that, since we are dealing with a **plane-concave** resonator, the beam waist of the TEM<sub>00</sub> Gaussian laser mode is located at the plane mirror, whereas its phase front at the curved mirror should fit the radius of curvature of the curved mirror. We can thus write [see also Eq.(4.7.13b) of PL]:

$$R = L_d \left[ 1 + \left( \frac{\pi w_0^2}{\lambda L_d} \right) \right] \quad (4)$$

where  $L_d = L - l + l/n \cong 87.7$  mm is the diffractive length of the resonator. Solving Eq.(4) with respect to  $w_0$  yields:

$$w_0^2 = \frac{\lambda L_d}{\pi} \left( \frac{R}{L_d} - 1 \right)^{1/2} = \frac{1.064 \mu\text{m} \times 8.77 \times 10^4 \mu\text{m}}{\pi} \left( \frac{100 \text{ mm}}{87.7 \text{ mm}} - 1 \right)^{1/2} \cong 1.11 \times 10^4 \mu\text{m}^2 \quad (5)$$

The ratio  $\delta = (w_0/w_p)^2$  is then given by  $\delta \cong 0.8$ , and, from Eqs.(1) and (3), the threshold pump power is calculated as  $P_{\text{th}} \cong 125$  mW. Notice that, since the Rayleigh range of the laser mode  $z_R = \pi w_0^2 / \lambda \cong 32.5$  mm is considerably larger than the rod thickness ( $l = 5$  mm), the assumption of a nearly constant mode spot size inside the gain medium is largely satisfied.

In order to calculate the laser slope efficiency when the pump power is  $x=10$  times larger than the minimum threshold value, given by Eq.(3), we need to estimate the transverse efficiency  $\eta_t$ , which, for a Gaussian pump distribution, can be evaluated by the help of Fig.7.11(b) of PL, which plots the behavior of transverse **efficiency** versus the ratio  $\delta = (w_0/w_p)^2$  in case of a Gaussian pump for  $x=10$ . In our case, we have  $\delta \cong 0.8$ , so that from an inspection of Fig.7.11(b) we may estimate  $\eta_t \cong 0.9$ . The quantum and coupling efficiencies are then readily calculated as:

$$\eta_q = \frac{h\nu}{h\nu_p} = \frac{\lambda_p}{\lambda} = \frac{800 \text{ nm}}{1064 \text{ nm}} \cong 0.75 \quad (6)$$

$$\eta_c = \frac{\gamma_2}{2\gamma} = -\frac{\ln(1-T)}{2\gamma} \cong \frac{T}{2\gamma} \cong 0.5, \quad (7)$$

whereas from the text of the problem the pumping efficiency is known to be  $\eta_p = 0.6$ . In conclusion, from Eq.(2) we finally obtain for the laser slope efficiency  $\eta \cong 20\%$ .

### 7.9A Estimate of internal laser losses.

Indicating by  $\gamma^{(1)}$  and  $\gamma^{(2)}$  the logarithmic losses of the Nd:YLF laser when the output coupler reflectivities are  $R_1=90\%$  and  $R_2=95\%$ , respectively, from the expression of the pump threshold for a four-level laser as given by Eq.(7.3.12) of PL, one obtains:

$$\frac{P_{th1}}{P_{th2}} = \frac{\gamma^{(1)}}{\gamma^{(2)}} \quad (1)$$

Notice that Eq.(1) is valid regardless of the spatial distribution of pump and laser modes provided that, in the two set of measurements, only the reflectivity of the output coupler is changed. Since  $\gamma^{(1)}=\gamma_i+\gamma_t/2$  and  $\gamma^{(2)}=\gamma_i+\gamma_t/2$ , where  $\gamma_t=-\ln R_1$  and  $\gamma_t=-\ln R_2$ , from Eq.(1) one obtains:

$$\frac{\gamma_i - \frac{1}{2} \ln R_1}{\gamma_i - \frac{1}{2} \ln R_2} = \frac{P_{th1}}{P_{th2}} \quad (3)$$

which can be solved with respect to  $\gamma_i$ , yielding:

$$\gamma_i = \frac{1}{2} \frac{P_{th2} \ln R_1 - P_{th1} \ln R_2}{P_{th2} - P_{th1}} \cong 0.03 \quad (4)$$

### 7.10A Calculation of optimum output coupling.

In case where transverse spatial variations of both pump and laser modes inside the gain medium are neglected, for the calculation of optimum output coupling we may use the laser rate-equations in the plane-wave approximation. From Eq.(7.5.3) and (7.5.4) of PL with  $\gamma_r=0$ , the optimum output coupling  $\gamma_{2opt}$  then turns out to be given by:

$$\gamma_{2opt} = 2\gamma_i(x_m^{1/2} - 1) \quad (1)$$

where  $\gamma_i$  are the internal logarithmic losses per-pass and  $x_m=P/P_{mth}$  is the ratio between the actual pump power  $P$  and the threshold pump power  $P_{mth}$  corresponding to zero output coupling, i.e. to  $\gamma_2=0$ . If  $P_{th}$  is the threshold pump power for an output coupling  $\gamma_2=-\ln R$ , then  $P_{mth}$  can be calculated as:

$$P_{mth} = \frac{\gamma_i}{\gamma_i - \frac{1}{2} \ln R} P_{th} \quad (2)$$

From Problem 7.9P, one has  $\gamma_i \approx 0.03$  and  $P_{th} = 1$  W for  $R = 0.9$ , so that from Eq.(2) one obtains  $P_{mth} \approx 363$  mW. Since the available pump power  $P$  is 5 W, from Eq.(1) it follows that:

$$\gamma_{2opt} = 2 \times 0.03 \times \left[ \left( \frac{5 \text{ W}}{0.363 \text{ W}} \right)^{1/2} - 1 \right] \approx 0.16 \quad (3)$$

corresponding to an output coupler with a reflectivity  $R_{opt} = \exp(-\gamma_{2opt}) \approx 85\%$ .

### 7.11A Longitudinal efficiency in a standing-wave laser.

The slope efficiencies of the two lasers, assuming equal values for quantum efficiency, pump efficiency and transverse efficiency, differ because of different output-coupling ( $\eta_c$ ) and longitudinal ( $\eta_l$ ) efficiencies. The output coupling efficiency is different in the two lasers because they have different output mirror transmission coefficients. In particular, for both a ring laser or a standing-wave laser with a one output coupler, we may write  $\eta_c = \gamma_2 / (\gamma_i + \gamma_2)$ , where  $\gamma_i$  denotes the internal laser losses *per round-trip* and  $\gamma_2$  the logarithmic loss due to the output coupler. Moreover, in a ring cavity the longitudinal efficiency is always equal to one, i.e.  $\eta_l^{(1)} = 1$ , whereas in a linear cavity it is always lower than one, due to the standing-wave pattern of the laser mode, and its value approaches one when the laser is operated well above threshold. In particular, close to threshold it can be shown that  $\eta_l^{(2)} = 2/3$ , whereas when the laser is operated at a pump level ten times above threshold, one has  $\eta_l^{(2)} = 8/9$  [see, for instance, Sec. 7.3.2 of PL]. The ratio of slope efficiencies  $\eta_l^{(1)}$  and  $\eta_l^{(2)}$  for the two lasers is then:

$$\frac{\eta_l^{(1)}}{\eta_l^{(2)}} = \frac{\eta_2^{(1)}}{\eta_2^{(2)}} \frac{\eta_l^{(1)}}{\eta_l^{(2)}} = \frac{\gamma_2^{(1)}(\gamma_2^{(2)} + \gamma_i)}{\gamma_2^{(2)}(\gamma_2^{(1)} + \gamma_i)} \frac{\eta_l^{(1)}}{\eta_l^{(2)}} \quad (1)$$

From the data of the problem, we have  $\gamma_2^{(1)} = 0.05$ ,  $\gamma_2^{(2)} = 0.1$  and  $\gamma_i = 0.05$ . When the lasers are operated close to threshold,  $\eta_l^{(2)} = 2/3$ , so that from Eq.(1) we get  $\eta_l^{(1)}/\eta_l^{(2)} \approx 1.125$ ; for the laser operated ten times above threshold,  $\eta_l^{(2)} = 8/9$ , and  $\eta_l^{(1)}/\eta_l^{(2)} \approx 0.844$ .

Complementary note:

It is worth deriving the analytical value  $\eta=2/3$  of the longitudinal efficiency of a standing-wave laser operated close to threshold by a direct analysis of rate-equations in which the standing-wave character of the cavity mode is taken into account. To this aim, let us consider a four-level laser made of an active medium of length  $l$ , transverse section  $A$  and refractive index  $n$ , placed inside a **Fabry-Perot** resonator of geometrical length  $L$ . From the spacedependent rate equations given by Eq.(E.I.9) of PL, it follows that, in steady-state conditions, the cavity photon number  $\phi$  in the lasing mode satisfies the equation:

$$\frac{c\sigma}{V} \int \frac{R_p |u|^2}{\frac{1}{\tau} + \frac{c\sigma}{V} |u|^2 \phi} dV = \frac{1}{\tau_c} \quad (2)$$

where  $R_p$  is the **pump** rate,  $\tau$  is the lifetime of the upper laser level,  $\tau_c$  is the cavity photon lifetime,  $\sigma$  is the transition cross-section at the frequency of cavity mode,  $u$  is the spacedependent field amplitude of cavity mode,  $V$  is the effective volume of the mode in the cavity, defined by Eq.(E.I.7) of PL, and the integral on the left hand side in Eq.(2) is extended over the volume of the active medium. As in this problem we are concerned with the influence of the standing-wave mode pattern on the laser slope **efficiency**, we will neglect the transverse dependence of both pump and cavity modes, i.e. we will assume the plane-wave approximation for the fields. Furthermore, we will limit our analysis to the case where the pump rate  $R_p$  is uniform along the longitudinal coordinate  $z$  of the cavity axis. In this case, we can perform the integral in Eq.(2) over the transverse variables  $(x,y)$ , obtaining:

$$\frac{\tau c\sigma A R_p}{V} \int_0^l \frac{|u(z)|^2}{1 + \frac{\tau c\sigma}{V} |u(z)|^2 \phi} dz = \frac{1}{\tau_c} \quad (3)$$

where  $u(z)=\sin(kz)$  is the **normalized** standing-wave pattern of the Fabry-Perot cavity mode. The output laser power  $P_{out}$  and the pump power  $P_p$  are related to  $\phi$  and  $R_p$ , respectively, by relations (7.2.18) and (6.2.6) of PL, i.e.:

$$P_{out} = \frac{\gamma_2 c}{2L_e} h\nu\phi \quad (4)$$

$$P_p = \frac{h\nu_p Al}{\eta_p} \quad (5)$$

where  $\eta_p$  is the pump efficiency,  $L_e=nl+L-l$  is the optical length of the cavity,  $\nu_p$  and  $\nu$  are the pump and laser **frequencies**, respectively, and  $\gamma_2$  is the **output-**

coupling logarithmic loss. From Eqs.(4) and (5), it then follows that the laser **slope efficiency**,  $\eta_s = dP_{out}/dP_p$ , is given by:

$$\eta_s = \eta_p \frac{h\nu}{h\nu_p} \frac{c}{2L_e l A} \frac{d\phi}{dR_p} \quad (6)$$

where the function  $\phi=\phi(R_p)$  is defined implicitly by Eq.(3). The threshold value  $R_{pth}$  is readily obtained from Eq.(3) by setting  $\phi=0$ , and it is given by:

$$R_{pth} = \frac{\int_0^l |u(z)|^2 dz}{\tau_c \sigma A \tau_e \int_0^l |u(z)|^4 dz} \quad (7)$$

If we **differentiate** both sides of Eq.(3) with respect to  $R_p$  and  $\phi$  and evaluate the equation so obtained at  $R=R_{pth}$  and  $\phi_{th}=0$ , we get:

$$\int_0^l |u(z)|^2 dz - R_{pth} \frac{\tau_c \sigma}{V} \left( \frac{d\phi}{dR_p} \right)_{R_{pth}} \int_0^l |u(z)|^4 dz = 0 \quad (8)$$

Substituting the expression of  $R_{pth}$  given by Eq.(7) in Eq.(8) and solving with respect to  $(d\phi/dR_p)_{R_{pth}}$ , we obtain:

$$\left( \frac{d\phi}{dR_p} \right)_{R_{pth}} = \tau_c A \frac{\left( \int_0^l |u(z)|^2 dz \right)^2}{\int_0^l |u(z)|^4 dz} \quad (9)$$

Since  $\tau_c = L_e / \gamma c$ , where  $y$  are the logarithmic losses per-pass [see Eq.(7.2.14) of PL], from Eq.(6) and Eq.(9), we can finally write the laser slope efficiency close to threshold in the form:

$$\eta_s = \eta_p \frac{h\nu}{h\nu_p} \frac{\gamma_2}{2\gamma} \eta_l \quad (10)$$

where we have introduced the longitudinal *efficiency*  $\eta_l$ :

$$\eta_l = \frac{1}{l} \frac{\left( \int_0^l |u(z)|^2 dz \right)^2}{\int_0^l |u(z)|^4 dz} \quad (11)$$

Equations (10) and (11) allow us to study the influence of the standing-wave cavity pattern on the laser slope efficiency. In a unidirectional ring cavity, we may assume  $u(z)=1$  independent of the longitudinal coordinate  $z$ , so that from Eq.(11) one obtains  $\eta=1$ . Conversely, in a Fabry-Perot cavity the field envelope is given by  $u(z)=\sin(kz)$ , where  $k=2\pi\nu/c$  is the wave number of the cavity mode. If we assume, as it is usual in most laser configurations, that the thickness  $l$  of the active medium is much larger than the laser wavelength  $\lambda=2\pi/k$ , the integrals in Eq.(11) take the simple form:

$$\int_0^l |u(z)|^2 dz = l \langle \sin^2 x \rangle \quad (12)$$

$$\int_0^l |u(z)|^4 dz = l \langle \sin^4 x \rangle \quad (13)$$

where  $\langle f(x) \rangle$  stands for  $(1/2\pi) \int_0^{2\pi} f(x) dx$ . Since:

$$\langle \sin^2 x \rangle = \frac{1}{2}, \quad \langle \sin^4 x \rangle = \frac{3}{8} \quad (14)$$

from Eqs.(11-13) we finally obtain  $\eta=2/3$ .

### 7.12A Dispersion relation for a Lorentzian line.

The relation between the refractive index  $n$  and the absorption coefficient  $\alpha$  for a homogeneously-broadened transition line is given by Eq.(7.10.2) of PL and reads:

$$n(\nu - \nu_0) = n_0 + \left( \frac{c}{2\pi\nu} \right) \left( \frac{\nu_0 - \nu}{\Delta\nu_0} \right) \alpha(\nu - \nu_0) \quad (1)$$

where  $n_0$  is the refractive index far from resonance,  $\nu_0$  the transition frequency,  $\Delta\nu_0$  the transition width (FWHM),  $\nu$  the frequency of the em wave probing the transition,  $c$  the speed of light in vacuum, and  $\alpha$  the absorption coefficient. For a Lorentzian line, the absorption coefficient is given by [see, e.g., Eqs.(2.4.33), (2.5.10) and (2.5.11) of PL]:

$$\alpha(\nu - \nu_0) = \frac{\sigma_a N}{[1 + 4(\nu - \nu_0)^2 / \Delta\nu_0^2]} \quad (2)$$

where  $\sigma_a$  is the peak absorption cross section and  $N$  the density of atoms. Note that the absorption coefficient at resonance, i.e. at  $\nu=\nu_0$ , is given by  $\alpha_p=\sigma_a N$ ; for

$N=1.58\times10^{19}$  ions/cm<sup>3</sup> and  $\sigma_s=1.22\times10^{-20}$  cm<sup>2</sup>, one then has  $\alpha_p\approx0.1928$  cm<sup>-1</sup>. For  $\nu=\nu_0+\Delta\nu_0/2$ , the absorption coefficient is simply half of its peak value, i.e.  $\alpha(\Delta\nu_0/2)=\alpha_p/2$ . Using these results and Eq.(1), it then turns out that the refractive index of ruby at resonance is equal to  $n_0$ , i.e. to the far-from-resonance value. At  $\nu=\nu_0+\Delta\nu_0/2$ , from Eq.(1) it follows that the refractive index differs from the off-resonance value  $n_0$  by the amount:

$$\Delta n = n(\Delta\nu_0/2) - n_0 = -\frac{c}{8\pi\nu} \alpha_p \equiv -\frac{\lambda_0 \alpha_p}{8\pi} \quad (3)$$

For  $\lambda_0=694.3$  nm and  $\alpha_p\approx0.1928$  cm<sup>-1</sup>, from Eq.(3) it follows that  $\Delta n\approx5.3\times10^{-7}$ . Notice that the contribution to the refractive index provided by the  $R_1$  transition line is very small compared to  $n_0$  and can be in practice neglected.

*Complementary note:*

Equation (1) relating the refractive index and the absorption coefficient for a **Lorentzian** atomic transition can be derived using a simple classical model of absorption and dispersion in a dielectric medium, the **Drude-Lorentz** model. In such a model, the optical electron of an atom displaced from its equilibrium position  $x=0$  by an applied electromagnetic (e.m.) field is pulled back towards its original position by an elastic force (the binding force), experiencing a frictional force which accounts for, e.g., collisions and dipole irradiation. The equation of motion for the electron displacement  $x$  is thus:

$$m \frac{d^2x}{dt^2} + \gamma \frac{dx}{dt} + m\omega_0^2 x = eE \quad (4)$$

where  $m$  and  $e$  are the mass and charge of the electron, respectively,  $\omega_0$  is the electron natural oscillation frequency,  $\gamma$  accounts for dissipation, and  $E(t)$  is the amplitude of the electric field of the e.m. wave incident on the atom. Notice that, in writing Eq.(4), the electron velocity  $dx/dt$  has been assumed much smaller than the velocity of light  $c$ , thus neglecting the magnetic force acting on the electron. If we consider a **monochromatic** field  $E(t)=E_0 \cos(\omega t)$  of angular frequency  $\omega$ , the solution to Eq.(4) can be easily found by making the Ansatz:

$$x(t) = x_0 \exp(i\omega t) + x_0^* \exp(-i\omega t) \quad (5)$$

where the complex amplitude  $x_0$  of the oscillation is readily obtained by inserting Eq.(5) into Eq.(4) and setting equals the terms oscillating as  $\exp(\pm i\omega t)$ . This yields:

$$x_0 = \frac{eE_0/m}{(\omega_0^2 - \omega^2) + i\omega\gamma/m} \quad (6)$$

The electric dipole induced by the incident field is hence:

$$\mathbf{p} = \mathbf{e}\mathbf{x} = \frac{e^2 / m}{(\omega_0^2 - \omega^2) + i\gamma\omega / m} E_0 \exp(i\omega t) + c.c. \quad (7)$$

where *c.c.* stands for complex conjugate. If we have *N* atoms per unit volume, the macroscopic polarization induced by the **e.m.** field is:

$$P = Np = \frac{Ne^2 / m}{(\omega_0^2 - \omega^2) + i\gamma\omega / m} E_0 \exp(i\omega t) + c.c. \quad (8)$$

From elementary electromagnetic theory, it is known that the polarization given by Eq.(8) implies a relative dielectric constant  $\epsilon_r$  of the medium given by:

$$\epsilon_r = n_0^2 + \frac{Ne^2 / m}{\epsilon_0 [(\omega_0^2 - m^2) + i\omega\gamma / m]} \quad (9)$$

where  $n_0$  (real) is the refractive index of the medium away from the resonance line at  $\omega = \omega_0$ . The absorption coefficient  $\alpha(\omega)$  and refractive index  $n(\omega)$  of the medium are then given by ( $\alpha > 0$  for an absorptive medium):

$$\alpha(\omega) = -\frac{\omega}{c} \text{Im} \sqrt{\epsilon_r} \quad (10)$$

$$n(\omega) = \text{Re} \sqrt{\epsilon_r} \quad (11)$$

where *c* is the velocity of light in vacuum. If we assume that the contribution to the dielectric constant (9) given by the resonant dipoles is smaller as compared to the bulk contribution  $(n_0)^2$ , we may assume:

$$\sqrt{\epsilon_r} \cong n_0 + \frac{Ne^2 / m}{2n_0\epsilon_0 [(\omega_0^2 - \omega^2) + i\omega\gamma / m]} \quad (12)$$

so that from Eqs.(10-12) we get:

$$\alpha(\omega) = \frac{Ne^2\gamma / m}{2n_0m\epsilon_0c} \frac{\omega^2}{(\omega_0^2 - \omega^2)^2 + \omega^2\gamma^2 / m^2} \quad (13)$$

$$n(\omega) = n_0 + \frac{Ne^2}{2mn_0\epsilon_0} \frac{(\omega_0^2 - \omega^2)}{(\omega_0^2 - \omega^2)^2 + \omega^2\gamma^2 / m^2} \quad (14)$$

In order to derive Eq.(1), we need to introduce the near-resonant approximation, which is **valid** for a weakly damped oscillator, i.e. for  $\Delta\omega_0/\omega_0 \ll 1$ , where  $\Delta\omega_0 = \gamma/m$ . As it will be shown below, this means that the linewidth  $\Delta\omega_0$  of the absorption curve is much smaller than the resonance frequency  $\omega_0$ , a condition

usually satisfied in the optical range of wavelengths. Since the resonant contribution in Eq.(9) vanishes when  $|\omega - \omega_0| > \Delta\omega_0$ , i.e. sufficiently far away from the resonance  $\omega_0$ , we may set in Eq.(9)  $(\omega^2 - \omega_0^2) \approx 2\omega_0(\omega - \omega_0)$  and  $\omega \approx \omega_0$ , so that from Eqs.(13) and (14) we obtain:

$$\alpha(\omega) = \frac{Ne^2\omega}{2n_0m\varepsilon_0c\omega_0\Delta\omega_0} \frac{1}{1 + \left[ \frac{2(\omega - \omega_0)}{\Delta\omega_0} \right]^2} \quad (15)$$

$$n(\omega) = n_0 - \frac{Ne^2}{n_0m\varepsilon_0\omega_0\Delta\omega_0^2} \frac{\omega - \omega_0}{1 + \left[ \frac{2(\omega - \omega_0)}{\Delta\omega_0} \right]^2} \quad (16)$$

Equation (15) shows that the absorption line is Lorentzian with a FWHM equal to  $\Delta\omega_0$ . A comparison of Eqs.(15) and (16) finally yields:

$$n(\omega) = n_0 - \frac{c(\omega - \omega_0)}{\omega\Delta\omega_0} \alpha(\omega) \quad (17)$$

Equation (17) reduces to Eq.(1) provided that the substitution  $\omega = 2\pi\nu$  is made.

### 7.13A Frequency pulling in a homogeneously-broadened laser.

The oscillation frequency  $\nu_L$  in a single-mode, homogeneously-broadened laser is given, as discussed in Sec.7.9 of PL, by the frequency pulling relation:

$$\nu_L = \frac{(\nu_0 / \Delta\nu_0) + (\nu_c / \Delta\nu_c)}{1/\Delta\nu_0 + 1/\Delta\nu_c} \quad (1)$$

where  $\nu_0$  is the center frequency of the laser transition,  $\nu_c$  is the frequency of the cold cavity mode closest to the center of the gain line, and  $\Delta\nu_c$  and  $\Delta\nu_0$  are the widths of cavity mode resonance and laser transition, respectively. The basic physical reason why the oscillation frequency  $\nu_L$  does not coincide, in general, with the cavity mode frequency  $\nu_c$ , but it is pulled toward the center of the gain line  $\nu_0$ , is that the atomic transition contributes to some extent to the refractive index of the medium, as it was shown, e.g., in problem 7.12P. The frequency dependence of the refractive index near the atomic resonance, usually neglected in the calculation of cavity mode resonance, is in fact responsible for the frequency pulling phenomenon. To prove Eq.(1), let us consider a Fabry-Perot optical cavity of geometrical length  $L$  containing an active medium of length  $l$  with a refractive index (bulk) no. As shown in problem 7.12P, the refractive

index of the gain medium, including the resonant contribution due to the laser transition, is given by [see Eq.(1) of Problem 7.14P]:

$$n(\nu) = n_0 + \frac{c(\nu - \nu_0)}{2\pi\Delta\nu_0\nu} g(\nu) \quad (2)$$

where  $g(\nu)$  is the gain coefficient. If  $\nu_L$  is the oscillation frequency, the phase shift of the laser field **after** a cavity round trip is hence given by:

$$\Delta\phi_L = 2 \frac{2\pi\nu_L}{c} [L - l + l n(\nu_L)] + \phi \quad (3)$$

where  $\phi$  takes into account possible phase shifts due to diffraction **and/or** reflection at the mirrors (see Sec. 5.2 of PL). As the field must reproduces itself after a cavity round-trip, one has:

$$\Delta\phi_L = 2m\pi \quad (4)$$

$m$  being an integer. This condition defines implicitly the oscillation frequency of the cavity filled with the gain medium. If  $\nu_c$  is the frequency of the cold cavity mode, one has manifestely:

$$2 \frac{2\pi\nu_c}{c} (L - l + l n_0) + \phi = 2m\pi \quad (5)$$

Combining Eqs.(2-5) one then obtains:

$$\nu_c L_e = \nu_L \left[ L_e + \frac{c(\nu_L - \nu_0)l}{2\pi\Delta\nu_0\nu_L} g(\nu_L) \right] \quad (6)$$

where  $L_e = L - l + l n_0$  is the optical length of the cavity. As the laser is in a **steady-state**, the round-trip gain equals cavity losses, **i.e.**:

$$g(\nu_L)l = \gamma \quad (7)$$

where  $\gamma$  is the total logarithmic loss per-pass. By extending the analysis given in Sec. 5.3 of PL, it can be easily shown that  $\gamma$  is related to the width  $\Delta\nu$ , of the cavity mode resonance by the relation:

$$\Delta\nu_c = \frac{c\gamma}{2\pi L_e} \quad (8)$$

Using Eqs.(7) and (8), Eq.(6) can be cast in the form:

$$\nu_c = \nu_L \left[ 1 + \frac{\Delta\nu_c}{\Delta\nu_0\nu_L} (\nu_L - \nu_0) \right] \quad (9)$$

## ANSWERS

Solving **Eq.(9)** with respect to  $\nu_L$  finally yields **Eq.(1)**.

### **7.14A Calculation of frequency pulling in a He-Xe laser.**

The width  $\Delta\nu_c$  of the cavity mode resonance is given by:

$$\Delta\nu_c = \frac{\gamma c}{2\pi L_e} = \frac{0.5 \times 10^8 \text{ ms}^{-1}}{2\pi \times 0.1 \text{ m}} \cong 79.6 \text{ MHz} \quad (1)$$

so that the ratio  $\Delta\nu_0/\Delta\nu_c$  between the width of Doppler-broadened laser transition and cavity mode resonance is:

$$\frac{\Delta\nu_0}{\Delta\nu_c} = \frac{200 \text{ MHz}}{79.6 \text{ MHz}} \cong 2.5 \quad (2)$$

Notice that, since  $\Delta\nu_c$  is **comparable** with  $\Delta\nu_0$ , a strong frequency pulling is expected when the laser cavity resonance  $\nu$ , is detuned apart from the center of the **gainline**  $\nu_0$ . The frequency difference  $\nu_L - \nu_c$  between the actual laser oscillation frequency and the cavity mode resonance is readily derived using the frequency pulling relation given by **Eq.(7.9.1)** of PL (see also Problem **7.13P**):

$$\nu_L - \nu_c = \frac{\nu_0 - \nu_c}{1 + \frac{\Delta\nu_0}{\Delta\nu_c}} = \frac{50 \text{ MHz}}{1 + 2.5} \cong 14.3 \text{ MHz} \quad (3)$$

Notice that, as expected, the frequency pulling is rather pronounced and it is indeed readily observed with a **3.51- $\mu\text{m}$**  He-Xe laser.

### **7.15A Quantum limit to the laser linewidth.**

The fundamental limit to the laser **linewidth** due to spontaneous emission noise in a single-longitudinal-mode is given by the **Schawlow-Towens** formula, which reads [**see, e.g., Eq.(7.9.2)** of PL]:

$$\Delta\nu_L = \frac{N_2}{N_2 - N_1} \frac{(2\pi\hbar\nu_L)(\Delta\nu_c)^2}{P} \quad (1)$$

where:  $N_1$  and  $N_2$  are populations of upper and lower laser levels, respectively;  $P$  is the output laser power;  $\nu_L$  is the frequency of the laser field; and  $\Delta\nu_c$  is the width of cavity mode resonance, given by:

$$\Delta\nu_c = \frac{1}{2\pi\tau_c} = \frac{\gamma c}{2\pi L_c} \quad (2)$$

In Eq.(2),  $\tau_c=L_c/(\gamma c)$  is the cavity photon lifetime and  $c$  the speed of light in vacuum. For  $\lambda_L=1064$  nm,  $\gamma=0.01$  and  $L_c=12$  cm, one has  $\nu_L=c/\lambda_L \approx 2.8195 \times 10^{14}$  Hz,  $\tau_c=L_c/(\gamma c) \approx 40$  ns, and, from Eq.(2),  $\Delta\nu_c \approx 3.98$  MHz. For the Nd:YAG laser, the lower laser level can be considered almost empty, i.e.  $N_2/N_1 \gg 1$ , so that we may assume in Eq.(1)  $N_2/(N_2-N_1) \approx 1$ . Using this approximation and for an output power  $P=100$  mW, from Eq.(1) we finally obtain:  $\Delta\nu_L \approx 0.186$  mHz. Notice that this linewidth limit is practically negligible as compared to environmental noise disturbances, such as cavity length fluctuations, which typically introduces a linewidth broadening of few tens of kHz in non-stabilized lasers, down to a few Hz using active stabilizing methods of cavity length.

*Complementary note:*

The fundamental limit to the monochromaticity of a continuous-wave single-mode laser, as given by the **Schawlow-Townes** formula [Eq.(1)], is established by spontaneous emission noise which originates from the quantum nature of the electromagnetic field. Although a proper treatment of spontaneous emission noise would require a full quantum theory of laser, it is possible to provide a simplified and heuristic derivation of the laser linewidth due to spontaneous emission by application of the energy-time uncertainty relation of quantum mechanics, which reads:

$$\Delta E \Delta t \geq A \quad (3)$$

This relation establishes a lower limit  $\Delta E$  to the energy uncertainty of a quantum-mechanical system in an energy measurement process that requires a time interval  $\Delta t$ . If  $\phi$  is the number of photons in the cavity mode and  $\nu_L$  their frequency, the energy  $E$  in the cavity mode is given by  $E=h\nu_L\phi$ , so that:

$$\Delta E = h\nu_L\Delta\phi + h\phi\Delta\nu_L \quad (4)$$

where  $\Delta\phi$  and  $\Delta\nu_L$  are the uncertainties of  $\phi$  and  $\nu_L$ , respectively. For a laser above threshold, the number of photons  $\phi$  may range typically from  $10^{10}$  to  $10^{16}$  (see Example 7.1 of PL), so that the uncertainty in the photon number  $\Delta\phi/\phi$  is expected to be much smaller than the uncertainty in the frequency  $\Delta\nu_L/\nu_L$ . This circumstance can be also understood by observing that, for a laser above threshold, the condition that the gain balances cavity losses in steady-state oscillation [see Eq.(7.3.4) of PL] corresponds to lock the amplitude of the **intracavity** field, i.e.  $\phi$ , but not its phase, whose fluctuations account for the uncertainty  $\Delta\nu_L$  in the frequency. Therefore we may neglect in Eq.(4) the first

term on the right hand side, so that, **after** substitution of Eq.(4) into Eq.(3), the **energy-uncertainty** relation takes the form:

$$\Delta\nu_L \geq \frac{1}{2\pi\phi\Delta t} \quad (5)$$

In order to evaluate  $\Delta t$ , it is worth observing that any kind of measurement of  $E$  should require a time interval  $\Delta t$  no longer than the spontaneous emission lifetime, **i.e.**  $1/\Delta t$  must be larger than the rate  $C$  of increase in cavity photons due to spontaneous emission. For a four-level laser, an inspection of Eq.(7.2.2) of PL reveals that  $1/\Delta t \approx C = V_a B N_2$ , so that Eq.(5) yields:

$$\Delta\nu_L \geq \frac{V_a B N_2}{2\pi\phi} \quad (6)$$

where  $B$  is the stimulated transition rate per photon per mode,  $V_a$  is the volume of the mode in the active medium, and  $N_2$  is the **population** of the upper laser level. It is then straightforward to rewrite Eq.(6) in the most standard form, given by Eq.(7.9.2) of PL, after observing that, if  $P$  is the output laser power,  $\tau_c = 1/(2\pi\Delta\nu_c)$  the cavity photon lifetime and  $N_c = N_2 - N_1$  the population inversion, one has  $P = h\nu_L\phi/\tau_c = 2\pi h\nu_L\phi\Delta\nu_c$  and  $BV_a = 1/\tau_c N_c = 2\pi\Delta\nu_c/(N_2 - N_1)$  [see Eq.(7.3.2) of PL], **i.e.:**

$$\phi = \frac{P}{2\pi h\nu_L\Delta\nu_c} \quad (7)$$

$$V_a B = \frac{2\pi\Delta\nu_c}{N_2 - N_1} \quad (8)$$

Substituting Eqs.(7) and (8) into Eq.(6), one finally obtains the **Schawlow-Townes formula** given by Eq.(1).

### 7.16A Tuning of a Ti:sapphire laser by a birefringent filter.

If  $L_e$  denotes the plate **thickness** along the beam direction within the plate, the frequency separation  $\Delta\nu_{fsr}$  between two consecutive maxima of the birefringent filter is given by [see, for instance, Eq.(7.6.2) of PL]:

$$\Delta\nu_{fsr} = \frac{c}{L_e(n_e - n_0)} \quad (1)$$

where  $c$  is the speed of light in vacuum and  $n_0$ ,  $n$ , the refractive indices for ordinary and extraordinary beam components, respectively. In terms of

wavelength separation  $\Delta\lambda_{fsr}$ , we may write  $\Delta\lambda_{fsr}=\lambda^2\Delta\nu_{fsr}/c$ , which can be easily derived by differentiating with respect to  $\lambda$  and  $\nu$  the relation  $\lambda=c/\nu$ . For  $n_0=1.535$ ,  $n_e=1.544$ ,  $\lambda=780$  nm and  $\Delta\lambda_{fsr}=6$  nm, we have  $\Delta\nu_{fsr}=c\Delta\lambda_{fsr}/\lambda^2 \approx 2.96 \times 10^{12}$  Hz, so that from Eq.(1) one readily obtains:  $L_e=c/[\Delta\nu_{fsr}(n_0-n_e)] \approx 11.27$  mm. The plate thickness L is then given by:

$$L = L_e \cos \theta_B' \quad (2)$$

where  $\theta_B'$  is the internal Brewster angle. If n denotes the average of  $n_0$  and  $n_e$ , the Brewster angle for the quartz plate is  $\theta_B = \tan^{-1} n \approx 57^\circ$ , so that, by Snell's law, the internal Brewster angle is  $\theta_B' = \sin^{-1}[(1/n)\sin\theta_B] \approx 33^\circ$ . From Eq.(2) with  $L_e \approx 11.3$  mm, we finally obtain  $L \approx 9.45$  mm.

### 7.17A Transverse mode selection.

Let us indicate by  $\gamma_{lm}^{(d)}$  the diffraction loss per-transit for the  $TEM_{lm}$  mode of the symmetric resonator and by  $\gamma_2 = -\ln(1-T_2) \approx 5.1\%$  the logarithmic loss due to the output coupling. Assuming that the unsaturated gain per-transit  $\alpha=0.1$  is the same for all transverse modes, in order to avoid laser oscillation on higher-order transverse modes the overall logarithmic loss per-pass  $\gamma_{lm} = \gamma_2/2 + \gamma_{lm}^{(d)}$  of higher-order  $TEM_{lm}$  modes must be larger than the unsaturated gain  $\alpha$ , i.e.:

$$\gamma_{lm}^{(d)} + \frac{\gamma_2}{2} > \alpha \quad (1)$$

Since we expect the diffraction losses to be an increasing function of mode order, it is sufficient to satisfy condition (1) for the lowest order  $TEM_{01}$  mode. This yields  $\gamma_{01}^{(d)} > 0.0745$ . Since the resonator is symmetric with a g-parameter equal to  $g=1-L/R=0.8$ , from Fig.5.13 of PL we see that the condition  $\gamma_{01}^{(d)} > 0.0745$  is satisfied provided that the Fresnel number  $N=a^2/\lambda L$  of the cavity is smaller than  $\approx 2$ . From this result, we obtain the maximum aperture diameter  $2a$  that ensures oscillation in the fundamental  $TEM_{00}$  mode as:

$$2a = 2(N\lambda L)^{1/2} \approx 2 \text{ mm} \quad (2)$$

### 7.18A Single longitudinal mode oscillation in an inhomogeneously-broadened laser.

Since the CO<sub>2</sub> laser transition is mainly Doppler broadened with a FWHM of the Gaussian gain curve  $\Delta\nu_0=50\text{ MHz}$ , when the laser is operated at a pump level twice the threshold value, all cavity modes with a **frequency detuned** apart from the center of the gain line by less than  $\Delta\nu_0/2$  are above **threshold** and can thus oscillate. If a cavity resonance coincides with the transition peak, **single-longitudinal mode** operation requires that the sideband cavity modes, spaced apart by  $\pm c/2L$  from the central mode, fall out of the gain line by a frequency greater than  $\Delta\nu_0/2$ , that is:

$$\frac{c}{2L} \geq \frac{\Delta\nu_0}{2} \quad (1)$$

Taking  $\Delta\nu_0=50\text{ MHz}$  and solving Eq.(1) with respect to L yields the requested maximum mirror spacing  $L_{MAX}=c/\Delta\nu_0=6\text{ m}$ .

### 7.19A Suppression of spatial hole burning by the twisted-mode technique.

Let us consider the interference of two circularly-polarized waves, with the same amplitude  $E_0$  and way of rotation, which counterpropagate along the  $z$  resonator axis. According to PL, to denote consistently the polarization way of rotation, we use the convention that the observer is always facing the incoming light beam. A simple and elegant solution to the problem can be obtained by using a polar representation, in the transverse plane ( $x,y$ ) of propagation, for the electric-field vectors of the two counterpropagating circularly-polarized waves. Denoting by  $\rho$  and  $\phi$  the amplitude and phase of the electric field and with reference to Fig.1, we may write for the two waves:

$$\rho_1 = E_0 \quad , \quad \phi_1 = kz - \omega t \quad , \quad \rho_2 = E_0 \quad , \quad \phi_2 = kz + \omega t + \phi_0 \quad , \quad (1)$$

where  $k=2\pi/\lambda$  is the **wavenumber** and  $\omega=kc$  the angular frequency of the waves, and  $\phi_0$  a possible phase delay between the two waves. Notice that, according to Eq.(1), the electric field vectors of the two waves rotate, in the transverse plane, with the same angular frequency  $\omega$  but in opposite ways, one clockwise the other counterclockwise. This is consistent with the circumstance that, for an observer facing the oncoming light beams, the two waves are both left (or right) circularly polarized. With the help of the graphic construction shown in Fig.1, it is evident that, according to the parallelogram sum rule, the vectorial sum of the

electric fields of the two circularly-polarized waves is a vector forming with the x-axis an angle  $\phi$  given by:

$$\phi = \frac{\phi_1 + \phi_2}{2} \quad (3)$$

Using Eq.(1), Eq.(3) yields:

$$\phi = kz + \phi_0 / 2 \quad (4)$$

From Eq.(4) it turns out that the angle  $\phi$  turns out to be independent of time t,

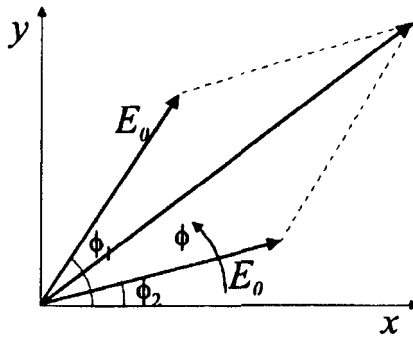


**Fig. 1** Interference of two counterpropagating circularly-polarized waves.

although  $\phi_1$  and  $\phi_2$  are not As a result, while the vectors representing the two circularly-polarized waves rotate in the transverse plane in opposite directions, their superposition has a fixed direction of vibration, which forms with the x-axis an angle  $\phi$  given by Eq.(4). This means that the total electric field is linearly polarized, and its amplitude oscillates in time between zero (when the two interfering waves add with opposite phase) and  $2E_0$  (when the two interfering waves add in phase). From Eq.(2), it then follows that:

- (i) at the reference plane  $z=0$ , the total electric field is linearly polarized with amplitude  $2E_0$  and forms with the x-axis and angle  $\phi(z=0)=\phi_0/2$ .
- (ii) at the plane  $z=d$ , the total electric field is still linearly polarized with the same amplitude  $2E_0$ , but forms with the x-axis the angle  $\phi(z=d)=\phi(z=0)+kd$ .

### 7.20A Single longitudinal mode selection by an intracavity etalon.

Assuming for the sake of simplicity that both the cavity length and the etalon tilting angle are tuned so that one cavity resonance and one transmission peak of the etalon coincide with the center of the gain line, the net gain per-transit experienced by the resonant mode is given by  $G_p \exp(-\gamma) \approx 1.25$ , where  $G_p=1.3$  is

the unsaturated peak gain and  $\gamma=0.04$  are the total losses per-pass, including output coupling loss and internal losses. If  $\Delta\nu=c/2L\approx150$  MHz is the frequency separation between adjacent longitudinal modes of the laser cavity, single longitudinal mode operation is ensured provided that all off-resonance longitudinal modes experience a loss larger than the gain, i.e.:

$$\exp(-\gamma)G_p g^*(m\Delta\nu)T(m\Delta\nu) < 1 \quad (1)$$

for any mode  $m=\pm 1, \pm 2, \pm 3, \dots$ . In Eq.(1),  $g^*(\nu)=\exp[-\ln 2(\nu/\Delta\nu_0)^2]$  is the Gaussian curve of the Doppler-broadened gain transition,  $\Delta\nu_0=3.5$  GHz is the FWHM of the curve, and  $T(\nu)$  is the transmission function of the **intracavity** etalon.  $T(\nu)$  is given by [see Eq.(4.5.6) of PL]:

$$T(\nu) = \frac{(1-R)^2}{(1-R)^2 + 4R\sin^2\left[\frac{2\pi l'\nu}{c}\right]} \quad (2)$$

where R is the reflectivity of the two etalon faces and  $l'=n,l\cos\theta\approx n,l=2.9$  cm for a small tilting angle  $\theta$ . Notice that the free-spectral-range of the etalon, given by  $\Delta\nu_{fsr}=c/2l'\approx5.17$  GHz, is much larger than the cavity axial mode separation  $\Delta\nu$  and comparable to the width of the gain curve. For longitudinal modes that fall under the first lateral peaks of the etalon transmission function, it is straightforward to show that Eq.(1) is satisfied since  $G_p\exp(-\gamma)g^*(\Delta\nu_{fsr})\approx0.27<1$ . Thus in order to ensure single longitudinal mode operation it is sufficient that Eq.(1) be satisfied in correspondence of the two longitudinal cavity modes adjacent the resonant mode, i.e. for  $m=\pm 1$ . This condition yields:

$$T(\Delta\nu) < \frac{1}{G_p \exp(-\gamma)g^*(\Delta\nu)} \approx 0.8 \quad (3)$$

which, with the help of Eq.(2), can be written as:

$$(1-R)^2 < 0.8 \left[ (1-R)^2 + 4R \sin^2\left(\pi \frac{\Delta\nu}{\Delta\nu_{fsr}}\right) \right] \quad (4)$$

Since  $\epsilon=\sin^2(\pi\Delta\nu/\Delta\nu_{fsr})\approx8.3\times10^{-3}$  is a small quantity, the inequality (4) can be easily solved with respect to (1-R), yielding at leading order  $1-R<4\epsilon^{1/2}$ , i.e.  $R>64\%$ . A more accurate estimation of R, obtained by an iterative procedure, yields  $R>70\%$ . The minimum finesse of the etalon is thus given by:

$$F = \frac{\pi R^{1/2}}{1-R} \approx 0.87 \quad (5)$$

# CHAPTER 8

## Transient Laser Behavior

### PROBLEMS

#### **8.1P Relaxation oscillations in a Nd:YAG laser.**

Calculate the relaxation oscillation frequency of a **Nd:YAG** laser when it is operated twice above threshold assuming a cavity length  $L=20\text{ cm}$ , a **Nd:YAG** rod of length  $l=0.8\text{ cm}$ , a refractive index of YAG  $n=1.82$ , an upper state laser lifetime  $\tau=230\text{ }\mu\text{s}$ , and an overall round-trip logarithmic loss  $\gamma=2\%$ .

#### **8.2P Noise spectrum of the output power for a four-level laser.**

Consider a single-mode four-level laser subjected to a continuous-wave pumping and assume that a Gaussian noise of white spectrum is superimposed to the continuous pump rate. Derive an analytical expression for the noise spectrum of the laser output power.

[Hint: **first** write down the rate-equations for the number of photons in the oscillating mode and for the population inversion, with a Gaussian noise term added to the pump rate; then linearize the rate-equations around the steady-state solution, obtained by neglecting the noise term, and study the noise property of the linearized system in the presence of this Gaussian white noise]  
(Level of *difficulty* higher than average)

#### **8.3P Fast Q-switching in a Nd:YLF laser.**

A flash-pumped **Nd:YLF** laser, operated in a pulsed regime and fast Q-switched by an **intracavity** Pockels cell, is made by a  $l=1\text{ cm}$  long active crystal with refractive index  $n=1.45$  placed at the center of a symmetric confocal resonator of length  $L=30\text{ cm}$ . The transmission of the cavity output coupler is  $T=20\%$  and the internal logarithmic laser losses per-pass are estimated to be  $\gamma_i \approx 5\%$ . Assuming a stimulated-emission cross-section  $\sigma_e=1.9 \times 10^{-19}\text{ cm}^2$  of **Nd:YLF** at

the laser wavelength  $\lambda=1053$  nm, calculate the energy and pulse duration of the Q-switched pulses when the energy of the pump pulse is twice the threshold value.

### **8.4P Calculation of the pulse energy and pulse duration in a repetitively Q-switched Nd:YAG laser.**

The Nd:YAG laser in Figs. 7.4 and 7.5 of PL is pumped at a level of  $P_{in}=10$  kW and repetitively Q-switched at a 10-kHz repetition rate by an acousto-optic modulator (whose insertion losses are assumed negligible). Calculate the energy and duration of the output pulses as well as the average power expected for this case.

### **8.5P Quarter-wave voltage in a Q-switch Pockels cell.**

Consider a Pockels cell in the so-called longitudinal configuration, i.e. with the dc field applied in the direction of the beam passing through the nonlinear crystal. In this case, the induced birefringence  $\Delta n=n_x-n_y$  is given by  $\Delta n=n_0^3 r_{63} V/L$ , where  $n_0$  is the ordinary refractive index,  $r_{63}$  is the appropriate nonlinear coefficient of the material,  $V$  is the applied voltage, and  $L$  is the crystal length. Derive an expression for the voltage required to keep the polarizer-Pockels-cell combination in Fig. 8.5a of PL in the closed position (quarter-wave voltage). Calculate the quarter-wave voltage at  $\lambda=1.06 \mu\text{m}$  in case of a  $\text{KD}_2\text{PO}_4$  Pockels cell assuming, for  $\text{KD}_2\text{PO}_4$ ,  $r_{63}=26.4 \times 10^{12} \text{ m/V}$  and  $n_0=1.51$ .

### **8.6P Active Q-switching in a three-level laser.**

Derive expressions for output energy and pulse duration that apply to a Q-switched three-level laser.

(Level of *difficulty* much higher than average)

**8.7P Calculation of the beam deflection angle by an acousto-optic modulator.**

A He-Ne laser beam with a wavelength (in air)  $\lambda=632.8 \text{ nm}$  is deflected by a  $\text{LiNbO}_3$  acousto-optic deflector operating in the Bragg regime at the acoustic frequency of 1 GHz. Assuming a sound velocity in  $\text{LiNbO}_3$  of  $7.4 \times 10^5 \text{ cm/s}$  and a refractive index  $n=2.3$ , calculate the angle through which the beam is deflected.

**8.8P Mode-locking of sidebands modes with random amplitudes.**

Suppose that a mode-locked signal has N sidebands all exactly in phase, but the amplitudes of the individual sidebands are randomly and uniformly distributed between zero and a maximum value  $E_0$ . Calculate the expectation values of the average output power in the N-mode signal and the peak power of the dominant mode-locked pulse in each period.

(Level of difficulty higher than average)

**8.9P Chirped Gaussian pulses with quadratic phase locking relations.**

Derive the analytical expression for the mode-locked pulse signal [Eq.(8.6.14) of PL] in case of Gaussian distribution of mode amplitudes and quadratic phase locking relations.

**8.10P On the periodicity of mode-locked signals.**

By approximating the sum over all modes in Eq.(8.6.10) of PL with an integral, an important characteristic of the output behavior is lost. What is it?

**8.11P Phase locking condition for second-harmonic mode-locking.**

Assume that the phase relation between consecutive longitudinal modes is such that  $\varphi_{l+1} - \varphi_l = \varphi_l - \varphi_{l-1} + \pi$  and the spectral amplitude is constant over  $2N$  modes. Show that the pulse repetition rate is now equal to  $2\Delta\nu$ , where  $\Delta\nu=c/2L$  is the separation of axial cavity modes.

[Hint: Let start to show that the phase locking relation is satisfied by assuming  $\varphi_l=0$  if  $l$  is even and  $\varphi_l=\pi/2$  if  $l$  is odd. Then write down the mode-locked signal as the sum of the superposition of longitudinal modes with odd and with even mode indices, and show that these two sums correspond to two pulse trains which are delayed in time by  $1/(2\Delta\nu)$ ]

(Level of difficulty much higher than average)

**8.12P Pulsewidth calculation in an actively mode-locked Nd:YAG laser.**

A Nd:YAG laser, oscillating at the wavelength  $\lambda=1064$  nm, is mode-locked by an acousto-optic modulator. Assuming a cavity length  $L=1.5$  m and a homogeneously-broadened gainline of width  $\Delta\nu_0 \approx 195$  GHz, calculate the expected pulsewidth. If the linewidth were inhomogeneously broadened, what would have been the expected pulsewidth?

**8.13P Gaussian pulse analysis of frequency mode-locking.**

Derive analytical expressions for pulsewidth and frequency chirp of Gaussian pulses in frequency mode-locking of a homogeneously-broadened laser.

(Level of difficulty higher than average. One should read first Appendix F of PL)

**8.14P Mode-locking in a He-Ne laser.**

Consider the He-Ne laser operating at the 632.8 nm transition, and assume that at room temperature the gainline is 'Doppler-broadened with a linewidth (FWHM)  $\Delta\nu_0 \approx 1.7$  GHz. If the laser is operated sufficiently far from threshold,

and the laser tube has a length of  $L=40$  cm, what is the expected pulse duration and the pulse repetition rate when the laser is mode-locked by an acousto-optic mode-locker?

### **8.15P Harmonic mode-locking of a laser in a linear cavity**

A laser system, made by a linear cavity of optical length  $L=2$  m, is mode-locked by placing an acousto-optic mode-locker inside the laser cavity at a distance  $d=L/4$  from the output mirror. Calculate the minimum value of the mode-locker frequency  $\nu_m$  needed to generate a mode-locked pulse train. What happens if the modulator is driven at a frequency twice its minimum value?

### **8.16P Calculation of pulse energy and peak power in a passively mode-locked Nd:YAG laser.**

A Nd:YAG laser, passively-mode locked by a fast saturable absorber, emits a pulse train at a repetition rate  $\nu_m=100$  MHz, each pulse having a duration  $\Delta\tau_p=10$  ps (FWHM of pulse intensity). The average output power is  $P_{av}=500$  mW. Calculate pulse energy and peak pulse power of the emitted pulse train.

### **8.17P Pulse duration in an idealized Kerr lens mode-locked Ti:Sapphire laser.**

Consider a Kerr lens mode-locked Ti:sapphire laser and assume that the total cavity **round-trip** losses can be written as  $2\gamma_r=2\gamma-kP$ , where  $P$  is the **peak intracavity** laser power and  $k \approx 5 \times 10^{-8} \text{ W}^{-1}$  is the nonlinear loss **coefficient** due to the Kerr lens mode-locking **mechanism**. Assuming a saturated round-trip gain of  $2g_0 \approx 0.1$ , a gain-bandwidth of 100 THz, and an **intracavity** laser energy of  $E=40$  nJ, calculate the pulse duration achievable in the limiting case where the effects of cavity dispersion and self-phase modulation can be neglected.

**8.18P Pulse duration in a soliton-type Ti:sapphire mode-locked laser.**

In a passively mode-locked **Ti:sapphire** the pulse shaping mechanism is mainly established by the interplay between negative dispersion of the cavity and self-phase modulation in the Kerr **medium**. Knowing that the intracavity group-velocity dispersion per-round-trip is  $\#''=-800 \text{ fs}^2$  and the nonlinear round-trip phase **shift** per unit power in the Kerr medium is  $\delta\approx 2\times 10^{-6} \text{ W}^{-1}$ , calculate the output pulse duration and pulse peak power assuming a linear cavity of length  $L=1 \text{ m}$ , an output coupling  $T=5\%$  and an average output power  $P_{av}=500 \text{ mW}$ .

**8.19P Pulse broadening in a quartz plate.**

Assuming a group-velocity dispersion (GVD) for quartz at  $\lambda\approx 800 \text{ nm}$  of  $50 \text{ fs}^2/\text{mm}$ , calculate the **maximum** thickness of a quartz plate that can be traversed by an initially **unchirped** 10-fs pulse, of Gaussian intensity profile, if the output pulse duration has not to exceed input pulse duration by more than 20%.  
[Hint: use results of Appendix G of PL]

**8.20P Self-imaging of a mode-locked pulse train.**

Consider the propagation of a mode-locked pulse train, at a repetition frequency  $v_m$  through a dispersive medium with a constant GVD equal to  $\beta_2$ . Show that, at the propagation distances  $L$ , from the entrance plane given by  $L_n=n/\pi\beta_2v_m^2$  ( $n=1,2,3,\dots$ ), the pulse train reproduces its original shape (**Talbot** images).

[Hint: write the electric field of the mode-locked pulse train as a sum of phase-locked axial modes and propagate each monochromatic component of the field along the dispersive medium assuming a parabolic law for the dispersion relation. Then show that, after propagation of a length multiple of the fundamental length  $L_T=1/\pi\beta_2v_m^2$ , the phase delay accumulated by each mode is an integer multiple of  $2\pi$ ]

## 8. TRANSIENT LASER BEHAVIOR

## ANSWERS

### 8.1A Relaxation oscillations in a Nd:YAG laser.

The relaxation oscillation frequency  $\omega'$  of a four-level **homogeneously**-broadened laser is given by Eq.(8.2.11) of PL. The laser parameters entering in this equation are **the** above-threshold parameter  $x$ , the upper-state laser lifetime  $\tau$ , and the photon lifetime  $\tau_c$ . According to Eq.(7.2.14) of PL, the photon lifetime  $\tau_c$  is given by:

$$\tau_c = \frac{L_e}{\gamma c} \cong 34 \text{ ns} \quad (1)$$

where  $L_e = L + (n-1)l \cong 20.65 \text{ cm}$  is the optical length of the resonator ( $L=20 \text{ cm}$  is the geometric cavity length,  $l=0.8 \text{ cm}$  is the length of the Nd:YAG rod,  $n=1.82$  its refractive index), and  $\gamma=0.02$  is the total logarithmic loss per-pass. From Eqs.(8.2.14) and (8.2.15) of PL one then has:

$$t_0 = \frac{2\tau}{x} = 230 \mu\text{s} \quad (2)$$

$$\omega = \sqrt{\frac{x-1}{\tau_c \tau}} \cong 355 \text{ kHz} \quad (3)$$

From Eq.(8.2.11) of PL we finally obtain:

$$\omega' = \sqrt{\omega^2 - \left(\frac{1}{t_0}\right)^2} \cong \omega \cong 355 \text{ kHz} \quad (4)$$

### 8.2A Noise spectrum of the output power for a four-level laser.

The starting point of the analysis for the calculation of the intensity noise spectrum  $S_{\sigma}(\omega)$  is provided by the rate equations for a **four-level** homogeneously-broadened laser in presence of a stochastic noise for the pump parameter. These equations are readily obtained from Eqs.(7.2.1a) and (7.2.1b) of PL as:

$$\frac{dN}{dt} = R_p - B\phi N - \frac{N}{\tau} + \xi_p \quad (1a)$$

$$\frac{d\phi}{dt} = V_a B \phi N - \frac{\phi}{\tau_c} \quad (1b)$$

where  $\xi_p(t)$  in Eq.(1a) is an additive delta-correlated stochastic term that accounts for the noise in the pump rate. Since the variance of noise is assumed to be small, we may linearize Eqs.(1a) and (1b) around the steady-state solution  $(N_0, \phi_0)$  by setting:

$$N = N_0 + \delta N, \phi = \phi_0 + \delta \phi \quad (2)$$

where  $\delta N, \delta \phi$  are small fluctuations of both population and photon number due to the noise term  $\xi_p(t)$ . The steady-state solution is obtained from Eqs.(1a) and (1b) by neglecting the noise term and setting equal to zero the time derivatives; this yields:

$$N_0 = \frac{1}{\tau_{arc}} \quad (3a)$$

$$\phi_0 = \frac{x-1}{\tau B} \quad (3b)$$

where  $x=R_p/R_{cp}$  and  $R_{cp}$  is the critical pump rate, given by Eq.(7.3.3) of PL. After inserting the Ansatz (2) in Eqs.(1a) and (1b), using Eqs.(3a) and (3b) and disregarding nonlinear terms like  $\delta \phi \delta N$  in the equation so obtained, one finds the following linearized equations for the fluctuations  $\delta N, \delta \phi$ :

$$\frac{d\delta N}{dt} = -\frac{x}{\tau} \delta N - BN_0 \delta \phi + \xi_p \quad (4a)$$

$$\frac{d\delta \phi}{dt} = BV_a \phi_0 \delta N \quad (4b)$$

To calculate  $\delta \phi(t)$  we substitute into Eq.(4a)  $\delta N(t)$  as obtained from Eq.(4b). We obtain the following differential second-order driven equation for  $\delta \phi$ :

$$\frac{d^2 \delta \phi}{dt^2} + \frac{x}{\tau} \frac{d\delta \phi}{dt} + \omega_0^2 \delta \phi = BV_a \phi_0 \xi_p \quad (5)$$

where we have set:

$$\omega_0^2 = B^2 V_a \phi_0 N_0 = \frac{x-1}{\tau_c \tau} \quad (6)$$

From the theory of linear systems in presence of a stationary noise, it is well-known that an input stationary noise, with power spectral density  $S_1(\omega)$ , is converted into an output stationary noise with a power spectral density  $S_2(\omega)$

given by  $S_2(\omega) = S_1(\omega)|H(\omega)|^2$ , where  $H(\omega)$  is the transfer function of the system. We thus have:

$$S_{\delta p}(\omega) = (BV_s \phi_0)^2 S_{\xi_p}(\omega) |H(\omega)|^2 \quad (7)$$

where  $S_{\xi_p}(\omega)$  is the spectral density of the noise source  $\xi_p$ ,  $S_{\delta p}(\omega)$  is the power spectrum for the fluctuations of photon number, and the transfer function of the system,  $H(\omega)$ , is obtained as the amplitude of the forced solution  $f(t) = H \exp(j\omega t)$  of the equation:

$$\frac{d^2 f}{dt^2} + \frac{x}{\tau} \frac{df}{dt} + \omega_0^2 f = \exp(j\omega t), \quad (8)$$

It is an easy exercise to show that:

$$H(\omega) = \frac{1}{\omega_0^2 - \omega^2 + jx\omega/\tau} \quad (9)$$

Since  $\xi_p(t)$  is assumed to be a **delta-correlated** Gaussian noise, the power spectrum  $S_{\xi_p}(\omega)$  is known to be frequency-independent (white noise). From Eq.(7) it follows that the power **spectrum** for the fluctuations in photon number,  $\delta p(t)$ , and hence in the output power,  $\delta P(t)$ , is proportional to  $|H(\omega)|^2$ . From Eq.(9) we thus finally obtain:

$$S_{\delta p}(\omega) \propto |H(\omega)|^2 = \frac{1}{(\omega_0^2 - \omega^2)^2 + x^2 \omega^2 / \tau^2} \quad (10)$$

### 8.3A Fast Q-switching in a Nd:YLF laser.

The pulse characteristics of the Q-switched Nd:YLF laser can be calculated using Eqs.(8.4.20) and (8.4.21) of PL, which provide analytical expressions for the pulse energy and pulse duration of a fast Q-switched four-level laser in terms of laser **parameters** (including logarithmic output coupling loss  $\gamma_2$ , beam area  $A_s$  in the gain medium, stimulatedemission cross-section  $\sigma_e$ , and cavity photon lifetime  $\tau_c$ ), energy utilization factor  $\eta_E$  and the ratio  $x = N_i/N_p$  by which threshold is exceeded. For the parameter values given in this problem, one has:

$$\gamma_2 = -\ln(1 - T) \approx 0.223 \quad (1)$$

$$\tau_c = \frac{L_e}{c\gamma} \approx 6.28 \text{ ns} \quad (2)$$

where  $T=0.2$  is the transmission of the output coupler,  $L_e=L+(n-1)l\approx30.45$  cm is the optical length of the cavity and  $\gamma=\gamma_2/2+\gamma_i\approx0.1616$  is the total logarithmic loss per-pass. To calculate the beam area  $A_b$  we first write  $A_b=\pi w_b^2/2$ , where  $w_b$  is the beam spot size inside the active crystal. For a confocal resonator  $w_b$  is seen from Eq.(5.5.11) of PL to be given by  $w_b=(L\lambda/2\pi)^{1/2}$ . In our case, however, the cavity length which enters in the previous equation is given by the so-called diffractive length of the resonator given by  $L_d=L-l+l/n\approx29.7$  cm. We thus get:

$$A_b = \frac{\pi w_b^2}{2} = \frac{L_d \lambda}{4} \approx 7.9 \times 10^{-4} \text{ cm}^2 \quad (3)$$

The energy utilization factor  $\eta_E$  corresponding to the ratio  $x=2$  can then be evaluated from Fig.8.11 of PL as  $\eta_E\approx0.8$ . From Eqs.(8.4.20) and (8.4.21) and using Eqs.(1-3), we finally obtain for the pulse energy and pulse duration the following numerical values:

$$\begin{aligned} E &= \frac{\gamma_2}{2} x \eta_E \frac{A_b}{\sigma_e} h\nu = \frac{0.223}{2} \times 1.6 \times \frac{7.9 \times 10^{-4} \text{ cm}^2}{1.9 \times 10^{-19} \text{ cm}^2} \times 6.63 \cdot 10^{-34} \text{ J} \cdot \text{s} \times \\ &\quad \times 2.849 \times 10^{14} \text{ s} \approx 0.14 \text{ mJ} \\ \Delta\tau_p &= \tau_c \frac{x \eta_E}{x - \ln x - 1} \approx 6.28 \text{ ns} \times 5.214 \approx 32.7 \text{ ns} \end{aligned}$$

### 8.4A Calculation of the pulse energy and pulse duration in a repetitively Q-switched Nd:YAG laser.

The energy and pulse duration of the Q-switch pulse are given by Eq.(8.4.17) and Eq.(8.4.21) of PL, respectively, where, according to the theory of repetitive Q-switching, the population inversions  $N_i$  and  $N_f$  before and after each pulse are determined as solutions of Eqs.(8.4.18) and (8.4.31) of PL. In our case, the following data are available: input pump power  $P_{in}=10$  kW, threshold pump power  $P_{th}=2.2$  kW, time between consecutive pulses  $\tau_p=0.1$  ms, and decay time  $\tau=0.23 \times 10^{-3}$  s. Thus we have  $x=P_p/P_{th}=4.545$  and  $f'=\tau/\tau_p=2.3$ . A graphic solution of the system of (8.4.18) and (8.4.31) gives for  $N_f/N_p$  and for  $N_f/N_i$  the following values (see also Fig.8.11 of PL):

$$\frac{N_i}{N_p} = 1.89 \quad , \quad \frac{N_f}{N_i} = 0.236 \quad (1)$$

The critical population inversion  $N_p$  assuming  $\gamma=0.1192$ ,  $\sigma=3.5 \times 10^{-19} \text{ cm}^2$  and  $l=7.5 \text{ cm}$ , turns out to be:

$$N_p = \frac{\gamma}{\sigma l} = 4.5 \times 10^{16} \text{ ions/cm}^3 \quad (2)$$

Taking for the active volume  $V_a$  the volume of the rod, the output pulse energy  $E$  is then given by Eq.(8.4.17) of PL ( $\gamma_2=0.1625$ ,  $V_a=2.37 \text{ cm}^3$ ,  $h\nu=1.87 \times 10^{-19} \text{ J}$ ):

$$E = \frac{\gamma_2}{2\gamma} (N_i - N_f)(V_a h\nu) = 19.8 \text{ mJ} \quad (3)$$

and thus the average power is:

$$P_{out} = \frac{E}{\tau_p} = 198 \text{ W} \quad (4)$$

Finally, the pulse duration is given by Eq.(8.4.21) of PL:

$$\Delta\tau_p = \tau_c \frac{N_i - N_f}{N_i - N_p - N_p \ln(N_i/N_p)} = 89.4 \text{ ns} \quad (5)$$

where  $\tau_c=L/c=15.7 \text{ ns}$  is the cavity photon lifetime [ $L=L+(n-1)l \approx 56.15 \text{ cm}$ ].

Note:

Notice that, since the pulse periodicity,  $\tau_p=1 \text{ ms}$ , is close to the decay time of population,  $\tau=0.23 \text{ ms}$ , the average output power  $P_{out}$  under repetitively Q-switching, as given by Eq.(4), is slightly less than the output power  $P'_{out}=(V_a h\nu/l\sigma\tau)(\gamma_2/2)(P_p/P_{th}-1)\approx211 \text{ W}$  under cw operation [see Eq.(7.3.9) of PL]. This means that most of the population inversion accumulated by the pumping process is converted into the lasing pulse. However, if the pulse periodicity were much larger than the population decay time, the average output power under Q-switching operation would be expected to be substantially smaller than the cw value  $P'_{out}$ , since in this case the population inversion between one pulse and the next is lost due to the radiative and non-radiative decays. For example, at a repetition rate of 1 kHz, corresponding to  $\tau_p=10 \text{ ms}$  and  $f=\nu/\tau_p=0.23$ , one would obtain from Eqs.(8.4.18) and (8.4.31)  $N_i/N_p=4.48$  and  $N_f/N_i=0.012$ , corresponding to a pulse energy  $E\approx59.4 \text{ mJ}$  and to an average output power  $P''_{out}\approx59.4 \text{ W}$ .

### 8.5A Quarter-wave voltage in a Q-switch Pockels cell.

Let us consider a combination of a Pockels cell and a polarizer, with the polarizer axis making an angle of  $45^\circ$  to the birefringence axes of the Pockels

cell. The linearly **polarized** light entering the Pockels cell is divided into two waves, with their electric fields (which are equal in amplitude, due to the orientation of the **polarizer**) along the two birefringence axes  $x$  and  $y$ . These two waves correspond to extraordinary and ordinary waves which propagate with two distinct phase velocities. After traversing the **thickness**  $L$  of the cell, the phase difference between ordinary and extraordinary waves is given by:

$$\Delta\phi = (k_1 - k_2)L = \frac{2\pi}{\lambda_0}(n_x - n_y)L \quad (1)$$

where  $\lambda_0$  is the wavelength in vacuum and  $n_x$ ,  $n_y$  are the ordinary and extraordinary refractive indices, respectively. After the cell, the transmitted wave is, in general, elliptically polarized. In particular, if  $\Delta\phi$  is an odd multiple of  $\pi/2$ , the light becomes circularly polarized. In order to convert the linearly polarized beam into a circularly polarized beam, the birefringence  $\Delta n = n_x - n_y$  must therefore satisfy the following condition:

$$\Delta n = n_x - n_y = \frac{(2m+1)}{L} \frac{\lambda_0}{4} \quad (2)$$

where  $m$  is a positive integer. From the data of the problem, we know that the birefringence  $\Delta n$  is related to the voltage  $V$  by the following expression:

$$\Delta n = n_0^3 r_{63} \frac{V}{L} \quad (3)$$

From Eqs.(2) and (3) we get:

$$V = \frac{(2m+1)\lambda_0}{4n_0^3 r_{63}} \quad (4)$$

The lowest voltage, obtained by setting  $m=0$  in Eq.(4), is referred to as the quarter-wave voltage. In case of a  $KD_2PO_4$  Pockels cell at  $\lambda=1.06 \mu m$ , assuming for  $KD_2PO_4$ ,  $r_{63}=26.4 \times 10^{-12} m/V$  and  $n_0=1.51$ , the quarter-wave voltage is given by:

$$V = \frac{\lambda_0}{4n_0^3 r_{63}} = 2.915 \text{ kV} \quad (5)$$

### 8.6A Active Q-switching in a three-level laser.

The analysis of fast active Q-switching in a three-level laser can be performed following the same technique developed in Sec. 8.4.4 of PL for a four-level

laser, starting from the rate-equations of a three-level laser discussed in detail in Problem 7.4P. Let  $N(t)=N_2-N_1$  and  $\phi(t)$  be the population inversion and cavity photon number in the lasing mode, respectively; in case of fast Q-switching, the evolution for  $N$  and  $\phi$ , after the switching time, can be obtained from the equations:

$$\frac{dN}{dt} = -2B\phi N \quad (1)$$

$$\frac{d\phi}{dt} = -\frac{\phi}{\tau_c} + B\phi V_a N \quad (2)$$

where  $B$  is the stimulated transition rate per-photon per-mode,  $\tau_c$  is the cavity photon lifetime, and  $V_a$  is the volume of the mode in the active medium. Notice that, as we are concerned with the formation of the Q-switch pulse, which is expected to occur on a time scale much shorter than the lifetime of upper laser level, we have neglected in Eq.(1) the change of population inversion  $N$  due to both pumping process and radiative/non-radiative decay of upper laser level, which occur on a slower time scale. Notice also that Eqs.(1) and (2) differ from the four-level laser counterparts [Eqs.(8.4.8a) and (8.4.8.b) of PL] by a factor 2 in the equation for the population inversion. This accounts for the physical circumstance that, in a three-level laser, any stimulated emission process corresponds to a unitary population transfer from the upper to the lower laser levels, thus contributing twice to the decrease of population inversion. The output pulse energy is given by [see also Eq.(8.4.16) of PL]:

$$E = \int_0^\infty P(t)dt = \left( \frac{\gamma_2 c}{2L_e} \right) h\nu \int_0^\infty \phi(t)dt \quad (3)$$

where  $P(t)$  is the output power and Eq.(7.2.18) of PL has been used. The integration in Eq.(3) can be easily carried out by integrating both sides of Eq.(2) from  $t=0$  to  $t=\infty$  and using the boundary conditions  $\phi(0)=\phi_i \approx 0$ ,  $\phi(\infty)=\phi_f \approx 0$  and Eq.(1). This yields:

$$\int_0^\infty \phi(t)dt = V_a \tau_c (N_i - N_f) / 2 \quad (4)$$

and thus:

$$E = \frac{\gamma_2}{2\gamma} V_a h\nu \frac{N_i - N_f}{2} \quad (5)$$

where  $N_i$  and  $N_f$  are the population inversion values before and after the Q-switching pulse, respectively. In order to determine  $N_f$ , it is useful to eliminate

the temporal variable in **Eqs.(1)** and (2) by considering the ratio between **Eqs.(1)** and (2). This yields:

$$\frac{d\phi}{dN} = -\frac{V_a}{2} \left[ 1 - \frac{N_p}{N} \right] \quad (6)$$

whose integration, with the initial condition  $\phi=0$ , gives:

$$\phi = \frac{V_a}{2} \left[ N_i - N - N_p \ln(N_i/N) \right] \quad (7)$$

where  $N_p = 1/V_a B \tau_c = \gamma \sigma l$  is the critical value of population inversion for the high-Q cavity. If we assume in **Eq.(7)**  $\phi \approx 0$ , we can obtain  $N/N_i$  as a function of  $N_p/N_i$  by an implicit equation, which reproduces exactly **Eq.(8.4.18)** of PL valid for a four-level laser. Notice that, a comparison of **Eq.(5)** with the similar equation found in case of a four-level laser [see **Eq.(8.4.17)** of PL], it follows that the output energy of the Q-switch pulse for a three-level laser is half of that of a four-level laser.

According to PL, the pulse duration is defined as  $\Delta\tau_p = E/P_p$ , where  $P_p$  is the peak power of the pulse. In order to determine the peak pulse power  $P_p$ , we note that, according to **Eq.(7.2.18)** of PL,  $P_p = (\gamma_2 c / 2L_e) h v \phi_p$ , where  $\phi_p$ , the peak of cavity photon, is obtained from **Eq.(7)** by setting  $N=N_p$ . This yields:

$$P_p = \frac{\gamma_2 c V_a}{4 L_e} h v N_p \left[ \frac{N_i}{N_p} - 1 - \ln \frac{N_i}{N_p} \right] \quad (8)$$

Since  $N_p = 1/V_a B \tau_c = \gamma \sigma l$  and  $1/\tau_c = c \gamma L_e$ , from **Eqs.(5)** and (8) we finally obtain for the pulse duration the following expression:

$$\Delta\tau_p = \tau_c \frac{(N_i - N_f)/N_p}{\frac{N_i}{N_p} - 1 - \ln \frac{N_i}{N_p}} \quad (9)$$

A comparison of **Eq.(9)** with **Eq.(8.4.21)** of PL shows that the expression for the pulse duration is the same for a three-level and a four-level Q-switched laser.

### 8.7A Calculation of the beam deflection angle by an acousto-optic modulator.

The acoustic wavelength, corresponding to the acoustic frequency  $v_a = 1$  GHz and assuming a velocity of sound in  $\text{LiNbO}_3$ ,  $v = 7.4 \times 10^5 \text{ cm/s}$ , is  $\lambda_a = v/v_a = 74$

$\mu\text{m}$ . Assuming that the acousto-optic deflector is operated in the Bragg regime, the beam is diffracted by an angle  $\theta' = \lambda/\lambda_a \approx 0.5^\circ$ , where  $\lambda = 632.8 \text{ nm}$  is the wavelength of the incident beam. Notice that, from Eq.(8.4.4) of PL, the Bragg **diffraction** regime is satisfied for a crystal length  $L' \gg 3.17 \text{ mm}$ .

### 8.8A Mode-locking of sidebands modes with random amplitudes.

The mode-locked signal  $E(t)$ , given by the superposition of  $N$  sideband modes all in phase with amplitudes  $A_n$ , can be written as:

$$E(t) = \sum_{n=1}^N A_n \exp(jn\omega t) \quad (1)$$

where  $\omega = 2\pi/T$  is the frequency separation between adjacent modes and  $A_n$  their amplitudes that, without loss of generality, may be assumed real-valued. Since the amplitudes  $A_n$  are stochastic variables uniformly distributed between zero and a maximum value  $E_0$ , the probability that  $A_n$  assumes a value in the interval  $(A \pm dA)$  is given by  $g(A)dA$ , where the probability density  $g(A)$  has the form:

$$g(A) = \begin{cases} 1/E_0 & \text{if } 0 < A < E_0 \\ 0 & \text{otherwise} \end{cases} \quad (2)$$

The time average power  $P_{av}$  carried by the mode-locked signal is given by:

$$P_{av} = \frac{1}{T} \int_0^T |E(t)|^2 dt = \sum_{n,m=1}^N \int_0^T A_n A_m \exp[j(n-m)\omega t] dt = \sum_{n=1}^N A_n^2 \quad (3)$$

The expectation value of  $P_{av}$  is thus:

$$\langle P_{av} \rangle = \sum_{n=1}^N \langle A_n^2 \rangle = \sum_{n=1}^N \int_{-\infty}^{\infty} A_n^2 g(A_n) dA_n = \frac{N}{E_0} \int_0^{E_0} A^2 dA = \frac{NE_0^2}{3} \quad (4)$$

In order to calculate the expectation value of the peak power of the dominant mode-locked pulse in each period, let us calculate the ensemble average of the instantaneous optical power, that is:

$$\langle P(t) \rangle = \langle |E(t)|^2 \rangle = \sum_{n,m=1}^N \langle A_n A_m \rangle \exp[j(n-m)\omega t] \quad (5)$$

If we assume that the variables  $A_n$ ,  $A_m$  are statistically independent for  $n \neq m$ , it follows that:

$$\langle A_n A_m \rangle = \int_{-\infty}^{\infty} \int_{-\infty}^{\infty} A_n A_m g(A_n) g(A_m) dA_n dA_m = \left( \int_{-\infty}^{\infty} A g(A) dA \right)^2 = \frac{E_0^2}{4} \quad (6)$$

Substitution of Eq.(6) into Eq.(5) yields:

$$\langle P(t) \rangle = \frac{E_0^2}{4} \sum_{n,m=1}^N \exp[i(n-m)\omega t] = \frac{E_0^2}{4} \left| \sum_{n=1}^N \exp(in\omega t) \right|^2 \quad (7)$$

From Eq.(7), it finally follows that the peak pulse power is attained at  $t=0$  and its expectation value is  $\langle P(t) \rangle_{peak} = N^2 E_0^2 / 4$ .

### 8.9A Chirped Gaussian pulses with quadratic phase locking relations.

The amplitude of pulse train envelope, obtained as a superposition of phase-locked cavity axial modes, is given by:

$$A(t) = \sum_{l=-\infty}^{\infty} A_l \exp(jl\Delta\omega t) \quad (1)$$

where, for a Gaussian amplitude distribution and quadratic phase locking relations, the complex amplitudes  $E_l$  are given by (see Eqs.(8.6.10) and (8.6.13) of PL):

$$E_l = E_0 \exp \left[ - \left( \frac{2l\Delta\omega}{\Delta\omega_L} \right)^2 \frac{\ln 2}{2} \right] \exp[j(l\varphi_1 + l^2\varphi_2)] \quad (2)$$

In Eqs.(1) and (2),  $\Delta\omega$  is the frequency separation between adjacent cavity axial modes,  $\Delta\omega_L$  is the bandwidth (FWHM) of the spectral intensity,  $\varphi_1$  and  $\varphi_2$  are two constants that define the phase locking condition. In case where a large number of longitudinal modes are oscillating, i.e. when  $\Delta\omega_L \gg \Delta\omega$ , the sum in Eq.(1) may be approximated by an integral over  $l$  from  $l=-\infty$  to  $l=\infty$  [see, however, Problem 8.10P]. Under this assumption, substitution of Eq.(2) into Eq.(1) yields:

$$A(t) \equiv E_0 \int_{-\infty}^{\infty} dl \exp(-c_1 l^2 + 2c_2 l) = E_0 \sqrt{\frac{\pi}{c_1}} \exp(c_2^2 / c_1) \quad (3)$$

where we have set:

$$c_1 = \left( \frac{2\Delta\omega}{\Delta\omega_L} \right)^2 \frac{\ln 2}{2} - j\varphi_2 \quad (4a)$$

$$c_2 = \frac{j\varphi_1}{2} + \frac{j\Delta\omega t}{2} \quad (4b)$$

Using Eqs.(4a) and (4b), the expression for the total electric field of the mode-locked pulse train can be cast in the final form:

$$E(t') \propto \exp(-\alpha t'^2) \exp(j\beta t'^2 + j\omega_0 t') \quad (5)$$

where  $t' = t + \varphi_1/\Delta\omega$  is a **restarted** time, and the constants  $\alpha$  and  $\beta$  are given by:

$$\alpha = \frac{\left(\frac{\Delta\omega}{2}\right)^2 \left(\frac{2\Delta\omega}{\Delta\omega_L}\right)^2 \frac{\ln 2}{2}}{\left(\frac{2\Delta\omega}{\Delta\omega_L}\right)^4 \frac{\ln^2 2}{4} + \varphi_2^2} \quad (6a)$$

$$\beta = \frac{\left(\frac{\Delta\omega}{2}\right)^2 \varphi_2}{\left(\frac{2\Delta\omega}{\Delta\omega_L}\right)^4 \frac{\ln^2 2}{4} + \varphi_2^2} \quad (6b)$$

Notice that, for a quadratic phase locking condition, the resulting pulse presents a linear frequency chirp, that is the instantaneous carrier frequency of the pulse is linearly swept in time according to  $\omega(t') = \omega_0 + 2\beta t'$  [see Eq.(5)]. In practice, **linearly-chirped** optical pulses can be generated in a homogeneously-broadened laser by using an **intracavity** phase modulator that produces a quadratic phase locking relation among the cavity axial modes (see Problem 8.13P).

### 8.10A On the periodicity of mode-locked signals.

By approximating the sum over all modes in Eq.(8.6.10) of PL with an integral, the frequency separation  $\Delta\omega$  between two consecutive modes becomes **infinitely** small. Thus the time separation between two successive pulses, given by  $\tau_p = 2\pi\Delta\omega$ , tends to infinity. Instead of obtaining a periodic **sequence** of pulses, separated by the cavity round-trip time, a single pulse is therefore obtained.

### 8.11A Phase locking condition for second-harmonic mode-locking.

If we **assume** the frequency of the lowest-order axial mode as the **carrier** frequency of the electric field, the pulse train envelope  $A(t)$ , obtained as a superposition of  $2N$  phase-locked axial modes with equal amplitudes  $E_0$ , reads:

$$A(t) = E_0 \sum_{l=1}^{2N} \exp(j\Delta\omega_l t + j\varphi_l) \quad (1)$$

where the phase-locking condition is **ruled** by the second-order **difference** equation:

$$\varphi_{l+1} - 2\varphi_l + \varphi_{l-1} = \pi \quad (2)$$

We can search for the general solution to **Eq.(2)** as a superposition of the solution to the homogeneous equation  $\varphi_{l+1} - 2\varphi_l + \varphi_{l-1} = 0$ , and of a forced solution. Two linearly-independent solutions to the homogeneous difference equation **are** readily found to be  $\varphi_l = l$  and  $\varphi_l = -l$ , and hence the general solution to the homogeneous equation is  $\varphi_l = c_1 + c_2 l$ , where  $c_1$  and  $c_2$  are arbitrary constants. A particular solution to **Eq.(1)** can be sought by the Ansatz:

$$\varphi_l = \alpha l^2 \quad (3)$$

where the constant  $\alpha$  in **Eq.(3)** has to be determined by substitution of **Eq.(3)** into **Eq.(2)**. This yields:

$$\alpha[(l+1)^2 - 2l^2 + (l-1)^2] = \pi \quad (4)$$

so that  $\alpha = \pi/2$ . In conclusion, the most general solution to the phase locking equation (2) is thus:

$$\varphi_l = c_1 + c_2 l + \frac{\pi}{2} l^2 \quad (5)$$

Notice that a **nonvanishing** value of  $c_1$  corresponds merely to a phase change of the field envelope  $A(t)$ , whereas with a suitable translation of the time origin we may assume  $c_1 = 0$ . Without loss of generality, we will thus assume in the following  $c_1 = c_2 = 0$ , so that from **Eq.(5)** we obtain:

$$\varphi_l = \frac{\pi}{2} l^2 = \begin{cases} 0 \pmod{2\pi} & \text{for } l = 2r \text{ even} \\ \pi/2 \pmod{2\pi} & \text{for } l = 2r + 1 \text{ odd} \end{cases} \quad (6)$$

Using Eq.(6), the pulse train envelope  $A(t)$ , as given by Eq.(1), can be cast in the useful form:

$$\begin{aligned} A(t) &= E_0 \sum_{r=1}^N \exp[j(2r-1)\Delta\omega t + j\pi/2] + E_0 \sum_{r=1}^N \exp(j2r\Delta\omega t) = \\ &= E_0 f(t)[1 - \exp(-j\Delta\omega t + j\pi/2)] \end{aligned} \quad (7)$$

where we have set:

$$f(t) = \sum_{r=1}^N \exp(2j\Delta\omega rt) = \exp[j\Delta\omega(N+1)t] \frac{\sin(\Delta\omega Nt)}{\sin(\Delta\omega t)} \quad (8)$$

and the well-known sum rule of a geometric progression has been used. The intensity of the output pulse train is thus given by:

$$|A(t)|^2 \propto 2|f(t)|^2 [1 + \sin(\Delta\omega t)] \quad (9)$$

In order to understand the pulse pattern as given by Eq.(9), let us observe that  $|A(t)|^2$  is the product of a rapidly oscillating periodic function  $|f(t)|^2$ , which shows narrow peaks of width  $\approx (\pi N \Delta\omega)$  at times  $t_n = n\pi/\Delta\omega$  ( $n=0, 1, 2, 3, \dots$ ) separated by  $T_{rep} = \pi/\Delta\omega$ , with the slowly-varying envelope  $[1 + \sin(\Delta\omega t)]$ . If the number of oscillating modes  $N$  is sufficiently large, we may therefore make the approximation  $[1 + \sin(\Delta\omega t)] \approx [1 + \sin(\Delta\omega t_n)] = 1$ , so that  $|A(t)|^2 \propto |f(t)|^2$ . This demonstrates that the output pulse train has a repetition frequency  $v_{rep} = 1/T_{rep} = 2(\Delta\omega/2\pi)$  which is twice the frequency separation  $\Delta\nu = \Delta\omega/2\pi$  of cavity axial modes.

### 8.12A Pulsewidth calculation in an actively mode-locked Nd:YAG laser.

For a homogeneously-broadened laser line, the pulse duration (FWHM) in an acousto-optic mode-locked laser is given approximately by Eq.(8.6.19) of PL:

$$\Delta\tau_p \cong \frac{0.45}{(\nu_m \Delta\nu_0)^{1/2}} \quad (1)$$

where  $\nu_m$  is the modulation frequency and  $\Delta\nu_0$  is the laser bandwidth. For a linear laser resonator of optical length  $L$ , the modulation frequency is given by  $\nu_m = c/2L$ , where  $c$  is the speed of light in vacuum. For a cavity length  $L=1.5$  m one has  $\nu_m=100$  MHz. Upon assuming  $\Delta\nu_0 \cong 195$  GHz, from Eq.(1) one then readily obtains  $\Delta\tau_p \cong 102$  ps. Notice that, if the gainline were inhomogeneously

broadened, the pulse duration would be given by **Eq.(8.6.18)** of PL and thus basically independent of the modulation frequency  $\nu_m$  and inversely proportional to the gain bandwidth  $\Delta\nu_0$ . In this case one would therefore obtain a pulse duration:

$$\Delta\tau_p \cong \frac{0.441}{\Delta\nu_0} \cong 2.3 \text{ ps} \quad (2)$$

which is much shorter than that obtained for the homogeneous line.

### 8.13A Gaussian pulse analysis of frequency mode-locking.

The theoretical framework to analyze frequency-modulation (FM) mode-locking is the same as that of amplitude-modulation (AM) mode-locking presented in details in Appendix F of PL. The basic idea is that, in steady-state mode-locking operation, a pulse circulating inside the laser cavity should reproduce its shape after each round-trip, apart for a possible phase delay. If  $\hat{U}_g$ ,  $\hat{U}_l$  and  $\hat{U}_m$  are the operators describing pulse propagation in the gain medium, loss element and phase modulator, we thus require:

$$\hat{U}_g \hat{U}_l \hat{U}_m A(t) = \exp(i\phi) A(t) \quad (1)$$

where  $A(t)$  is the envelope of the steady-state pulse circulating in the cavity and  $\phi$  is a possible phase delay. The expressions of  $\hat{U}_g$  and  $\hat{U}_l$  are the same as those found for AM mode-locking and given by **Eqs.(F.1.13)** and **(F.1.15)** of PL, respectively. In case of phase modulation, we have  $\hat{U}_m = \exp[j\gamma_m \cos(\omega_m t)]$ , where  $\omega_m$  is the modulation frequency and  $\gamma_m$  the modulation index. Since we expect the pulse passing through the modulator in correspondence of a **stationary** point (either a maximum or a **minimum**) of the phase modulation, we may approximate the cosine modulation by a parabolic law near the **extrema** and set, for small modulation indices ( $\gamma_m \ll 1$ ):

$$\hat{U}_m = 1 \pm j\gamma_m [1 - (\omega_m^2 t^2 / 2)] \quad (2)$$

where the upper (lower) sign has to be chosen according to pulse passing through the modulator in correspondence of maxima (minima) of phase modulation. As briefly discussed in the note at the end of the problem, this circumstance is related to the fact that, if a pulse would not pass **through** the modulator in correspondence of either a minimum or maximum of the phase modulation, in a transient stage it would be attracted toward one of the extrema of the phase modulation owing to the finite gain bandwidth of the active medium. After inserting **Eqs.(F.1.13), (F.1.15)** and (2) into **Eq.(1)** and using the

conditions  $[(g_0, \gamma, \gamma_m, |\phi|) \ll 1]$ , we obtain for the pulse envelope the following differential equation:

$$\left\{ g_0 \left[ 1 + \left( \frac{2}{\Delta\omega_0} \right)^2 \frac{d^2}{dt^2} \right] - \gamma \pm j\gamma_m \left( 1 - \frac{\omega_m^2 t^2}{2} \right) - j\phi \right\} A(t) = 0 \quad (3)$$

A Gaussian pulse solution to Eq.(2) with a complex pulse parameter can be sought in the form:

$$A(t) \propto \exp[-(\alpha + j\beta)t^2/2] \quad (4)$$

where  $\alpha$  is a real positive constant which establishes the pulse duration and  $\beta$  is a real, either positive or negative, constant which establishes pulse chirping. After substitution of Eq.(4) into Eq.(3), it is straightforward to show that Eq.(4) is a solution to Eq.(3) provided that:

$$\alpha = \frac{\sqrt{2}}{2} \sqrt{\frac{\gamma_m}{2g_0}} \left( \frac{\omega_m \Delta\omega_m}{2} \right) \quad (5a)$$

$$\beta = \pm\alpha \quad (5b)$$

with  $g_0$  and 4 such that:

$$g_0 = \gamma + \alpha g_0 \left( \frac{2}{\Delta\omega_0} \right)^2 \quad (6a)$$

$$\phi = \pm\gamma_m - \beta g_0 \left( \frac{2}{\Delta\omega_0} \right)^2 \quad (6b)$$

Notice that, as opposed to AM mode-locking, the Gaussian pulses in a FM mode-locking are chirped with a chirp parameter  $\beta/\alpha = \pm 1$ , the sign of chirp being determined by the passage of the pulse in the modulator in correspondence of either maxima or minima of the phase perturbation. Notice also that, owing to a non-vanishing value of  $\beta$ , from Eq.(8.6.16) of PL it turns out that the time-bandwidth product  $\Delta\tau_p \Delta\nu_L$  is larger than the minimum value of 0.441 predicted by the Fourier theorem by a factor of  $2^{1/2}$ , i.e. one has for FM mode-locking  $\Delta\tau_p \Delta\nu_L \approx 0.63$ .

Note:

In the answer to the problem we have limited our attention to the determination of a stationary pulse solution, that reproduces its shape after propagation in one round-trip, neglecting the dynamical aspects that are important to assess the stability of the pulse solution. It is important pointing out that one could prove

that the Gaussian pulse solution, as given by Eqs.(4) and (5), is stable. In particular, it can be shown that any initial pulse **that** passes through the modulator at an arbitrary instant is attracted toward either a **maximum** or a minimum of the phase perturbation, which are therefore the possible attractors for the pulse. From a physical viewpoint, this is due to the fact that, if the center of the pulse is detuned from either a maximum or minimum of the phase modulation, it would experience a frequency shift when passing through the modulator. This effect is counteracted by the finite bandwidth of the gain medium, which push the pulse spectrum toward the center of the **gainline**. In the time domain, this corresponds to lock the center of the pulse toward a point of

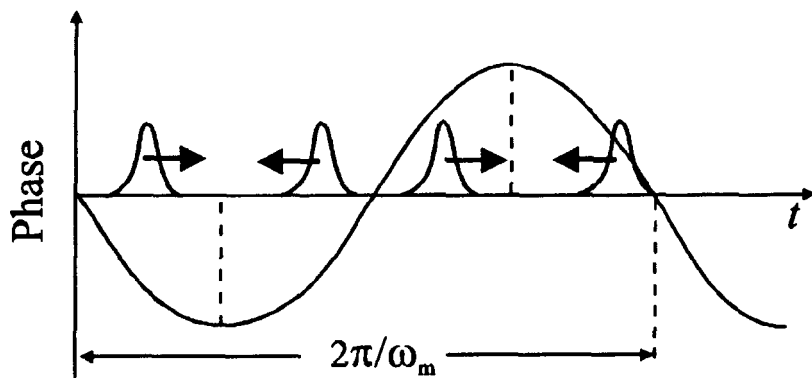


**Fig.8.1** Schematic of the **sinusoidal** phase modulation showing the attraction of detuned optical pulses toward the stationary points of phase perturbation.

stationary phase modulation. In particular, it can be shown that an initial detuned pulse will be attracted toward the stationary point of the phase perturbation which has the same curvature of phase modulation as that experienced by the initial pulse (see Fig.8.1). The existence of two possible attractors for the FM mode-locking, corresponding to **the** double sign in Eq.(5b), is in practice the cause of an undesirable switching of the laser operation between the two different steady-state conditions.

### 8.14A Mode-locking in a He-Ne laser.

Since the **gainline** is inhomogeneously broadened, for the laser operating well above threshold the oscillating bandwidth tends to cover the entire gain bandwidth. In **particular**, assuming a Gaussian distribution for the amplitudes of

mode-locked modes, we can **estimate** the pulse duration from **Eq.(8.6.18)** of PL, i.e.:

$$\Delta\tau_p \cong \frac{0.441}{\Delta\nu_0} \cong 0.26 \text{ ns} \quad (1)$$

The pulse repetition rate is **determined** by the frequency spacing of cavity axial modes and is thus given by:

$$\nu_p = \frac{c}{2L} \cong 375 \text{ MHz} \quad (2)$$

### 8.15A Harmonic mode-locking of a laser in a linear cavity

An easy answer to the problem can be provided by exploiting the time-domain picture of mode-locking in a laser (see **Sec. 8.6.2** of PL). A necessary condition for a pulse to propagate consistently inside a laser cavity with internal loss modulation is that the pulse passes through the modulator in correspondence of minima of loss modulation. If a pulse passes through the modulator at time  $t$ , **after** reflection from the output mirror it passes again through the modulator at time  $t' = t + (2d/c)$ , where  $d$  is the optical distance between the modulator (here assumed, for simplicity, of negligible thickness) and the output mirror, and  $c$  is the velocity of light in vacuum. For consistency, we require that the transit time  $2d/c$  be an integer multiple of the modulation period  $T_m = 1/\nu_m$ . This yields:  $\nu_m = m(c/2d)$ , with  $m=1, 2, 3, \dots$ . If  $d$  is an integer fraction of the cavity length  $L$ , i.e.  $d=L/N$ , we finally obtain:

$$\nu_m = mN \frac{c}{2L} \quad (1)$$

where both  $m$  and  $N$  are integer numbers. The minimum value of cavity loss modulation requested to achieve laser mode-locking corresponds to  $m=1$ , i.e.  $\nu_m = N(c/2L)$ . For  $N=4$  and  $L=2$  m, one obtains  $\nu_m = 300 \text{ MHz}$ . In case where the modulation frequency is twice this minimum value, during a transit time  $t'-t$  there are two minima of loss modulation, which can allocate two distinct pulses. The result is to increase by a factor of two the repetition-rate of the mode-locked pulse train.

Note:

Notice that the acousto-optic cell must be driven at a frequency half of the required modulation frequency (see discussion at page 341 of PL).

### 8.16A Calculation of pulse energy and peak power in a passively mode-locked Nd:YAG laser.

In a passively mode-locked laser **with** homogeneous **gainline and** fast saturable absorber, the steady-state pulse amplitude is described by a hyperbolic **sech**ant function, so that the output pulse power can be written as:

$$P(t) = P_p \operatorname{sech}^2(t/\tau_p) \quad (1)$$

where  $P_p$  is the pulse peak power and  $\zeta$  is related to the duration  $\Delta\tau_p$  of the pulse intensity (**FWHM**) by  $\zeta \cong \Delta\tau_p/1.76$ . The pulse energy  $E$  and average optical power of the pulse train  $P_{av}$  are obviously given by:

$$E = \int_{-\infty}^{\infty} P(t) dt = P_p \int_{-\infty}^{\infty} \operatorname{sech}^2(t/\tau_p) dt \quad (2)$$

$$P_{av} = \nu_m E \quad (3)$$

where  $\nu_m$  is the repetition frequency of the pulse train. With the substitution  $\xi = t/\tau_p$  and taking into account that:

$$\int_{-\infty}^{\infty} \operatorname{sech}^2 \xi d\xi = 2 \quad (4)$$

from Eqs.(2) and (3) one easily obtains:

$$E = 2P_p \tau_p \cong 1.13 P_p \Delta\tau_p \quad (5)$$

$$P_{av} \cong 1.13 \nu_m P_p \Delta\tau_p \quad (6)$$

For  $\Delta\tau_p=10$  ps,  $\nu_m=100$  MHz and  $P_{av}=500$  mW, from Eq.(6) one readily obtains  $P_p \cong 442.5$  W and thus, from Eq.(4),  $E \cong 5$  nJ.

### 8.17A Pulse duration in an idealized Kerr lens mode-locked Ti:Sapphire laser.

In case of passive mode-locking by a fast saturable absorber, the pulse duration is approximately given by Eq.(8.6.22) of PL, which reads:

$$\Delta\tau_p \cong \frac{0.79}{\Delta\nu_0} \left( \frac{g_0}{\gamma} \right)^{1/2} \left( \frac{P_s}{P_p} \right)^{1/2} \quad (1)$$

where  $\Delta\nu_0$  is the **gainbandwidth** (FWHM),  $2g_0$  is the round-trip saturated gain,  $\gamma'$  is the low-intensity single-pass loss of the saturable absorber,  $P_s$  is the saturation power of the absorber and  $P_p$  is the peak power of the pulse. In **case** of a **Kerr-lens** mode-locking, the equivalent action of the fast saturable absorber is provided by the **nonlinear** (i.e. powerdependent) loss **introduced** by the **intracavity** aperture, which leads to a powerdependent loss coefficient per round-trip given by:

$$2\gamma_s = 2\gamma - kP \quad (2)$$

where  $\gamma$  is the linear loss and  $k$  is the nonlinear loss coefficient. To obtain the expression for  $\Delta\tau_p$  which applies to our **case**, we first notice that, for a saturable absorber, one can write [see Eq.(8.6.20) of PL]:

$$2\gamma_s = 2\gamma - 2\gamma' \left( \frac{P}{P_s} \right) \quad (3)$$

A comparison of **Eqs.(2)** and (3) then leads to the following simple equivalence between the **parameters** which apply for the two cases:

$$\frac{P_s}{\gamma'} = \frac{2}{k} \quad (4)$$

From **Eqs.(1)** and (4) one then gets:

$$\Delta\tau_p = \frac{0.79}{\Delta\nu_0} \left( \frac{2g_0}{kP_p} \right)^{1/2} \quad (5)$$

To relate the pulse duration  $\Delta\tau_p$  to the pulse energy  $E$  rather than to its peak power  $P_p$ , we first observe that, for a hyperbolic sechanted pulse, one has (see Problem 8.16P):

$$P_p = \frac{E}{1.13\Delta\tau_p} \quad (6)$$

The substitution of the expression for  $P_p$  given by **Eq.(6)** into **Eq.(5)** readily leads to the following expression for the pulse duration:

$$\Delta\tau_p \cong \frac{1.13}{E} \left( \frac{0.79}{\Delta\nu_0} \right)^2 \left( \frac{2g_0}{k} \right) \quad (7)$$

Inserting in **Eq.(7)** the numerical values of the problem:  $E=40$  nJ,  $2g_0 \cong 0.1$ ,  $\Delta\nu_0 \cong 100$  THz and  $k \cong 5 \times 10^{-8}$  W<sup>-1</sup>, one obtains  $\Delta\tau_p \cong 3.5$  fs.

### 8.18A Pulse duration in a soliton-type Ti:sapphire mode-locked laser.

The **pulse** duration in a **solitary-type** mod-locking is given by Eq.(8.6.41) of PL, which reads explicitly:

$$\Delta\tau_p = \frac{3.53|\phi''|}{\delta E} \quad (1)$$

where  $E$  is the **intracavity** pulse energy,  $\phi''$  is the total group-velocity dispersion per-round-trip in the cavity, and  $\delta$  is the nonlinear phase shift in the Kerr medium per round-trip and per unit optical power. For a small output coupling, the *intracavity* pulse energy  $E$  is related to the average *output* power  $P_{av}$  by the following relation:

$$E \cong \frac{P_{av}T_R}{T} \quad (2)$$

where  $T_R=2L/c$  is the cavity round-trip time and  $T$  is the transmission of the output coupler. For  $L=1.5$  m, one obtains  $T_R=10$  ns and then, for  $P_{av}=500$  mW and  $T=0.05$ , Eq.(2) yields  $E\cong100$  nJ. Substituting this value for the pulse energy into Eq.(1) and assuming  $|\phi''|=800$  fs<sup>2</sup> and  $\delta\cong2\times10^{-6}$  W<sup>-1</sup>, one obtains  $\Delta\tau_p\cong14$  fs. In order to evaluate the pulse peak power, let us recall that, for a sech-like pulse shape, the pulse peak power  $P_p$  is related to the pulse energy  $E$  and pulse duration  $\Delta\tau_p$  by the relation (see Problem 8.16P):

$$P_p \cong \frac{E}{1.13\Delta\tau_p} \quad (3)$$

From Eq.(3) with  $\Delta\tau\cong14$  fs and  $E=100$  nJ, one obtains:  $P_p\cong6.3$  MW

### 8.19A Pulse broadening in a quartz plate.

**A** Gaussian pulse that propagates inside a dispersive medium with constant group-velocity dispersion  $\beta_2$  maintains its Gaussian shape, but both pulse duration and frequency chirp change during propagation. In particular, the pulse duration of an initially **unchirped** Gaussian pulse increases during propagation in the dispersive medium. For a medium of thickness L, the pulse duration,  $\tau_p'$ ,

at the exit of the medium is related to the pulse duration at the input,  $\tau_p$ , by the relation [see Eq.(G.15) of PL]:

$$\tau'_p = \tau_p \left[ 1 + \left( \frac{L}{L_D} \right)^2 \right]^{1/2} \quad (1)$$

where  $L_D = \tau_p^2 / |\beta_2|$  is the dispersion length of the pulse in the medium. Since the FWHM of the Gaussian-pulse intensity profile AT, is related to  $\tau_p$  by  $\Delta\tau_p = 2(\ln 2)^{1/2} \tau_p$ , for  $\Delta\tau_p = 10$  fs and  $\beta_2 = 50 \text{ fs}^2/\text{mm}$ , one has  $\tau_p \approx 6$  fs and  $L_D \approx 0.72$  mm. If we require  $\tau'_p < 1.2 \tau_p$ , from Eq.(1) we obtain:

$$\frac{L}{L_D} = \sqrt{\left( \frac{\tau'_p}{\tau_p} \right)^2 - 1} \leq 0.66 \quad (2)$$

The maximum permitted thickness of the quartz plate is thus  $L_{MAX} \approx 0.66 L_D \approx 0.47$  mm.

### 8.20A Self-imaging of a mode-locked pulse train.

The electric field  $E(t)$  for the mode-locked pulse train at the entrance of the dispersive medium can be written as a superposition of phase-locked modes with angular frequency separation  $\omega_m = 2\pi\nu_m$  and complex amplitudes  $E_l$ , i.e.:

$$E(t) = \exp(j\omega_0 t) \sum_{l=-\infty}^{\infty} E_l \exp(j\omega_m l t) \quad (1)$$

where  $\omega_0$  is the optical carrier frequency for the mode  $l=0$ . Each monochromatic component at frequency  $\omega_0 + \omega_m l$  propagates in the dispersive medium with a propagation constant  $\beta = \beta(\omega_0 + \omega_m l)$ , where  $\beta(\omega)$  is the dispersion relation of the medium. The electric field at distance  $z$  from the entrance of the medium is thus given by:

$$E(z, t) = \sum_{l=-\infty}^{\infty} E_l \exp[j(\omega_0 + l\omega_m) t - j\beta(l) z] \quad (2)$$

where  $\beta(l) = \beta(\omega_0 + l\omega_m)$ . In case of constant group-velocity dispersion (GVD), the dispersion relation  $\beta(\omega)$  can be approximated by a parabolic law, i.e.:

$$\beta(\omega) = \beta_0 + \beta_1(\omega - \omega_0) + \frac{1}{2} \beta_2 (\omega - \omega_0)^2 \quad (3)$$

where  $\beta_0 = \beta(\omega_0)$ ,  $\beta_1 = (d\beta/d\omega)_{\omega_0}$ , and  $\beta_2 = (d^2\beta/d\omega^2)_{\omega_0}$  is the GVD parameter. Using Eq.(3), Eq.(2) can be cast in the form:

$$E(z, t) = \exp[j(\omega_0 t - \beta_0 z)] \sum_{l=-\infty}^{\infty} E_l \exp[j\omega_m l(t - \beta_1 z)] \exp(-j\beta_2 \omega_m^2 l^2 z/2) \quad (4)$$

An inspection of Eq.(4) reveals that, at the propagation distances multiplies of the fundamental length  $L_T = 1/(\pi\beta_2 v_m^2)$ , i.e. at  $z = L_n = nL_T$  ( $n = 1, 2, 3, \dots$ ), the phase of the exponential term in the last term of Eq.(4) is an integer multiple of  $2n$ ; regardless of the value of the mode index  $l$ , so that one has:

$$E(L_n, t) = \exp[j(\omega_0 t' - \phi)] \sum_{l=-\infty}^{\infty} E_l \exp(j\omega_m l t') \quad (5)$$

where  $t' = t - \beta_1 L_n$  is a **retarded** time and  $\phi = L_n(\beta_1 \omega_0 - \beta_0)$  a constant **phase** term. A comparison of Eq.(5) with Eq.(1) shows that, at the propagation distances  $L_n$ , the pulse train reproduces exactly its shape, both in intensity and phase, apart for inessential time and phase delays. Notice that this property is valid regardless of the values of mode amplitudes  $E_l$ , i.e. it is independent of the mode-locked pulse shape. It is worth pointing out that this self-imaging of the initial pulse train counteracts the effect of dispersion which initially broadens each mode-locked pulse. This effect, however, requires strictly a periodic pulse train which extends from  $t = -\infty$  to  $t = \infty$ . In practice it is well reproduced by a finite sequence of pulses provided that the number of pulses is large. The self-imaging property ceases to be valid if the initial waveform is not periodic.

#### Note:

The self-imaging phenomenon, by means of which a periodic field propagating in a dispersive medium reproduces its original shape at suitable propagation distances, is analogous to the Talbot effect of diffractive optics well-known since the end of the XVIII century. This analogy finds its explanation in the formal equivalence between pulse propagation in quadratic dispersive media and spatial diffraction of scalar wave fields.

# CHAPTER 9

## Solid-State, Dye, and Semiconductor Lasers

### PROBLEMS

#### 9.1P Slope efficiency in a Ti:Al<sub>2</sub>O<sub>3</sub> laser.

A Ti:Al<sub>2</sub>O<sub>3</sub> laser is longitudinally pumped by the focused beam of an Ar<sup>+</sup> laser at the pump wavelength  $\lambda_p = 514$  nm. A wavelength tuner is inserted in the cavity, forcing the laser to oscillate at 850 nm. Assume a round trip loss of the cavity  $\gamma_{rt} = 10\%$ , an output mirror reflectivity  $R = 95\%$  and a pump efficiency  $\eta_p = 30\%$ . Assume also that the laser is under optimum pumping conditions. Calculate the laser slope efficiency.

#### 9.2P Output power from a Nd:YAG laser.

A Nd:YAG laser is transversely pumped at 808 nm. The laser mode has a spot size  $w_0 = 1.4$  mm; the stimulated emission cross-section is  $\sigma_e = 2.8 \times 10^{-19}$  cm<sup>2</sup> and the upper level lifetime is  $\tau = 230 \mu\text{m}$ . Assume that an output coupler with a transmission  $T = 12\%$  is used and that the pump threshold is  $P_{th} = 48.8$  W. Calculate the pump power required to obtain an output power  $P_{out} = 45$  W from this laser.

#### 9.3P A Nd:YVO<sub>4</sub> laser in the fog.

A laser company shows to a buyer the performances of a new Nd:YVO<sub>4</sub> laser in the open air. The laser shows a **threshold pump** power  $P_{th} = 1$  W; at a pump power  $P_p = 7$  W the output power is  $P_{out} = 1$  W. Suddenly a dense fog falls in the exposition area; owing to the increased losses inside the laser cavity, the threshold pump power doubles. Calculate the output power delivered by the laser in these conditions for the same pump power  $P_p$ . Assume for simplicity that the presence of fog inside the laser cavity doesn't affect the pump efficiency.

## PROBLEMS

### 9.4P A green solid-state laser.

A green solid-state laser, using **Nd:YAG** as active material, is based on intra-cavity second-harmonic conversion of the laser radiation. The second-harmonic crystal is inserted near the output mirror. The transmission of the output coupler is  $T_{gr} = 99.9\%$  at 532 nm and  $T_{ir} = 0.01\%$  at 1064 nm; the laser rod is longitudinally pumped at 808 nm. Assume that: the (optical) pump efficiency is  $\eta_p = 45\%$ ; the saturation intensity for **Nd:YAG** is  $2.9 \times 10^7 \text{ W/m}^2$ ; the mode spot size inside the rod is  $w_t = 120 \mu\text{m}$ ; the **laser** is operating under optimum pumping conditions and the loss per single pass is  $\gamma_t = 3\%$  at 1064 nm, in the absence of second harmonic generation. The power conversion in the nonlinear crystal can be expressed as  $P_{2\omega} = \kappa (P_\omega)^2$ , where:  $P_\omega$  is the power at 1064 nm entering the crystal;  $P_{2\omega}$  is the power at 532 nm emerging from the crystal;  $\kappa = 10^{-2} \text{ W}^{-1}$  is the conversion coefficient. Calculate which is the pump power required in this laser for an output power  $P_{out} = 2 \text{ W}$  at 532 nm.  
(Level of difficulty higher than average)

### 9.5P Yb:YAG laser vs. Nd:YAG laser.

Two large laser companies are strong competitors in the market of solid state lasers. Company A builds a **Nd:YAG** laser, a few months later the **company B** builds an **Yb:YAG** laser. The two lasers are longitudinally pumped under optimum pumping conditions; the mode spot size in the **Yb:YAG** rod is five times smaller than in the **Nd:YAG**. Moreover the pump efficiencies in the two lasers are the same. Company A states that the **Nd:YAG** laser has a pump threshold 3.6 times larger than the **Yb:YAG** laser of B. Assuming a single pass loss  $\gamma = 6\%$  in the two lasers, calculate the **Yb:YAG** rod length. Use numerical values reported in the following table:

	<b>Nd:YAG (1% at. w.)</b>	<b>Yb:YAG (6.5% at. w.)</b>
$N_t (10^{20} \text{ cm}^{-3})$	1.38	8.97
$\tau (\text{ms})$	0.23	1.16
$\sigma_e (10^{-20} \text{ cm}^2)$	28	1.8
$\sigma_a (10^{-20} \text{ cm}^2)$	-	0.12
$\lambda (\text{nm})$	1064	1030
$\lambda_p (\text{nm})$	808	941

where:  $N_t$  is the population of active species in the medium;  $\tau$  is the upper laser level lifetime;  $\sigma_e$  is the effective stimulated emission cross-section at the laser

wavelength  $\lambda$ ;  $a_e$  is the effective absorption cross-section at the laser wavelength;  $\lambda_p$  is the pump wavelength.

### 9.6P Anisotropy in a Cr:LiSAF laser rod.

A Ph.D. student inserts a Cr:LiSAF rod inside a laser cavity. The rod, having  $10^{20}$  Cr<sup>+3</sup> ions/cm<sup>3</sup> concentration, is longitudinally pumped at 670 nm; the pump beam is polarized along the vertical direction. A tuner forces the laser to oscillate at 850 nm and selects only the vertical polarization, which coincides with the direction of the Cr:LiSAF optical axis. The student observes that, owing to the anisotropy of Cr:LiSAF, the pump threshold increases three times upon 90° rotation of the rod around the cavity axis. Calculate the rod length using the numerical values reported in the following table:

Cr:LiSAF	Direction //	Direction ⊥
$\sigma_e (10^{-20} \text{ cm}^2)$	5	1.8
$\sigma_p (10^{-20} \text{ cm}^2)$	5	2.3

where:  $a_e$  is the effective stimulated emission cross-section at the laser wavelength;  $\sigma_p$  is the absorption cross-section at the pump wavelength; the symbols // and ⊥ refer to a direction of the Cr:LiSAF optical axis, parallel and perpendicular to the light polarization direction respectively.

[Hint: the answer to this problem requires a graphical or numerical solution of a non linear equation.]

### 9.7P Threshold pump power in longitudinal pumping: ground and excited states contribution.

Establish the expression for the threshold pump power of a laser in longitudinal pumping configuration, if ground-state absorption, characterized by a loss per pass  $\gamma_g$ , and excited-state absorption, characterized by an excited-state absorption cross-section  $\sigma_{ESA}$ , are taken into account. Compare the result with Eq. (6.3.20) of PL.

**9.8P Threshold pump power in a dye laser: triplet-triplet contribution.**

Establish the expression for the threshold pump power of a longitudinally pumped dye laser, when intersystem crossing, with rate  $k_{ST}$ , triplet-triplet absorption, with cross-section  $\sigma_T$  and triplet decay, with lifetime  $\tau_T$ , are taken into account. Assume Gaussian profiles for both pump and mode beams. Compare this expression to that derived in problem 9.7.

**9.9P Slope efficiency in a dye laser.**

Consider a **rhodamine-6G** laser **oscillating at 580-nm** wavelength and pumped at **514 nm** by an  $\text{Ar}^+$  laser. Assume optimum pumping conditions, with a pump spot size of **100  $\mu\text{m}$**  and with **80%** of the pump power absorbed in the dye jet stream; assume also an output coupling of **3%**, an internal loss per pass of **1%**, a lifetime for the first excited singlet state of **5 ns**. Calculate the slope efficiency of this laser in the absence of intersystem crossing. Assume now an intersystem crossing rate  $k_{ST} \approx 10^7 \text{ s}^{-1}$ , a stimulated emission cross-section for the laser transition  $\sigma_e = 1.5 \times 10^{-16} \text{ cm}^2$ , an absorption cross-section for the triplet-triplet transition  $\sigma_T = 0.5 \times 10^{-16} \text{ cm}^2$  and a triplet lifetime  $\tau_T \approx 0.1 \mu\text{s}$ . Calculate the effective slope **efficiency** and compare it to the previous result.

[Hint: you should first solve problem 9.8 before answering this problem.]

**9.10P A laser cascade.**

Consider a laser system made of a cascade of three lasers: a laser, emitting at **500 nm**, that pumps a  $\text{Ti:Al}_2\text{O}_3$  laser, that pumps a **Nd:YAG** laser. Suppose that the green laser has a threshold power  $P_{th} = 0.75 \text{ W}$  and a slope **efficiency**  $\eta_{s1} = 13\%$ , the  $\text{Ti:Al}_2\text{O}_3$  laser **has** a threshold power  $P_{th} = 1.7 \text{ W}$  and a slope **efficiency**  $\eta_{s2} = 15\%$  and the **Nd:YAG** laser has a threshold power  $P_{th} = 1 \text{ W}$  and a slope efficiency  $\eta_{s3} = 12\%$ . Calculate the pump power that must be provided to the green laser to get an output power  $P_{out} = 0.75 \text{ W}$  from the **Nd:YAG** laser.

**9.11P Longitudinal modes in a semiconductor laser.**

Consider a semiconductor laser with a cavity length  $L = 350 \mu\text{m}$ . Assuming that the gain line has a bandwidth  $\Delta\nu_L = 380 \text{ GHz}$  and that the group index of

semiconductor is  $n_g = n + v(dn/dv) = n - \lambda(dn/d\lambda) = 3.6$ , calculate the number of longitudinal modes which fall within this line. How much long the laser cavity should be to achieve single mode oscillation?

### 9.12P Beam astigmatism in a semiconductor laser.

Assume that the beam, at the exit face of a semiconductor laser, is spatially coherent. Assume that the transverse field distributions along the directions parallel and perpendicular to the junction, have Gaussian profiles with spot sizes  $w_{\parallel}$  and  $w_{\perp}$  respectively. Assume also that, for both field distributions, the location of the beam waists occur at the exit face. Given these assumptions, derive an expression for the propagation distance at which the beam becomes circular. Taking  $w_{0\parallel} = 2.5 \mu\text{m}$  and  $w_{0\perp} = 0.5 \mu\text{m}$  at the beam waist, calculate the value of this distance for  $\lambda = 850 \text{ nm}$ .

### 9.13P Current threshold in a GaAs/AlGaAs laser.

Consider a **double-heterostructure** (DH) laser consisting of a **GaAs** active layer between two **AlGaAs** cladding layers, which emits at  $\lambda = 840 \text{ nm}$ . Assume a carrier density at transparency  $N_{tr} = 1.2 \times 10^{18} \text{ carriers/cm}^3$ , a cavity length  $L = 300 \mu\text{m}$ , a differential gain  $a = 3.6 \times 10^{-16} \text{ cm}^2$ , a radiative lifetime  $\tau_r = 4 \text{ ns}$ , a thickness of the active layer  $d = 100 \text{ nm}$ , an internal quantum efficiency  $\eta_i = 0.95$  and a total loss per pass  $\gamma = 1.43$ . Assume also that the refractive index of the active layer and of the cladding layers are  $n_1 = 3.6$  and  $n_2 = 3.4$  respectively. Calculate the current density at threshold required in this laser.

### 9.14P Slope efficiency in a GaAs/AlGaAs laser.

The expression for the output power  $P_{out}$  of a semiconductor laser is [see Eq. (9.4.14) of PLJ]:

$$P_{out} = \left[ \frac{(I - I_{th})\eta_i h\nu}{e} \right] \left( \frac{\ln(R)}{\ln(R) - \alpha L} \right)$$

where:  $I$  is the operating current;  $I_{th}$  is the threshold current;  $\eta_i$  is the internal quantum efficiency;  $v$  is the laser frequency;  $R$  is the reflectivity of the output mirrors;  $a$  is the internal loss coefficient and  $L$  is the cavity length.

Starting from this equation, derive an expression for the laser slope **efficiency**. Calculate then the slope efficiency of a **GaAs/AlGaAs** laser for an applied voltage  $V = 1.8$  V. Assume a cavity length  $L = 300 \mu\text{m}$ , an internal quantum efficiency  $\eta_i = 0.95$ , a reflectivity of the two end faces  $R = 32\%$ , a loss coefficient  $a = 10 \text{ cm}^{-1}$  and an emission wavelength  $\lambda = 850 \text{ nm}$ .

### 9.15P Distributed feedback in a semiconductor laser.

**Fabry-Perot-type** semiconductor lasers generally oscillate on several longitudinal modes (see Fig. 9.28 of PL). To achieve oscillation on a single mode, distributed feedback (DFB) structures are widely used. Consider the DFB laser shown in Fig. 9.29b of PL. Calculate the period  $A$  of refractive index modulation assuming that the laser oscillates on a single mode at  $\lambda = 1550 \text{ nm}$  and that the average refractive index in the semiconductor is  $n_0 = 3.5$ .

### 9.16P Current threshold in a quantum-well laser.

Consider a quantum-well (QW) laser consisting of a **GaAs** active layer with thickness  $d = 10 \text{ nm}$  between two **AlGaAs** cladding layers, which **emits** at  $\lambda = 840 \text{ nm}$ . Assume a carrier density at transparency  $N_{tr} = 1.2 \times 10^{18} \text{ carriers/cm}^3$ , a cavity length  $L = 300 \mu\text{m}$ , a differential gain  $a = 6 \times 10^{-16} \text{ cm}^2$ , a radiative lifetime  $\tau_r = 4 \text{ ns}$ , an internal quantum efficiency  $\eta_i = 0.95$ , a total loss per pass  $\gamma = 1.43$ , and a confinement factor  $\Gamma = 1.8 \times 10^{-2}$ . Calculate the current density at threshold required for this laser. Compare the result to that obtained for the DH semiconductor laser considered in problem 9.13.

### 9.17P Carrier density in a VCSEL at threshold.

Consider a vertical-cavity surface-emitting laser (VCSEL) consisting of an active layer sandwiched between two Bragg reflectors. Assume that: the active layer consists of a multiple quantum well **structure** with effective thickness  $d = 30 \text{ nm}$ ; the cavity length (including spacing layers) is  $L = 2 \mu\text{m}$ ; the reflectivity of the two mirrors is  $R = 99\%$ ; the loss **coefficient** is  $a = 18 \text{ cm}^{-1}$ ; the differential gain is  $a = 6 \times 10^{-16} \text{ cm}^2$  and the **carrier** density at **transparency** is  $N_{tr} = 1.2 \times 10^{18} \text{ carriers/cm}^3$ . Calculate the **carrier** density at threshold in this laser.

## ANSWERS

### **9.1A Slope efficiency in a Ti:Al<sub>2</sub>O<sub>3</sub> laser.**

The slope efficiency  $\eta_s$  of a four-level laser can be written as [see Eq. (7.3.12) of PL]:

$$\eta_s = \eta_p \left( \frac{\gamma_2}{2\gamma} \right) \left( \frac{hv}{hv_p} \right) \left( \frac{A_b}{A} \right) \quad (1)$$

where:  $\eta_p$  is the pump efficiency;  $\gamma$  is the single-pass loss;  $\gamma_2$  is the output coupler loss;  $v$  is the laser emission frequency;  $v_p$  is the pump frequency;  $A$  is the cross-sectional area of the active medium and  $A_b$  is the cross-sectional area of the laser mode. For longitudinal pumping under optimum conditions, the mode spot size and the spot size of the pump beam are equal, so that  $A = A_b$ . To calculate the slope efficiency we can assume  $2\gamma \approx \gamma_n = 0.1$ ; the output coupler loss can be calculated as  $\gamma_2 = -\ln(1-T_2) \approx -\ln(R_2) = 0.05$ , where  $T_2$  and  $R_2$  are the transmission and the reflectivity of the output mirror [see Eq. (7.2.6) of PL]. Upon inserting in Eq. (1) the other numerical values given in the problem, we obtain  $\eta_s = 9.1\%$ .

### **9.2A Output power from a Nd:YAG laser.**

The output power  $P_{out}$  for a four-level laser can be expressed as [see Eq. (7.3.9) of PL]:

$$P_{out} = (A_b I_s) \left( \frac{\gamma_2}{2} \right) \left( \frac{P_p}{P_{th}} - 1 \right) \quad (1)$$

where:  $A_b$  is the cross-sectional area of the laser mode;  $\gamma_2$  is the output coupler loss;  $P_p$  and  $P_{th}$  are the *pump* power and the threshold pump power respectively;  $I_s = h\nu/\sigma\tau$  is the saturation intensity for a four-level system [see Eq. (2.8.24) of PL]. The output coupler loss can be calculated as  $\gamma_2 = -\ln(1-T_2) = 0.128$ , where  $T_2$  is the output mirror transmission. Using the other numerical values given in the problem, Eq. (1) can be rewritten as:

$$P_{out} = 0.2196 (P_p - P_{th}) \quad (2)$$

From Eq. (2) one can easily calculate that the input *pump* power  $P_p$  required to get an output power of  $P_{out} = 45$  W, is  $P_p = 253.7$  W.

### 9.3A A Nd:YVO<sub>4</sub> laser in the fog.

If we consider the expressions for the pump power at threshold  $P_{th}$  in a four level laser [see Eq. (6.3.20-22) of PL], we can note that  $P_{th}$  is always proportional to the single pass loss  $\gamma$  inside the laser resonator, irrespective of whether the laser rod is pumped in longitudinal or transverse direction. Moreover, according to the problem, the presence of fog inside the cavity doesn't affect the pump efficiency; we can also assume that both the cross-sectional areas of the active medium ( $A$ ) and of the laser mode ( $A_b$ ) don't change owing to the fog presence. For these reasons the observed doubling of  $P_{th}$  simply corresponds to a doubling of  $\gamma$ . Consider now the expression for the slope efficiency  $\eta_s$  in a four-level laser [see Eq. (7.3.14) of PL]:

$$\eta_s = \eta_p \eta_c \eta_q \eta_t \quad (1)$$

where:  $\eta_p$  is the pump efficiency;  $\eta_c = \gamma_2/2\gamma$  is the output coupling efficiency;  $\eta_q = h\nu h\nu_p$  is the laser quantum efficiency and  $\eta_t = A_b/A$  is the transverse efficiency. In Eq. (1) only  $\eta_c$  changes when the cavity losses increase; from the previous discussion it follows that the doubling of  $\gamma$  corresponds to a decrease of  $\eta_s$  to half its initial value. To calculate the initial  $\eta_s$  we can simply use the relation:

$$P_{out} = \eta_s (P_p - P_{th}) \quad (2)$$

where  $P_{out}$ ,  $P_p$  and  $P_{th}$  are the output laser power, the pump power and the pump power at threshold, respectively. Inserting in Eq. (2) the numerical values given in the problem, we get  $\eta_s = (116) = 16.7\%$  for the initial value of the slope efficiency. After the fog appearance we get  $\eta_{s,fog} = (1112) = 8.3\%$ ; in this situation the threshold pump power doubles, so that  $P_{th,fog} = 2$  W. Substituting these new values in Eq. (2), we obtain the new output power  $P_{out,fog} = 0.42$  W.

### 9.4A A green solid-state laser.

The laser will be described in the following with the help of Fig. 9.1.

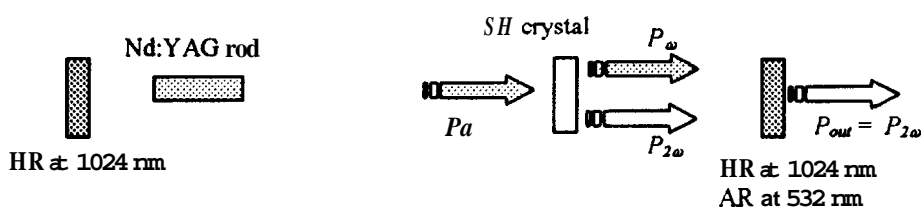


Fig. 9.1 Cavity scheme.

For simplicity we will assume that the output coupler has 100% reflectivity (HR) at 1064 nm and 100% transmission (AR) at 532 nm; moreover we will assume that the second harmonic (SH) produced by the laser beam travelling inside the non linear crystal from the right to the left, will be completely absorbed by the **Nd:YAG** rod, so that no other losses, except the output coupling and the internal ones, are considered.

On the basis of these assumptions and considering the relationship between the power at **1064 nm** and the SH power generated in the crystal, the output loss can be written as:

$$\gamma_2 = -\ln(1-T_2) \approx \kappa P_\omega \quad (1)$$

where  $T_2$  is the effective **transmission** of the output coupler.

On the other hand the (second harmonic) output power from the laser,  $P_{out}$ , can be expressed as:

$$P_{out} = (A_b I_s) \left( \frac{\gamma_2}{2} \right) \left( \frac{P_p}{P_{th}} - 1 \right) \quad (2)$$

where:  $A_b$  is the cross-sectional area of the laser mode;  $\gamma_2$  is the output coupler loss;  $P_p$  and  $P_{th}$  are the pump power and the threshold pump power respectively;  $I_s = h\nu/\sigma\tau$  is the saturation intensity for a four-level system [see Eq. (2.8.24) of PL]. The pump power at threshold, under optimum pumping conditions, can be written as [see Eq. (7.3.12) of PL]:

$$P_{th} = \frac{\gamma}{I_s} \frac{h\nu_p A}{\sigma} \quad (3)$$

where:  $\eta_p$  is the pump **efficiency**;  $\nu_p$  is the pump frequency;  $A$  is the cross-sectional area of the active **medium**;  $\gamma$  is the single-pass loss. Note **that**, for longitudinal pumping under optimum conditions, the mode spot size and the spot size of the pump beam are equal, so that  $A = A_b$ .

We can rewrite Eq. (1) with the help of the conversion relation in the crystal [ $P_{2\omega} = \kappa(P_\omega)^2$ ] as:

$$\gamma_2 \approx \kappa P_\omega = (\kappa P_{2\omega})^{1/2} = (\kappa P_{out})^{1/2} \quad (4a)$$

Moreover the single-pass loss is related to the output coupler loss by the expression [see Eq. (7.2.8) of PL]:

$$\gamma = \gamma_i + \frac{\gamma_2}{2} = \gamma_i + \frac{(\kappa P_{out})^{1/2}}{2} \quad (4b)$$

Substituting Eq. (3) into Eq. (2) and using, in the resulting equation, the expressions of  $\gamma_2$  and  $\gamma$  given by Eqs. (4a) and (4b), we get :

$$P_{out} = (\kappa P_{out})^{1/2} \left[ \frac{A_b}{A} \frac{h\nu_p}{h\nu_p} \eta_p \frac{P_p}{2\gamma_i + (\kappa P_{out})^{1/2}} - \frac{A_b I_s}{2} \right] \quad (5)$$

Inverting Eq. (5) to get  $P_p$  as a function of  $P_{out}$ , we then obtain:

$$P_p = \frac{A}{A_b} \frac{h\nu_p}{h\nu} \frac{2\gamma_i + (\kappa P_{out})^{1/2}}{\eta_p} \left[ \frac{A_b I_s}{2} + \left( \frac{P_{out}}{\kappa} \right)^{1/2} \right] \quad (6)$$

Inserting in Eq. (6) the numerical values given in the problem, we obtain that the pump power required to obtain an output power  $P_{out} = 2 \text{ W}$  is  $P_p = 8.72 \text{ W}$ .

### 9.5A Yb:YAG laser vs. Nd:YAG laser.

The pump power at threshold in a four-level laser, under optimum pumping conditions, can be written as [see Eq. (7.3.12) of PL]:

$$P_{th} = \frac{\gamma}{\eta_p} \frac{h\nu_p}{\tau} \frac{A}{\sigma_e} \quad (1)$$

where:  $\eta_p$  is the pump efficiency;  $\nu_p$  is the pump frequency;  $A$  is the cross-sectional area of the active medium;  $\gamma$  is the single-pass loss;  $\tau$  is the upper laser level lifetime and  $\sigma_e$  is the effective stimulated emission cross-section. This expression can be used for the Nd:YAG laser mentioned in the problem.

The Yb:YAG is a quasi-three level laser; the pump power at threshold, under optimum pumping conditions, can than be written as [see Eq. (7.4.4) of PL]:

$$P_{th} = \frac{\gamma}{\eta_p} \left( 1 + \frac{\sigma_a N_t l}{\gamma} \right) \frac{h\nu_p}{\tau} \frac{A}{\sigma_e + \sigma_a} \quad (2)$$

where:  $\sigma_a$  is the effective absorption cross-section;  $l$  is the Yb:YAG rod length;  $N_t$  is the total population in the medium. According to the problem, the ratio between threshold powers of Nd:YAG and Yb:YAG lasers is equal to 3.6. Using Eq. (2-3) and asswning the same losses and pump efficiencies in the two lasers, we get:

$$\frac{P_{th,Yb}}{P_{th,Nd}} = \frac{A_{Yb}}{A_{Nd}} (\sigma_e)_{Nd} \left[ \frac{1 + \sigma_a N_t l / \gamma}{\sigma_e + \sigma_a} \right]_{Yb} \frac{(h\nu_p / \tau)_{Yb}}{(h\nu_p / \tau)_{Nd}} = 0.278 \quad (3)$$

where material parameters for the two lasers are indicated by the indexes Nd and Yb, respectively. Inverting Eq. (3) to get the Yb:YAG rod length  $l$  as a function of the other quantities, we get:

$$l_{yb} = \frac{\gamma}{(\sigma_a N_t)_{yb}} \left[ 0.278 \frac{A_{Nd}}{A_{yb}} \frac{(\sigma_e + \sigma_a)_{yb}}{(\sigma_e)_{Nd}} \frac{(\tau \lambda_p)_{yb}}{(\tau \lambda_p)_{Nd}} - 1 \right] \quad (4)$$

where  $\lambda_p$  is the pump wavelength. According to the problem, the mode spot size in the **Nd:YAG** rod is 5 times larger than in **Yb:YAG**, so that  $A_{Nd}/A_{yb} = 25$ . Inserting in Eq. (4) the numerical values given in the problem, we get an **Yb:YAG** rod length  $l_{yb} \approx 1$  mm.

### 9.6A Anisotropy in a Cr:LiSAF laser rod.

The pump power at threshold in a four-level laser, under optimum pumping conditions, can be written as [see Eq. (7.3.12) of PL]:

$$P_{th} = \frac{\gamma}{\eta_p} \frac{h\nu_p}{\tau} \frac{A}{\sigma_e} \quad (1)$$

where:  $\eta_p$  is the pump efficiency;  $\nu_p$  is the pump frequency;  $A$  is the cross-sectional area of the active medium;  $y$  is the single-pass loss;  $\tau$  is the upper laser level lifetime and  $\sigma_e$  is the effective stimulated emission cross-section. Owing to the **anisotropy** of **Cr:LiSAF**, the stimulated emission cross-section and the pump absorption inside the active medium change when the student rotates the rod. For this reason the pump **efficiency** also changes when the rod is rotated. In the following we will assume that the rod rotation doesn't change either the cavity losses or the mode spot size. According to the problem and using Eq. (1), the ratio between the pump powers at threshold can be written as:

$$\frac{P_{th}^{\parallel}}{P_{th}^{\perp}} = \frac{\eta_p^{\perp}}{\eta_p^{\parallel}} \frac{\sigma_e^{\perp}}{\sigma_e^{\parallel}} = \frac{1}{3} \quad (2)$$

where the symbols  $\parallel$  and  $\perp$  refer to a direction of the **Cr:LiSAF** optical axis, parallel and perpendicular to the light polarization direction, respectively.

To calculate the pump efficiency, we recall that  $\eta_p$  is given by [see Eq. (6.2.5) of PL]:

$$\eta_p = \eta_r \eta_t \eta_a \eta_{pq} \quad (3)$$

where:  $\eta_r$  is the radiative efficiency;  $\eta_t$  is the transfer efficiency;  $\eta_a = [1 - \exp(-\alpha l)]$  is the absorption efficiency, where  $a$  is the absorption coefficient of the active material and  $l$  the rod length;  $\eta_{pq}$  is the energy **quantum** efficiency. Assuming that the quantities  $\eta_r$ ,  $\eta_t$ ,  $\eta_{pq}$  don't change after rod rotation, we can rewrite Eq. (2), with the help of Eq. (3), as:

$$\frac{1}{3} = \frac{1 - \exp(-\alpha^\perp l)}{1 - \exp(-\alpha^\parallel l)} \frac{\sigma_e^\perp}{\sigma_e^\parallel} \quad (4)$$

To calculate the absorption coefficients  $\alpha$  we can use the relation:

$$\alpha = \sigma_p N_t \quad (5)$$

where  $\sigma_p$  is the absorption cross-section at the pump wavelength and  $N_t$  the total population of  $\text{Cr}^{+3}$  ions in the Cr:LiSAF rod. Note that in Eq. (5) we assume implicitly that the absorption in the active material is not saturated. With the help of Eq. (5), we can rewrite Eq. (4) as:

$$\sigma_e^\parallel [1 - \exp(-\sigma_p^\parallel N_t l)] = 3 \sigma_e^\perp [1 - \exp(-\sigma_p^\perp N_t l)] \quad (6)$$

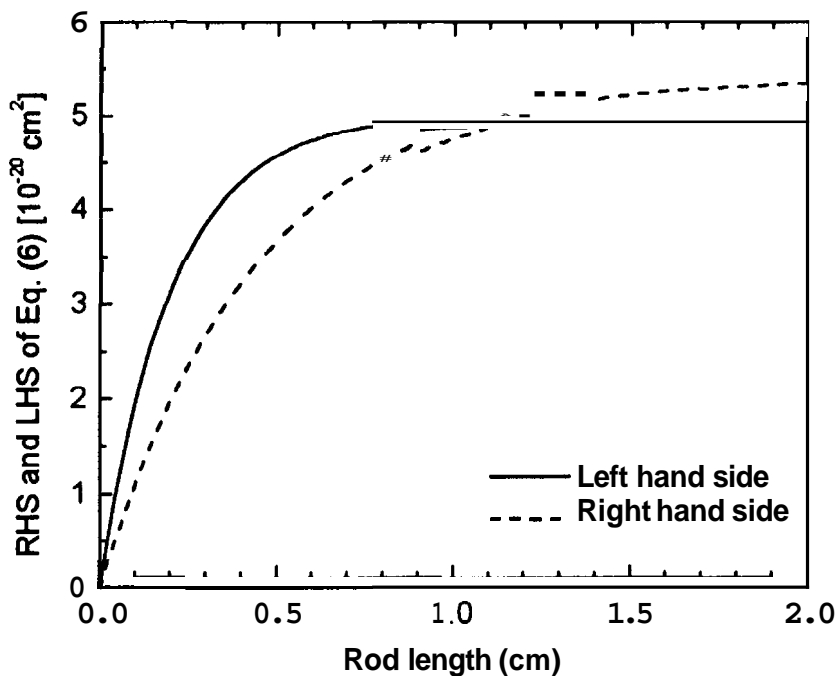


Fig. 9.2 Graphical solution of Eq. (6)

This expression is a non linear equation in the variable  $l$ . A solution can be obtained by graphical or numerical methods. To perform a graphical solution, we plot in Fig. 9.2 the right hand side (RHS) and the left hand side (LHS) of Eq. (6) as a function of  $l$  and then we look for the intersection between the two curves.

Using numerical values given in the problem, we find an intersection at  $I = 1.1 \text{ cm}$ , which represent the required solution to the **problem**. Note that the solution corresponding to the intersection at  $I = 0 \text{ cm}$  has no physical meaning and can be discarded. It is worth noting that there are no other intersections between the two **curves**.

### 9.7A Threshold pump power in longitudinal pumping: ground and excited states contribution.

Let us consider the scheme for energy levels in the active medium shown in Fig. 9.3, where transition A indicates the stimulated transition while transitions B and C indicate absorption processes from the upper laser level and ground level respectively.

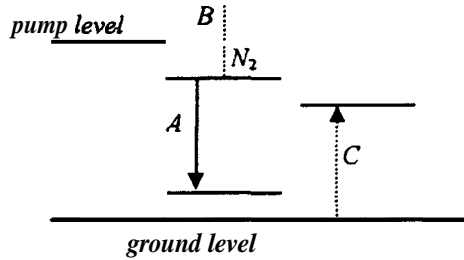


Fig. 9.3 Energy level scheme

In the presence of laser action, stimulated transition A competes with absorption from transitions B and C. To derive the expression for the threshold pump power, we need first to establish the expression for the critical population  $N_{2c}$  in the upper **laser** level. This quantity can be calculated assuming that, when the laser is at threshold, the single pass gain equals the losses in the cavity. This condition can be written as:

$$\sigma_e N_{2c} l = \gamma + \sigma_{ESA} N_{2c} l + \gamma_a \quad (1)$$

where:  $\sigma_e$  is the stimulated emission cross-section for the laser transition A;  $\sigma_{ESA}$  is the absorption cross-section for the transition B;  $\gamma$  is the single pass loss due to the cavity and  $\gamma_a$  is the single pass loss due to ground state absorption (transition C). From Eq. (1) one gets:

$$N_{2c} = \frac{\gamma + \gamma_a}{(\sigma_e - \sigma_{ESA})l} \quad (2)$$

The critical pump rate  $R_{pc}$  is determined assuming that all the excited population decays by spontaneous emission at threshold [see Eq. (6.3.18) of PL]. Thus:

$$R_{pc} = \frac{N_{2c}}{\tau} = \frac{\gamma + \gamma_a}{(\sigma_e - \sigma_{ESA})l\tau} \quad (3)$$

where  $\tau$  is the upper laser level lifetime.

In longitudinal pumping configuration, the pump rate is related to the pump power  $P_p$  by [see Eq. (6.3.12) of PLJ]:

$$R_p = \eta_p \left( \frac{P_p}{h\nu_p} \right) \frac{2}{\pi(w_0^2 + w_p^2)l} \quad (4)$$

where:  $\eta_p$  is the pump efficiency;  $\nu_p$  is the pump frequency;  $l$  is the active medium length;  $w_0$  is the mode spot size and  $w_p$  is the pump spot size. With the help of Eqs. (3) and (4), the threshold pump power can then be expressed as:

$$P_{th} = \frac{(\gamma + \gamma_a)}{\eta_p} \frac{h\nu_p}{\tau} \frac{\pi(w_0^2 + w_p^2)}{2(\sigma_e - \sigma_{ESA})} \quad (5)$$

The comparison of this result with Eq. (6.3.20) of PL shows that the pump power at threshold increases with respect to an ideal laser for two reasons:

(a) the increase in single-pass loss from  $\gamma$  to  $(\gamma + \gamma_a)$ ; (b) the decrease in the net single pass gain, due to excited state absorption, which can be thought as a change in the effective stimulated emission cross-section from  $a_s$  to  $(a_s - \sigma_{ESA})$ .

### 9.8A Threshold pump power in a dye laser: triplet-triplet contribution.

Let consider the scheme for energy levels in a dye molecule shown in Fig. 9.4 [see section 9.3 of PL]:

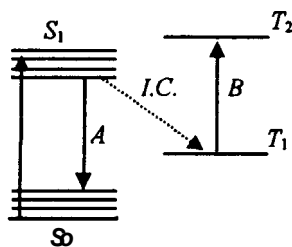


Fig. 9.4 Energy levels in the dye.

The laser transition (**A**) take place between the lowest vibrational level of the excited state  $S_1$  and a set of vibrational levels in the ground state  $S_0$ . Both  $S_0$  and  $S_1$  are called *singlet* states, because in these states the total electronic spin in the dye molecule is zero. The generation, by electromagnetic interaction, of excited states with non-zero spin is forbidden, because the ground-state spin is zero and the spin is conserved in photoinduced excitations. Some population can however accumulate on a state with non-zero spin (triplet state  $T_1$  in Fig. 4) due to a **non-radiative transition**, namely by *intersystem crossing* (*I.C.*) from  $S_1$  population. States  $T_1$  and  $T_2$  are referred to as *triplet* states, because total electronic spin in the dye molecule is one. Triplet state  $T_1$  can absorb radiation at the laser wavelength to produce triplet states with higher energy ( $T_2$  in Fig. 4). This absorption mechanism competes with laser action. To determine the effect of triplet-triplet absorption on threshold pump power of a dye laser, we must first calculate the triplet population  $N_T$  generated by intersystem crossing. In cw regime the generation rate of triplets by intersystem crossing equals the triplet decay rate. This can be expressed as:

$$k_{ST} N_2 = \frac{N_T}{\tau_T} \quad (1)$$

where  $N_2$  is the population of the  $S_1$  upper laser level,  $k_{ST}$  is the intersystem crossing rate and  $\tau_T$  is the triplet lifetime.

From Eq. (1) one gets:

$$N_T = k_{ST} \tau_T N_2 \quad (2)$$

To obtain the threshold pump power, we have to determine the critical population  $N_{2c}$  in the upper laser level. This quantity can be calculated assuming that, when the laser is at threshold, the single pass gain equals the losses in the cavity. This condition can be written as:

$$\sigma_e N_{2c} l = \gamma + \sigma_T N_T l \quad (3)$$

where:  $\sigma_e$  is the stimulated emission cross-section for the laser transition (A);  $\sigma_T$  is the absorption cross-section for the triplet-triplet transition (B);  $\gamma$  is the single pass loss in the cavity;  $l$  is the active medium length.

With the help of Eq. (2) one can rewrite Eq. (3) as:

$$N_{2c} = \frac{\gamma}{(\sigma_e - \sigma_T k_{ST} \tau_T) l} \quad (4)$$

The critical pump rate  $R_{pc}$  is now established by assuming that all the excited population decays at threshold by spontaneous emission or by intersystem crossing [see Eq. (6.3.18) of PL]. Thus:

$$R_{pc} = \frac{N_{2c}}{\tau} = \frac{\gamma}{(\sigma_e - \sigma_T k_{ST} \tau_T) l \tau} \quad (5)$$

where  $\tau$  is the upper laser level lifetime. Note that the decay time constant  $\tau$  is given by the combination of the radiative decay and of the decay due to intersystem crossing, according to the relation:

$$\frac{1}{\tau} = \frac{1}{\tau_r} + k_{ST}$$

where  $\tau_r$  is the radiative lifetime.

In longitudinal pumping configuration, the pump rate is related to the pump power  $P_p$  by [see Eq. (6.3.12) of PL]:

$$R_p = \eta_p \left( \frac{P_p}{h \nu_p} \right) \frac{2}{\pi(w_0^2 + w_p^2) l} \quad (6)$$

where:  $\eta_p$  is the pump efficiency;  $\nu_p$  is the pump frequency;  $P_p$  is the pump power;  $l$  is the active medium length;  $w_0$  is the mode spot size and  $w_p$  is the pump spot size. With the help of Eqs. (5) and (6), the threshold pump power can then be written as:

$$P_{th} = \frac{\gamma}{\eta_p} \frac{h \nu_p}{\tau} \frac{\pi(w_0^2 + w_p^2)}{2(\sigma_e - \sigma_T k_{ST} \tau_T)} \quad (7)$$

The comparison of this result with that of Eq. (6.3.20) of PL shows that the pump power at threshold is again increased with respect to the ideal laser. This behavior is due to the decrease in the single-pass net gain owing to triplet-triplet absorption and can be thought as a change in the effective stimulated emission cross-section from  $\sigma_e$  to  $(\sigma_e - \sigma_T k_{ST} \tau_T)$ . Note that, in spite of the small amount of intersystem crossing rate, this change can be quite large owing to the long triplet lifetime. A small contribution to the increase of  $P_{th}$  is also given by the small reduction of the upper laser level lifetime  $\tau$ , with respect to the radiative lifetime  $\tau_r$ , due to intersystem crossing.

### 9.9A Slope efficiency in a dye laser.

To calculate the slope efficiency, we consider the expression for the output power from the laser,  $P_{out}$ :

$$P_{out} = (A_b I_s) \left( \frac{\gamma_2}{2} \right) \left( \frac{P_p}{P_{th}} - 1 \right) \quad (1)$$

where:  $A_b$  is the cross-sectional area of the laser mode;  $\gamma_2$  is the output coupler loss;  $P_p$  and  $P_{th}$  are the pump power and the **threshold** pump power respectively;  $I_s = h\nu/\sigma_e\tau$  is the saturation intensity for a four-level system at the laser frequency  $\nu$  [see Eq. (2.8.24) of PL]. With the help of Eq. (1), the slope efficiency  $\eta_s$  can be written as [see Eq. (7.3.10) of PL]:

$$\eta_s = \frac{dP_{out}}{dP_p} = \frac{A_b I_s \gamma_2}{P_{th} 2} \quad (2)$$

In the case of a dye laser, the pump power at threshold in longitudinal pumping configuration can be written as [see answer 9.8]:

$$P_{th} = \frac{\gamma}{\eta_p} \frac{h\nu_p}{\tau} \frac{\pi(w_0^2 + w_p^2)}{2(\sigma_e - \sigma_T k_{ST} \tau_T)} \quad (3)$$

where:  $\gamma$  is the single pass loss in the cavity;  $\gamma$  is the pump efficiency;  $\nu_p$  is the pump frequency;  $\tau$  is the upper laser level lifetime;  $w_0$  is the mode spot size;  $w_p$  is the pump spot size;  $\sigma_e$  is the stimulated emission cross-section for the laser transition;  $\sigma_T$  is the absorption cross-section for the triplet-triplet transition;  $k_{ST}$  is the intersystem crossing rate and  $\tau_T$  is the triplet lifetime. Note that, under optimum **pumping** condition, one has  $w_0 = w_p$ .

Inserting Eq. (3) in Eq. (2) one obtains the following expression:

$$\eta_s = \eta_p \frac{\gamma_2}{2\gamma} \frac{h\nu}{h\nu_p} \frac{2A_b}{\pi(w_0^2 + w_p^2)} \frac{\sigma_e - \sigma_T k_{ST} \tau_T}{\sigma_e} \quad (4)$$

We can rearrange Eq. (4), as:

$$\eta_s = \eta_p \eta_c \eta_q \eta_A \eta_g \quad (5)$$

where:  $\eta_p$  is the pump efficiency;  $\eta_c = \gamma_2/2\gamma$  is the output coupling efficiency;  $\eta_q = h\nu/h\nu_p$  is the laser quantum efficiency;  $\eta_A = 2A_b / \pi(w_0^2 + w_p^2)$  is the area efficiency and  $\eta_g = (\sigma_e - \sigma_T k_{ST} \tau_T) / \sigma_e$ . Note that  $\eta_g$  can be thought as a **gain efficiency**, giving the ratio between the net gain and the theoretical gain achievable in the absence of triplet absorption. Inserting in Eq. (5) the numerical values given in the problem, one sees that the slope efficiency in the absence of intersystem crossing would be  $\eta_{s0} = 43\%$ . Owing to intersystem crossing, this value is lowered to  $\eta_s = \eta_{s0} \eta_g = 29\%$ .

## ANSWERS

### 9.10A A laser cascade.

The expression for the output power  $P_{out}$  from a laser is given by:

$$P_{out} = \eta_s (P_p - P_{th}) \quad (1)$$

where:  $\eta_s$  is the slope efficiency and  $P_p$ ,  $P_{th}$  are the pump power and the pump power at threshold, respectively. On the basis of Eq. (1) the output power  $P_{out3}$  from the Nd:YAG laser is:

$$P_{out3} = \eta_{s3} (P_{p2} - P_{th3}) \quad (2)$$

where:  $\eta_{s3}$  is the slope efficiency of the Nd:YAG laser;  $P_{th3}$  is the pump power at threshold in the Nd:YAG laser;  $P_{p2}$  is the pump power provided by the Ti:Sapphire laser. Eq. (2) can be rewritten using Eq. (1) to express the output power from the Ti:Sapphire laser:

$$P_{out3} = \eta_{s3} [\eta_{s2} (P_{p1} - P_{th2}) - P_{th3}] \quad (3)$$

where:  $\eta_{s2}$  is the slope efficiency of the Ti:Sapphire laser;  $P_{th2}$  is the pump power at threshold of the Ti:Sapphire laser,  $P_{p1}$  is the pump power provided by the green laser. Eq. (3) can be rewritten again using Eq. (1) to express the output power from the green laser:

$$P_{out3} = \eta_{s3} \{ \eta_{s2} [\eta_{s1} (P_p - P_{th1}) - P_{th2}] - P_{th3} \} \quad (4)$$

where:  $\eta_{s1}$  is the slope efficiency of the green laser;  $P_{th1}$  is the pump power at threshold of the green laser;  $P_p$  is the electrical pump power provided to the green laser. One can readily solve Eq. (4) to obtain  $P_p$  as a function of the other variables:

$$P_p = \frac{P_{out} + \eta_{s3} P_{th3} + \eta_{s3} \eta_{s2} P_{th2} + \eta_{s3} \eta_{s2} \eta_{s1} P_{th1}}{\eta_{s1} \eta_{s2} \eta_{s3}} \quad (5)$$

Using in Eq. (5) the numerical values given in the problem, one gets  $P_p = 385.6 \text{ W}$ .

### 9.11A Longitudinal modes in a semiconductor laser.

The resonance frequencies of the modes can be approximately written as  $v = lc / 2nL$ , where:  $l$  is an integer;  $c$  is the speed of light in vacuum;  $n$  is the refractive index of the semiconductor and  $L$  is the cavity length. From the preceding expression one readily gets  $n v = l(c / 2L)$ . From this expression, since  $n$  is a function of  $v$ , i.e.  $n = n(v)$ , the change in frequency  $\Delta v$  corresponding to a change in  $l$  of  $\Delta l = 1$ , can approximately be calculated from

the equation  $\Delta n v + n A v = (c/2L)$ . From this equation, approximately writing  $\Delta n = (dn/dv)\Delta v$ , one readily gets:

$$\Delta v = \frac{c}{2n_g L} \quad (1)$$

where

$$n_g = \frac{n}{1 + v(dn/dv)} = \frac{n}{1 - \lambda(dn/d\lambda)} \quad (2)$$

is the material group index. If the **gain linewidth** of the semiconductor is  $A\nu_L$ , the number of modes falling within this linewidth can approximately be calculated as (see Fig. 9.5):

$$N \cong \frac{\Delta\nu_L}{\Delta\nu} + 1 = \frac{2n_g L \Delta\nu_L}{c} + 1 \quad (3)$$

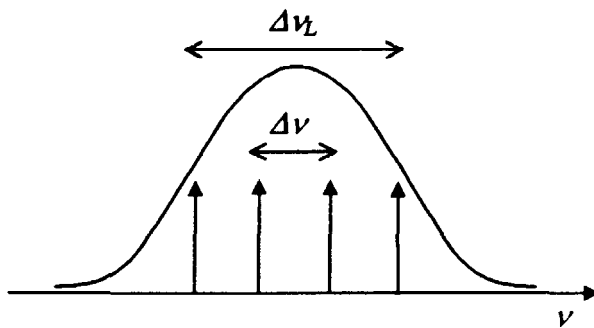


**Fig. 9.5** Gain line and oscillating modes

Using the numerical values given in the problem, one gets  $N = 4$ . To obtain single mode oscillation, one should have  $A\nu > \Delta\nu_L$ . According to Eq. (1), this would correspond to a cavity length  $L < 115 \mu m$ .

### 9.12A Beam astigmatism in a semiconductor laser.

The spot size  $w$  of a gaussian beam can be expressed as a function of the propagation distance  $z$  according to the following relation:

$$w^2(z) = w_0^2 \left[ 1 + \left( \frac{\lambda z}{\pi w_0^2} \right)^2 \right] \quad (1)$$

where  $w_0$  is the spot size in the beam waist and  $\lambda$  is the wavelength of the beam [see Eq. (4.7.16-17) of PL]. The origin of coordinate  $z$  must coincide with the beam waist.

An astigmatic **gaussian** beam, such as that emerging from a semiconductor laser, can be represented with the help of two spot sizes,  $w_{\parallel}(z)$  and  $w_{\perp}(z)$ , **corresponding** respectively to the direction parallel and perpendicular to the diode **junction**.

According to Eq. (I), these two quantities can be written as:

$$w_{\perp}^2(z) = w_{0\perp}^2 \left[ 1 + (\lambda z / \pi w_{0\perp}^2)^2 \right] \quad (2a)$$

$$w_{\parallel}^2(z) = w_{0\parallel}^2 \left[ 1 + (\lambda z / \pi w_{0\parallel}^2)^2 \right] \quad (2b)$$

where  $w_{0\parallel}$  and  $w_{0\perp}$  are **the** spot sizes at the beam waist for the two directions. To calculate the coordinate  $z_c$  where the beam is circular, we can simply equate the two spot sizes at position  $z_c$ :

$$w_{\perp}^2(z_c) = w_{\parallel}^2(z_c) \quad (3)$$

Using Eqs. (2a) and (2b) in Eq. (3), we get:

$$w_{0\parallel}^2 - w_{0\perp}^2 = \frac{\lambda^2 z_c^2}{\pi^2} \left[ \frac{w_{0\parallel}^2 - w_{0\perp}^2}{w_{0\parallel}^2 w_{0\perp}^2} \right] \quad (4)$$

from which  $z_c$  can readily be obtained as:

$$z_c = \frac{\pi w_{0\parallel} w_{0\perp}}{\lambda} \quad (5)$$

Inserting in Eq. (5) the numerical values given in the problem, we get  $z_c = 4.6 \mu\text{m}$ .

### 9.13A Current threshold in a GaAs/AlGaAs laser.

The current density at threshold  $J_{th}$  in a semiconductor laser is related to the carrier density at threshold  $N_{th}$  by the following relation [see Eq. (9.4.3) of PL]:

$$J_{th} = \left( \frac{e d}{\eta_i \tau_r} \right) N_{th} \quad (1)$$

where:  $e = 1.6 \times 10^{-19}$  C is the electron charge;  $d$  is the thickness of the active layer;  $\eta_i$  is the internal quantum **efficiency**, which is the fraction of **carriers** that combine **radiatively** in the active layer;  $\tau_r$  is the radiative recombination time. To calculate  $J_{th}$  we need to establish the carrier density at threshold. From a balance between gain and losses in the semiconductor, derive the following expression for  $N_{th}$  [see Example 9.1 of PL]:

$$N_{th} = \left( \frac{\gamma}{\sigma L \Gamma} \right) + N_{tr} \quad (2)$$

where:  $y$  is the total loss per pass;  $\sigma$  is the differential gain;  $L$  is the length of the active medium;  $\Gamma$  is the **beam** confinement factor, **which** represents the fraction of the beam power actually in the active layer. For a given laser wavelength  $\lambda$ , the beam confinement factor can be calculated if the refractive indexes of the active layer ( $n_1$ ) and of the cladding layer ( $n_2$ ) are known. To this purpose we can use the approximate relation [see Example 9.1 of PL]:

$$\Gamma \approx \frac{D^2}{2 + D^2} \quad (3)$$

where:

$$D = 2\pi(n_1^2 - n_2^2)^{1/2} \frac{d}{\lambda} \quad (4)$$

With the **help** of Eqs. (1) and (2), the current density at threshold can be written as:

$$J_{th} = \left( \frac{ed}{\eta_i \tau_r} \right) \left[ \left( \frac{\gamma}{\sigma L \Gamma} \right) + N_{tr} \right] \quad (5)$$

Upon inserting into Eq. (4) the numerical values given in the problem, we get  $D = 0.885$ ; using this value in Eq. (3) gives  $\Gamma = 0.2814$ . Inserting this value in Eq. (5) together with the other data given in the problem, one obtains  $J_{th} = 703 \text{ A/cm}^2$ .

### 9.14A Slope efficiency in a GaAs/AlGaAs laser.

The electrical power  $P$  spent in the semiconductor laser can be expressed as  $P = VI$ , where  $V$  is the operating voltage across the laser diode and  $I$  is the operating current flowing inside. As a first approximation the voltage can be

considered constant over a broad current range, so that the slope efficiency  $\eta_s$  of the laser diode can be calculated as:

$$\eta_s = \frac{d P_{out}}{d P} \approx \frac{d P_{out}}{V dI} \quad (1)$$

where  $P_{out}$  is the output power of the laser. From the expression of  $P_{out}$  given in the problem and with the help of Eq. (1), one obtains:

$$\eta_s = \left( \frac{\eta_i h \nu}{V e} \right) \left( \frac{\ln(R)}{\ln(R) - \alpha L} \right) \quad (2)$$

Inserting the numerical values given in the problem, one gets  $\eta_s = 61\%$ .

### 9.15A Distributed feedback in a semiconductor laser.

A distributed feedback laser consists of an active medium in which a periodic thickness variation is produced in one of the cladding layers forming part of the heterostructure. Owing to this structure, the mode oscillating in the laser cavity experiences a modulation of the effective refractive index  $n_{eff}(z)$  along the propagation direction  $z$ . This modulation can be represented by [see Eq. (9.4.16) of PL]:

$$n_{eff}(z) = n_0 + n_s \sin[(2\pi z/A) + \varphi] \quad (1)$$

where  $A$  is the pitch of the periodic thickness change. The modulation in refractive index induces scattering of the laser mode in both the forward and backward direction. According to Bragg's diffraction theory, a constructive interference develops among the scattered components, if the following relation holds:

$$\lambda = \lambda_B = 2\langle n_{eff} \rangle A \quad (2)$$

where:  $\lambda$  is the mode wavelength;  $\lambda_B$  is the Bragg wavelength;  $\langle n_{eff} \rangle$  is the average value of the refractive index inside the laser cavity. With the help of Eq. (1), we can rewrite Eq. (2) as:

$$A = \lambda / 2n_0 \quad (3)$$

Inserting in Eq. (3) the numerical values given in the problem, we obtain  $A = 221.5 \text{ nm}$ .

### 9.16A Current threshold in a quantum-well laser.

As already derived in answer 9.13, the current density at threshold  $J_{th}$  in a semiconductor laser can be written as [see also Eq. (9.4.13) of PL]:

$$J_{th} = \left( \frac{ed}{\eta_i \tau_r} \right) \left[ \left( \frac{\gamma}{\sigma L \Gamma} \right) + N_{tr} \right] \quad (1)$$

where: e is the electron charge; d is the thickness of the active layer;  $\eta_i$  is the internal **quantum efficiency**, which is the **fraction** of carriers that combine radiatively in the active layer;  $\tau_r$  is the radiative recombination time;  $\gamma$  is the total loss per pass;  $\sigma$  is the differential gain; L is the length of the active medium;  $\Gamma$  is the beam confinement factor, which represents the fraction of the beam power actually in the active layer. Inserting the numerical values given in the problem, we obtain  $J_{th} = 236 \text{ A/cm}^2$ .

Comparing this result to that obtained in answer 9.13, we see that the current density at threshold in a Quantum Well laser is about 3 times **smaller** than that in a standard Double-Heterostructure laser. The reasons for this unexpected result are the following: (a) The reduction in the active layer thickness by an order of magnitude. (b) The increase of the differential gain,  $\sigma$ , in the QW structure, arising by electron and hole quantum confinement, which partially compensates the decrease of the beam confinement factor  $\Gamma$  [see Sect. 3.3.5 of PL].

### 9.17A Carrier density in a VCSEL at threshold.

The expression for the **carrier** density at threshold  $N_{th}$  can be derived from a balance between gain and losses in the semiconductor, according to the following expression [see Eq. (9.4.9) of PL]:

$$N_{th} = \left( \frac{\gamma}{\sigma d \Gamma} \right) + N_{tr} \quad (1)$$

where:  $\gamma$  is the total loss per pass;  $\sigma$  is the differential gain; d is the length of the active medium;  $\Gamma$  is the beam confinement factor, which represents the fraction of the beam power actually in the active layer. In a VCSEL laser the beam confinement factor can be assumed  $\Gamma \approx 1$ , owing to the cavity structure. To calculate the single pass loss we can use the relation [see Example 9.4 of PL]:

$$\gamma = -\ln(R) + \alpha L \quad (2)$$

where: R is the reflectivity of the two mirrors; L is the cavity length and  $\alpha$  is the loss coefficient inside the semiconductor. Inserting in Eq. (3) the numerical values given in the problem, we get  $\gamma=1.37\%$ . Inserting this value in Eq. (1) and using the remaining values given in the problem, we obtain  $N_{th} = 8.81 \times 10^{18}$  carriers/cm<sup>3</sup>. The comparison of this result with the **carrier** density at transparency, shows that the **carrier** density at threshold in this laser is dominated by the loss term ( $\gamma/\sigma d$ ).

# **CHAPTER 10**

## **Gas, Chemical, Free-Electron, and X-Ray Lasers**

### **PROBLEMS**

#### **10.1P Low-density laser emitting in the infrared.**

List at least four lasers, using a low-density active medium, whose wavelengths fall in the infrared.

#### **10.2P Low-density laser emitting in the UV - soft X region.**

List at least four lasers, using a low-density active medium, whose wavelengths fall in the UV to **soft** X-ray region. **Which** problems are faced in achieving laser action in the **W** or **X-ray** region?

#### **10.3P High-power lasers for material processing.**

Metal-working applications require a laser with a **cw** output  $> 1 \text{ kW}$ . Which lasers meet this requirement?

#### **10.4P Internal structure of He-Ne lasers.**

The basic design of a He-Ne laser is shown in Fig. 10.2 of PL. Explain the reasons for using a large tubular cathode and for confining the electrical discharge inside the **central** capillary.

**10.5P Maximum output power in He-Ne lasers.**

The population inversion in He-Ne lasers is not directly proportional to current density  $\mathbf{J}$  in the discharge; explain the reasons for such behavior and show that an optimum value occurs for the current density in the discharge.

**10.6P Internal structure of high-power  $\text{Ar}^+$  lasers.**

The schematic diagram of a high-power argon laser is shown in Fig. 10.7 of PL. Explain the function of tungsten disks and the reasons for the presence of off-center holes. Why the pump efficiency of this laser increases applying a magnetic field parallel to the laser tube?

**10.7P Output vs. pump power in  $\text{Ar}^+$  lasers.**

The pump rate  $R_p$  in argon lasers is approximately proportional to the square of current density  $J^2$  in the discharge. Thus the relationship between pump power  $P_p$  and output power  $P_{out}$  is not linear. Assuming a constant voltage drop across the laser tube, calculate the output power of such laser as a function of pump power. Compare the result with Eq. (7.3.9) of PL, which is valid only for a linear dependence of pump rate on  $P_p$ .

**10.8P Current density in a low power  $\text{CO}_2$  laser.**

Consider a  $\text{CO}_2$  laser with slow **axial** flow of the gas mixture; the diameter of the laser tube is  $D_0 = 1.5$  cm. Assuming a voltage drop  $V = 7500$  V along the laser tube and a uniform distribution of the current density across the tube, calculate the current density required for a pump power  $P_p = 250$  W. Establish the values of voltage drop and current density corresponding to the same pump power and for a tube diameter  $D = 2D_0$ .

**10.9P Voltage drop in a low power  $\text{CO}_2$  laser tube.**

Assume that the gas mixture of a  $\text{CO}_2$  laser is made of  $\text{CO}_2$ ,  $\text{N}_2$  and He with relative ratios of partial pressures of 1:2:3. For this **mixture** the optimum value of the ratio between the applied electric field  $E$  and the total gas pressure  $p$  is  $E/p = 10 \text{ V}/(\text{cm} \times \text{torr})$ . The optimum value of the product between  $p$  and the

tube diameter  $D$  is  $pD = 22.5$  cmxtorr. Assuming a diameter  $D = 1$  cm and a tube length  $l = 50$  cm, calculate the voltage drop across the tube. Which is the current density required to provide a pump power  $P_p = 225$  W?

### 10.10P Rotational transitions in a CO<sub>2</sub> laser.

Knowing that the **maximum** population of the upper laser level of a CO<sub>2</sub> molecule occurs for the rotational quantum number  $J' = 21$  [see Fig. 10.11 of PL] and assuming a **Boltzmann** distribution, calculate the rotational constant  $B$ . Assume a temperature  $T = 400$  K, corresponding to an energy  $kT/hc \cong 280$  cm<sup>-1</sup>. Calculate also the frequency spacing between two adjacent rotational laser transitions. [Hint: to answer this problem you have to read § 3.1 of PL.]

### 10.11P Mode locking of a CO<sub>2</sub> laser.

Consider a CO<sub>2</sub> laser with high enough pressure to have all its rotational lines merged together. If this laser is mode-locked, what is the order of magnitude of the expected laser pulse width?

### 10.12P ASE threshold for a N<sub>2</sub> laser.

Consider a "mirrorless" nitrogen laser using a gas mixture of 960 mbar of He and 40 mbar of N<sub>2</sub> at room temperature, with a discharge length  $l = 30$  cm and a tube diameter  $D = 1$  cm. Assume a stimulated emission cross-section  $\sigma_e = 40 \times 10^{-14}$  cm<sup>2</sup> and a fluorescence quantum yield  $\phi \cong 1$ . The **threshold** for amplified spontaneous emission (ASE) in this laser is given by the condition [see Eq. (2.9.4b) of PL]:

$$G = [4\pi(\ln G)^{1/2}]/(\phi \Omega)$$

where  $G$  is the single pass gain in the **discharge** and  $\Omega = \pi D^2/(4l^2)$  is the emission solid angle. Calculate the density  $N_2$  of excited molecules required to reach the threshold for ASE.

[Hint: the answer to this problem requires a graphical or numerical solution of the previous non linear equation. Alternatively, since  $(\ln G)^{1/2}$  is a slowly varying function of  $G$ , one can solve the previous equation by an iterative method, **i.e.** assuming first a given value of  $G$  to be used in  $(\ln G)^{1/2}$ , then calculating the new value of  $G$  and so on.]

**10.13P Pump power in a KrF excimer laser at threshold.**

Consider a KrF excimer laser which operates in a pulsed regime. The density of the KrF **excimers** at laser threshold is  $N_{th} = 4 \times 10^{11} \text{ cm}^{-3}$ . Assuming **an** upper laser level lifetime  $\tau = 10 \text{ ns}$ , evaluate the **minimum** pump rate required for this laser. **Assume** that: the **pump** efficiency is  $\eta_p = 1$ ; **the** average energy required to excite a (KrF)<sup>\*</sup> molecule is  $E_p \approx 7.5 \text{ eV}$ ; the discharge volume is  $157 \text{ cm}^3$ ; the duration of the current pulse is  $\tau_p = 10 \text{ ns}$ . Calculate the **peak** pump power and the pump energy at threshold.

**10.14P Cold reaction in a HF chemical laser.**

Consider the "cold reaction"  $\text{F} + \text{H}_2 \rightarrow \text{HF}^+ + \text{H}$  occurring in a HF chemical laser. Assuming a reaction energy of **31.6 kcal/mole**, calculate the energy released for each molecular reaction.

**10.15P Transition linewidths in the soft-X-ray spectral region.**

Consider the laser **transition** occurring in  $\text{Ar}^{8+}$  (Neon-like Argon) at  $\lambda = 46.9 \text{ nm}$ . Assuming **an** ion temperature  $T_i = 10^4 \text{ K}$  and an  $\text{Ar}^{8+}$  mass  $M = 39.9$  atomic **units**, calculate the Doppler broadening for this transition. Assuming a radius of the  $\text{Ar}^{8+}$  approximately equal to the atomic radius of Neon ( $a \approx 51 \text{ pm}$ ) and also assuming that the dipole moment of the dipole-allowed transition is  $\mu \approx ea$ , calculate the spontaneous emission lifetime of the transition. Calculate then the linewidth for natural broadening and compare it to that for Doppler broadening.

**10.16P A free-electron laser operating in the soft-X-ray region.**

Consider a **free-electron** laser (FEL) operating at **the** emission wavelength  $\lambda = 46.9 \text{ nm}$ . Assume an undulator period  $\lambda_u = 10 \text{ cm}$  and **an** **undulator** parameter  $K \approx 1$ . Calculate **the** electron energy required in this operating conditions. Assuming a length of the magnets array  $l = 10 \text{ m}$ , calculate the emission linewidth and compare the result to those established in problem **10.15**.

## ANSWERS

### 10.1A Low-density laser emitting in the infrared.

Laser action in the infrared region can be obtained using molecular gases as **low-density** active media. Among molecular lasers we can mention: (a) **CO<sub>2</sub>** lasers, with laser action **occurring** between some roto-vibrational levels of CO<sub>2</sub> molecule in the ground electronic **state**; two laser transitions are observed around **9.6** and **10.6 μm** respectively. (b) CO lasers, in which laser action occurs very efficiently owing to cascading effects between a set of roto-vibrational levels of CO molecule; laser transition occurs at **-5 μm**. (c) **CH<sub>3</sub>F** lasers, whose laser action occurs between rotational levels of an excited vibrational level of the molecule; laser emission occurs around **496 μm**.

We recall also that, among chemical lasers emitting in the **infrared**, the most notable example is the HF laser, whose emission takes place between **2.7** and **3.3 μm**, involving transition between several **roto-vibrational** levels of the HF molecule.

### 10.2A Low-density laser emitting in the UV - soft X region.

Laser action in the ultraviolet to soft-X-ray region can be achieved using excited ions or molecules in gas phase as low-density active media. Among lasers emitting in the near-W region, we can mention: (a) The He-Cd laser, with laser action occurring between some excited states of the **Cd<sup>+</sup>** ion; two main laser transitions **are observed** at **325** and **416 nm**. (b) The N<sub>2</sub> laser, in which laser action occurs between two vibronic levels (**i.e.** between the first excited electronic state and the ground state of the molecule); the emission takes place at **337 nm**. Owing to the circumstance that the lifetime of the lower laser level is larger than that of the upper level, this is a self-terminating laser. (c) Excimer lasers, in which the upper laser level consists of an excited dimer and the lower level consists of the dissociating dimer. Notable examples **are ArF** laser (emitting at **193 nm**) and **KrF** laser (emitting at **248 nm**). (d) Lasers emitting in the soft-X region are generally based on transitions occurring in multiple ionised atoms. As an example we can mention the **Ar<sup>8+</sup>** (Neon-like Argon) laser, emitting at 46.9 nm. The generation of the excited medium can be achieved in these cases either by strong photoionization of a target using powerful laser pulses, or by ionization of a gas using fast, **powerful** electrical discharge. In both cases amplified spontaneous emission is achieved in the active medium.

Many problems must be overcome to achieve laser action in the **W** and soft-X regions: (1) For wavelengths between 200 and 150 nm, almost all the optical materials (air included) absorb; for this reason special materials must be used for laser windows, dielectric mirrors and lenses. To avoid strong absorption **from** air, laser beams must propagate in vacuum. (2) In the soft-X-ray region (below 50 nm), the difference in refractive index between various materials becomes very small; for this reason **multilayer** dielectric **mirrors** require a large number of layers (~40) and are, accordingly, very lossy. For this reason optical resonator are not used and directional emission can take place only as amplified spontaneous emission ("mirror-less lasing"). (3) Lifetime of laser transitions in the X-ray region is extremely short (up to some femtoseconds); for this reason strong population inversion and very fast pumping mechanisms are required in X-ray lasers.

### **10.3A High-power lasers for material processing.**

Owing to the high slope efficiency (**15-25%**), CO<sub>2</sub> laser can be produced with high cw output power: in fast axial-flow lasers, 1 **kW** per unit discharge length can be achieved. In transverse-flow lasers, output powers of a few **kW** per unit discharge length are easily obtained; this result is however attained with a lower quality of laser beam. Output powers up to a few kW can also be attained with both lamp-pumped and diode-pumped ( $\lambda_p \cong 810$  nm) **Nd:YAG** lasers and with longitudinally-pumped ( $\lambda_p \cong 950$  nm) **Yb:YAG** lasers. Optical to optical laser efficiency up to 40 % has been demonstrated with **Nd:YAG** lasers.

High power laser are used for cutting, drilling, welding, surface hardening and surface metal alloying; lower power are used also for surface marking.

### **10.4A Internal structure of He-Ne lasers.**

Upon excitation of the He-Ne mixture by electrical discharge, the positive ions produced in the discharge are collected by the cathode. Owing to the relatively large value of the mass of the ions, a large momentum is transferred to the cathode which is thus subjected to damage. Increasing the cathode area helps in withstanding such collisions **from** positive ions. The confinement of electrical discharge by the capillary allows increase of population inversion, thus lowering the pump power at threshold. A way to understand this circumstance is to recall that in gas lasers an optimum value for the product  $pD$  exists, where p is the pressure of the gas mixture and D the diameter of the discharge tube. For a given current **density**, the pump rate by electron-atom collisions is proportional to p and hence to  $D^{-1}$ . Thus using small capillary diameters allows an increase in

pump rate and hence in laser gain. A lower limit to capillary diameter is set by the **appearance** of losses induced by **diffraction**. Most He-Ne lasers operate with a bore diameter of -2 mm.

### 10.5A Maximum output power in He-Ne lasers.

In He-Ne lasers the main pumping process occurs through excitation of He atoms in a metastable state by electron impact; Ne excitation is then achieved by resonant energy transfer. The rate of He excitation in steady state **must** equal the **rate** of deexcitation due to electron collisions and to collisions with the walls. Thus the excited He population  $N^*$  can be related to the total He population  $N_t$  by the following expression:

$$N_t k_1 J = N^* (k_2 + k_3 J)$$

where:  $\mathbf{J}$  is the current density in the discharge; the constant  $k_1$  accounts for excitation by electron collisions;  $k_2$  is the rate of deexcitation by collisions with the walls and  $k_3$  takes into account **de-excitation** by electron collisions. Thus the population  $N_2$  in the Ne upper laser level will be related to the population in the ground state  $N_g$  by a similar relation:

$$N_2 = N_g \frac{aJ}{b + cJ} \quad (1)$$

where  $a$ ,  $b$  and  $c$  are constants. On the other hand the population in the lower

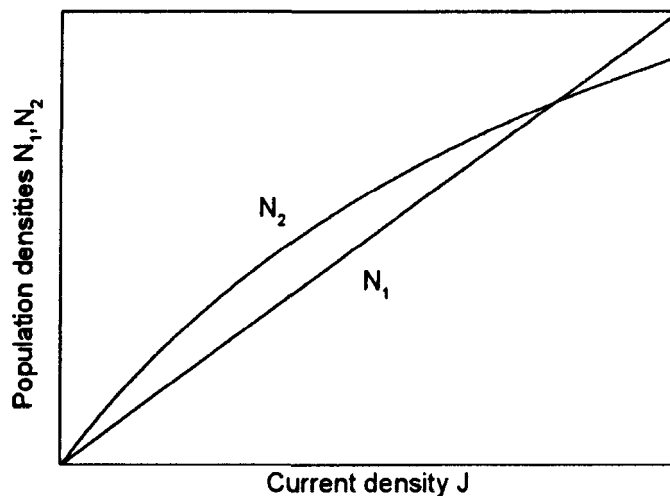


Fig. 10.1: Upper and lower level populations of Ne in a He-Ne laser as a function of current density.

laser level  $N_1$  increases linearly with  $\mathbf{J}$ , owing to direct excitation by electron collisions of Ne **atoms**. We *can* thus write:

$$N_1 = d J \quad (2)$$

where  $d$  is again a constant. In Fig. 10.1  $N_1$  and  $N_2$  are plotted as a function of the current density  $\mathbf{J}$ . We can see that an optimum value of  $\mathbf{J}$  occurs **i.e.**, for which the population inversion  $\Delta N = N_2 - N_1$  **is** maximized.

For this reason, He-Ne lasers are equipped with a power supply that provides the optimum current density to the discharge.

### 10.6A Internal structure of high-power Ar<sup>+</sup> lasers.

The use of a confining structure for the electrical discharge, allows laser oscillation to be found in a TEM <sub>$\infty$</sub>  mode and limits the current needed by the laser. The presence of high temperature argon ions requires a structure with **low-erosion** property and providing a strong heat dissipation. Tungsten disks allow for both these two features. Owing to **the** strong electric field in the discharge, ion migration towards **the** cathode occurs. At the cathode these. ions are neutralized by the electrons emitted, whicht results in accumulation of Ar neutral atoms. To allow a redistribution of the gas, some return paths are provided through off-center holes made in the tungsten disks; such holes, being **off-center**, avoid the occurrence of secondary current flows between the electrodes. The presence of a static magnetic field parallel to the discharge, confines electrons and ions by **Lorentz** force near the tube axis, thus providing an increase of pump rate and a reduction of wall damages by ion and electron collisions.

### 10.7A Output vs. pump power in Ar<sup>+</sup> lasers.

The pump rate  $R_p$  in an Ar<sup>+</sup> laser is approximately proportional to the square of the current density  $\mathbf{J}$  flowing in the laser tube [see answer 6.18A]:

$$R_p \propto J^2 \quad (1)$$

According to Eq. (7.2.18) and Eqs. (7.3.5-6) of PL, the output power  $P_{out}$  of a four level laser **can** be expressed as:

$$P_{out} = \frac{A_b I_s \gamma_2}{2} \left( \frac{R_p}{R_{cp}} - 1 \right) \quad (2)$$

where:  $A_b$  is the cross-sectional area of the laser mode;  $\gamma_2$  is the output coupler loss;  $R_p$  and  $R_{cp}$  are the pump rate and the critical pump rate respectively;  $I_s = h\nu/\sigma\tau$  is the saturation intensity for a four-level system [see Eq. (2.8.24) of PL]. If we let  $V_0$  be the voltage drop across the discharge, we can express the pump power  $P_p$  as:

$$P_p = AV_0J \quad (3)$$

where  $A$  is the cross-sectional area of the discharge. We further assume that  $V_0$  is independent of the current density  $J$ . Inserting the value obtained for  $J$  by Eq. (3) in Eq. (1) and then using the resulting expression for  $R_p$  in Eq. (2), we obtain:

$$P_{out} = \frac{A_b I_s \gamma_2}{2} \left( \frac{P_p^2}{P_{th}^2} - 1 \right) \quad (4)$$

where  $P_{th}$  is the pump power at threshold. Eq. (4) shows that in an  $\text{Ar}^+$  laser the output power  $P_{out}$  increases according to a quadratic law in  $P_p$ . Comparing this result with that of Eq. (7.3.9) of PL, we can see that the output power increases faster with  $P_p$  than in ordinary lasers; the laser slope efficiency  $dP_{out}/dP_p$  is then expected to increase linearly with pump power.

### 10.8A Current density in a low power $\text{CO}_2$ laser.

Assuming a constant voltage drop  $V_0$  along the laser tube and a constant current density  $J$  across the tube, we can express the pump power  $P_p$  as:

$$P_p = AV_0J \quad (1)$$

where  $A$  is the cross-sectional area of the discharge. The area  $A$  is then given by:

$$A = \frac{\pi D_0^2}{4} \quad (2)$$

Inserting Eq. (2) in Eq. (1), we can calculate the current density as:

$$J = \frac{4P_p}{\pi D_0^2 V_0} \quad (3)$$

Using the numerical values given in the problem, we obtain from Eq. (3)  $J = 0.019 \text{ A/cm}^2$ . From the scaling laws of a **gas** laser discharge [see Eq. (6.4.23a-b) of PL], one sees that doubling the **tube** diameter requires a reduction of both pressure and electric field to half their original values. In particular, this correspond to a reduction of the operating voltage to half its **original** value, **i.e.** to 3750 V. Doubling of the **tube** diameter corresponds to increase the area A four times. Accordingly from Eq. (1) one sees that, for the same pump power, the required **current** density is  $J' = 0.0094 \text{ A/cm}^2$ , **i.e.** half its initial value.

### 10.9A Voltage drop in a low power CO<sub>2</sub> laser tube.

Assuming that the laser is operating under optimum conditions, the pressure  $p$  inside the laser tube can be calculated using the optimum value of the product  $pD$  and the value given for **the** tube diameter D. From the optimum value of the  $\mathcal{E}/p$  ratio, we then get  $\mathcal{E} = 225 \text{ V/cm}$ . The voltage drop across the laser tube is then given by  $V = \mathcal{E} l$ , where I is the tube length. From the previous equation, one obtains  $V = 11.2 \text{ kV}$ .

The current density J flowing in the tube is then related to the pump power  $P_p$  by the expression:

$$J = \frac{4P_p}{\pi D^2 V} \quad (1)$$

Inserting in Eq. (1) the numerical values, we get  $J = 0.025 \text{ A/cm}^2$ .

### 10.10A Rotational transitions in a CO<sub>2</sub> laser.

According to Eq. (3.1.10) of PL the most heavily populated **rotational-vibrational** level is the one corresponding to the quantum number  $J'$  satisfying the relation:

$$(2J'+1) = \sqrt{2kT/B} \quad (1)$$

where: k is the **Boltzmann** constant; T is the **temperature** of the molecule; B is the rotational constant of the molecule. Note that in CO<sub>2</sub> molecules, only rotational levels with odd values of  $J'$  are populated, owing to **symmetry** reasons. Inserting in Eq. (1) the numerical values given in the problem, we get  $B = 5.97 \times 10^{-24} \text{ J}$ , corresponding to a frequency in wavenumbers of  $0.3 \text{ cm}^{-1}$ . The rotation energy  $E_r$  of a given rotational level characterized by the rotational quantum number  $J'$  is then given by:

$$E_r = B J' (J'+1) \quad (2)$$

For the **CO<sub>2</sub>** molecule (and in general for linear or diatomic molecules), the selection rule for allowed transitions between two roto-vibrational levels requires:

$$\Delta J = J'' - J' = \pm 1 \quad (3)$$

where **J''** is the rotational quantum number in the lower level and **J'** the quantum number in the upper level.

Using Eq. (2) and Eq. (3), we can calculate the energy separation between two adjacent rotational lines in the **roto-vibrational** laser transition. Recalling that only odd rotational levels are occupied, we can assume that the two adjacent rotational lines we are considering corresponds respectively to upper levels with quantum numbers **J'** and **J'+2**. Let us focus our discussion to transitions following the rule **A J = -1**. The difference in energy **A E** between two adjacent transitions is given by **A E = A E<sub>2</sub> - A E<sub>1</sub>**, where **A E<sub>2</sub>** is the **difference** between the upper level energies and **A E<sub>1</sub>** is the difference between the lower level energies of the two transitions. Thus, according to Eq. (2) and Eq. (3):

$$\begin{aligned} \Delta E_2 &= B(J'+2)(J'+3) - B J' (J'+1) \\ \Delta E_1 &= B[(J'+2) - 1](J'+2) - B(J'-1)J' \end{aligned}$$

After some simple algebra, we obtain **A E = 4 B** and correspondingly the frequency difference between the two lines is  **$\Delta\nu = A E / h = 3.6 \times 10^{10}$  Hz**. The same result is found for transitions following the rule **A J = 1**.

### 10.11A Mode locking of a CO<sub>2</sub> laser.

Let us **assume** that the width of the gain line, when all rotational lines are merged, is related to the width of the population distribution of the upper rotational levels. In the following we will also focus our attention to one of the two rotational branch of the laser transition (**e.g.** to the transitions obeying the **rule A J = -1**, **see** answer 10.10A). From Fig. 10.11 of PL we can see that the population density is mainly concentrated among levels with quantum number **11 < J' < 41**. Since only odd rotational levels are occupied and since the frequency spacing between two adjacent rotational lines is **A v = 3.6 × 10<sup>10</sup> Hz** [**see** answer 10.10A], the width of the gain line is approximately given by **A ν<sub>tot</sub> = A v (41-11)/2 = 15 A v**, **i.e.** equal to **A ν<sub>tot</sub> = 0.15 THz**. The pulse width under mode-locking operation is then approximately equal to **Δτ<sub>p</sub> ≈ 1/Δ ν<sub>tot</sub> = 1.8 ps**.

### 10.12A ASE threshold for a N<sub>2</sub> laser.

For a given value of the single pass gain G in the laser tube, the density  $N_2$  of excited molecules can be calculated from the expression:

$$G = \exp[\sigma_e N_2 I] \quad (1)$$

where  $\sigma_e$  is the stimulated emission cross-section and  $I$  the discharge length. The value of G corresponding to threshold for ASE is then obtained upon solving the non-linear equation given in the problem [see Eq. (2.9.4b) of PL]:

$$G = [4\pi(\ln G)^{1/2}]/(\phi \Omega) \quad (2)$$

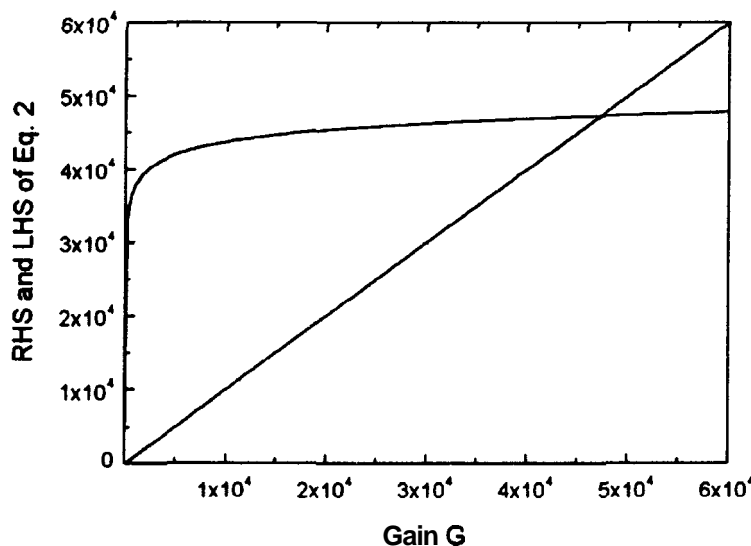


Fig. 10.2 Graphical solution of Eq. (2)

Eq. (2) is valid in the limit  $G \gg 1$ , which is generally satisfied in nitrogen lasers. A solution can be obtained by graphical or numerical methods. To perform a graphical solution, we plot in Fig. 10.2 the right hand side (RHS) and the left hand side (LHS) of Eq. (2) as a function of G and then we look for intersections between the two curves. Using the numerical values given in the problem, the intersection is seen to correspond to  $G = 4.7 \times 10^4$ . Inserting this value in Eq. (1), the corresponding value for the excited population turns out to be  $N_2 = 8.97 \times 10^{11}$  molecules/cm<sup>3</sup>.

Alternatively, since  $(\ln G)^{1/2}$  is a slowly varying function of G, one can solve Eq. (2) by an iterative method, i.e. assuming first a given value of G to be used in the RHS of Eq. (2), then calculating the new value of G and so on. It's easy to show that the convergence of this method is very fast; in the following table we

report the first four steps of the iteration, starting with an initial gain of  $G = 2 \times 10^4$ .

Step n.	$G$	RHS of Eq. (2)
1	$2 \times 10^4$	$4.532 \times 10^4$
2	$4.532 \times 10^4$	$4.715 \times 10^4$
3	$4.715 \times 10^4$	$4.724 \times 10^4$
4	$4.724 \times 10^4$	$4.724 \times 10^4$

### 10.13A Pump power in a KrF excimer laser at threshold.

Excimer lasers generally operate in pulsed regime; for this reason the steady-state solutions to rate equations cannot be applied. We therefore proceed with an analysis in the transient regime.

To calculate the minimum pump rate  $R_{pc}$  required (critical pump rate), we will assume that  $R_{pc}$  is constant during the duration of the pump pulse  $\tau_p$ . Thus, for time  $t$  in the interval  $0 < t < \tau_p$ , the rate equation for the excited population  $N$  at threshold becomes:

$$\frac{dN}{dt} + \frac{N}{\tau} = R_{pc} \quad (1)$$

where  $\tau$  is the lifetime of the laser transition. Assuming no population at time  $t = 0$ , one can readily show that the solution of Eq. (1) is:

$$N(t) = R_{pc} \tau [1 - e^{-t/\tau}] \quad (2)$$

If we impose that the excited population at the end of the pump pulse equals the population at threshold, we get:

$$N(\tau_p) = N_{th} = R_{pc} \tau [1 - e^{-\tau_p/\tau}] \quad (3)$$

From Eq. (3), using the values given for  $\tau$  and  $\tau_p$ , we get the expression for the critical pump rate as:

$$R_{pc} = \frac{N_{th}}{\tau} \frac{e}{(e-1)} \quad (4)$$

From the numerical values given in the problem, we obtain  $R_{pc} = 6.33 \times 10^{19} \text{ cm}^{-3} \text{ s}^{-1}$ . It is worth noting that Eq. (4) differs from the steady state expression by a numerical factor depending on the ratio between pump duration and lifetime of excited molecules. The minimum peak pump power  $P_p$  is then readily calculated as:

$$P_p = R_{pc} V_a E_{ex} \quad (5)$$

where  $V_a$  is the volume of the active medium and  $E_{ex}$  is the excitation energy for a single molecule. From Eq. (5), using the calculated value for  $R_{pc}$  and the given values of  $V_a$  and  $E_{ex}$ , we get  $P_p = 11.93 \text{ kW}$ . The corresponding **minimum** pulse energy is expected to be  $E_{min} = P_p \tau_p = 0.12 \text{ mJ}$ . It should be noted, however, that the pump **efficiency** expected for this laser is approximately equal to the laser slope **efficiency** and hence equal to  $-1\%$ . The actual peak pump power and energy, at threshold, are therefore expected to be  $-100$  time larger than the value given above.

### 10.14A Cold reaction in a HF chemical laser.

Let us consider the "cold reaction"  $\text{F} + \text{H}_2 \rightarrow \text{HF}^+ + \text{H}$  occurring in a HF chemical laser. Assuming a reaction energy  $E = 31.6 \text{ kcal/mole}$ , the energy  $E_m$  released for each molecular reaction is given by:

$$E_m = E / N_A \quad (1)$$

where  $N_A = 6.022 \times 10^{23} \text{ molecules/mole}$  is the Avogadro number. Inserting in Eq. (1) the numerical values, we get  $E_m = 1.37 \text{ eV}$ . Note that the vibrational frequency of the HF molecule corresponds to a wavelength  $\lambda = 2.7 \mu\text{m}$ . The corresponding transition energy is then **approximately**  $\Delta E_v \approx 0.44 \text{ eV} \approx E_m/3$ . This means that the "cold reaction" can leave the HF molecule in an excited state **as high as** the  $v = 3$  vibrational level [see Fig. 10.22 of PL].

### 10.15A Transition linewidths in the soft-X-ray spectral region.

The linewidth  $\Delta\nu_0^*$  of a Doppler-broadened transition is given by [see Eq. (2.5.18) of PL]:

$$\Delta\nu_0^* = 2\nu_0 \left( \frac{2kT_i}{Mc^2} \ln 2 \right)^{1/2} \quad (1)$$

where:  $\nu_0$  is the transition frequency;  $k$  is the **Boltzmann** constant;  $T_i$  is the temperature of the ion ensemble;  $M$  is the ion mass and  $c$  is the speed of light. Inserting in Eq. (1) the numerical values given in the problem, we get  $\Delta\nu_0^* = 72.5 \text{ GHz}$ . The natural broadening  $\Delta\nu_{nat}$  of the **same** transition is given by:

$$\Delta \nu_{nat} = \frac{1}{2\pi\tau_{sp}} \quad (2)$$

where  $\tau_{sp}$  is the spontaneous emission lifetime. This lifetime can be calculated using the expression [see Eq. (2.3.15) of PL]:

$$\tau_{sp} = \frac{3h\epsilon_0 c^3}{16\pi^3 \nu_0^3 |\mu|^2} \quad (3)$$

where:  $h$  is the **Planck** constant;  $\epsilon_0$  is the **vacuum** dielectric constant and  $\mu$  is the dipole moment of the transition. Inserting in Eq. (3) the numerical values given in the problem, we get  $\tau_{sp} = 55$  ps. From Eq. (2) we then obtain  $\Delta \nu_{nat} = 2.9$  GHz. One can note that Doppler broadening still predominates over natural broadening in this wavelength region. Since, however, one has  $\Delta \nu_{nat}/\Delta \nu_0 \propto \nu_0^{-2}$ , the two broadening mechanisms may become comparable for an increase of the transition frequency and hence a decrease of the corresponding wavelength by less than an order of magnitude.

### 10.16A A free-electron laser operating in the soft-X-ray region.

The emission wavelength  $\lambda$  of a free-electron laser (FEL) is related to the energy  $E$  of the electrons by the relation [see Eq. (10.4.6) of PL]:

$$\lambda = \frac{\lambda_q}{2} \left( \frac{m_0 c^2}{E} \right)^2 (1 + K^2) \quad (1)$$

where:  $\lambda_q$  is the undulator period;  $m_0$  is the electron mass at rest;  $c$  is the speed of light;  $K$  the undulator parameter. Inverting Eq. (1), we get the electron energy as:

$$E = m_0 c^2 \sqrt{\frac{\lambda_q}{2\lambda_0} (1 + K^2)} \quad (2)$$

Using the numerical values given in the problem, we get from Eq. (2)  $E = 747$  MeV. Note the large value of electron energy which is required at this short wavelength. The emission linewidth  $\Delta \nu$  is then given by the expression:

$$\Delta \nu = \frac{\nu_0}{2N} \quad (3)$$

where  $\nu_0$  is the transition frequency and N is the number of undulators in the FEL. Assuming  $N \approx l/\lambda_q$ , where  $l$  is the length of the undulator array, we obtain  $A v = 32$  THz. The comparison of this value with that obtained in the previous problem and at the same wavelength in Neon-like Argon, shows that the linewidth of the FEL laser is  $\sim 400$  times larger.

# CHAPTER 11

## Properties of Laser Beams

### PROBLEMS

#### 11.1P Complex degree of coherence for a quasi monochromatic wave.

Consider a quasi-monochromatic wave with a mean frequency  $\langle\omega\rangle$ . Show that the complex degree of coherence  $\gamma^{(1)}(\tau)$  can be written in the form  $\gamma^{(1)}(\tau)=|\gamma^{(1)}(\tau)| \exp[j(\langle\omega\rangle\tau-\psi(\tau))]$ , where  $|\gamma^{(1)}(\tau)|$  and  $\psi(\tau)$  are slowly-varying functions of  $\tau$  on a time scale  $2\pi/\langle\omega\rangle$ .

#### 11.2P Measurement of the spatial coherence by a Young interferometer.

A Young interferometer is used to measure the spatial coherence between two points  $P_1$  and  $P_2$  on a wave front of an electromagnetic wave. The interference pattern produced by the light diffracted from two holes at  $P_1$  and  $P_2$ , made on a opaque screen, is observed on a second screen, placed beyond the **first** one. Measurements **are** made around a point P equidistant from  $P_1$  and  $P_2$ . The visibility of fringes obtained in this way is  $V_p=0.6$ . The ratio  $r=\langle I_1 \rangle / \langle I_2 \rangle$  between the average field intensities  $\langle I_1 \rangle$  and  $\langle I_2 \rangle$ , measured in P when either one of the two holes in  $P_1$  and  $P_2$  are closed, is  $r=0.2$ . Calculate the magnitude of the first-order spatial degree of colierence between points  $P_1$  and  $P_2$ .

#### 11.3P Destroy of spatial coherence by rotation of a ground glass.

A piece of transparent ground glass is placed before the two holes of a Young interferometer and rotated rapidly. Under this condition, it is found that a

spatially coherent radiation does not produce any interference fringes. Explain this observation.

### 11.4P Comparison of temporal coherence between a thermal source and a laser.

Calculate the temporal coherence length  $L_\infty$  of a mercury vapor lamp emitting in the green portion of the **spectrum** at a wavelength of 546 nm with an emission bandwidth  $\Delta\lambda \approx 0.01$  nm. Then compare this coherence length to **that** of a **Nd:YAG** laser operating at a wavelength of 1064 nm with an emission spectral width of  $\Delta\nu \approx 10$  kHz.

### 11.5P Temporal coherence of white light.

Consider a white light with uniform spectrum between  $\lambda_1 = 400$  nm and  $\lambda_2 = 700$  nm. Estimate the bandwidth and coherence time of this white light and show that its coherence length is of the order of the wavelength.

### 11.6P Relation between first-order degree of temporal coherence and fringe visibility in a Michelson interferometer.

With reference to Fig.11.4 of PL, consider a Michelson interferometer for measuring the degree of **temporal** coherence of an electromagnetic wave at a point  $r$ . Show that the fringe visibility  $V_p(\tau)$  of the interference pattern, as obtained by **varying** the time delay  $\tau$  introduced by the two **arms** of the interferometer, is equal to the modulus of the first-order complex degree of temporal coherence, i.e.  $V_p(\tau) = |\gamma^{(1)}(r, r, \tau)|$ .

### 11.7P Degree of temporal coherence for a low-pressure discharge lamp.

Calculate the first-order degree of temporal coherence  $\gamma^{(1)}(\tau)$  for a low-pressure gas discharge lamp assuming that the emitted light has a Gaussian power spectrum centered at the frequency  $\omega_0$  with a **FWHM**  $\Delta\omega_0$ . Assuming that the

coherence time  $\tau_c$  of the light is equal to the half-width at half-maximum (HWHM) of  $|\gamma^{(1)}(\tau)|$ , shows that  $\tau_c = (4 \ln 2) / \Delta\omega_0$ .

### 11.8P Temporal coherence of a gas laser oscillating on N axial modes.

An idealized model of the normalized power spectral density of a gas laser oscillating in  $(2N+1)$  equal-intensity axial modes is:

$$S(\nu) = \frac{1}{2N+1} \sum_{n=-N}^N \delta(\nu - \nu_0 + n\Delta\nu)$$

where  $\nu_0$  is the frequency of the central mode and  $\Delta\nu$  is the frequency separation of adjacent cavity axial modes. Show that the corresponding envelope of the complex degree of coherence is:

$$\gamma(\tau) = \left| \frac{\sin[(2N+1)\pi\tau\Delta\nu]}{(2N+1)\sin(\pi\tau\Delta\nu)} \right|$$

### 11.9P An interference experiment with partially coherent light.

A mercury arc lamp, emitting a quasi-monochromatic radiation at  $\lambda=546.1$  nm, is placed behind a circular aperture with a diameter  $d=0.1$  mm in an opaque screen. Beyond this first screen there containing two pin-holes of equal diameter. Interference fringes from light diffracted by the two pin-holes are observed on a third screen, at a distance  $L=3$  m from the second one. Calculate the separation  $s$  between the two pin-holes at which the visibility of fringes, around a point on the screen equally distant from the two holes, is  $V_p=0.88$ .

### 11.10P Spatial coherence of the light from the sun.

Consider the light from the sun and assume that the sun can be treated as a disk source of incoherent light with a diameter  $d \approx 13.92 \times 10^8$  m. Assume that the observation is made on the earth using narrow-band interference filters centered at  $\lambda \approx 550$  nm. Assume also that the distance between the earth and the sun is  $z \approx 1.5 \times 10^{11}$  m. Calculate the linear dimensions on the earth over which the light from the sun spatially coherent?

**11.11P An astronomic calculation based on spatial coherence of stellar radiation,**

The radiation at  $\lambda \approx 550$  nm emitted by star **Betelgeuse** and observed at two points on the earth shows a spatial coherence of  $\gamma = 0.88$  if the distance between the two points is  $r \approx 80$  cm. Provide an estimate of the angle subtended by the star at the earth.

**11.12P Beam divergence of a partially-coherent laser beam.**

A **Nd:YAG** laser beam, operating at the wavelength  $\lambda = 1064$  nm with a diameter of  $D \approx 6$  mm and approximately a constant intensity distribution over its cross section, has a divergence  $\theta \approx 3$  mrad. Show that the laser beam is not diffraction-limited and estimate the diameter of the coherence area. Let the beam then pass through an attenuator whose power transmission  $T$  varies with radial distance  $r$  according to  $T(r) = \exp[-(2r/w_0)^2]$  with  $w_0 = 0.5$  mm, so that the beam, after the attenuator, has a Gaussian intensity profile with spot size  $w_0$ . What is the divergence of the transmitted beam and how it is compared with the divergence of a perfectly-coherent Gaussian beam of spot-size at the beam waist  $w_0$  ?

**11.13P Focusing of a perfectly-coherent spatial beam.**

A plane wave of circular cross section, uniform intensity and perfect spatial coherence is focused by a lens. What is the increase in intensity at the focal plane compared to that of the incident wave ?

**11.14P  $M^2$  factor of a Nd:YAG laser.**

The near-field transverse intensity profile of a **Nd:YAG** laser beam at  $\lambda = 1064$  nm wavelength is, to a good approximation, Gaussian with a diameter (FWHM)  $D \approx 4$  mm. The half-cone beam divergence, measured at the half-maximum point

of the far-field intensity distribution, is  $\theta \approx 3 \text{ mrad}$ . Calculate the corresponding  $M^2$  factor.

### **11.15P Brightness of a high-power CO<sub>2</sub> laser.**

A high-power CO<sub>2</sub> laser, oscillating on the  $\lambda = 10.6 \mu\text{m}$  transition, emits a TEM<sub>00</sub> beam with a **beam** waist  $w_0 = 1 \text{ cm}$  and an optical power  $P = 1 \text{ kW}$ . Calculate the brightness B of the laser and the peak laser intensity that would be produced by focusing the laser beam in the focal plane of a lens with focal **length**  $f = 20 \text{ cm}$ .

### **11.16P Grain size of the speckle pattern as observed on a screen.**

The speckle pattern observed when an expanded He-Ne **laser beam** at  $\lambda = 632 \text{ nm}$  illuminates a **diffusing** area of diameter  $D = 0.5 \text{ cm}$  shows a grain size of  $d_g \approx 0.6 \text{ mm}$ . **Provide** an estimate of **the** distance L of the scattered surface from the observation plane.

### **11.17P Grain size of the speckle pattern as seen by a human observer.**

Consider the same problem **11.16P** and assume that the speckle pattern is seen by a human observer that looks at the scattering surface. What is the apparent grain size on the scattering surface observed by the human eye ? Assume for the eye a pupil diameter  $D = 1.8 \text{ mm}$ .

### **11.18P Correlation function and power spectrum of a single-longitudinal mode laser.**

The electric field of a single-longitudinal mode laser is well described by  $E(t) = A \exp[j\omega_0 t + j\varphi(t)]$ , where  $\omega_0$  is the central laser wavelength, A can be taken as a constant real amplitude, and  $\varphi(t)$  is a **random** phase describing a random-walk process. Assuming for  $\Delta\varphi(\tau) = \varphi(t+\tau) - \varphi(t)$  a Gaussian probability distribution, given by:

$$f(\Delta\varphi) = \frac{1}{(4\pi|\tau|/\tau_c)^{1/2}} \exp\left[-\frac{\tau_c\Delta\varphi^2}{4|\tau|}\right],$$

where  $\tau_c$  is the time constant associated to the random walk, show that the autocorrelation function  $I^{(1)}(\tau) = \langle E(t+\tau)E^*(t) \rangle$  of the electric field is given by:

$$I^{(1)}(\tau) = \exp(j\omega_0\tau) \exp(-|\tau|/\tau_c)$$

Then show that the power spectrum of the laser field is lorentzian with a FWHM given by  $\Delta\nu = 1/\pi\tau_c$ .

(Level of difficulty higher than average)

## ANSWERS

### **11.1A Complex degree of coherence for a quasi monochromatic wave.**

Let us consider a linearly-polarized quasi monochromatic wave with a mean optical frequency  $\langle \omega \rangle$ . We can write the magnitude of its electric field, at point  $\mathbf{r}$  and time  $t$ , in the form:

$$E(\mathbf{r}, t) = A(\mathbf{r}, t) \exp(j \langle \omega \rangle t) \quad (1)$$

where  $A(\mathbf{r}, t)$ , the complex amplitude of electric field, varies slowly over an optical period, i.e.

$$\left| \frac{1}{A} \frac{\partial A}{\partial t} \right| \ll \langle \omega \rangle \quad (2)$$

For a stationary and **ergodic** field, the ensemble average  $\Gamma^{(1)} = \langle E(\mathbf{r}_1, t_1) E^*(\mathbf{r}_2, t_2) \rangle$  depends solely on the time difference  $\tau = t_2 - t_1$  and can be calculated by taking the time average as:

$$\Gamma^{(1)}(\mathbf{r}_1, \mathbf{r}_2, \tau) = \lim_{T \rightarrow \infty} \frac{1}{T} \int_0^T E(\mathbf{r}_1, t + \tau) E^*(\mathbf{r}_2, t) dt \quad (3)$$

Substituting Eq.(1) into Eq.(3) yields:

$$\Gamma^{(1)}(\mathbf{r}_1, \mathbf{r}_2, \tau) = \Theta(\tau) \exp[j \langle \omega \rangle \tau] \quad (4)$$

In Eq.(4), we have set:

$$\Theta(\tau) = \frac{1}{T} \lim_{T \rightarrow \infty} \int_0^T A(\mathbf{r}_1, t + \tau) A^*(\mathbf{r}_2, t) dt \quad (5)$$

and, for the sake of simplicity, we have not indicated explicitly the dependence of  $\Theta$  on the spatial variables  $\mathbf{r}_1$  and  $\mathbf{r}_2$ . The complex degree of coherence [see, e.g., Eq.(11.3.8) of PL] is then given by:

$$\gamma^{(1)}(\tau) = \frac{\Gamma^{(1)}(\mathbf{r}_1, \mathbf{r}_2, \tau)}{\left[ \Gamma^{(1)}(\mathbf{r}_1, \mathbf{r}_1, 0) \Gamma^{(1)}(\mathbf{r}_2, \mathbf{r}_2, 0) \right]^{1/2}} = \varepsilon(\tau) \exp(j \langle \omega \rangle \tau) \quad (6)$$

where we have set:

$$\varepsilon(\tau) = \frac{\Theta(\mathbf{r}_1, \mathbf{r}_2, \tau)}{[\Theta(\mathbf{r}_1, \mathbf{r}_1, 0)\Theta(\mathbf{r}_2, \mathbf{r}_2, 0)]^{1/2}} \quad (7)$$

From Eq.(7), taking into account the definition of  $\Theta(\tau)$  [see Eq.(5)] and Eq.(2), it is an **easy** exercise to prove that  $\varepsilon(\tau)$  is a slowly-varying function of over one optical cycle. In fact, notice that the dependence of  $\varepsilon(\tau)$  on  $\tau$  is provided solely by the numerator of Eq.(7), i.e. by  $\Theta(\tau)$ . The value of  $\Theta$  at an incremental time delay  $\tau + \Delta\tau$ , with  $\omega\Delta\tau \ll 1$ , can be calculated from Eq.(5) by expanding the function  $A(t + \tau + \Delta\tau)$ , appearing under the sign of integral, in power series around  $t + \tau$ . Thus, at leading order,  $\Theta(\tau + \Delta\tau)$  equals  $\Theta(\tau)$ , i.e.  $\Theta(\tau)$  varies slowly over one optical cycle.

### 11.2A Measurement of the spatial coherence by a Young interferometer.

The visibility  $V_p$  of fringes is related to the first-order complex degree of coherence  $\gamma^{(1)}(\mathbf{r}_1, \mathbf{r}_2, 0)$  by the relation [see Eq.(11.3.12) of PL]:

$$V_p = \frac{2(\langle I_1 \rangle \langle I_2 \rangle)^{1/2}}{\langle I_1 \rangle + \langle I_2 \rangle} |\gamma^{(1)}(\mathbf{r}_1, \mathbf{r}_2, 0)| \quad (1)$$

where  $\langle I_1 \rangle$  and  $\langle I_2 \rangle$  are the average intensities measured on the screen when either one of the two holes is closed. If we set  $r = \langle I_1 \rangle / \langle I_2 \rangle$ , solving Eq.(1) with respect to  $\gamma^{(1)}$  yields:

$$|\gamma^{(1)}| = V_p \frac{1+r}{2\sqrt{r}} \quad (2)$$

For  $r=0.2$  and  $V_p=0.6$ , from Eq.(2) we obtain  $|\gamma^{(1)}| \approx 0.8$ .

### 11.3A Destroy of spatial coherence by rotation of a ground glass.

The expression for the instantaneous intensity of the interference field observed at a point P on a screen in a Young's interferometer is given by [see Eq.(11.3.17) of PL]:

$$I(t) = I_1(t + \tau) + I_1(t) + 2 |K_1 K_2| \operatorname{Re}[E(\mathbf{r}_1, t + \tau) E^*(\mathbf{r}_2, t)] \quad (1)$$

where:  $I_1$  and  $I_2$  are the instantaneous intensities at point P due to the emission from points  $P_1$  and  $P_2$  alone, respectively;  $\tau = (L_2/c) - (L_1/c)$  is the difference between time delays of light propagating from the two diffracting holes  $P_1$  and  $P_2$  to point P, respectively; c is the speed of light in vacuum; and  $K_1, K_2$  are the **diffraction** factors for the two holes. If we limit our attention to the case of a monochromatic wave at **frequency**  $\omega$  with perfect spatial and temporal coherence, **Eq.(1)** yields:

$$I = I_1 + I_2 + 2\sqrt{I_1 I_2} \cos(\omega\tau) \quad (2)$$

The last term in **Eq.(2)** is responsible for the occurrence of an interference pattern on the screen, i.e. of maxima and minima of the intensity I when the observation point P is varied on the screen. When a ground glass is placed before the two holes,  $E(\mathbf{r}_1, t+\tau)$  and  $E(\mathbf{r}_2, t)$  will acquire the phase shifts  $\phi_1$  and  $\phi_2$ , due to the thickness of the ground glass at points  $\mathbf{r}_1$  and  $\mathbf{r}_2$ , respectively. Instead of **Eq.(2)** we will now have:

$$I(t) = I_1 + I_2 + 2\sqrt{I_1 I_2} \cos(\omega\tau + \Delta\phi) \quad (3)$$

where  $\Delta\phi = \phi_1 - \phi_2$ . Since the thickness variation,  $\Delta L$ , of a ground glass is usually larger than the optical wavelength, the phase difference  $\Delta\phi = 2\pi n \Delta L / \lambda$ , where n is the glass refractive index, will be a random number between 0 and  $2\pi$ . If now the glass is put into rotation,  $\Delta\phi$  will become a random function of time. As a consequence, the intensity pattern observed on the screen (e.g., position of maxima and minima) will change in a random fashion in time. For an observation time longer than the period of rotation, it then turns out that the interference pattern is completely washed out and a uniform intensity pattern is observed.

#### 11.4A Comparison of temporal coherence between a thermal source and a laser.

For a non-monochromatic radiation, the temporal coherence length  $L_{co}$  is given by:

$$L_{co} = c\tau_{co} \quad (1)$$

where  $\tau_{co}$ , the coherence time, is related to the spectral bandwidth  $\Delta\nu$  of the radiation by:

$$\tau_{co} \cong \frac{1}{\Delta\nu} \quad (2)$$

For a near monochromatic radiation, with central wavelength  $\lambda_0$  and bandwidth  $\Delta\lambda$  ( $\Delta\lambda \ll \lambda_0$ ), one has  $\Delta\nu = |\Delta(c/\lambda)| \approx (c/\lambda_0^2)\Delta\lambda$ , so that from Eq.(2) one has:

$$\tau_{co} \approx \frac{\lambda_0^2}{c\Delta\lambda} \quad (3)$$

Substitution of Eq.(3) into Eq.(1) yields:

$$L_{co} \approx \frac{\lambda_0^2}{\Delta\lambda} \quad (4)$$

For the mercury vapor lamp, one has  $\lambda_0=546$  nm and  $\Delta\lambda=0.01$  nm, so that from Eq.(4) it follows that:

$$L_{co} \approx \frac{546^2 \text{ nm}^2}{0.01 \text{ nm}} = 2.98 \text{ cm} \quad (5)$$

For the Nd:YAG laser, one has  $\Delta\nu \approx 10$  kHz and hence, from Eqs.(1) and (2), one has 1 ms and  $L_{co} \approx c\tau_{co} = 3 \times 10^4 \text{ m} = 30 \text{ km}$ !

### 11.5A Temporal coherence of white light.

The bandwidth of the white light can be calculated as

$$\Delta\nu = \left( \frac{c}{\lambda_2} - \frac{c}{\lambda_1} \right) \approx 3.2 \times 10^{14} \text{ s}^{-1} \quad (1)$$

where  $\lambda_2=700$  nm and  $\lambda_1=400$  nm are the wavelengths at the boundary of the white spectrum. The coherence time is hence  $\tau_{co} \approx 1/\Delta\nu \approx 3 \times 10^{-15}$  s. The coherence length is then given by [see also Eq.(4) of Problem P11.4]:

$$L_{co} = c\tau_{co} \approx 933 \text{ nm} \quad (2)$$

which is of the same order as the optical wavelength.

### 11.6A Relation between first-order degree of temporal coherence and fringe visibility in a Michelson interferometer.

$$\tau_{co} \approx 0.$$

Let us consider the Michelson interferometer, shown in Fig.11.4 of PL, and assume that the incoming beam is split by a 50% beam splitter ( $S_1$ ) into two beams of equal intensity. These beams are then reflected by the two 100%-

reflectivity mirrors ( $S_2$  and  $S_3$ ) and, after partial transmission through the beam splitter  $S_1$ , they interfere in C. The electric field in a section of path C can be thus written as:

$$E(t) = K_1 E\left(t - \frac{2L_2}{c}\right) + K_2 E\left(t - \frac{2L_3}{c}\right) \quad (1)$$

where  $L_2$  and  $L_3$  are the optical lengths of the two arms of the interferometer as taken from an initial reference plane, and  $K_1$ ,  $K_2$  are complex coefficients that account for reflection and transmission at the beam splitter  $S_1$  and mirrors  $S_2$  and  $S_3$ . For a 50% reflectivity beam splitter, we can take  $|K_1|=|K_2|$  and, without loss of generality, we may assume  $K_1$  and  $K_2$  real-valued. Notice that a nonvanishing phase difference between  $K_1$  and  $K_2$  would lead merely to a shift of the interference fringes. The intensity of the interfering beam is then given by:

$$I = E(t)E^*(t) = I_0\left(t - \frac{2L_2}{c}\right) + I_0\left(t - \frac{2L_3}{c}\right) + 2K^2 \operatorname{Re}\left[E^*\left(t - \frac{2L_2}{c}\right)E\left(t - \frac{2L_3}{c}\right)\right] \quad (2)$$

where  $K=K_1=K_2$  and  $I_0(t)=K^2E(t)E^*(t)$ . If we take the time average of both sides in Eq.(2) and assume stationary fields, we obtain:

$$\langle I \rangle = 2 \langle I_0 \rangle + 2 \langle I_0 \rangle \operatorname{Re} \left[ \frac{\langle E\left(t - \frac{2L_3}{c}\right)E^*\left(t - \frac{2L_2}{c}\right) \rangle}{\langle E(t)E^*(t) \rangle} \right] \quad (3)$$

We now recognize that the expression in the square brackets on the right hand side of Eq.(3) is equal to the first-order temporal degree of coherence, i.e.

$$\gamma^{(1)}(\tau) = \frac{\langle E\left(t - \frac{2L_3}{c}\right)E^*\left(t - \frac{2L_2}{c}\right) \rangle}{\langle E(t)E^*(t) \rangle} \quad (4)$$

where  $\tau=2(L_3/c-L_2/c)$  is the time delay experienced by the two beams in the interferometer. For a quasi-monochromatic wave the complex degree of coherence can be written as:

$$\gamma^{(1)}(\tau) = |\gamma^{(1)}(\tau)| \exp[j\omega\tau - j\psi(\tau)] \quad (5)$$

where  $|\gamma^{(1)}(\tau)|$  and  $\psi(\tau)$  are slowly varying functions of  $\tau$  as compared to  $\exp(j\omega\tau)$ , the exponential term. After substitution of Eq.(4) into Eq.(3) and using Eq.(5), we finally obtain:

$$\langle I \rangle = 2 \langle I_0 \rangle \left[ 1 + |\gamma^{(1)}(\tau)| \cos(\omega\tau - \psi) \right] \quad (6)$$

**Notice** that, since both  $|\gamma^{(1)}(\tau)|$  and  $\psi(\tau)$  are slowly varying function of  $\tau$ , the modulation of  $\langle I \rangle$  corresponding to the variations in length of an interferometer arm is due primarily to the  $\omega\tau$  term in the argument of the cosine function. Therefore the local values of minima and maxima of  $\langle I \rangle$ , observed when one arm of the interferometer is changed, are given by

$$\langle I \rangle_{\max} = 2 \langle I_0 \rangle \left[ 1 + |\gamma^{(1)}(\tau)| \right] \quad (7a)$$

$$\langle I \rangle_{\min} = 2 \langle I_0 \rangle \left[ 1 - |\gamma^{(1)}(\tau)| \right] \quad (7b)$$

The visibility of the interferometer fringes is defined by:

$$V_p = \frac{\langle I_{\max} \rangle - \langle I_{\min} \rangle}{\langle I_{\max} \rangle + \langle I_{\min} \rangle} \quad (8)$$

Substitution of Eqs.(7a) and (7b) into Eq.(8) then yields:

$$V_p = |\gamma^{(1)}(\tau)| \quad (9)$$

### 11.7A Degree of temporal coherence for a low-pressure discharge lamp.

From the text of the problem we know that the power spectrum  $W(\omega)$  of the electric field  $E(t)$  emitted by the low-pressure discharge lamp is given by:

$$W(\omega) = \exp \left[ - \left( 2\sqrt{\ln 2} \frac{\omega - \omega_0}{\Delta\omega_0} \right)^2 \right] \quad (1)$$

where  $\omega_0$  is the central frequency of the light and  $\Delta\omega_0$  is the FWHM of the spectrum. For the Wiener-Kintchine theorem, the power spectrum of the electric field  $E(t)$  is equal to the Fourier transform of the autocorrelation function  $I^{(1)}(\tau) = \langle E(t+\tau) E^*(t) \rangle$ , i.e.:

$$I^{(1)}(\tau) = \int_{-\infty}^{\infty} W(\omega) \exp(j\omega\tau) d\omega \quad (2)$$

If we substitute Eq.(1) into Eq.(2) we obtain:

$$\Gamma^{(1)}(\tau) = \int_{-\infty}^{\infty} \exp \left[ - \left( 2\sqrt{\ln 2} \frac{\omega - \omega_0}{\Delta\omega_0} \right)^2 + j\omega\tau \right] d\omega \quad (3)$$

To calculate the integral on the right hand side in Eq.(3), we make the change of variables  $\omega' = \omega - \omega_0$ . Equation (3) can then be written as:

$$\Gamma^{(1)}(\tau) = \exp(j\omega_0\tau) \int_{-\infty}^{\infty} \exp(-\alpha\omega'^2 + \beta\omega') d\omega' \quad (4)$$

where we have set:

$$\alpha = \left( \frac{2\sqrt{\ln 2}}{\Delta\omega_0} \right)^2 \quad (5a)$$

$$\beta = j\tau \quad (5b)$$

Taking into account that [see, for instance, the solution to the Problem 4.9A]:

$$\int_{-\infty}^{\infty} \exp(-\alpha x^2 + \beta x) dx = \sqrt{\frac{\pi}{\alpha}} \exp\left(\frac{\beta^2}{4\alpha}\right) \quad (6)$$

from Eqs.(4) and (5) we obtain:

$$\Gamma^{(1)}(\tau) = e^{-j\omega_0\tau} \frac{\sqrt{\pi\Delta\omega_0}}{2\sqrt{\ln 2}} \exp\left[-\frac{\tau^2}{4(2\sqrt{\ln 2}/\Delta\omega_0)^2}\right] \quad (7)$$

After normalization, the complex degree of temporal coherence  $\gamma^{(1)}(\tau)$  is then given by:

$$\gamma^{(1)}(\tau) = \frac{\Gamma^{(1)}(\tau)}{\Gamma^{(1)}(0)} = \exp(j\omega_0\tau) \exp\left[-\frac{\tau^2}{4(2\sqrt{\ln 2}/\Delta\omega_0)^2}\right] \quad (8)$$

If we define the coherence time  $\tau_{\text{co}}$  as the HWHM of the magnitude of  $|\gamma^{(1)}(\tau)|$ , from Eq.(8) one readily follows that:

$$\tau_{\text{co}} = \frac{4\ln 2}{\Delta\omega_0} \quad (9)$$

Notice that, according to the general relation between **temporal** coherence and monochromaticity, the coherence time  $\tau_{\text{co}}$  turns out to be inversely proportional to the spectral bandwidth. The **particular** value of the proportionality factor appearing on the right hand side in Eq.(9) depends upon the particular definition of  $\tau_{\text{co}}$  and  $\Delta\omega_0$  adopted in the problem.

### 11.8A Temporal coherence of a gas laser oscillating on N axial modes.

Owing to the **Wiener-Kintchine** theorem, the power spectral density  $S(\nu)$  is given by the Fourier transform of the autocorrelation function  $\Gamma^{(1)}(\tau) = \langle E(t+\tau)E^*(t) \rangle$ , and hence:

$$\Gamma^{(1)}(\tau) = \int_{-\infty}^{\infty} S(\nu) \exp(2\pi j\nu\tau) d\nu \quad (1)$$

For a **gas** laser oscillating on  $(2N+1)$  modes, we have:

$$S(\nu) = \frac{1}{2N+1} \sum_{n=-N}^N \delta(\nu - \nu_0 + n\Delta\nu) \quad (2)$$

where  $\nu_0$  is the frequency of the central mode and  $\Delta\nu$  is the frequency separation between two consecutive axial modes. Substituting Eq.(2) into Eq.(1) and taking into account the well-known property of the  **$\delta$ -function**,

$$\int_{-\infty}^{\infty} \delta(\nu - a) f(\nu) d\nu = f(a) \quad (3)$$

one obtains:

$$\Gamma^{(1)}(\tau) = \frac{1}{2N+1} \sum_{n=-N}^N \exp[2\pi j(\nu_0 - n\Delta\nu)\tau] \quad (4)$$

The sum on the right hand side in Eq.(4), which is analogous to that found, e.g., in the theory of mode-locking [see Sec. 8.6.1 of PL], can be reduced to that of a geometric progression of argument  $a = \exp(-2\pi j\Delta\nu\tau)$  after setting  $l = n+N$ . This yields:

$$\sum_{n=-N}^N \exp[2\pi j(\nu_0 - n\Delta\nu)\tau] = \exp(2\pi j\nu_0\tau) \frac{\sin[(2N+1)\pi\Delta\nu\tau]}{\sin(\pi\Delta\nu\tau)} \quad (5)$$

Substitution of Eq.(5) into Eq.(4) yields:

$$\Gamma^{(1)}(\tau) = \exp(2\pi j\nu_0\tau) \frac{\sin[(2N+1)\pi\Delta\nu\tau]}{(2N+1)\sin(\pi\Delta\nu\tau)} \quad (6)$$

The complex degree of coherence  $\gamma^{(1)}(\tau)$  is then given by:

$$\gamma^{(1)}(\tau) = \frac{\langle E(t+\tau)E^*(t) \rangle}{\langle E(t)E^*(t) \rangle} = \frac{\Gamma^{(1)}(\tau)}{\Gamma^{(1)}(0)} = \exp(2\pi j\nu_0\tau) \frac{\sin[(2N+1)\pi\Delta\nu\tau]}{(2N+1)\sin(\pi\Delta\nu\tau)} \quad (7)$$

where we have used the relation  $I^{(1)}(0)=1$ , which can be readily obtained by taking the limit of  $I^{(1)}(\tau)$ , given by Eq.(6), for  $\tau \rightarrow 0$ . According to the result of Problem 11.1P, the complex degree of coherence  $\gamma^{(1)}(\tau)$  is seen to be given by the product of the fast oscillating exponential term  $\exp(2\pi j v_0 \tau)$  with a slowly-varying envelope, given by:

$$|\gamma^{(1)}(\tau)| = \left| \frac{\sin[(2N+1)\pi\Delta\nu\tau]}{(2N+1)\sin(\pi\Delta\nu\tau)} \right| \quad (8)$$

### 11.9A An interference experiment with partially coherent light.

When the observation point is equally distant from the two pin-holes, the visibility of fringes  $V_p$  coincides with the magnitude of the complex degree of spatial coherence,  $|\gamma^{(1)}(\mathbf{r}_1, \mathbf{r}_2, 0)|$ , where  $\mathbf{r}_1$  and  $\mathbf{r}_2$  are the coordinates of the centers of the two holes. In order to calculate the degree of spatial coherence, one has to resort to the Van Cittert-Zernike theorem, which provides an expression of the spatial degree of coherence of a quasi-monochromatic beam emitted from an incoherent source. Observation is made in the far-field plane of an aperture of the same dimensions of the source. In particular, for the diffraction pattern from a circular aperture of diameter  $d$ , observed at a distance  $L$  from the aperture, it turns out that  $|\gamma^{(1)}(\mathbf{r}_1, \mathbf{r}_2, 0)|=0.8$  when the distance  $s=|\mathbf{r}_1 - \mathbf{r}_2|$  between the points  $\mathbf{r}_1$  and  $\mathbf{r}_2$  symmetrically located compared to the beam center is given by [see Eq.(11.3.43) of PL]:

$$s \cong 0.16 \frac{\lambda L}{d} \quad (1)$$

For  $\lambda=546.1$  nm,  $L=3$  m and  $d=0.1$  mm, from Eq.(1) one obtains  $s \cong 2.6$  mm.

### 11.10A Spatial coherence of the light from the sun.

The light emitted by a spatially incoherent source, such as the sun, acquires a partial degree of coherence during propagation. In particular, according to the Van Cittert-Zernike theorem, if  $d$  is the diameter of the sun,  $z$  the distance of the earth from the sun, and  $\lambda$  the mean wavelength of the light, the spatial degree of coherence on the earth assumes a value of 0.88 for a linear distance  $r$  given [see Eq.(11.3.43) of PL]:

$$r \cong 0.16 \left( \frac{\lambda z}{d} \right) \quad (1)$$

For  $\lambda=550$  nm,  $d=13.92 \times 10^8$  m,  $z=1.5 \times 10^{11}$  m, from Eq.(1) one obtains  $r \approx 0.01$  mm.

### 11.11A An astronomic calculation based on spatial coherence of stellar radiation.

Indicating by  $\theta$  the angle subtended by the star at the earth, one has  $\theta \approx d/z$ , where  $z$  is the distance between star and earth and  $d$  is the star diameter. For  $\gamma(1)=0.88$ , we have from Eq.(11.3.43) of PL:

$$\theta = \frac{d}{z} \approx 0.16 \frac{\lambda}{r} \quad (1)$$

where  $r$  is the distance between two points on earth and  $A$  is the wavelength of the radiation which has been considered. For  $\lambda=550$  nm and  $r=80$  cm, from Eq.(1) one readily obtains  $\theta \approx 1.1 \times 10^{-7}$  rad.

### 11.12A Beam divergence of a partially-coherent laser beam.

The divergence  $\theta'_d$  of a diffraction-limited beam with constant amplitude over a circular area with diameter  $D$  is given by Eq.(11.4.6) of PL, i.e.:

$$\theta'_d = 1.22 \frac{\lambda}{D} \quad (1)$$

where  $\lambda$  is the laser wavelength. For the Nd:YAG laser, one has  $\lambda=1064$  nm, and hence from Eq.(1) with  $D=6$  mm one obtains  $\theta'_d \approx 0.216$  mrad. Since  $\theta_d$  is larger than  $\theta'_d$  (about 14 times), the beam is not diffraction-limited. The diameter  $D_c$  of coherence area can be estimated from Eq.(11.4.9) of PL as:

$$D_c = \frac{\beta \lambda}{\theta_d} \quad (2)$$

where  $\beta$  is a numerical factor, of the order of unity, whose value depends upon how  $\theta_d$  and  $D_c$  are precisely defined. If we assume, for instance,  $\beta=2/\pi$ , which applies to a Gaussian beam [see Eq.(11.4.7) of PL], we obtain:

$$D_c \approx \frac{2\lambda}{\pi \theta_d} \approx 226 \mu\text{m} \quad (3)$$

If the beam is passed through the attenuator, the beam intensity profile just after the attenuator has a Gaussian shape with a spot size  $w_0$ . However, the beam is not Gaussian because it is not **diffraction** limited: a simple attenuation cannot change its spatial coherence and hence the divergence  $\theta_d$  of the beam, which remains equal to  $\approx 3$  mrad. For comparison, the divergence of a diffraction-limited Gaussian beam with spot size  $w_0=0.5$  mm would be:

$$\theta_d = \frac{\lambda}{\pi w_0} \approx 0.68 \text{ mrad} \quad (4)$$

### 11.13A Focusing of a perfectly-coherent spatial beam.

The diffraction pattern produced in the focal plane of a lens by a beam with uniform amplitude distribution over a circular cross-section is given by the Airy formula [see Eq.(11.4.3) of PL]:

$$I_f(r) = I_0 \left[ \frac{2\pi J_1\left(\frac{\pi r D}{\lambda f}\right)}{\frac{\pi r D}{\lambda f}} \right]^2 \quad (1)$$

where  $J_1$  is the Bessel function of first order,  $\lambda$  is the beam wavelength,  $f$  is the focal length of the focusing lens,  $D$  the beam diameter, and  $r$  the radial coordinate in the focal plane. Taking into account that, at  $r \rightarrow 0$ , the expression in the brackets of Eq.(1) tends to unity, we recognize that  $I_0$  is the beam intensity at the center of the diffraction pattern, i.e. for  $r=0$ . In order to calculate the ratio  $I_0/I_i$  between the focused beam intensity  $I_0$  and the intensity  $I_i$  of the incoming uniform beam, let us observe that the optical power  $P_i$  for an input beam of uniform intensity over a diameter  $D$  is obviously given by:

$$P_i = \frac{\pi D^2}{4} I_i \quad (2)$$

On the other hand, neglecting power losses due to absorption and diffraction at the lens, one can calculate  $P_i$  by integration of the intensity distribution in the focal plane, i.e.

$$P_i = 2\pi \int_0^\infty I_f(r) r dr \quad (3)$$

Using **Eq.(1)**, the integral on the right hand side in **Eq.(3)** can be calculated in a closed form, and the result is expressed by **Eq.(11.4.4)** of PL, i.e.:

$$P_i = I_0 \left( \frac{4\lambda^2 f^2}{\pi D^2} \right) \quad (4)$$

A comparison of **Eqs.(2)** and (4) then yields:

$$\frac{I_0}{I_i} = \left( \frac{\pi D^2}{4\lambda f} \right)^2 = (N.A.)^4 \left( \frac{\pi f}{4\lambda} \right)^2 \quad (5)$$

where  $N.A.=D/f$  is the lens **numerical aperture**. As an example, assuming  $N.A.=0.5$ ,  $\lambda=1064$  nm and  $f=10$  cm, one gets from **Eq.(5)** ( $I_0/I_i) \approx 3.4 \times 10^8$ .

### 11.14A $M^2$ factor of a Nd:YAG laser.

The divergence for a multimode laser beam is given by **Eq.(11.4.20)** of PL, which reads:

$$\theta_d = M^2 \frac{\lambda}{\pi w_0} \quad (1)$$

For a Gaussian beam,  $w_0$  is the spot size at the beam waist, defined as the half-width at 1/e of the amplitude of electric field distribution at the plane of beam waist,  $\theta_d$  is the half-angle at 1/e of the far-field **distribution**, and  $M^2$  is the  $M^2$ -factor of the beam. If  $D$  and  $\theta_d'$  are the beam diameter and the **half-cone** of beam divergence measured by taking the FWHM of the Gaussian beam intensity at the plane of the beam waist and in the far-field plane, respectively, one has  $D=w_0(2 \ln 2)^{1/2}$  and  $\theta_d'=(2 \ln 2)^{1/2} \theta_d/2$ . From **Eq.(1)** we then obtain:

$$M^2 = \frac{\pi w_0 \theta_d}{\lambda} = \frac{\pi w_0 \theta_d'}{\lambda \ln 2} \quad (2)$$

For  $D=4$  mm,  $\lambda=1064$  nm and  $\theta_d'=3$  mrad, from **Eq.(2)** we obtain  $M^2 \approx 51$ .

### 11.15A Brightness of a high-power CO<sub>2</sub> laser.

The brightness of a laser source, defined as the power emitted by the laser per unit of beam area and emission solid angle, is given by [see **Eq.(11.6.1)** of PL]:

$$B = \frac{4P}{\lambda^2} \quad (1)$$

where  $P$  is the laser power and  $\lambda$  the laser wavelength. For  $P=1 \text{ kW}$  and  $\lambda=10.6 \mu\text{m}$ , we then obtain  $B \approx 3.56 \times 10^9 \text{ W/cm}^2 \times \text{sr}$ . The beam spot size  $w_1$  produced at the focal plane of a lens with focal length  $f$  is given by:

$$w_1 \approx f\theta_d = f \frac{\lambda}{\pi w_0} \quad (2)$$

where  $\theta_d = \lambda/\pi w_0$  is the beam divergence and  $w_0$  the beam waist. If we denote by  $I_0$  the laser peak intensity in the focal plane, one has:

$$P = 2\pi \int_0^\infty I_0 r \exp\left(-\frac{2r^2}{w_1^2}\right) = \frac{\pi w_1^2}{2} I_0 \quad (3)$$

If we substitute the expression of  $w_1$  given by Eq.(2) into Eq.(3) and solving the resulting equation with respect to  $I_0$ , we finally obtain:

$$I_0 = \frac{2\pi P w_0^2}{f^2 \lambda^2} \quad (4)$$

For  $P=1 \text{ kW}$ ,  $w_0=1 \text{ cm}$ ,  $f=20 \text{ cm}$  and  $\lambda=10.6 \mu\text{m}$ , from Eq.(4) one has  $I_0 \approx 14 \text{ MW/cm}^2$ .

### 11.16A Grain size of the speckle pattern as observed on a screen.

An approximate expression for the grain size  $d_g$  of the scattered light observed on a screen at distance  $L$  from the diffuser is given by [see Eq.(11.5.2) of PL]:

$$d_g \approx \frac{2\lambda L}{D} \quad (1)$$

where  $\lambda$  is the laser wavelength and  $D$  the beam diameter. For  $\lambda=632 \text{ nm}$ ,  $D=0.5 \text{ cm}$  and  $d_g=0.6 \text{ mm}$ , from Eq.(1) we then obtain:

$$L \approx \frac{D d_g}{2\lambda} = \frac{0.5 \text{ cm} \times 0.6 \text{ mm}}{2 \times 632 \times 10^{-6} \text{ mm}} \approx 237 \text{ cm} \quad (2)$$

### 11.17A Grain size of the speckle pattern as seen by a human observer.

If we assume that the whole aperture  $D'$  of eye pupil is illuminated by light diffracted by each individual **scatterer**, we can estimate the apparent grain size of the speckle pattern as seen by the **human** observer as [see Eq.(11.5.4) of PL]:

$$d_{\text{ag}} = \frac{2\lambda L}{D'} \quad (1)$$

where  $L$  is the distance between the scattering surface and the human eye. For  $L=237 \text{ cm}$ ,  $D'=1.8 \text{ mm}$  and  $\lambda=632 \text{ nm}$ , from Eq.(1) one obtains  $d_{\text{ag}} \approx 1.7 \text{ mm}$ .

### 11.18A Correlation function and power spectrum of a single-longitudinal mode laser.

The **first-order** correlation **function** for the electric field  $E(t)=A \exp[j\omega_0 t + j\varphi(t)]$  with constant amplitude  $A$  is readily calculated as:

$$\Gamma^{(1)}(\tau) = \langle E(t + \tau) E^*(t) \rangle = |A|^2 \exp(j\omega_0 \tau) \langle \exp(j\Delta\varphi) \rangle \quad (1)$$

where we have set:

$$\Delta\varphi = \varphi(t + \tau) - \varphi(t) \quad (2)$$

If we assume that the phase difference  $\Delta\varphi$  undergoes a phase **diffusion** process (random walk),  $\Delta\varphi$  is a Gaussian stationary process with a first-order probability density given by:

$$f(\Delta\varphi) = \frac{1}{(4\pi |\tau|/\tau_c)^{1/2}} \exp\left(-\frac{\tau_c \Delta\varphi^2}{4|\tau|}\right) \quad (3)$$

The ensemble average appearing on the right-hand-side in Eq.(1) can be thus calculated as:

$$\langle \exp(j\Delta\varphi) \rangle = \int_{-\infty}^{\infty} f(\Delta\varphi) \exp(-j\Delta\varphi) d\Delta\varphi \quad (4)$$

The integral on the right hand-side in Eq.(4) is a generalized Gaussian integral which can be calculated analytically in a closed form [see, e.g., Eq.(6) in the solution of Problem 11.7]. After integration one obtains:

$$\langle \exp(j\Delta\phi) \rangle = \exp\left(-\frac{|\tau|}{\tau_c}\right) \quad (5)$$

Substituting Eq.(5) into Eq.(1) leads to the following expression for the first-order correlation function:

$$\Gamma^{(1)}(\tau) = |A|^2 \exp(j\omega_0\tau) \exp(-|\tau|/\tau_c) \quad (6)$$

The power spectrum of the laser field can be calculated as the Fourier transform of the autocorrelation function  $\Gamma^{(1)}$ . We then have:

$$\begin{aligned} S(\nu) &= \int_{-\infty}^{\infty} \exp(-2\pi j\nu\tau) \Gamma^{(1)}(\tau) d\tau = |A|^2 \int_{-\infty}^{\infty} \exp[-2\pi j(\nu - \nu_0)\tau] \exp(-|\tau|/\tau_c) d\tau = \\ &= 2|A|^2 \operatorname{Re} \left\{ \int_0^{\infty} \exp[-2\pi j(\nu - \nu_0)\tau] \exp(-\tau/\tau_c) d\tau \right\} = \frac{2|A|^2}{\tau_c \left[ \frac{1}{\tau_c^2} + 4\pi^2(\nu - \nu_0)^2 \right]} \end{aligned} \quad (7)$$

where we have set  $\nu_0 = \omega_0/2\pi$ . The power spectrum of the laser field is thus lorentzian with a FWHM given by  $\Delta\nu = 1/\pi\tau_c$ .



## CHAPTER 12

# Laser Beam Transformation: Propagation, Amplification, Frequency Conversion, Pulse Compression, and Pulse Expansion

## PROBLEMS

### 12.1P Propagation of a multimode beam.

The multimode beam of a **Nd:YAG** laser ( $\lambda \approx 1.06 \mu\text{m}$ ) with an output power of 5 W is sent to a target at a distance of 10 m from the beam waist. Assuming that the near-field transverse intensity profile is, to a good approximation, Gaussian with a diameter (FWHM) of  $D = 5 \text{ mm}$  and that the  $M^2$  factor can be taken as  $M^2 \approx 40$ , calculate the spot size parameter and the radius of curvature of the phase front at the target position.

### 12.2P Amplification of long pulses by a **Nd:YAG** amplifier.

The output of a Q-switched **Nd:YAG** laser ( $E = 100 \text{ mJ}$ ,  $\tau_p = 20 \text{ ns}$ ) is amplified by a 6.3-mm diameter **Nd:YAG** amplifier having a small signal gain of  $G_0 = 100$ . Assume that: (a) the lifetime of the lower level of the transition is much shorter than  $\tau_p$ ; (b) the beam transverse intensity profile is uniform; (c) the effective peak cross section for stimulated emission is  $\sigma \approx 2.6 \times 10^{-19} \text{ cm}^2$ . Calculate the energy of the amplified **pulse**, the corresponding amplification, and the fraction of the energy stored in the amplifier that is extracted by the incident pulse.

### 12.3P Amplification of short pulses by a **Nd:YAG** amplifier.

Referring to Problem 12.2, assume now that the input pulse duration is much shorter than the lifetime  $\tau_l$  of the lower laser level ( $\tau_l \approx 100 \text{ ps}$ ). Assume that: (a)

the peak cross section of the  $^4F_{3/2} \rightarrow ^4I_{1/2}$  transition is  $\sigma_{23} \approx 6.5 \times 10^{-19} \text{ cm}^2$ ; (b) the fractional **population** of the lower laser sublevel of the  $^4I_{1/2}$  state is  $f_{13} \approx 0.187$ ; (c) the **fractional** population of the upper laser sublevel of the  $^4F_{3/2}$  state is  $f_{22} \approx 0.4$ . Calculate the energy of the amplified pulse and the corresponding amplification.

### 12.4P Extraction efficiency of a two-pass amplifier.

The output of a **Nd:YAG** laser ( $E_0 = 50 \text{ mJ}$ ,  $\tau_p = 50 \text{ ns}$ ) is amplified in a **5.6-mm** diameter **Nd:YAG** amplifier, in a two-pass configuration. The small signal gain for the first pass is  $G_0 = 4.8$ . Assume that: (a) the lifetime of the lower level of the transition is much shorter than  $\tau_p$ ; (b) the **beam** transverse intensity profile is uniform; (c) the effective peak cross section for stimulated emission is  $\sigma \approx 2.6 \times 10^{-19} \text{ cm}^2$ . Calculate the extraction **efficiency** of the double-pass **amplifier**.

[Hint: The unsaturated gain **coefficient**,  $g'$ , for the second pass is given by  $g' = g(1 - \eta_1)$ , where  $g$  and  $\eta_1$  are the gain coefficient and the extraction efficiency of the first pass, respectively].

### 12.5P Saturation fluence in a quasi-three-level amplifier.

Show **that**, in an amplifier medium working on a quasi-three-level scheme, the rate of change of population inversion can be written in the same way as for a four-level amplifier provided that the saturation energy fluence  $\Gamma_s$  is expressed as  $\Gamma_s = h\nu / (\sigma_e + \sigma_a)$ , where  $\sigma_e$  and  $\sigma_a$  are the emission and absorption cross section of the transition.

### 12.6P Maximum output fluence from an amplifier with losses.

If amplifier losses cannot be neglected the output fluence  $\Gamma(l)$  does not continue increasing with input fluence but it is limited to a maximum value  $\Gamma_m$ . Show that  $\Gamma_m \approx g\Gamma_s/\alpha$ , where:  $g$  is the unsaturated gain coefficient of the amplifier;  $\alpha$  is the absorption coefficient;  $\Gamma_s$  is the saturation fluence.

[Hint: in Eq.(12.3.11) of PL assume  $\exp(-l\Gamma_s) \approx 0$ ].

### **12.7P Theoretical limit to the maximum intensity of an amplifier.**

Show that the **maximum** focused intensity which can be obtained from a **gain** material of area S is limited to  $I_{\max} \approx (h\nu^3 \Delta\nu_0 S / \sigma^2)$ , where  $\sigma$  is the emission cross section at frequency  $\nu$  and  $\Delta\nu_0$  is the fluorescence bandwidth.

[Hints: For efficient energy extraction from an amplifier one **must** work near saturation. Consider the relationship between the **minimum** pulse duration and the fluorescence bandwidth. Then consider that the **beam** size at focus is limited by the wavelength].

### **12.8P Index of refraction of an extraordinary wave in a uniaxial crystal.**

A uniaxial crystal has  $n_o=1.5$  and  $n_e=2$ , where  $n_o$  and  $n_e$  are the ordinary and extraordinary indices, respectively. Calculate the index of refraction of an **extraordinary** wave travelling in a direction making **an** angle of  $30^\circ$  with respect to the optic **axis** of the crystal.

### **12.9P Double refraction in a uniaxial crystal.**

A laser beam enters a **20-mm-thick** uniaxial crystal with **an** incidence angle of  $45^\circ$ . The input and output faces of the crystal are parallel to each other and are perpendicular to the optic axis. The ordinary and extraordinary indices of the crystal are:  $n_o=3$  and  $n_e=2$ . Calculate the lateral separation of the ordinary and extraordinary rays at the output face of the crystal.

### **12.10P Second harmonic conversion of a Ti:sapphire laser in a BBO crystal.**

The frequency of a **Ti:sapphire** laser beam ( $\lambda=780$  nm) is doubled in a BBO crystal. The refractive indices of the crystal can be described by the following Sellmeier equations:

$$n_o^2 = 2.7405 + \frac{0.0184}{\lambda^2 - 0.0179} - 0.0155 \lambda^2$$

$$n_e^2 = 2.3730 + \frac{0.0128}{\lambda^2 - 0.0156} - 0.0044 \lambda^2$$

where the wavelength is in  $\mu\text{m}$ . Calculate the phase-matching angles for both type-I and type-II second harmonic generation.

[The calculation of the phase-matching angle in the case of type-II second harmonic generation requires a graphical solution]

### 12.11P Second harmonic conversion efficiency in a KDP crystal.

For type-I second harmonic generation and for an incident beam intensity of 100  $\text{MW/cm}^2$  at  $\lambda=1.06 \mu\text{m}$ , calculate the second harmonic conversion **efficiency** in a perfectly phase-matched **2.5-cm-long** KDP crystal (for KDP one has  $n \approx 1.5$ , and  $d_{\text{eff}} = d_{36} \sin \theta_m = 0.28 \times 10^{-12} \text{ m/V}$ , where  $\theta_m \approx 50^\circ$  is the phase-matching angle).

### 12.12P Second harmonic generation with a Gaussian beam.

Consider a Gaussian beam incident on a nonlinear crystal of length  $l$ . Show that, in the case of perfect phase matching ( $\Delta k=0$ ), the conversion efficiency,  $\eta$ , for second harmonic generation is given by:

$$\eta = \frac{P_{2\omega}(l)}{P_\omega(0)} = \frac{2}{\epsilon_0 c^3} \frac{\omega^2 d^2 l^2}{n^3} \frac{P_\omega(0)}{\pi w_0^2}$$

where:  $\omega$  is the laser fundamental frequency;  $l$  is the crystal length;  $P_\omega(0)$  is the input power;  $P_{2\omega}(l)$  is the output second harmonic power;  $d$  is the effective nonlinear coefficient;  $n$  is the refractive index ( $n_\omega = n_{2\omega} = n$ ) at phase-matching;  $w_0$  is the spot size at the beam waist. Assume that the beam Rayleigh range is much longer than crystal length so that the intensity is nearly independent of the propagation coordinate within the crystal.

[Hints: Express Eq.(12.4.55) of PL in terms of the intensities  $I_{2\omega}(l)$  and  $I_\omega(0)$ ; since  $z_R \gg l$  the beam intensity at the fundamental frequency within the crystal can be written as  $I_\omega(z, r) \approx I_0 \exp(-2r^2/w_0^2)$ . Then calculate the input and the second harmonic power].

(Level of **difficulty** higher than average)

### 12.13P Frequency doubling of a Gaussian beam in a KDP crystal.

Under optimum focusing condition, corresponding to a crystal length equal to the confocal **parameter**,  $b$ , of the beam ( $b=2 z_R$  where  $z_R$  is the **beam Rayleigh range**), the **second harmonic** conversion efficiency,  $\eta$ , of a Gaussian **beam** is given by:

$$\eta = \frac{P_{2\omega}(l)}{P_\omega(0)} \Big|_{l=2z_R} = \frac{2\omega^3 d^2 l}{\pi \epsilon_0 c^4 n^2} P_\omega(0)$$

where:  $\omega$  is the laser fundamental frequency;  $l$  is the crystal length;  $P_\omega(0)$  is the input power;  $P_{2\omega}(l)$  is the output second harmonic power;  $d$  is the effective nonlinear coefficient;  $n$  is the refractive index ( $n_\omega=n_{2\omega}=n$ ) at phase-matching. Calculate the second harmonic conversion **efficiency** in a perfectly phase-matched **2.5-cm-long** KDP crystal, for an incident Gaussian beam at  $\lambda=1.06 \mu\text{m}$  having a peak intensity of  $100 \text{ MW/cm}^2$  (for KDP one has  $n \approx 1.5$  and  $d_{\text{eff}}=0.28 \times 10^{-12} \text{ m/V}$ ).

### 12.14P Effective nonlinear coefficient of a KDP crystal.

Show that, in a crystal with  **$\bar{4}2m$**  point group **symmetry** (e.g., KDP) and type-I phase-matching, the effective nonlinear **coefficient**,  $d_{\text{eff}}$ , can be expressed as  $d_{\text{eff}} = -d_{36} \sin(2\phi) \sin\theta$ , where  $\theta$  is the angle between the propagation vector and the z-axis, and  $\phi$  is the angle that the projection of the propagation vector in the **x-y** plane makes with the x-axis of the crystal.

[**Hints:** For the  **$\bar{4}2m$**  point group symmetry only  $d_{14}$ ,  $d_{25}$  and  $d_{36}$  are nonzero, and these three d coefficients are equal. Write the electric field components along the x-, y- and z-axes. The nonlinear polarization along the i-axis is then given by  $P_i^{2\omega} = 2 \sum_{m=1}^6 \epsilon_0 d_{im}^{2\omega} (EE)_m$ . Assume **that** the effective polarization has the correct orientation to generate an extraordinary second harmonic beam. Finally, obtain  $d_{\text{eff}}$  from  $P(2\omega) = 2 \epsilon_0 d_{\text{eff}} E^2(\omega)$ .]

(Level of *difficulty* higher than average)

**12.15P Threshold pump intensity of an optical parametric oscillator.**

Calculate the threshold pump intensity for a doubly resonant and degenerate optical parametric oscillator consisting of a 5-cm-long  $\text{LiNbO}_3$  crystal pumped at  $\lambda_3=0.5 \mu\text{m}$  ( $\lambda_1=\lambda_2=1 \mu\text{m}$ ), using the following data:  $n_1=n_2=2.16$ ,  $n_3=2.24$ ,  $d=6\times 10^{-12} \text{ m/V}$ ,  $\gamma_1=\gamma_2=2\times 10^{-2}$ . If the pumping beam is focused in the crystal to a spot with a diameter of  $100 \mu\text{m}$ , calculate the resulting threshold pump power.

**12.16P Collinear parametric generation in a BBO crystal.**

Calculate the phase-matching angle for **collinear** parametric generation ( $\omega_3=\omega_1+\omega_2$ ) in a **BBO** crystal with type-I phase matching, considering a pump beam at wavelength  $\lambda_3=400 \text{ nm}$  and a signal beam at wavelength  $\lambda_1=560 \text{ nm}$ . The refractive indices of BBO can be described by the Sellmeier equations given in Problem 12.10. For beam propagation along a direction making an angle  $\theta$  with the **z-axis**, the extraordinary refractive index,  $n_3^e(\theta)$ , at wavelength  $\lambda_3$  can be expressed as [see Eq. (4) of 12.8A]:

$$n_3^e(\theta) = \frac{n_3^o n_3^e}{\sqrt{(n_3^o)^2 \sin^2 \theta + (n_3^e)^2 \cos^2 \theta}}$$

where  $n_3^o$  and  $n_3^e$  are the **ordinary** and extraordinary refractive indices, respectively.

Repeat the same calculation assuming  $\lambda_1=700 \text{ nm}$ .

[Hint: For type-I sum-frequency generation in a negative crystal an **ordinary** ray at  $\omega_1$  (signal) combines with an ordinary ray at  $\omega_2$  (idler) to generate an extraordinary ray at the sum frequency  $\omega_3=\omega_1+\omega_2$ ]

**12.17P Noncollinear parametric generation in a BBO crystal.**

Calculate the phase-matching angles for noncollinear parametric generation ( $\omega_3=\omega_1+\omega_2$ ) in a BBO crystal with type-I phase matching, considering a pump beam at wavelength  $\lambda_3=400 \text{ nm}$  and a signal beam at wavelengths  $\lambda_1=560 \text{ nm}$  and  $\lambda_2=700 \text{ nm}$ . Assume an angle  $\alpha=3.7^\circ$  between the extraordinary pump wave-vector and the ordinary signal wave-vector. The refractive indices of BBO can be described by the Sellmeier equations given in Problem 12.10.

Repeat the same calculation assuming  $\alpha=5^\circ$ .

[Hint: Write the vectorial phase-matching equation,  $\mathbf{k}_1 + \mathbf{k}_2 = \mathbf{k}_3$ , and consider the two equations obtained upon projection of this equation in the direction of  $\mathbf{k}_3$  and in the direction orthogonal to  $\mathbf{k}_3$ ]

### 12.18P Nonlinear index $n_2$ of sapphire.

The refractive index of a medium, taking into account both its linear and nonlinear component, can be written either as  $n = n_0 + n_2 I$ , where  $I$  is the beam intensity, or as  $n = n_0 + \bar{n}_2 |E|^2$ , where  $|E|$  is the electric field amplitude. Find the relationship between  $n_2$  and  $\bar{n}_2$ . Use this relationship to obtain the value of  $\bar{n}_2$  of sapphire, knowing that  $n_0 \approx 1.7$  and  $n_2 \approx 3.45 \times 10^{-16} \text{ cm}^2/\text{W}$ .

### 12.19P Pulse spectral broadening due to self-phase modulation in a Kerr medium.

Show that the maximum spectral broadening due to self-phase modulation in a Kerr medium of length  $L$  for a pulse whose intensity is changing in time as  $I(t) = I_0 \exp(-t^2/\tau_0^2)$  (Gaussian pulse) is given by:

$$\Delta\omega_{max} = \omega_{max} - \omega_0 \approx 0.86 \frac{n_2 \omega_0 L I_0}{c \tau_0}$$

where  $n_2$  is the coefficient of the nonlinear index of the medium and  $\omega_0$  is the central **frequency** of the pulse spectrum. In the calculation neglect the dispersion and the absorption of the Kerr medium, and assume a uniform profile of the **beam** intensity.

### 12.20P Spectral broadening of a 20-fs pulse in a hollow fiber filled with argon

Using the expression for  $\Delta\omega_{max}$  given in the previous problem, calculate the spectral broadening of a 20-fs,  $40\text{-}\mu\text{J}$  energy, Gaussian pulse at  $\lambda=800$  nm, propagating in a 60-cm-long hollow fiber with inner radius  $a=80\text{ }\mu\text{m}$ , filled with argon at a pressure of 0.4 bar. Assume an uniform beam intensity profile with an effective area given by  $A_{eff}=\pi w^2$ , where  $w=2a/3$  is the spot size of the laser beam

at the input face of the fiber (the nonlinear index of argon per unit pressure is  $n_2/p=9.8\times10^{-24}\text{ m}^2/(\text{W bar})$ ).

### 12.21P Group delay dispersion of a medium.

Show **that** the group delay dispersion (GDD) of a medium of length L and refractive index  $n(\lambda)$  is given by:  $\text{GDD}=\phi''=\frac{\lambda^3 L}{2\pi c^2} \frac{d^2 n(\lambda)}{d\lambda^2}$ , where  $\phi''=d^2\phi/d\omega^2$ .

### 12.22P Dispersion-induced broadening of a 10-fs pulse in a fused silica plate.

A 10-fs **unchirped** Gaussian pulse with central wavelength  $\lambda_0=800\text{ nm}$  enters a **1-mm-thick** fused silica plate. Assuming that the group delay dispersion of fused silica at 800 nm is  $36.16\text{ fs}^2$  calculate the pulse broadening at the output of the plate as due to dispersion.

[**Hint:** Pulse temporal broadening is given by  $\Delta\tau_d \approx \phi''(\omega_0) A\omega$ , where  $\Delta\omega$  is the pulse bandwidth (for a Gaussian pulse one has:  $\Delta\omega \tau_p = 2\pi 0.441$ , where  $\tau_p$  is the pulse duration)]

## ANSWERS

### 12.1A Propagation of a multimode beam.

For a Gaussian intensity profile,  $I(r) = I_0 \exp(-2r^2/W_0^2)$ , the spot size of the input beam is related to the diameter (FWHM) D, by the following relationship:

$$\exp(-D^2/2W_0^2) = 1/2 \quad (1)$$

which gives:

$$W_0 = D/(2 \ln 2)^{1/2} = 4.2 \text{ mm} \quad (2)$$

The spot size at the beam waist of the embedded Gaussian beam can be calculated as:

$$w_0 = W_0 / \sqrt{M^2} \cong 0.66 \text{ mm} \quad (3)$$

The corresponding **Rayleigh** range is given by:

$$z_R = \pi w_0^2 / \lambda = 1.29 \text{ m} \quad (4)$$

The spot size and the radius of curvature of the embedded Gaussian beam at the target position ( $l=10 \text{ m}$ ) are obtained, using Eqs. (4.7-17a-b) of PL, respectively as:

$$w(l) = w_0 [1 + (l/z_R)^2]^{1/2} = 5.16 \text{ mm} \quad (5a)$$

$$R(l) = l [1 + (z_R/l)^2] = 10.17 \text{ m} \quad (5b)$$

The wave-front radius of curvature of the multimode beam coincides with that of the embedded Gaussian beam. The spot size parameter,  $W(l)$ , of the multimode beam is given by:

$$W(l) = \sqrt{M^2} w(l) \geq 32.6 \text{ mm} \quad (6)$$

## 12.2A Amplification of long pulses by a Nd:YAG amplifier.

Since the lifetime of the lower level of the transition is much shorter than pulse **duration**, the amplifier behaves as a four-level system. The **saturation** energy fluence is then given by Eq. (12.3.2) of PL:

$$\Gamma_s = \frac{h\nu}{\sigma} = \frac{hc}{\lambda\sigma} = 0.719 \text{ J/cm}^2 \quad (1)$$

The input fluence is given by:

$$\Gamma_{in} = E_{in} / S = 0.321 \text{ J/cm}^2 \quad (2)$$

where  $S=0.312 \text{ cm}^2$  is the area of the amplifier rod. The output fluence,  $\Gamma_{out}$ , can be calculated using Eq. (12.3.12) of PL:

$$\Gamma_{out} = \Gamma_s \ln\{1 + [\exp(\Gamma_{in}/\Gamma_s) - 1]G_0\} \quad (3)$$

where  $G_0$  is the small signal gain. Using Eqs. (1-3) we obtain  $\Gamma_{out} = 2.91 \text{ J/cm}^2$ . The energy of the amplified pulse is thus given by:

$$E_{out} = \Gamma_{out} S = 907 \text{ mJ} \quad (4)$$

The corresponding amplification, G, is calculated as:

$$G = E_{out} / E_{in} = 9.07 \quad (5)$$

The energy stored in the amplifier is given by:

$$E_{stored} = N_0 l S h\nu = g l S (h\nu/\sigma) = S \Gamma_s \ln G_0 = 1032 \text{ mJ} \quad (6)$$

where  $N_0$  is the amplifier upper level population before the arrival of the laser pulse, and  $g=\sigma N_0$  is the unsaturated gain **coefficient** of the amplifier, related to the small signal gain  $G_0$  by:  $G_0=\exp(gl)$ . The fraction,  $\eta$ , of the energy stored in the amplifier that is extracted by the incident pulse is given by:

$$\eta = \frac{E_{out} - E_{in}}{E_{stored}} \cong 78.2 \% \quad (7)$$

## 12.3A Amplification of short pulses by a Nd:YAG amplifier.

Since the pulse duration is much shorter than the lifetime of the lower level of the transition the saturation energy fluence is given by:

$$\Gamma_s = \frac{h\nu}{\sigma_e + \sigma_a} \quad (1)$$

where  $\sigma_e$  and  $\sigma_a$  are the effective emission and absorption cross section of the upper and lower levels of the transition, respectively. They can be obtained from Eqs. (2.7.21a) and (2.7.21b) of PL as:

$$\sigma_e = \sigma_{23}^e = f_{22} \sigma_{23} \cong 2.6 \times 10^{-19} \text{ cm}^2 \quad (2a)$$

$$\sigma_a = \sigma_{32}^a = f_{13} \sigma_{23} \cong 1.2 \times 10^{-19} \text{ cm}^2 \quad (2b)$$

(since sublevels 3 and 2 of the lower and upper state have the same degeneracy we have  $\sigma_{32} = \sigma_{23}$ ). Using Eqs. (2a) and (2b) in Eq. (1) one obtains:

$$\Gamma_s = \frac{hc}{\lambda(\sigma_e + \sigma_a)} = 0.493 \text{ J/cm}^2 \quad (3)$$

Using Eq. (12.3.12) of PL [see also Eq. (3) of the previous problem], the output fluence can be calculated as  $\Gamma_{out} = 2.23 \text{ J/cm}^2$ . The energy of the amplified pulse is given by:

$$E_{out} = \Gamma_{out} S = 697 \text{ mJ} \quad (4)$$

The corresponding amplification, G, is:

$$G = E_{out} / E_{in} = 6.97 \quad (5)$$

## 12.4A Extraction efficiency of a two-pass amplifier.

We will calculate the output energy fluence using the notation shown in Fig.12.1. The energy fluence after the first amplification pass,  $\Gamma_1$ , is calculated using Eq. (12.3.12) of PL [see also Eq. (3) of 12.2A], where  $\Gamma_{in} = \Gamma_0$ :

$$\Gamma_0 = E_0 / S = (50 \times 10^{-3} / 0.246) \text{ J/cm}^2 = 0.203 \text{ J/cm}^2$$

and  $\Gamma_s = 0.719 \text{ J/cm}^2$  (see Eq. (1) of 12.2A). We thus obtain:

$$\Gamma_1 = \Gamma_s \ln \{1 + [\exp(\Gamma_0 / \Gamma_s) - 1] G_0\} = 0.678 \text{ J/cm}^2 \quad (1)$$

The output energy,  $E_1$ , is obtained as:  $E_1 = \Gamma_1 S = 167 \text{ mJ}$ . The extraction efficiency,  $\eta_1$ , is:

$$\eta_1 = \frac{E_1 - E_0}{E_{stored}} = \frac{E_1 - E_0}{S \Gamma_s \ln G_0} = 0.42 \quad (2)$$

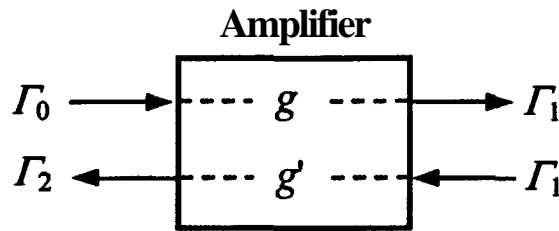


Fig. 12.1 Schematic configuration of a double-pass amplifier.

A mirror at the output of the gain medium now returns the beam a second time through the amplifier. The output fluence,  $\Gamma_2$ , after the second pass is obtained, again using Eq. (12.3.12) of PL, as:

$$\Gamma_2 = \Gamma_s \ln\{1 + [\exp(\Gamma_1 / \Gamma_s) - 1]G_0'\} \quad (3)$$

In this **case** the input energy fluence is the output of the first pass and the small signal gain,  $G_0'$ , is smaller than  $G_0$  because energy has been extracted from the gain medium on the first pass. The unsaturated gain coefficient,  $g'$ , for the second pass is given by  $g' = \sigma N_0'$ , where  $N_0'$  is the amplifier upper level population after the first amplification pass. Therefore one can write:

$$g' = \sigma N_0' = \sigma N_0 (1 - \eta_l) = g (1 - \eta_l) \quad (4)$$

where  $g$  is the unsaturated gain coefficient for the first pass. The small signal gain  $G_0'$  is thus calculated as:

$$G_0' = \exp(g' l) = \exp[g l (1 - \eta_l)] = (G_0)^{1-\eta_l} = 2.48 \text{ J/cm}^2 \quad (5)$$

Using the calculate value of  $G_0'$  in Eq. (3) we obtain  $\Gamma_2 = 1.14 \text{ J/cm}^2$ . The energy of the amplified pulse is given by:

$$E_2 = \Gamma_2 S = 281 \text{ mJ} \quad (6)$$

The corresponding extraction **efficiency** of the double-pass amplifier is:

$$\eta_2 = \frac{E_2 - E_0}{E_{stored}} = \frac{E_2 - E_0}{S \Gamma_s \ln G_0} = 0.83 \quad (7)$$

Note:

This problem shows that a double-pass **configuration** provides a **significant** improvement of the amplifier characteristics, as clearly shown by Fig. 12.2, which displays the extraction **efficiency** for **one-** and two-pass amplifier as a function of the input energy fluence normalized to the saturation fluence, for two **different** values of the small signal gain  $G_0$ .

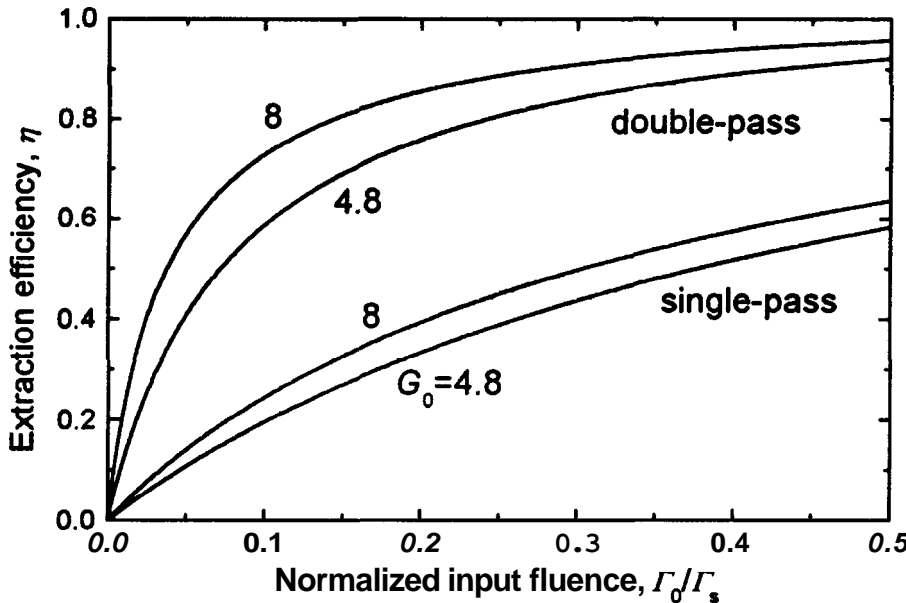


Fig. 12.2 Extraction efficiency of a single- and double-pass amplifier as a function of the normalized input fluence for two different values of the small signal gain  $G_0$ .

### 12.5A Saturation fluence in a quasi-three-level amplifier.

We will assume that pumping to the amplifier upper level and subsequent spontaneous decay can be neglected during passage of the pulse and that the transition is homogeneously broadened. Under these conditions the rate of change of the upper state population in a quasi-three-level amplifier can be written as:

$$\frac{dN_2}{dt} = -W_e N_2 + W_a N_1 = -\frac{\sigma_e I}{h\nu} N_2 + \frac{\sigma_a I}{h\nu} N_1 \quad (1)$$

where  $\sigma_e$  and  $\sigma_a$  are the effective cross sections for stimulated emission and absorption, respectively. Equation (1) can be written in the following way:

$$\frac{dN_2}{dt} = -\frac{\sigma_e I}{h\nu} (N_2 - \frac{\sigma_a}{\sigma_e} N_1) = -\frac{\sigma_e I}{h\nu} N \quad (2)$$

where we have defined the population inversion,  $N$ , as [see also Eq. (7.2.23) of PL]:

$$N = N_2 - \frac{\sigma_a}{\sigma_e} N_1 \quad (3a)$$

The total population in the two levels,  $N_t$ , is then given by:

$$N_t = N_1 + N_2 \quad (3b)$$

Using Eqs. (3a) and (3b) one can obtain  $N_2$  in terms of  $N$  and  $N_t$ :

$$N_2 = \frac{\sigma_e}{\sigma_e + \sigma_a} (N + \frac{\sigma_a}{\sigma_e} N_t) \quad (4)$$

The substitution of Eq. (4) in the left-hand side of Eq. (2) then leads to:

$$\frac{dN}{dt} = -\frac{\sigma_e + \sigma_a}{h\nu} IN = -\frac{NI}{\Gamma_s} \quad (5)$$

where we have defined  $\Gamma_s = h\nu/(\sigma_e + \sigma_a)$  as the saturation energy fluence.

## 12.6A Maximum output fluence from an amplifier with losses.

The differential equation which, for an amplifier, establishes the evolution of the pulse fluence,  $\Gamma(z)$ , vs propagation length  $z$  is given by Eq. (12.3.11) of PL:

$$\frac{d\Gamma}{dz} = g\Gamma_s[1 - \exp(-\Gamma/\Gamma_s)] - \alpha\Gamma \quad (1)$$

where:  $g$  is the **unsaturated** gain coefficient;  $\alpha$  is the absorption coefficient;  $\Gamma_s$  is the saturation fluence. For large values of  $\Gamma$  (i.e., for  $g \gg \alpha$ ) we can write

$$\exp(-\Gamma/\Gamma_s) \approx 0 \quad (2)$$

Equation (1) can then be written as:

$$\frac{d\Gamma}{dz} = g\Gamma_s - \alpha\Gamma \quad (3)$$

so that, upon integration, one gets:

$$\int_{\Gamma(0)}^{\Gamma(z)} \frac{d\Gamma}{g\Gamma_s - \alpha\Gamma} = \int_0^z dz \Rightarrow \ln \frac{g\Gamma_s - \alpha\Gamma(z)}{g\Gamma_s - \alpha\Gamma(0)} = -\alpha z$$

The output fluence is thus given by:

$$\Gamma(z) = \frac{g\Gamma_s}{\alpha} - \left[ \frac{g\Gamma_s}{\alpha} - \Gamma(0) \right] \exp(-\alpha z) \quad (4)$$

From Eq. (4) one can readily see that the **maximum** obtainable energy fluence is somewhat less than the value  $\Gamma_m = g\Gamma_s/\alpha$ .

### 12.7A Theoretical limit to the maximum intensity of an amplifier.

The maximum fluence **that** can be obtained from an amplifier without a significant temporal distortion of the amplified pulse is approximately given by the saturation fluence  $\Gamma_s = h\nu/\sigma$ . Therefore, the maximum peak power,  $P_{max}$ , that can be obtained from **an** amplifier of cross-section area  $S$  can be written as

$$P_{max} \cong \frac{\Gamma_s S}{\tau_{min}} = \frac{h\nu S}{\sigma \tau_{min}} \quad (1)$$

where  $\tau_{min}$  is the minimum achievable pulse **duration**. If the amplified beam is focused by a lens to a focal spot of diameter  $d$ , the maximum peak intensity in this spot will be given by

$$I_{max} \cong \frac{P_{max}}{d^2} = \frac{h\nu S}{\sigma \tau_{min} d^2} \quad (2)$$

We now know **that** the minimum pulse duration is related to the fluorescence bandwidth,  $\Delta\nu_0$ , by the relation

$$\tau_{min} \cong \frac{1}{\Delta\nu_0} \quad (3)$$

On the other hand, the minimum spot diameter is limited by the pulse wavelength. Therefore, **the** maximum focused intensity can be written as

$$I_{max} = \frac{h\nu \Delta\nu_0 S}{\sigma \lambda^2} = \frac{h\nu^3 \Delta\nu_0 S}{\sigma c^2} \quad (4)$$

*Note:*

In the case of a **Yb:phosphate** amplifier one has:  $\Gamma_s = 40 \text{ J/cm}^2$ ,  $\tau_{min} = 20 \text{ fs}$  and  $\lambda = 1030 \text{ nm}$ . For a  $1-\text{cm}^2$  area of this gain medium one then gets from Eq.(1)

$P_{max} \approx 2$  PW, while the **maximum** peak intensity at the beam focus is seen from Eqs. (3) and (4) to be given by  $I_{max} \approx 2 \times 10^{23}$  W/cm<sup>2</sup>.

### 12.8A Index of refraction of an extraordinary wave in a uniaxial crystal.

For a positive uniaxial crystal ( $n_e > n_o$ ) and for beam propagation in the z-y plane, Fig. 12.3 shows **the section of the normal surface** for extraordinary wave with the z-y plane. The equation of the ellipse shown in the figure is given by

$$\frac{y^2}{n_e^2} + \frac{z^2}{n_o^2} = 1 \quad (1)$$

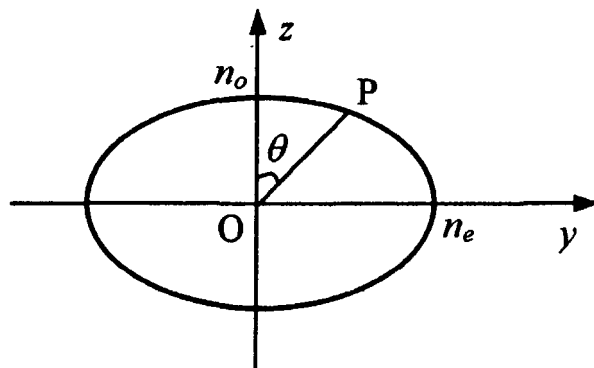


Fig. 12.3 **Normal** index surface of a positive uniaxial crystal

For beam propagation **along** the direction  $\theta$ , the value of  $n_e = n_e(\theta)$  is given **by** the **length** of the segment OP in Fig. 12.3. It is therefore convenient to express the coordinate **y** and **z** in **terms** of  $n_e(\theta)$  and  $\theta$ .

$$y = n_e(\theta) \sin \theta \quad (2a)$$

$$z = n_e(\theta) \cos \theta \quad (2b)$$

Using these relations, Eq. (1) can be transformed to:

$$\frac{[n_e(\theta)]^2}{n_e^2} \sin^2 \theta + \frac{[n_e(\theta)]^2}{n_o^2} \cos^2 \theta = 1 \quad (3)$$

which gives:

$$n_e(\theta) = \frac{n_o n_e}{\sqrt{n_o^2 \sin^2 \theta + n_e^2 \cos^2 \theta}} \quad (4)$$

Substituting the numerical values of the problem into Eq. (4) we get  $n_e(30^\circ)=1.59$ .

### 12.9A Double refraction in a uniaxial crystal.

The phenomenon illustrated in this problem is referred to as double refraction. We consider separately the ordinary and extraordinary rays. In the case of the ordinary ray the calculation is straightforward. Applying Snell's law we have:

$$n \sin \theta_i = n_o \sin \theta_o \quad (1)$$

where  $n$  is the refractive index of the external medium (air,  $n=1$ ),  $\theta_i$  is the incidence angle and  $\theta_o$  is the refraction angle of the ordinary ray. In the case of the extraordinary ray Snell's law gives:

$$n \sin \theta_i = n_e(\theta_e) \sin \theta_e \quad (2)$$

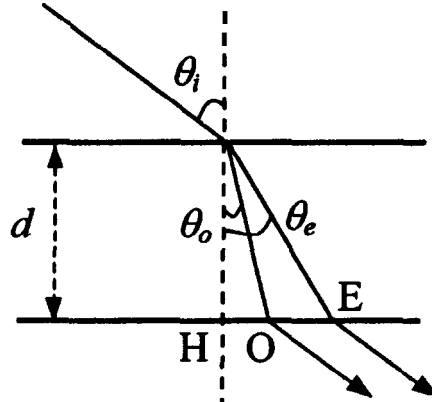


Fig. 12.4 Double refraction.

where  $\theta_e$  is the refraction angle of the extraordinary ray. Since the optic axis of the crystal is perpendicular to the crystal surface,  $n_e(\theta_e)$  can be calculated using Eq. (4) of the previous answer. After some straightforward calculations we obtain:

$$\sin \theta_e = \frac{n_e \sin \theta_i}{\sqrt{n_o^2 n_e^2 - (n_o^2 - n_e^2) \sin^2 \theta_i}} \quad (3)$$

The lateral **separation** of the **ordinary** and **extraordinary** rays at the output **surface** of the crystal is given by (see Fig. 12.4):

$$OE = d (\tan \theta_e - \tan \theta_o) \quad (4)$$

Using the numerical values given in the problem we get  $\theta_o=13.63^\circ$ ,  $\theta_e=14.14^\circ$  and  $OE \approx 0.19 \text{ mm}$

### 12.10A Second harmonic conversion of a Ti:sapphire laser in a BBO crystal.

$\beta$ -barium borate ( $\beta\text{-BaB}_2\text{O}_4$ ) is a negative uniaxial crystal. In the case of type-I second harmonic generation (SHG) an ordinary ray at  $\omega$  combines with an ordinary ray at  $\omega$  to give an extraordinary ray at  $2\omega$ , or, in symbols,  $o_\omega + o_\omega \rightarrow e_{2\omega}$ . To satisfy the phase-matching condition ( $k_{2\omega}=2k_\omega$ ) we can then propagate the **fundamental** wave at an angle  $\theta_m$  to the optic axis such that:

$$n_e(2\omega, \theta_m) = n_o(\omega) \quad (1)$$

Using Eq. (4) of Answer 12.8 in the left-hand side of Eq. (1), the equation gives:

$$\frac{n_o(2\omega) n_e(2\omega)}{\sqrt{n_o^2(2\omega) \sin^2 \theta_m + n_e^2(2\omega) \cos^2 \theta_m}} = n_o(\omega) \quad (2)$$

This equation can be solved for  $\sin^2 \theta_m$  to obtain:

$$\sin^2 \theta_m = \frac{[n_o(2\omega)/n_o(\omega)]^2 - 1}{[n_o(2\omega)/n_e(2\omega)]^2 - 1} \quad (3)$$

The ordinary and extraordinary refraction indices of the fundamental and second-harmonic radiation can be obtained from the **Sellmeier** equations upon putting  $\lambda=0.78 \mu\text{m}$  and  $\lambda=0.39 \mu\text{m}$ , respectively. We get:

$$\begin{aligned} n_o(0.78 \mu\text{m}) &= 1.6620 \\ n_e(0.78 \mu\text{m}) &= 1.5466 \\ n_o(0.39 \mu\text{m}) &= 1.6957 \\ n_e(0.39 \mu\text{m}) &= 1.5704 \end{aligned} \quad (4)$$

Using Eq. (3) we then obtain the phase-matching angle as  $\theta_m=29.78^\circ$ .

In the case of type-II SHG in a negative uniaxial crystal an ordinary ray at  $\omega$

combines with an extraordinary ray at  $\omega$  to give an extraordinary ray at  $2\omega$ , or, in symbols,  $e_\omega + e_\omega \rightarrow e_{2\omega}$ . The phase-matching condition in this case is given by:

$$k_o(\omega) + k_e(\omega, \theta_m) = k_e(2\omega, \theta_m) \quad (5)$$

which, in terms of the refractive indexes, can be written as follows:

$$\frac{1}{2}[n_o(\omega) + n_e(\omega, \theta_m)] = n_e(2\omega, \theta_m) \quad (6)$$

Using Eq. (4) of 12.8A, Eq. (6) can be solved graphically, as shown in Fig. 12.5. From Fig. 12.5 we obtain  $\theta_m = 43.15^\circ$ .

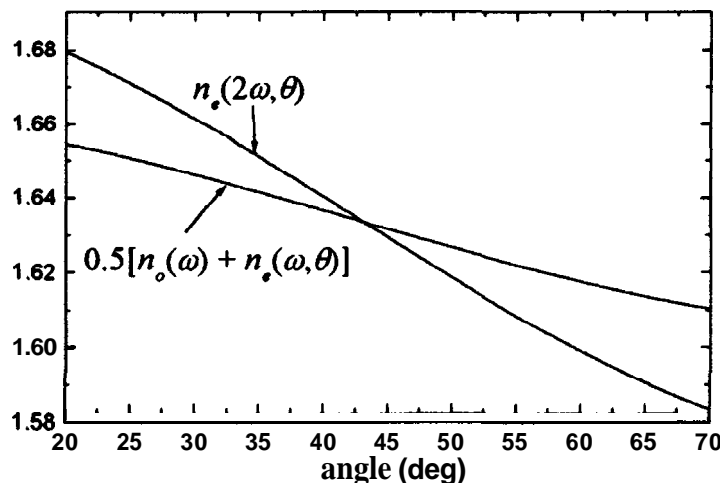


Fig. 12.5 Graphical determination of the phase-matching angle for type-II second harmonic generation

*Note:*

Using Eq. (3) and Eq. (6) it is simple to compute with a numerical code the SHG tuning curves (i.e., the phase-matching angle vs the fundamental wavelength) for type-I and type-II phase matching. In the case of BBO crystal the tuning curves are shown in Fig. 12.6.

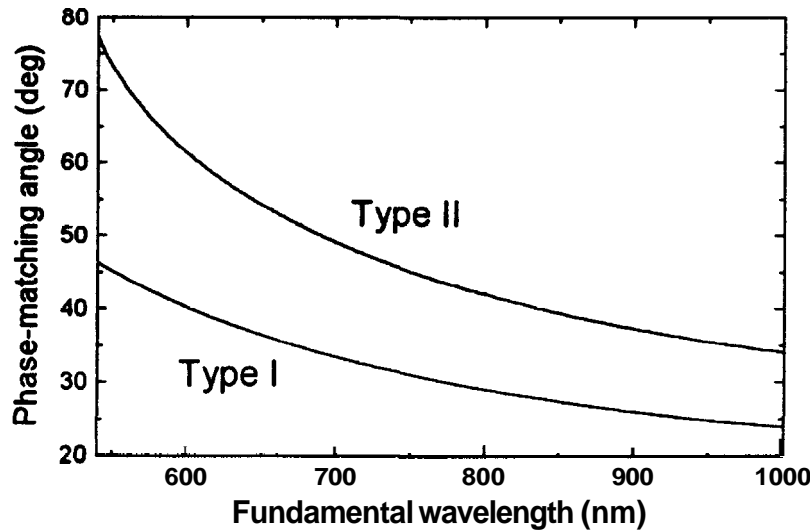


Fig. 12.6 Tuning curves for type-I and type-II second harmonic generation in BBO

### 12.11A Second harmonic conversion efficiency in a KDP crystal.

From Eq. (12.4.58a) of PL the second harmonic conversion efficiency is obtained as:

$$\eta = \frac{I_{2\omega}(z)}{I_\omega(0)} = \frac{|E'_{2\omega}|^2}{|E'_\omega(0)|^2} = [\tanh(z/l_{SH})]^2 \quad (1)$$

where  $l_{SH}$  can be obtained from Eq. (12.4.52) of PL. For perfect phase-matching we can write  $n_\omega = n_{2\omega} = n$  so that Eq.(12.4.52) transforms to:

$$l_{SH} = \frac{\lambda n}{2\pi d_{eff} |E_\omega(0)|} \quad (2)$$

Since  $|E_\omega(0)| = [2ZI_\omega(0)]^{1/2}$ , where  $Z=1/\epsilon_0 c \approx 377 \Omega$  is the free-space impedance (see Problem 2.1), we get:

$$l_{SH} = \frac{\lambda n}{2\pi d_{eff} [2ZI_\omega(0)]^{1/2}} = 3.3 \text{ cm} \quad (3)$$

Substituting the value calculate for  $l_{SH}$  in Eq. (1) and assuming  $z=2.5$  cm, we obtain  $\eta=40.9\%$ .

### 12.12A Second harmonic generation with a Gaussian beam.

From Eq. (12.4.55) of PL we have:

$$|E'_{2\omega}(l)|^2 = |E'_\omega(0)|^2 \frac{\sin^2(\Delta k l/2)}{(\Delta k l_{SH}/2)^2} \quad (1)$$

where:  $E'_\omega = (n_\omega)^{1/2} E_\omega$  and  $E'_{2\omega} = (n_{2\omega})^{1/2} E_{2\omega}$ ;  $l_{SH}$  is given by Eq. (12.4.52) of PL:

$$l_{SH} = \frac{\lambda (n_\omega n_{2\omega})^{1/2}}{2\pi d |E_\omega(0)|} \quad (2)$$

where  $d$  is the effective coefficient for second harmonic generation. Using Eq. (2), Eq. (1) can be written as follows:

$$n_{2\omega} |E_{2\omega}(l)|^2 = n_\omega |E_\omega(0)|^4 \frac{\omega^2 d^2 l^2}{c^2 n_\omega n_{2\omega}} \frac{\sin^2(\Delta k l/2)}{(\Delta k l/2)^2} \quad (3)$$

For perfect phase matching one has  $\Delta k=0$  and  $n_\omega=n_{2\omega}=n$ . Since the beam intensity can be expressed as  $I = \epsilon_0 c n |\mathbf{E}|^2 / 12$ , using Eq. (3) we obtain:

$$I_{2\omega}(l) = \frac{2\omega^2 d^2 l^2}{\epsilon_0 c^3 n^3} I_\omega^2(0) \quad (4)$$

Assuming that  $z_R \gg l$ , the intensity of the incident wave is nearly independent of  $z$  within the crystal so that one can write:

$$I(z, r) \approx I_0 \exp(-2r^2/w_0^2) \quad (5)$$

where  $w_0$  is the beam spot size at the beam waist. Equation (4) can be re-written as follows:

$$I_{2\omega}(l, r) = \frac{2\omega^2 d^2 l^2}{\epsilon_0 c^3 n^3} I_\omega^2(0, r) \quad (6)$$

The input power,  $P_\omega(0)$ , is given by:

$$P_\omega(0) = \int_0^{+\infty} I_\omega(0, r) 2\pi r dr = \int_0^{+\infty} 2\pi r I_0 \exp(-2r^2/w_0^2) dr = I_0 \pi w_0^2 / 2 \quad (7)$$

The second harmonic power,  $P_{2\omega}(l)$ , can be calculated using Eq. (6):

$$\begin{aligned} P_{2\omega}(l) &= \int_0^{+\infty} I_{2\omega}(l, r) 2\pi r dr = \frac{2\omega^2 d^2 l^2}{\epsilon_0 c^3 n^3} \int_0^{+\infty} I_\omega^2(0, r) 2\pi r dr = \\ &= \frac{2\omega^2 d^2 l^2}{\epsilon_0 c^3 n^3} I_0^2 \frac{\pi w_0^2}{4} \end{aligned} \quad (8)$$

Using Eqs.(7) and (8) the conversion efficiency is calculated as:

$$\eta = \frac{P_{2\omega}(l)}{P_\omega(0)} = \frac{2\omega^2 d^2 l^2}{\epsilon_0 c^3 n^3} \frac{P_\omega(0)}{\pi w_0^2} \quad (9)$$

*Note:*

According to Eq. (9) in a crystal of length  $l$  and with a given input power, the second harmonic output power can be increased by decreasing  $w_0$ . This is true until the Rayleigh range of the input beam,  $z_R = \pi w_0^2 n / \lambda$ , becomes comparable to the crystal length. Further reduction of  $w_0$  cause a spread of the beam inside the crystal, thus leading to a reduction of the intensity and of the second harmonic conversion efficiency. It can be shown that the optimal focusing condition is obtained when the beam confocal parameter is equal to the crystal length (i.e.,  $2z_R=l$ ). In this case the conversion efficiency becomes:

$$\eta = \left. \frac{P_{2\omega}(l)}{P_\omega(0)} \right|_{l=2z_R} = \frac{2\omega^3 d^2 l}{\pi \epsilon_0 c^4 n^2} P_\omega(0) \quad (10)$$

### 12.13A Frequency doubling of a Gaussian beam in a KDP crystal.

The input power at fundamental frequency,  $P_\omega(0)$ , is related to the peak intensity  $I_0$  by the equation  $P_\omega(0) = (\alpha w_0^2 / 2) I_0$  [see also Eq. (7) of 12.12A], where  $w_0$  is the spot size at the beam waist. Under optimum focusing conditions,  $w_0$  must be such that  $2(\pi w_0^2 n / \lambda) = l$  so that:

$$w_0 = \left( \frac{\lambda l}{2\pi n} \right)^{1/2} \quad (1)$$

The fundamental power is therefore given by:

$$P_\omega(0) = \frac{\pi w_0^2}{2} I_0 = \frac{l \lambda}{4n} I_0 = 4.4 \times 10^3 \text{ W} \quad (2)$$

The conversion efficiency is then calculated as:

$$\eta = \frac{2\omega^3 d_{eff}^2 l}{\pi \epsilon_0 c^4 n^2} P_\omega(0) = 19.2 \% \quad (3)$$

### 12.14A Effective nonlinear coefficient of a KDP crystal.

The nonlinear polarization for second harmonic generation can be written in the following simple way:

$$P(2\omega) = 2 \epsilon_0 d_{eff} E^2(\omega) \quad (1)$$

where  $d_{eff}$  is the effective nonlinear coefficient which includes all the summations that apply to the particular interaction geometry. Here we will consider the case of type-I phase-matching second **harmonic** generation in KDP, which belong to the  $\bar{4}2m$  point group symmetry and is a negative uniaxial ( $n_e < n_o$ ). The nonlinear polarization at frequency  $2\omega$  can be written in contracted notation as:

$$P_i^{2\omega} = 2 \sum_{m=1}^6 \epsilon_0 d_{im}^{2\omega} (EE)_m \quad (2)$$

The abbreviated field notation is:  $(EE)_1 \equiv E_x^2$ ,  $(EE)_2 \equiv E_y^2$ ,  $(EE)_3 \equiv E_z^2$ ,  $(EE)_4 \equiv 2E_y E_z$ ,  $(EE)_5 \equiv 2E_x E_z$ ,  $(EE)_6 \equiv 2E_x E_y$ .

In the case of KDP we then obtain:

$$P_x(2\omega) = 4 \epsilon_0 d_{36} E_y E_z \quad (3a)$$

$$P_y(2\omega) = 4 \epsilon_0 d_{36} E_z E_x \quad (3b)$$

$$P_z(2\omega) = 4 \epsilon_0 d_{36} E_x E_y \quad (3c)$$

where the z-axis is taken along the optic axis of the crystal. For type-I phase matching an ordinary ray (***o*-ray**) at  $\omega$  combines with an ordinary ray at  $2\omega$  to

give an extraordinary ray (e-ray) at  $2\omega$ , or, in symbols,  $o_\omega + o_\omega \rightarrow e_{2\omega}$ . The interaction geometry is shown in Fig. 12.7. The components of the electric field at  $\omega$  are:

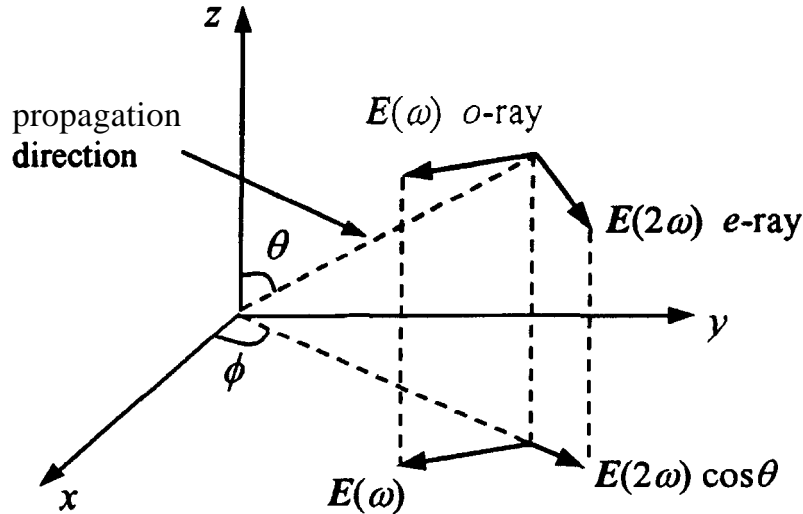


Fig. 12.7 Interaction geometry for type-I phase-matching in a negative uniaxial crystal.

$$E_x = |E(\omega)| \sin \phi \quad (4a)$$

$$E_y = -|E(\omega)| \cos \phi \quad (4b)$$

$$E_z = 0 \quad (4c)$$

Using Eqs. (3) and (4) the components of the second harmonic polarization are given by:

$$P_x = P_y = 0 \quad (5a)$$

$$P_z = -4 \epsilon_0 d_{36} \sin \phi \cos \phi |E(\omega)|^2 \quad (5b)$$

The effective polarization with the correct orientation to generate a second harmonic extraordinary wave must be orthogonal to the direction of the vector  $E(\omega)$  and to the propagation direction. This polarization must then be directed as the vector  $E(2\omega)$  shown in Fig. 12.7. From this figure we then obtain:

$$\begin{aligned} P_{eff}(2\omega) &= P_z \sin \theta = -4 \epsilon_0 d_{36} \sin \phi \cos \phi \sin \theta |E(\omega)|^2 = \\ &= -2 \epsilon_0 d_{36} \sin(2\phi) \sin \theta |E(\omega)|^2 \end{aligned} \quad (6)$$

The comparison of Eq. (6) with Eq. (1) show that:

$$d_{\text{eff}} = -d_{36} \sin(2\phi) \sin \quad (7)$$

### 12.15A Threshold pump intensity of an optical parametric oscillator.

Using the expression of the threshold intensity  $I_{3th}$  for a doubly resonant oscillator given in Example 12.4 of PL, and substituting the numerical values, we obtain:

$$I_{3th} = \frac{n_3}{2Z d^2} \frac{n_1 n_2 \lambda_1 \lambda_2}{(2\pi l)^2} \gamma_1 \gamma_2 = 156 \text{ W/cm}^2 \quad (1)$$

where:  $Z=1/\epsilon_0 c \approx 377 \Omega$  is the free-space impedance;  $\lambda_1$  and  $\lambda_2$  are the wavelengths of the signal and idler waves, respectively;  $l$  is the crystal length;  $n_1$ ,  $n_2$  and  $n_3$  are the refractive indexes of the crystal at the wavelength of the signal, idler and pump waves, respectively;  $\gamma_1$  and  $\gamma_2$  are the logarithmic losses of the laser cavity at the signal and idler wavelengths, respectively.

The threshold pump power is then given by:

$$P_{3th} = I_{3th} S = 12.3 \text{ mW} \quad (2)$$

where  $S$  is the cross-section of the focused beam.

### 12.16A Collinear parametric generation in a BBO crystal.

For type-I parametric generation in a negative uniaxial crystal an **extraordinary** ray at frequency  $\omega_3$  (pump) generates an ordinary ray at  $\omega_1$  (signal) and an ordinary ray at  $\omega_2$  (idler) or, in symbols,  $o_{\omega_1} + o_{\omega_2} \rightarrow e_{\omega_3}$ . For this process we can write the energy conservation equation:

$$\hbar \omega_1 + \hbar \omega_2 = \hbar \omega_3 \quad (1)$$

and the momentum conservation equation (phase-matching):

$$\hbar \mathbf{k}_1 + \hbar \mathbf{k}_2 = \hbar \mathbf{k}_3 \quad (2)$$

where  $\mathbf{k}_i = \omega_i \mathbf{n}_i / c = 2\pi n_i / \lambda_i$ , ( $i = 1, 2, 3$ ). From Eq. (1) the idler wavelength,  $\lambda_2$ , can be calculated:

$$\frac{1}{\lambda_1} + \frac{1}{\lambda_2} = \frac{1}{\lambda_3} \Rightarrow \lambda_2 = \frac{\lambda_1 \lambda_3}{\lambda_1 - \lambda_3} \quad (3)$$

From Eq. (2), assuming a **collinear** configuration, the phase-matching condition can be written as:

$$\frac{n_1}{\lambda_1} + \frac{n_2}{\lambda_2} = \frac{n_3}{\lambda_3} \quad (4)$$

where  $n_i = n(\omega_i)$ . For type-I phase matching in a negative crystal, from Eq. (4) we get:

$$n_3^e(\theta_m) = \frac{\lambda_3}{\lambda_1} n_1^o + \frac{\lambda_3}{\lambda_2} n_2^o \quad (5)$$

where  $\theta_m$  is the phase-matching angle. From Eq. (5) with the help of the expression for  $n_3^e(\theta)$  given in the problem we readily see that the phase-matching angle can be calculated from the equation:

$$\sin^2 \theta_m = \frac{[n_3^o / n_3^e(\theta_m)]^2 - 1}{(n_3^o / n_3^e)^2 - 1} \quad (6)$$

Assuming  $\lambda_1=560$  nm and  $\lambda_3=400$  nm, from Eq. (3) we obtain the idler wavelength  $\lambda_2=1400$  nm. From the Sellmeier equations the ordinary indexes at the three wavelengths and the extraordinary index at the pump wavelength can be calculated:  $n_1^o=1.673$ ,  $n_2^o=1.649$ ,  $n_3^o=1.693$ ,  $n_3^e=1.569$ . From Eq. (5) we then readily calculate the required pump extraordinary index for phase matching as  $n_3^e(\theta_m)=1.666$ . The phase matching angle is then calculated from Eq. (6):  $\theta_m=26.63^\circ$ .

Repeating the same procedure for a wavelength  $\lambda_1=700$  nm, we obtain the following numerical results:  $\lambda_2=933$  nm,  $n_1^o=1.665$ ,  $n_2^o=1.658$ ,  $n_3^e(\theta_m)=1.662$ ,  $\theta_m=28.76^\circ$ .

## 12.17A Noncollinear parametric generation in a BBO crystal,

The energy conservation and the momentum conservation (phase matching) can again be written as [see 12.16A]:

$$\hbar \omega_1 + \hbar \omega_2 = \hbar \omega_3 \quad (1)$$

$$\hbar \mathbf{k}_1 + \hbar \mathbf{k}_2 = \hbar \mathbf{k}_3 \quad (2)$$

where, for noncollinear geometry, the vectorial Eq. (2) can be represented as shown in Fig. 12.8. From Eq. (2) one can get two scalar equations upon projecting the equation along the direction of  $\mathbf{k}_3$  and along the direction orthogonal to  $\mathbf{k}_3$ . From Fig. 12.8 one then readily gets:

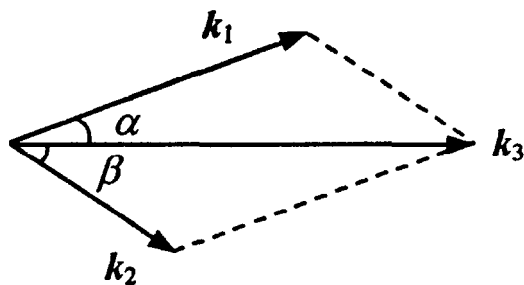


Fig. 12.8 Phase-matching condition in noncollinear parametric generation

$$k_1 \cos \alpha + k_2 \cos \beta = k_3 \quad (3a)$$

$$k_1 \sin \alpha = k_2 \sin \beta \quad (3b)$$

where  $\alpha$  is the angle between  $\mathbf{k}_1$  and  $\mathbf{k}_3$ , and  $\beta$  is the angle between  $\mathbf{k}_2$  and  $\mathbf{k}_3$ . From Eq. (3b)  $\beta$  is obtained as:

$$\sin \beta = \frac{k_1}{k_2} \sin \alpha = \frac{n_1^o}{n_2^o} \frac{\lambda_2}{\lambda_1} \sin \alpha \quad (4)$$

Using Eq. (3a) one finds:

$$n_3^e(\theta_m) = n_1^o \frac{\lambda_3}{\lambda_1} \cos \alpha + n_2^o \frac{\lambda_3}{\lambda_2} \cos \beta \quad (5)$$

Using Eq. (6) of the previous problem and Eq. (5) the phase-matching angle can be calculated.

Assuming  $\lambda_1=560$  nm and  $\lambda_3=400$  nm, the idler wavelength is obtained from Eq. (3) of 12.16A as  $\lambda_2=1400$  nm. From the Sellmeier equations the ordinary indexes at the three wavelengths and the extraordinary index at the pump wavelength can be calculated:  $n_1^o=1.673$ ,  $n_2^o=1.649$ ,  $n_3^o=1.693$ ,  $n_3^e=1.569$ . From Eq. (4) we get, for  $\alpha=3.7^\circ$ :  $\beta=9.42^\circ$ . Using Eq. (5) we find  $n_3^e(\theta_m)=1.657$ . From Eq. (6) of 12.16A we obtain the phase-matching angle:  $\theta_m=31.15^\circ$ .

Repeating the same calculations for  $\alpha=3.7^\circ$  and  $\lambda_1=700$  nm we obtain:

$$\lambda_2=933 \text{ nm}, \beta=4.96^\circ, n_3^e(\theta_m)=1.657, \theta_m=31.10^\circ.$$

If we now assume  $\alpha=5^\circ$ , we obtain the following results:

$$(a) \text{ for } \lambda_1=560 \text{ nm} (\lambda_2=1400 \text{ nm}): \beta=12.77^\circ, n_3^e(\theta_m)=1.650, \theta_m=34.71^\circ.$$

$$(b) \text{ for } \lambda_1=700 \text{ nm} (\lambda_2=933 \text{ nm}): \beta=6.7^\circ, n_3^e(\theta_m)=1.653, \theta_m=32.97^\circ.$$

*Note:*

In the case of noncollinear sum-frequency generation in a BBO crystal pumped at 400 nm, if the angle,  $\alpha$ , between the pump and the signal wave-vectors is set at  $\alpha=3.7^\circ$ , the phase-matching angle is nearly constant over a large signal wavelength range in the visible. Figure 12.9 shows the phase-matching tuning curves for different values of  $\alpha$ , ranging from  $\alpha=0^\circ$  (collinear geometry) to  $\alpha=5^\circ$ . This peculiar property of BBO has been used in optical parametric oscillators (OPOs) and amplifiers (OPAs) to generate ultrashort signal and idler pulses tunable in the visible and near infrared. Pulses as short as 4.5 fs have been generated using a noncollinear OPA based on BBO pumped by the second harmonic of an amplified Ti:sapphire laser system.

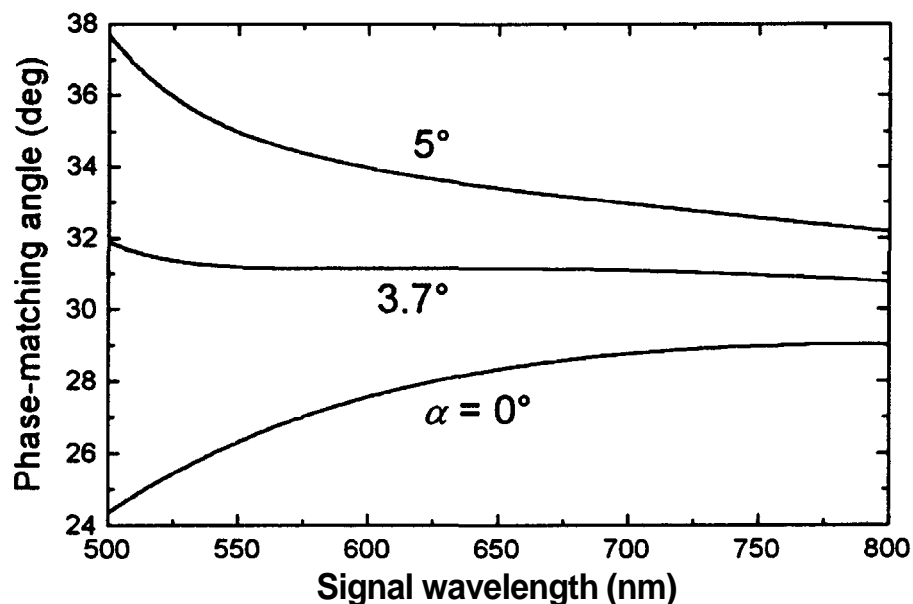


Fig. 12.9 Phase-matching curves for type-I sum-frequency generation in BBO pumped at 400 nm, for different values of the pump-signal angle,  $\alpha$ .

### 12.18A Nonlinear index $n_2$ of sapphire.

The intensity of an e.m. wave is given by (see 2.1A):

$$I = \frac{1}{2} \epsilon_0 c n_0 |E|^2 \quad (1)$$

where  $n_0$  is the low-intensity refractive index. Using Eq. (1) the refractive index of the Kerr medium can be written as follows:

$$n = n_0 + n_2 I = n_0 + n_2 \frac{1}{2} \epsilon_0 c n_0 |E|^2 = n_0 + \bar{n}_2 |E|^2 \quad (2)$$

where:

$$\bar{n}_2 = \frac{1}{2} \epsilon_0 c n_0 n_2 \quad (3)$$

In the case of sapphire, since  $n_0 \approx 1.7$  and  $n_2 \approx 3.45 \times 10^{-16} \text{ cm}^2/\text{W}$ , we get:

$$\bar{n}_2 = 7.78 \times 10^{-23} \text{ m}^2/\text{V}^2 \quad (4)$$

### 12.19A Pulse spectral broadening due to self-phase modulation in a Kerr medium.

Due to self-phase modulation (SPM) a light pulse of uniform intensity profile, that travels a distance  $L$  in a Kerr medium, acquires a phase given by Eq. (8.6.38) of PL:

$$\varphi(t, L) = \omega_0 t - \frac{\omega_0 (n_0 + n_2 I) L}{c} \quad (1)$$

where  $I$  is the light pulse intensity and  $n_0$  is the low-intensity refractive index of the medium. The instantaneous carrier frequency of the pulse is then obtained from Eq. (1) as:

$$\omega(t, L) = \frac{d\varphi}{dt} = \omega_0 - \frac{\omega_0 n_2 L}{c} \frac{dI}{dt} \quad (2)$$

For a Gaussian pulse with intensity

$$I(t) = I_0 \exp(-t^2 / \tau_0^2) \quad (3)$$

the pulse duration  $\tau_p$  (FWHM) is related to  $\tau_0$  by the following relationship:

$$\tau_p = 2 \sqrt{\ln 2} \tau_0 \approx 1.665 \tau_0 \quad (4)$$

Using the expression of pulse intensity given by Eq. (3) into Eq. (2), we obtain:

$$\Delta\omega(t, L) = \omega(t, L) - \omega_0 = \frac{2\omega_0 n_2 L I_0}{c \tau_0^2} t \exp(-t^2 / \tau_0^2) \quad (5)$$

Spectral broadening is **symmetric** with respect to the center of the pulse. Figure 12.12 of PL shows the temporal behavior of  $\Delta\omega(t, L)$  obtained using Eq. (5). In order to calculate the maximum spectral broadening, we have to calculate the **maximum** value of  $\Delta\omega(t, L)$ . This can be simply done by equating to zero the time derivative of  $\Delta\omega(t, L)$ :

$$\frac{d \Delta\omega}{dt} = \frac{2\omega_0 n_2 L I_0}{c \tau_0^2} \left( 1 - \frac{2t^2}{\tau_0^2} \right) \exp(-t^2 / \tau_0^2) = 0 \quad (6)$$

which gives  $t = \pm\tau_0 / \sqrt{2}$  (the plus sign corresponds to the maximum, while the minus sign corresponds to the minimum of  $\Delta\omega(t, L)$ ).

We thus obtain:

$$\Delta\omega_{max} = \Delta\omega(\tau_0 / \sqrt{2}) = \sqrt{2} \exp\left(-\frac{1}{2}\right) \frac{\omega_0 n_2 L I_0}{c \tau_0} \approx 0.86 \frac{\omega_0 n_2 L I_0}{c \tau_0} \quad (7)$$

## 12.20A Spectral broadening of a 20-fs pulse in a hollow fiber filled with argon.

For a Gaussian pulse, the time variation of the pulse power **can** be written as  $P(t) = P_0 \exp[-(t/2\tau_p)^2 \ln 2]$ , where  $\tau_p$  is the width of the pulse (**FWHM**).

Since the pulse energy is given by  $E = \int_{-\infty}^{+\infty} P(t) dt$ , we readily obtain that pulse peak power,  $P_0$ , is related to the pulse energy by the equation:

$$P_0 = \frac{2(\ln 2)^{1/2}}{\sqrt{\pi}} \frac{E}{\tau_p} \approx 0.94 \frac{E}{\tau_p} = 1.88 \text{ GW} \quad (1)$$

The peak intensity of the pulse is then readily calculated as:

$$I_0 = \frac{P_0}{A_{eff}} = \frac{P_0}{\pi(2a/3)^2} \cong 2.1 \times 10^{17} \text{ W/m}^2 \quad (2)$$

To calculate  $\Delta\omega_{max}$  from the expression given in 12.19P we observe that, in our case: (i)  $\omega_0 = 2\pi c/\lambda \cong 2.36 \times 10^{15} \text{ s}^{-1}$ ; (ii) since the pulse parameter  $\tau_0$  is related to  $\tau_p$  by  $\tau_0 = \tau_p / 2\sqrt{\ln 2}$  we obtain  $\tau_0 = 12 \text{ fs}$ ; (iii) we have  $n_2 = 0.4 \times 9.8 \times 10^{-24} \text{ m}^2 \text{ IW} \cong 3.92 \times 10^{-24} \text{ m}^2 \text{ 1W}$ ; (iv)  $L = 60 \text{ cm}$ . Using these data and the value for  $I_0$  given by Eq. (2) we obtain  $\Delta\omega_{max} \cong 2.78 \times 10^{14} \text{ s}^{-1}$ . The expected spectral broadening is then:

$$\Delta\omega = 2\Delta\omega_{max} \cong 5.56 \times 10^{14} \text{ s}^{-1} \quad (3)$$

*Note:*

Assuming that the chirp introduced by the SPM can be completely compensated by an ideal compressor, we could obtain a compressed pulse of duration  $\tau_p$  given by:

$$\tau_p = 0.441/(\Delta\omega/2\pi) = 4.98 \text{ fs}$$

## 12.21A Group delay dispersion of a medium.

The phase introduced by the propagation in a dispersive medium of length  $L$  is:

$$\phi(\omega) = n(\omega)\omega L/c \quad (1)$$

When a short pulse in the visible or near-infrared spectral region passes through the material, the longer wavelengths travel faster than the shorter wavelengths, thus introducing a positive chirp on the pulse. The group delay dispersion (GDD) of a medium is defined as:  $\text{GDD} \equiv \phi'' \equiv d^2\phi/d\omega^2$ . We can now express GDD as a function of  $\lambda$  rather than of  $\omega$ . To this purpose, we first express the phase  $\phi(\omega)$  as a function of wavelength  $\lambda$ :

$$\phi(\omega) = n(\omega)\omega L/c = 2\pi L n(\lambda)/\lambda \quad (2)$$

We then calculate  $d\phi/d\omega$  and  $d^2\phi/d\omega^2$ :

$$\frac{d\phi(\omega)}{d\omega} = \frac{d\phi(\lambda)}{d\lambda} \frac{d\lambda}{d\omega} = -\frac{\lambda^2}{2\pi c} \frac{d\phi(\lambda)}{d\lambda} = \frac{L}{c} \left( n - \lambda \frac{dn}{d\lambda} \right) \quad (3)$$

$$\frac{d^2\phi(\omega)}{d\omega^2} = -\frac{\lambda^2}{2\pi c} \frac{d}{d\lambda} \left[ \frac{L}{c} \left( n - \lambda \frac{dn}{d\lambda} \right) \right] = \frac{\lambda^3 L}{2\pi c^2} \frac{d^2n(\lambda)}{d\lambda^2} \quad (4)$$

### 12.22A Dispersion-induced broadening of a 10-fs pulse in a fused silica plate.

Pulse broadening due to dispersion,  $\Delta\tau_d$ , is given approximately by Eq. (8.6.31) of PL:

$$\Delta\tau_d \approx \varphi''(\omega_0) |\Delta\omega| = \text{GDD} A_w \quad (1)$$

where  $A_w$  is the pulse bandwidth and GDD is the group delay dispersion of the medium. Assuming an unchirped input pulse of Gaussian profile the pulse bandwidth is related to pulse duration  $\tau_p$  by:

$$\Delta\omega = 2\pi 0.441/\tau_p = 2.77 \times 10^{14} \text{ s}^{-1} \quad (2)$$

The temporal broadening of the pulse arising from dispersion is therefore given by:

$$\Delta\tau_d \approx \text{GDD} A_w = 10 \text{ fs} \quad (3)$$

For a Gaussian pulse, the original pulse duration  $\tau_p$ , and the pulse broadening,  $\Delta\tau_d$ , must be combined quadratically:

$$\tau_{out} = (\tau_p^2 + \Delta\tau_d^2)^{1/2} = 14.14 \text{ fs} \quad (4)$$